Universitat Autònoma de Barcelona

Genetic dissection of fruit quality and ripening traits in melon

Lara Pereira García

UNIVERSITAT AUTÒNOMA DE BARCELONA

Facultat de Biociències

Dept. Biologia Animal, Biologia Vegetal i Ecologia

Genetic dissection of fruit quality and ripening traits in melon

Dissertation presented by Lara Pereira García for the degree in Doctor of Biology and Plant Biotechnology by the Universitat Autònoma de Barcelona (UAB).

This work was performed in the Centre for Research in Agricultural Genomics (CRAG).

Thesis directors		Tutor	PhD candidate
Jordi Garcia-Mas	Marta Pujol Abajo	Benet Gunsé	Lara Pereira García

Barcelona, May 2018

Index of contents

List of Figures

List of Tables

List of Digital Supplementary Material

List of abbreviations

ACC	1-aminocyclopropane-1-carboxylate
ABA	Abscisic acid
ABS	Abscission
ALF	Abscission layer formation
AZ	Abscission Zone
ACO	ACC oxidase
ACS	ACC synthase
BC	Backcross
bp	Base pair
cM	centiMorgan
CD	Chlorophyll degradation
Chr	Chromosome
COV	Coefficient of variance
CV	Coefficient of variation
CI	Confident Interval
DAP	Days after pollination
EABS	Earliness of abscission
EALF	Earliness of abscission layer formation
EARO	Earliness of aroma production
ECD	Earliness of chlorophyll degradation
DAPP	Earliness of ethylene peak
DAPE	Earliness of ethylene production

eV	electron Volt
ETR	Ethylene Receptors
ERF	Ethylene Responsive Factors
ECOL	External color of immature fruit
FIR	Flesh firmness
FAO	Food and Agriculture Organization
FD	Fruit diameter
FL	Fruit length
FP	Fruit perimeter
FW	Fruit weight
GC	Gas chromatography
GC-FID	Gas chromatography - flame ionization detector
GC-MS	Gas chromatography - mass spectrometry
GDP	Genotype depth
GBS	Genotyping-by-sequencing
HAR	Harvest date
Hyb	Hybrid, F1
INDELs	Insertions and deletions
IL	Introgression Line
kb	Kilobase
KW	Kruskal-Wallis
LOQ	Limit of quantification
LG	Linkage group

LOD	Logarithms of the odds
MAS	Marked-assisted selection
MEM	Maximal exact matches
Max	Maximum
ETH	Maximum ethylene production
Mb	Megabase
Min	Minimum
MV	Missing Values
MOT	Mottled rind
NIL	Near-isogenic line
NGS	Next-Generation Sequencing
NR	Number of reads
ppm	Parts per million
PS	Piel de Sapo
PCA	Principal Component Analysis
ARO	Production of aroma
PTV	Programmable temperature vaporization
qPCR	quantitative Polymerase Chain Reaction
QTL	Quantitative Trait Loci
RIL	Recombinant Inbred Line
RFLPs	Restricted Fragment Length Polymorphisms
RT	Room temperature
SN	Seed number

SW	Seed weight
SIM	Selected ion monitoring
FS	Shape index
SNP	Single Nucleotide Polymorphism
SSC	Soluble Solid Content
TILLING	Targeting Induced Local Lesions in Genomes
CAR	Total carotenoids
TF	Transcription factor
Ved	Védrantais
WEP	Width of ethylene peak
YELL	Yellowing of mature rind

Summary

Summary

Melon (*Cucumis melo* L.) is an important crop worldwide, with a production of around 31 million tons during 2016. Although traditionally breeding programs have been focused on agronomic traits, fruit quality has become a main goal recently. Fruit quality is a complex concept, including diverse traits related to fruit appearance, nutritional and organoleptic traits. Many of these traits are associated to fruit ripening, which is the process that the fruit undergoes to become edible to promote seed dispersal. Fruits are classified according to their ripening behavior into climacteric, when the plant hormone ethylene is synthesized in an autocatalytic way at the onset of ripening, and non-climacteric, in which ethylene has not a major role. The main goal of this work was to study the genetic basis of fruit quality and fruit ripening in melon.

We have developed a Recombinant Inbred Line (RIL) population from a cross between two elite cultivars, "Védrantais", highly climacteric, and "Piel de Sapo", non-climacteric. The phenotypic diversity in fruit quality and ripening-associated traits, including ethylene production, has been thoroughly studied. A high-density genetic map was constructed using SNPs and INDELs obtained through a genotyping-by-sequencing experiment. A first QTL mapping experiment revealed five major genes and 33 QTLs governing fruit appearance (flesh and rind color, presence of sutures, mottled rind), fruit morphology, sugar content and seed weight. A second QTL mapping experiment identified 14 QTLs modifying ethylene production and ripening-associated traits, as chlorophyll degradation and abscission layer formation. Among them, we highlight a major QTL, *ETHQV8.1*, involved in ethylene production that was affecting almost all the studied traits, located in a 500-kb interval in chromosome VIII.

In order to genetically dissect the fruit ripening process in melon, in addition to the mentioned RIL population, we studied a climacteric near-isogenic line, 8M35, with "Piel de Sapo" background and containing an introgression from the exotic accession PI 161375. 8M35 carries a QTL, *ETHQB3.5*, delimited in a region of 5 Mb in chromosome III. A positional cloning strategy was followed to fine map *ETHQB3.5*, generating a diverse set of subNILs. After multiple evaluations of different subNILs, we determined that at least two different genetic factors should be involved in triggering climacteric ripening in 8M35. One of them, named *ETHQB3.5.1*, which is responsible for the major part of the variation, was delimited to a 500-kb region containing 63 annotated genes.

Finally, two reciprocal introgression line (IL) collections were developed, using both "Védrantais" and "Piel de Sapo" as recurrent and donor parental lines, respectively. Recurrent backcrosses were performed in both directions and marker-assisted selection was performed in each generation to select both the target introgressions and the desired background. The current IL collections, covering approximately 95% of the donor parental genome, are formed by 38 ILs. We performed a preliminary phenotyping that allowed to validate some of the QTLs mapped in the RIL population for both fruit quality and fruit ripening traits. In addition, two segregating families of ILs with "Piel de Sapo" background were used to fine map *ETHQV8.1*, allowing to narrow down the region to a 150-kb interval containing 14 candidate genes.

As a summary, this PhD thesis has contributed to improving our knowledge about the genetics of fruit quality and particularly fruit ripening in melon, proposing some important QTLs that will be further explored in the future. Our work suggests that climacteric behavior in melon is a complex and quantitative trait controlled by polygenic inheritance, rather than a qualitative class as described traditionally in the literature.

Resumen

El melón (*Cucumis melo* L.) es un importante cultivo a nivel mundial, con una producción de 31 millones de toneladas durante el año 2016. Aunque tradicionalmente los programas de mejora genética se han focalizado en el comportamiento agronómico del cultivo, la calidad de fruto se ha convertido recientemente en un objetivo principal. La calidad del fruto es un concepto complejo, que incluye diversos caracteres relacionados con la apariencia visual del fruto y su calidad nutricional y organoléptica. Muchos de estos caracteres están asociados a la maduración de fruto, que es el proceso que sufre el fruto para transformarse en un alimento atractivo para promover la dispersión de la semilla. Los frutos son clasificados, en base a su comportamiento durante la maduración, en climatéricos, cuando la hormona vegetal etileno es sintetizada de manera autocatalítica al comienzo del proceso de maduración, y como no climatéricos, para los cuales el etileno no tiene un papel importante. El principal objetivo de este trabajo ha sido estudiar las bases genéticas de la calidad y la maduración del fruto en melón.

Hemos desarrollado una población de líneas puras recombinantes (RIL) a partir del cruce entre dos variedades élite, "Védrantais", altamente climatérica, y "Piel de Sapo", no climatérica. La diversidad fenotípica en la calidad de fruto y los caracteres asociados a la maduración, incluyendo la producción de etileno, han sido estudiados en profundidad. Un mapa genético de alta densidad ha sido construido usando SNPs e INDELs obtenidos a través de un experimento de *genotyping-by-sequencing*. Un primer experimento de mapeo de QTLs reveló cinco genes mayores y 33 QTLs implicados en la apariencia visual del fruto (color de piel y de pulpa, presencia de suturas, moteado de la piel), morfología de fruto, contenido en azúcares y peso de semilla. Un segundo experimento de mapeo de QTLs identificó 14 QTLs implicados en la producción de etileno y otros caracteres asociados a la maduración, como la degradación de clorofila o la formación de una capa de abscisión. Entre ellos, podemos destacar un QTL mayor, *ETHQV8.1*, implicado en la producción de etileno que afectó a prácticamente todos los caracteres estudiados, localizado en un intervalo de 500 kb en el cromosoma VIII.

Para diseccionar genéticamente la maduración del fruto en melón, además de la mencionada población de RILs, estudiamos la línea casi isogénica (NIL) climatérica 8M35, con el fondo genético de Piel de Sapo y una introgresión de la accesión exótica PI 161375. 8M35 porta el QTL *ETHQB3.5*, delimitado en una región de 5Mb del

cromosoma III. Se ha seguido una estrategia de clonaje posicional para proceder al mapeo fino de *ETHQB3.5*, generando un juego diverso de subNILs. Tras múltiples evaluaciones de diferentes subNILs, determinamos que al menos dos factores genéticos diferentes deben estar implicados en el desencadenamiento de la maduración climatérica en la línea 8M35. Uno de ellos, nombrado *ETHQB3.5.1*, es responsable de la mayor parte del fenotipo y fue delimitado a una región de 500 kb que contiene 63 genes anotados.

Finalmente, dos colecciones de introgresiones recíprocas han sido desarrolladas, utilizando "Védrantais" y "Piel de Sapo", ambos como líneas parentales recurrente y donante, respectivamente. Se efectuaron retrocruzamientos recurrentes en las dos direcciones y se realizó una selección asistida por marcadores en cada generación, para seleccionar tanto la introgresión diana como el fondo genético deseado. Las colecciones actuales, que cubren aproximadamente el 95% del genoma de la línea parental donante, están formadas por 38 líneas de introgresión. Hemos realizado un fenotipado preliminar que ha permitido validar algunos de los QTLs mapeados en la población de RILs, tanto para calidad como para maduración de fruto. Además, dos familias segregantes de líneas de introgresión con el fondo genético de "Piel de Sapo" se han usado para el mapeo fino de *ETHQV8.1*, permitiendo reducir la región de *ETHQV8.1* a un intervalo de 150 kb que contiene 14 genes candidatos.

Como resumen, esta tesis doctoral ha contribuido a mejorar el conocimiento sobre la genética de la calidad y particularmente la maduración de fruto en melón, proponiendo algunos QTLs importantes que serán explorados en mayor profundidad en el futuro. Nuestro trabajo sugiere que el comportamiento climatérico en melón es un carácter complejo y cuantitativo, controlado por una herencia poligénica, más que una clase cualitativa como ha sido descrito tradicionalmente en la literatura.

Resum

El meló (*Cucumis melo* L.) és un cultiu important a nivell mundial, amb una producció de més de 31 milions de tones durant l'any 2016. Malgrat que tradicionalment els programes de millora genètica s'han focalitzat en el comportament agronòmic del cultiu, la qualitat del fruit s'ha convertit recentment en un objectiu principal. La qualitat del fruit és un concepte complex, que inclou diversos caràcters relacionats amb l'aparença visual del fruit i la seva qualitat nutricional i organolèptica. Molts d'aquests caràcters estan associats a la maduració del fruit, que és el procés que pateix el fruit per transformar-se en un aliment atractiu per promoure la dispersió de la llavor. Els fruits són classificats en base al seu comportament durant la maduració en climatèrics, quan l'hormona vegetal etilè és sintetitzada de manera autocatalítica al començament del procés de maduració, i no climatèrics, pels quals l'etilè no té un paper important. El principal objectiu d'aquest treball ha estat estudiar les bases genètiques de la qualitat i la maduració del fruit en meló.

Hem desenvolupat una població de línies pures recombinants (RIL) a partir del creuament de dues varietats èlit, "Védrantais", altament climatèrica, i "Piel de Sapo", no climatèrica. La diversitat fenotípica en la qualitat del fruit i els caràcters associats a la maduració, incloent la producció d'etilè, han estat estudiats en profunditat. S'ha construït un mapa genètic d'alta densitat fent servir SNPs i INDELs obtinguts mitjançant un experiment de *genotyping-by-sequencing*. Un primer experiment de mapeig de QTLs va revelar cinc gens majors i 33 QTLs implicats en l'aparença visual del fruit (color de la pell i la polpa, presència de sutures i taques a la pell), morfologia del fruit, contingut en sucres i pes de la llavor. Un segon experiment de mapeig de QTLs va permetre identificar 14 QTLs implicats en la producció d'etilè i altres caràcters associats a la maduració, com la degradació de la clorofil·la o la formació d'una capa d'abscisió. Entre ells, podem destacar un QTL major, *ETHQV8.1*, implicat en la producció d'etilè que afecta pràcticament tots els caràcters estudiats, localitzat en un interval de 500 kb al cromosoma VIII.

Per tal de diseccionar genèticament la maduració del fruit en meló, a més de l'esmentada població de RILs, vam estudiar la línia quasi isogènica (NIL) climatèrica 8M35, amb el fons genètic de "Piel de Sapo" i una introgressió de l'accessió exòtica PI 161375. 8M35 conté el QTL *ETHQB3.5*, delimitat en una regió de 5 Mb del cromosoma III. S'ha seguit una estratègia de clonatge posicional per procedir al mapeig fi de *ETHQB3.5*, generant un joc divers de subNILs. Després de múltiples avaluacions de diferents subNILs, vam determinar que com a

mínim dos factor genètics diferents han d'estar implicats en el desencadenament de la maduració climatèrica de la línia 8M35. Un d'ells, anomenat *ETHQB3.5.1*, és responsable de la major part del fenotip i ha estat delimitat a una regió del 500 kb que conté 63 gens anotats.

Finalment, dues col·leccions d'introgressions recíproques han estat desenvolupades, fent servir "Védrantais" i "Piel de Sapo", ambdós com línies parentals recurrent i donant, respectivament. Es van efectuar retrocreuaments recurrents en les dues direccions i es va realitzar una selecció assistida per marcadors en cada generació, per tal de seleccionar tant l' introgressió diana com el fons genètic desitjat. Les col·leccions actuals, que cobreixen aproximadament el 95% del genoma de la línia parental donant, estan formades per 38 línies d'introgressió. Hem realitzat un fenotipat preliminar que ha permès validar alguns dels QTLs mapejats a la població de RILs tant per qualitat com per maduració del fruit. A més, dues famílies segregants de línies d'introgressió amb el fons genètic de "Piel de Sapo" s'han fet servir pel mapeig fi de *ETHQV8.1*, permetent reduir la regió de *ETHQV8.1* a un interval de 150 kb que conté 14 gens candidats.

Com a resum, aquesta tesi doctoral ha contribuït a millorar el coneixement sobre la genètica de la qualitat i particularment la maduració del fruit en meló, proposant alguns QTLs importants que seran explotats en major profunditat en el futur. El nostre treball suggereix que el comportament climatèric en meló és un caràcter complex i quantitatiu, controlat per una herència poligènica, més que una classe qualitativa com la que ha estat descrita històricament a la literatura.

Main introduction

Melon

Origin and phylogeny

Melon (*Cucumis melo* L.) is a diploid species (2n=2x=24) from the *Cucurbitaceae* family that has been cultivated for at least 4,000 years. The *Cucurbitaceae* family contains around a thousand species in almost a hundred genus, being *Cucumis* and *Citrullus* the most economically important (Renner and Schaefer 2016). More than fifty species belong to the *Cucumis* genus, including other important crops as *Cucumis sativus* (cucumber) (Pitrat 2016).

The origin of melon has traditionally been placed in Africa, but recently it has been suggested that melon was originated in India (Sebastian et al. 2010). According to Sebastian et al. (2010), a substantial part of the *Cucumis* genus, including species of varied geographical origin, has been underestimated in phylogeny and diversity studies; and proposed that deepening into Asian and Australian accessions could improve our knowledge about melon domestication.

Classically, melon was divided in two subspecies, *Cucumis melo* L. ssp. *melo* and *Cucumis melo* L. ssp. *agrestis*, which were differentiated by their ovaries; the ssp. *melo* presents long and hairy ovaries/young fruits, and the ssp. *agrestis*, short and glabrous ovaries/young fruits. However, wild melons are found in both subspecies (Pitrat 2013). Melon accessions have been further divided in botanical groups, according mainly to fruit traits. The latter classification includes 19 groups, some of them divided in subgroups, and is based on phenotypic criteria (Figure I.1). Most of these phenotypic traits are related to fruit characteristics as size, shape, external appearance and quality, but also to seed traits (Pitrat 2016).

Economic importance and breeding

Melon is a crop with huge economic importance worldwide, with more than 31 million tons produced and one and a half million cultivated hectares in 2016. The actual yield is around 2,500 kg per hectare, and is increasing continuously during the last decades as consequence of technical improvements and breeding. The first producer, with most than 50% of the total world production, is China. Spain, in the eighth position, had a total production of almost seven hundred thousand tons in 2016. The major part of the Spanish

production (410 thousand tons in 2013) was exported, contributing substantially to farmers' economy (FAO, 2017).

Figure I.1. Pictures representing the great diversity in fruit traits within the melon species. a. *agrestis* group b. *flexuosus* group c. *dudaim* group d. e. *cantalupensis* group f. g. h. *inodorus* group. Adapted from Pitrat (2016).

Due to the importance of melon as a crop, breeding companies have done an effort during the last decades to improve melon cultivars. Cultivated accessions can be found in both melon subspecies, and generally a specific breeding program is followed for each botanical group, pursuing different goals depending on the variety. The increasing availability of genetic and genomic knowledge in the species has generated a new source of tools to improve cultivars, focusing not only on the agronomical aspects of the crop (disease resistance, tolerance to abiotic stresses) but also on the nutritional and organoleptic aspects of the fruits.

Genetic and genomic resources

The broad diversity that can be observed in melon (Figure I.1) is a powerful tool for both research and breeding, allowing to investigate the genetic basis of agronomic and organoleptic traits and later on apply this knowledge in breeding programs. Several mapping populations have been developed through decades, from F2 to near-isogenic line (NIL) populations, generally by crossing two divergent varieties with different origin.

The segregation obtained in these populations was used to determine which genetic regions are associated to the phenotype, which are called quantitative trait loci (QTLs) (Eduardo et al. 2007; Paris et al. 2008; Argyris et al. 2017; Díaz et al. 2017; Galpaz et al. 2018).

The genotyping of these populations with molecular markers, from Restriction Fragment Length Polymorphisms (RFLP) to Single Nucleotide Polymorphisms (SNP), allowed to construct genetic maps, lately used to perform QTL mapping analysis. The fast development of sequencing technologies and the vast amount of available genetic resources of melon, as EST databases, BAC-end sequences and genetic maps, were useful to obtain in 2012 a high quality reference genome (Garcia-Mas et al. 2012). This sequence contains 82.5% of the estimated melon genome size (375 Mb of 454 Mb). After masking the repetitive fraction of the genome, corresponding principally to transposable elements, around 27 thousand genes were annotated. Recent improvements of the genome assembly, anchoring and annotation have been performed (Argyris et al. 2015; Ruggieri et al. 2018). Lately, other melon accessions have been re-sequenced, allowing to study the genetic diversity of melon, including not only SNP/INDEL polymorphisms, but also structural variation and transposon insertions, which are very common in plants (Sanseverino et al. 2015). Low-coverage re-sequencing and genotyping-by-sequencing (GBS) are cost-effective techniques that have been used in melon to obtain a high number of polymorphisms, principally SNPs and INDELs (Nimmakayala et al. 2016; Gur et al. 2017; Pavan et al. 2017; Hu et al. 2018).

In addition to sequence variation, many efforts have been done during the last years to understand several melon processes from a transcriptomic perspective. The use of microarrays and RNA-seq to identify differential expressed genes in a spatiotemporal axis and/or in several varieties led to a comprehensive landscape to understand specific processes as fruit ripening and abscission zone formation, among others (Corbacho et al. 2013; Saladié et al. 2015). Recently, a new method was proposed to perform QTL mapping analysis, including expression-QTLs, using RNA-seq data to obtain both markers and phenotypes; it has proven to be very efficient, allowing to identify QTL intervals containing only a few dozens of genes (Galpaz et al. 2018).

Another important resource, especially in order to validate potential candidate genes, are TILLING (Targeting Induced Local Lesions in Genomes) collections, a strategy that combines mutagenesis and high-throughput screenings, which has proven its efficiency

in functional genomics (Till et al. 2003). One of the most used TILLING populations in melon was developed from "Charentais Mono", a variety from the *cantalupensis* group with high importance in European and American markets. Since "Charentais Mono" is a typical climacteric variety with elevated ethylene production, the TILLING collection has been used principally to study the function of different genes related to fruit ripening (Dahmani-Mardas et al. 2010). A second TILLING population was produced in melon, in this case using "Piel de Sapo", a non-climacteric variety from the *inodorus* group, mainly consumed in Spain (González et al. 2011).

However, the best methodology to achieve functional validation of genes is the generation of transgenic or gene-edited plants. Transgenesis in melon has been described (Ayub et al. 1996; Giner et al. 2017), but the efficiency of the regeneration protocol is low and many of the obtained plants are usually tetraploid. The new and highly efficient technique CRISPR-Cas9, already used in many species for genome editing, has not been reported yet in melon.

Fruit quality

Fruit quality is a wide concept including many aspects of organoleptic, nutritional and appearance traits. The major part of fruit quality traits are related to fruit ripening and will be reviewed and discussed later on. But also some important fruit traits as size, shape and appearance are independent of fruit ripening.

Fruit size and shape have been largely studied in tomato. These traits, already defined in the ovary, are determined by both the number of cells and their size (Monforte et al. 2014). The inheritance of these traits is complex and polygenic, which is not totally understood yet. The knowledge of the molecular basis of fruit size and shape in tomato has been reviewed in Monforte et al. (2014); in addition, a new gene affecting fruit size was identified recently (Mu et al. 2017). In melon, extensively work has been performed to decipher the genetic basis of these traits, and multiple QTLs were mapped, but the underlying genes have not been cloned yet (Monforte et al. 2014).

Fruit appearance, referred as visual aspect of fruits, is governed by many different traits and varies greatly depending on the melon accession (Pitrat 2016) (Figure I.1). Some of them are the presence of sutures, ribbing, mottling of the rind, netting and external color.

They have been widely used in both breeding and taxonomy, but their inheritance is not well-known (Dogimont 2011). The most studied is the external color of fruits, determined by the accumulation of chlorophyll, flavonoids and carotenoids (Tadmor et al. 2010). The external color of immature fruit can be white or green; the trait is governed by a monogenic inheritance gene already described and mapped in chromosome VII (Dogimont 2011). Later, when the fruit grows and ripe, more pigments are synthetized or degraded, changing the final color of the fruit. The loss of the green pigment chlorophyll modifies the final color of the fruit, which is an ethylene-dependent trait in melon (Pech et al. 2008). In addition, other pigments as carotenoids and flavonoids are synthetized during ripening, but generally in an ethylene-independent manner. The most studied is the accumulation of naringenin chalcone, a yellow flavonoid pigment, which is controlled by *CmKFB*, a Kelch domain-containing F-box gene (Feder et al. 2015).

Fruit ripening

Fleshy fruits are key as main source of vitamins, minerals, fiber and antioxidants, playing an important role in human nutrition. The development and ripening of fruits has a major importance due to the economic and nutritional relevance and the scientific interest from a biological perspective. After fruit set, a phase of growth is mainly leaded by auxins, with subsequent periods of cell division and expansion of the ovary tissues (Seymour et al. 2013). When the fruit has achieved the adequate size and the seeds are completely developed, a series of changes are triggered to become attractive to consumers, with the ultimate aim of seed dispersal.

Classically, fruits have been divided in two types: climacteric and non-climacteric. When the ripening process is driven by the gaseous hormone ethylene, the fruits are classified as climacteric. The onset of ripening is determined by a peak of ethylene followed by an increase on the respiration rate, which triggers a myriad of physiological and metabolic changes (Lelievre et al. 1997). During the last decades, the molecular insights of fruit ripening have been revealed principally in tomato, the model crop for fruit development (Giovannoni 2007). Other examples of climacteric fruits are banana, avocado and apple.

In non-climacteric fruits, the ethylene and respiration levels remain basal, having no specific role in ripening. Strawberry, orange and grape are examples of non-climacteric species. Although much less is known about non-climacteric fruit ripening mechanisms,

abscisic acid has been described as a major player in the strawberry ripening process (Chai et al. 2011; Li et al. 2011).

Fruit ripening in the model crop tomato

Ethylene biosynthesis and perception

The biosynthetic pathway of ethylene is composed of two steps: the first one is the conversion of s-adenosyl-L-methionine (SAM) to aminocyclopropane-1-carboxylic acid (ACC) by the enzyme ACC synthase (ACS); and the second one is the conversion of ACC into ethylene by ACC oxidase (ACO) (Figure I.2) (Gapper et al. 2013). Both enzymes are encoded by multigenic families, but specific genes (*SlACS2*, *SlACS4* and *SlACO1*) are responsible of ethylene biosynthesis during ripening. The limiting enzyme is ACS, and both the induction of the enzyme and its stability are main control points of ethylene biosynthesis. The stability of ACS is probably controlled by the 26S proteasome, since the enzyme is stable when phosphorylated and is degraded after de-phosphorylation (Gapper et al. 2013).

The perception and signal transduction of ethylene has been well characterized in *Arabidopsis*, and the orthologous genes in tomato have been identified. The ethylene receptors, ETR, are localized in the endoplasmic reticulum and are negative regulators; when ethylene is absent, the signaling of the hormone is repressed (Figure I.2). There are seven ethylene receptors in tomato that act in a semi-redundant way, and three of them have a role in fruit ripening. Downstream the receptors, altering the ethylene perception in a tissue-specific manner, the *green-ripe* (Gr) gene is found, carrying an unknown and highly conserved domain (Barry and Giovannoni 2006). Also downstream the receptors, and interacting physically with them, there is the *CONSTITUTIVE TRIPLE RESPONSE 1* (*CTR1*) gene, a RAF MAP kinase kinase kinase (Kieber et al. 1993). In *ctr1 Arabidopsis* mutants, a constitutive ethylene response is observed, demonstrating its function as negative regulator. In *Arabidopsis* there is only one copy of *CTR1*, but in tomato it is encoded by a multigenic family of three members which are functionally redundant, since either of them complement the *ctr1 Arabidopsis* mutant (Adams-Phillips et al. 2004). The next step of the signal transduction is *ETHYLENE INSENSITIVE 2* (*EIN2*), a transmembrane protein located at the endoplasmic reticulum that acts as positive regulator of ethylene (Hu et al. 2010). *EIN2* is phosphorylated by *CTR1*, possibly regulating the movement of the protein to the nucleus or its degradation via the 26S

proteasome (Ju et al. 2012). A family of *ETHYLENE INSENSITIVE 3* (*EIN3*) transcription factors are acting downstream *EIN2* as positive regulators, binding to a specific promoter sequence called primary ethylene-response ethylene (PERE) of the *ETHYLENE RESPONSIVE FACTOR 1* (*ERF1*) (Solano et al. 1998; Tieman et al. 2001). In tomato, three homologs of the *Arabidopsis EIN3* had been identified. As for *EIN2*, the protein turnover via the 26S proteasome is suggested to play a role in regulating the stability of *EIN3*. The ERF genes compose a large, multigenic family that shares a conserved domain that binds to a specific sequence denominated GCC box, activating different genetic programs to trigger the observed phenotypic responses (Solano et al. 1998).

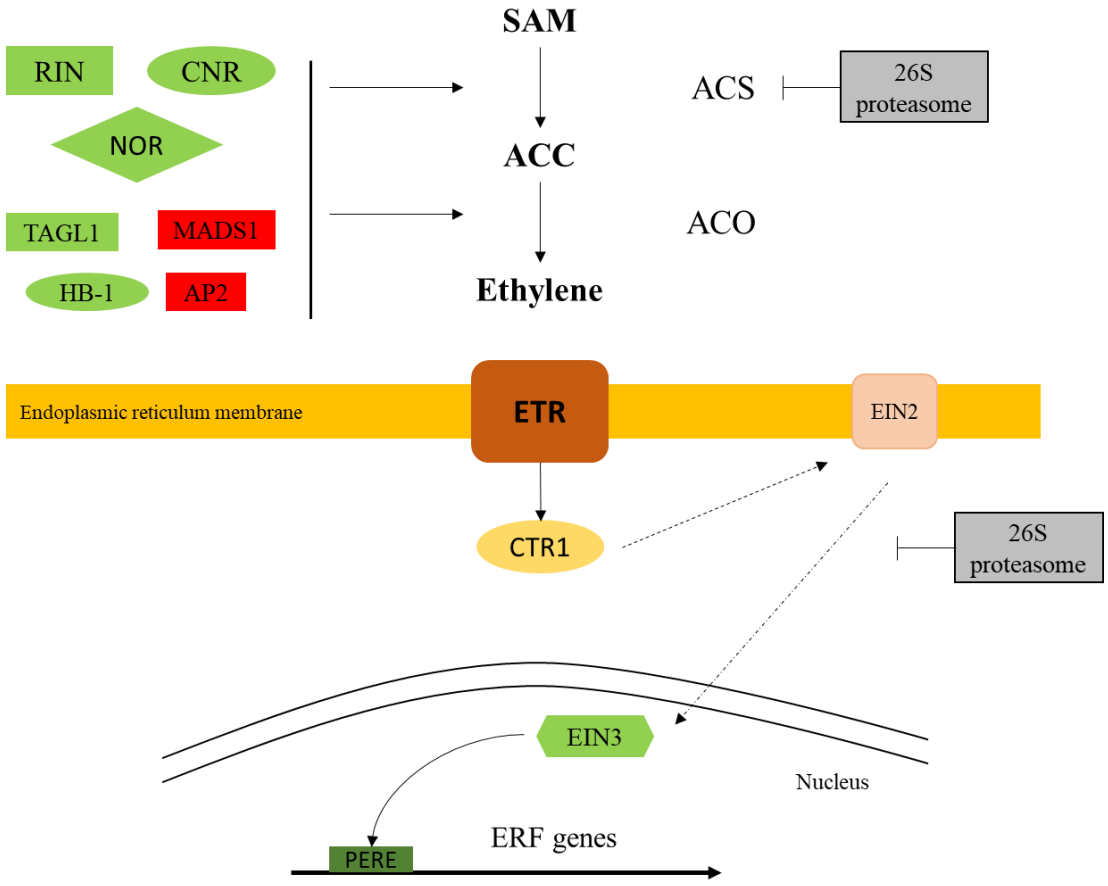

Figure I.2. Ethylene biosynthesis and transduction. The two enzymes of the pathway, ACC synthase (ACS) and ACC oxidase (ACO), are regulated by a complex network of transcription factors (green, activators and red, repressors) and via 26S proteasome. When the hormone reaches the cell, it binds to the receptors (ETR), which are located in the endoplasmic reticulum membrane. The kinase CTR1 and other secondary messengers activate the signaling pathway, causing finally the gene expression of Ethylene Responsive Factors (ERF) genes. Adapted from Vegas (2014).

Transcriptional regulation of ethylene in fruit ripening

Tomato mutants have been essential to decipher the genetic factors involved in climacteric ripening regulation. The complex genetic network controlling the process is not totally understood yet, but several genes have been cloned and characterized during the last years (Giovannoni 2007).

Classically, three factors have been described as master regulators of climacteric fruit ripening: RIN, a SEPALLATA MADS-box transcription factor (TF), CNR, a SQUAMOSA promoter binding protein, and NOR, a NAC TF. The *ripening inhibitor* (*rin*) mutant presented a strong repression of all the ripening symptoms, including the ethylene burst, large sepals and loss of inflorescence determinacy (Figure I.2) (Vrebalov et al. 2002). The positional cloning of the RIN locus showed that two MADS-box genes were affected, *LeMADS-RIN*, responsible for the ripening phenotype, and *LeMADS-MC*, causing the sepal modification. *LeMADS-RIN* has been considered as essential in fruit ripening regulation and its expression and interaction with other genes has been deeply studied (Ito et al. 2008; Osorio et al. 2011; Fujisawa et al. 2012; Qin et al. 2012; Fujisawa et al. 2013). The RIN homologs of other species, both climacteric and non-climacteric, have also been related to fruit ripening (Seymour et al. 2011; Elitzur et al. 2016). However, a recent work has shown that RIN, although alters significantly the fruit ripening process, is not required for fruit ripening initiation, as the *rin* mutant is not a null mutation but a gain-of-function mutant (Ito et al. 2017). *LeSPL-CNR* was identified by positional cloning in the mutant *Colorless non-ripening*, which shows a colorless and mealy pericarp (Manning et al. 2006). This phenotype is caused by a stable epimutation, which caused high levels of cytosine methylation in the promoter of *LeSPL-CNR*, reducing its expression. Although no physical interaction has been detected between CNR and RIN, the RIN DNA-binding activity was reduced in the *Cnr* mutant (Martel et al. 2011). Finally, a NAC-domain protein identified in the *non-ripening* (*nor*) mutant is considered essential for fruit ripening and is suggested to be acting upstream RIN (Osorio et al. 2011; Giovannoni et al. 2017).

In addition, many other transcription factors, although not essential to trigger the ripening process, are involved in fruit ripening, leading to ripening-deficient plants. *LeHB-1* encodes a class-I homeodomain leucine zipper protein that binds to the promoter of ACO1; its silencing provokes a delay in ripening, besides other alterations in flower development (Lin et al. 2008). *TAGL1*, an AGAMOUS MADS-box orthologue of

Arabidopsis SHATTERPROOF, is regulating both fruit development and ripening; the autocatalytic synthesis of ethylene is greatly reduced in the mutant and the most obvious effect is the reduction in total carotenoid content, mainly lycopene, that confers orange color to the ripe fruit (Vrebalov et al. 2009). *SlAP2a* was the first negative regulator of fruit ripening characterized in tomato, with *SlAP2a* RNAi lines producing five-fold increase of ethylene when compared to the wild type and altering the carotenoid content (Chung et al. 2010). AP2a probably functions downstream the master regulators CNR, NOR and RIN, moreover CNR can bind directly to a promoter element of AP2a (Karlova et al. 2011). *SlMADS1* was also described as a repressive modulator of ethylene biosynthesis and fruit ripening, acting through direct binding to RIN (Dong et al. 2013). Other two MADS-box containing proteins, TDR4/FUL1 and MBP7/FUL2, orthologues of the FRUITFUL *Arabidopsis* factor, are modulating carotenoid biosynthesis, cell-wall metabolism and aroma production but the ethylene biosynthesis is not altered, indicating that they act downstream ethylene or in a totally independent way (Bemer et al. 2012). *SlFYFL*, another gene encoding the MADS-box orthologue of *Arabidopsis* FYF, acts as a negative regulator of ethylene biosynthesis and fruit ripening, specifically modulating the abscission zone development (Xie et al. 2014). FYFL interacts physically with other MADS-box proteins as RIN and MADS1. Another described positive modulator of fruit ripening is *SlNAC4*, whose silencing delayed ripening around three days and reduced ethylene production, carotenoid content and fruit softening (Zhu et al. 2014). *SlNAC4* could not be induced by ethylene and its expression is not altered in *rin* mutants, suggesting that it acts upstream of RIN. Another NAC factor, *SlNAC1*, is a positive modulator of fruit ripening, affecting ethylene production, fruit pigmentation and fruit softening (Meng et al. 2016).

In summary, the insights in tomato fruit ripening have shown that a complex transcriptional network, mainly integrated by NAC and MADS-box TFs, is governing the process.

Competence to ripen: DNA demethylation

Ethylene, besides having an essential role in fruit ripening, is governing many other physiological processes as plant defense, shoot and root differentiation, sex determination and flower and leaf senescence. To differentiate the physiological function of the hormone, two systems have been defined: system 1, auto-inhibitory and operating in all tissues including fruits, responsible of responses to ethylene other than ripening, and

system 2, autocatalytic and responsible of the ethylene burst during ripening (Lelievre et al. 1997). Before the transition from system 1 to system 2, the fruit has not the competence to ripen, even if exogenous ethylene is applied (McMurchie et al. 1972; Giovannoni et al. 2017).

Since the characterization of the epimutant *Cnr*, it has been hypothesized that DNA methylation could play a role in fruit ripening. The use of chemical inhibitors of DNA methylation proved that cytosine demethylation triggers, at least partially, the transition from system 1 to system 2, allowing fruit ripening (Zhong et al. 2013). Silencing of *SlDML2*, the DEMETER-like DNA demethylase that plays a main role in tomato fruit, delayed and limited ripening (Liu et al. 2015). The observed fruit ripening defects were correlated with the absence of demethylation of the promoters of key ripening genes as *NOR* and *RIN*. These findings were corroborated by a CRISPR-Cas9 mutant of *SlDML2*, which presented a high number of silenced ripening-related genes (flavonoid and carotenoid biosynthesis and ethylene pathway) (Lang et al. 2017).

Another epigenetic modification that has been suggested to modify fruit ripening is histone deacetylation (Guo et al. 2017). The repression of *SlHDA*, a fruit-specific histone deacetylase, provokes the up-regulation of ethylene-related and ripening-associated genes, causing an evident phenotype in fruits.

Recently, a genetic-epigenetic model has been proposed, suggesting that both the transcriptional network and the epigenetic changes have major impact in ripening, in addition to other unexplored candidates, as *WRKY* and *NAGTHA* gene families with ripening-associated expression (Giovannoni et al. 2017). In addition, a new spatial perspective is starting to prevail, focusing on the distinct transcriptional and phenotypic profiles in different tissues. It has been suggested that the locular tissue surrounding the seeds could have a major role in early ripening.

Ripening in non-climacteric fruits

Non-climacteric fruits do not present a burst of ethylene nor a peak of respiration, although they show a complete ripening process that overlaps to a high extent with the physiological responses induced by ethylene in climacteric fruits. Strawberry has been accepted as a non-climacteric model, since the ethylene peak at the onset of respiration is absent. However, some recent studies support that ethylene may have a role in strawberry ripening (Cherian et al. 2014).

The major regulator of strawberry fruit ripening is the plant hormone abscisic acid (ABA) (Li et al. 2011). ABA treatment accelerates the change of fruit color and softening in strawberry, while ABA inhibitors block fruit ripening. Besides fruit ripening, ABA is a phytohormone involved in the regulation of many important processes, as seed dormancy, seedling growth and adaptation to adverse conditions, among many others (Raghavendra et al. 2010).

ABA is synthetized via a complex biosynthetic pathway using carotenoids as first precursors (Seo and Koshiba 2002). The early steps of ABA biosynthesis, converting zeaxanthin into xanthophylls, are located in the plastids. The oxidative cleavage of xanthophylls to produce xanthosin, catalyzed by 9-cis-epoxycarotenoid dioxygenase (NCED) also happens in plastids. The later steps to transform xanthosin to ABA are performed in the cytosol, and alternative pathways that involve different enzymes have been described. Concerning ABA perception and signaling, two pathways have been proposed in *Arabidopsis*: the PYR1-PP2C-SnRK2 pathway and the ABAR-WRKY40-ABI5 pathway (Raghavendra et al. 2010). In the first route, located in the cytosol, ABA induces the interaction of PYR1, which is an ABA receptor, and a protein phosphatase 2C (PP2C), which subsequently activates a sucrose non-fermenting-related kinase 2 (SnRK2), leading to a phosphorylation cascade of downstream factors (Chai et al. 2011). The second pathway is initiated by the plastid ABA receptor ABAR/CHLH that recruits the TF WRKY40 from the nucleus to the cytoplasm, causing a de-repression of the ABA responses (Rushton et al. 2012).

In strawberry, the involvement of enzymes from both the biosynthetic pathway and the signaling components in fruit ripening have been studied. Although stable transgenic strawberries are problematic to obtain, the virus-induced gene silencing technique has been used to study the effects of ABA-related genes in strawberry fruits. Down-regulation of *FaPYR1*, the orthologue of the *Arabidopsis* ABA receptor gene *PYR1*, altered significantly ABA content and expression of ABA-responsive genes in addition to a marked delay of fruit ripening (Chai et al. 2011). Silencing of *FaNCED1*, one of the major biosynthetic enzymes, caused a ripening delay and ABA treatment was able to rescue the wild-type phenotype (Jia et al. 2011). An analogous result in fruit ripening was observed when down-regulating the plastid receptor *FaCHLH/ABAR*, because as expected, the wild-type phenotype was not rescued by applying exogenous ABA (Jia et al. 2011).

Other important signals modulating fruit ripening in strawberry are sugars as sucrose, glucose and turanose (Jia et al. 2013). The chemical treatment of immature fruits with these molecules accelerates fruit ripening, obtaining fully red fruits after only eight days, while the negative control remained white. Silencing of a fruit-specific sucrose transporter, *FaSUT1*, exerted a significant inhibition of fruit ripening, and its overexpression had the opposite effect, accelerating fruit ripening. In addition, sucrose was regulating the expression of *FaNCED*, which encodes one of the key enzymes of ABA biosynthesis, suggesting that sucrose partially controls strawberry fruit ripening by modulating ABA content.

Although the mechanisms inducing and modulating fruit ripening in non-climacteric fruits seemed to be ethylene-independent, two MADS-box TFs, *FaMADS9* and *FaSHP*, are positive regulators of strawberry fruit ripening (Seymour et al. 2011; Daminato et al. 2013). In other non-climacteric species, as pepper, the orthologues of RIN could have also a role in fruit ripening (Dong et al. 2014). These facts suggest that most probably climacteric and non-climacteric ripening share some overlapped mechanisms.

Ripening-associated traits

The biological aim of the ripening process is to become attractive to the consumers for seed dispersal. Many metabolic and physiological changes are triggered in both climacteric and non-climacteric species to achieve this objective in an efficient manner. Most of these modifications are related with fruit flavor, a concept including taste and smell, in which many different molecules are involved.

Sugars and acids accumulation

The sweetness of fruits is a central trait for fruit quality and is mainly determined by the total sugar content (also referred as soluble solid content) and the ratios between different sugars. During fruit growth it accumulates sugars in the form of starch, due to an influx from other vegetative tissues. When the fruit ripens, the starch is decomposed in hexose sugars, as glucose and fructose (Matsukura 2016). However, the type of sugars accumulated during ripening is highly dependent on the species (Osorio and Fernie 2014).

The main step controlling sugar metabolism in tomato fruit is the enzyme invertase (Osorio and Fernie 2014). Different types of invertases have been described depending on their localization in the cell, and the most determinant for fruit quality seemed to be

the cell-wall invertase LIN5, which was identified using an introgression line of tomato. The effect of LIN5 in soluble solid content was confirmed by silencing the corresponding gene, obtaining significant lower sugar content (Zanor et al. 2009).

Another major component of flavor is the organic acids content, since the taste and the flavor of the fruits is determined by the sugar/organic acid ratio, and they also act as precursors of other secondary metabolites (Osorio and Fernie 2014). The activity of different metabolic pathways, as glycolysis and the tricarboxylic acid cycle, determines the organic acid content. The main organic acids in fruits are citrate and malate, both intermediate components of the tricarboxylic acid cycle, and also glutamate (Klee 2010).

Carotenoid accumulation and chlorophyll degradation

Carotenoids are a type of isoprenoids that are almost exclusively synthetized in the plastids of plant cells. Their functions are related to the absorption of the excess of light energy and also as precursors of plant hormones, among others. They are responsible of many of the colors that can be observed in nature, as yellow, orange and red. Animals cannot synthesize carotenoids, so they should incorporate them in their diets. Due to their nutritional and healthy benefits, increasing efforts are ongoing to understand and modify carotenoid content in fruits (McQuinn et al. 2015).

During ripening, the chloroplasts of fruit tissues differentiate to chromoplasts, a specialized organelle that mainly stores carotenoids. The structure of the carotenoid-bearing bodies differs depending on the species, probably due to the main type of carotenoid accumulated. In tomato, the dominant structures are the crystalloid bodies of lycopene. The two major metabolic changes are the biosynthesis of carotenoids and the loss of the components involved in photosynthesis and biogenesis of thylakoids. During the transition from chloroplast to chromoplasts, a down-regulation of many photosynthetic genes strongly decreases the photosynthetic activity, finishing with a disintegration of the thylakoid membranes. The chlorophyll is degraded and the fruit structures lose the characteristic green color (Pech et al. 2014).

In parallel, the biosynthesis of carotenoids is activated. The methylerythritol 4-phosphate pathway produces isopentenyl diphosphate, which could be considered the initial substrate of the pathway. Subsequent condensations of isoprenoid molecules lead to geranylgeranyl pyrophosphate, which suffers other modifications to be converted in a varied set of carotenoids (McQuinn et al. 2015). Most of the enzymes of the pathway are

de-regulated during ripening, increasing the gene expression of enzymes of the first reactions of the pathway (*PSY1*, *ZDS* and *CRTISO*) and down-regulating the enzymes downstream the pathway to avoid carotenoid cleavage. Specifically, *PSY1* expression is generally considered as a ripening symptom (Bemer et al. 2012; Zhu et al. 2014; Meng et al. 2016).

Fruit softening

To become palatable, one of the most important changes is fruit softening. Softening is the consequence of changes in firmness, meaning the force necessary to deform the surface of the fruit, and texture, a more sensorial and subjective concept (Tucker 2014). Although changes in texture during ripening are desirable for the consumer in an adequate level, they have also negative consequences, as an increase in pathogen susceptibility. An excessive softening, generally appearing at the later stages of ripening, could lead to an undesirable texture and complicates the transport and storage of fruits (Goulao and Oliveira 2008).

Different factors contribute to fruit softening, as decrease in cell turgor, physiological changes in membranes, degradation of starch and cell-wall and apoplast modifications. However, the latter is considered as the main reason of texture changes in fruit ripening (Goulao and Oliveira 2008).

The dissolution of the middle lamella (intercellular space) and the disruption of primary cell wall are the main processes provoking fruit softening (Goulao and Oliveira 2008). The middle lamella is formed mainly by pectins, and the fruit primary cell-wall consists in cellulose, hemicelluloses (xyloglucan is the most abundant in tomato), pectins and structural proteins (Tucker 2014; Wang et al. 2018). Structural modifications of the polymers forming the cell wall include mainly solubilisation and depolymerisation. In tomato, the main changes are the solubilisation and depolymerisation of polyuronides and the depolymerisation of xyloglucan, maintaining the cellulose fraction almost intact. However, the softening process is specific for each species and the observed changes may vary greatly (Goulao and Oliveira 2008).

Multiple enzymes act coordinately to modify the cell wall structure. Generally, they are classified in pectolytic enzymes, including endo- and exo-polygalacturonases, pectate lyases and β-galacturonases, and non-pectolytic enzymes, as endo-1,4-β-glucanases, xyloglucan hydrolases and expansins (Goulao and Oliveira 2008). Traditionally,

polygalacturonases were considered as the main responsible enzymes for texture changes and they have been deeply studied. They were proposed to have a role in post-harvest behavior, but the silencing of these enzymes did not alter substantially fruit texture. Similar results were observed in transgenic plants with reduced activity of other cell-wall modifying enzymes, as pectin methylesterase, galactanase and expansins, suggesting that a coordinated activity of several enzymes leading to a remodeling of cell wall is necessary for an adequate fruit softening (Goulao and Oliveira 2008; Wang et al. 2018).

However, a recent work has demonstrated that the repression of a pectate lyase is sufficient to achieve a firmer tomato fruit with improved shelf-life without affecting any other fruit quality trait (Uluisik et al. 2016). Pectate lyase is acting principally in tricellular junctions, breaking the de-esterified pectins that contribute to cell-to-cell adhesion and allowing the subsequent action of other cell-wall modifying enzymes.

Aroma profile

The aroma, determined by a mixture of a wide range of volatile organic compounds, plays an essential role in fruit flavor. Some of these compounds are very potent, contributing substantially to the aroma profile, although they are present in very low concentrations. Not only is the final amount of volatiles important for flavor, but also its relative composition.

Fruit volatiles are classified in four main groups: volatiles derived from carotenoids, fatty acid volatiles, terpenoid volatiles and amino acid derived volatiles. The carotenoid-derived volatiles, also called apocarotenoids, are the product of a cleavage of carotenoids, either by non-enzymatic oxidation or by the action of carotenoid dioxygenase. Fatty-acid derived volatiles are synthesized principally by the lipoxygenase pathway, using linoleic and linolenic acid as substrates. The key enzymes of the pathway are hydroperoxide lyase, alcohol dehydrogenase and alcohol acyltransferase. The most important fatty-acid volatiles in tomato are cis-3-hexanal and trans-2-hexenal, both defined as green flavor compounds. The terpenoids are the most abundant volatiles in tomato, belonging to mono-, sesqui- and diterpenoids. They are synthesized by terpene synthases, a gene family formed by 29 potentially functional enzymes in tomato. Concerning the amino acid derived volatiles, phenylalanine-derived volatiles (guiacol, eugenol, methylsalicytale) compounds contribute greatly to tomato aroma, much more than

branched chain volatiles (isobutyl acetate, 2-methylbutanal/ol) (Tohge et al. 2014; Zhang and Chen 2014).

Biosynthesis of many volatile compounds is triggered by ethylene during fruit ripening, and coincides with the chloroplast-to-chromoplast transition. Transgenic lines with down-regulated ACS and ripening mutants as *rin* and *nor* presented reduced levels of a range of volatiles, including trans-2-hexenal, cis-3-hexenal and geranylacetone, among others (Wang et al. 2016).

Abscission zone formation

When plant organs become useless or damaged, the plant activates mechanisms to shed them from its body. After ripening, the fruit is prepared to be consumed and the seeds are ready to be dispersed, so many species form an abscission zone (AZ) in the pedicel to separate the fruit from the plant. Normally, AZ formation is induced by ethylene and is formed by several layers of small, undifferentiated cells at the junction between the organ and the main body of the plant (Ito and Nakano 2015).

Tomato mutants have been used to characterize the genetic regulators of this process. The first cloned gene was *JOINTLESS*, a MADS-box TF which plays a central role in AZ development in tomato flower and fruit (Mao et al. 2000). MACROCALIX, another MADS-box identified in the *rin* mutant (Vrebalov et al. 2002), was proved to regulate AZ formation by direct interaction with JOINTLESS (Nakano et al. 2012). Two additional MADS-box TFs were described as AZ development modulators, *SLMBP21* (Liu et al. 2014; Roldan Gomez et al. 2017) and *SlFYFL* (Xie et al. 2014). It has been hypothesized that they could form heterodimers to regulate the expression of genes involved in meristem identity and cell wall modification, leading to AZ formation (Nakano et al. 2012; Xie et al. 2014). These mutants, especially *jointless-2*, a mutant of *SlMBP21*, have been broadly utilized in breeding programs, since non-abscising fruits facilitate the harvest process and improve the quality of tomato for both industry and fresh market (Roldan Gomez et al. 2017).

Melon, an alternative model for fruit ripening

Unlike most of fleshy fruit species, melon species includes climacteric and non-climacteric varieties. The existence of sexually-compatible varieties showing a range of climacteric behavior allows to develop segregating populations, a powerful tool to

decipher the genetic control of this trait (Ezura and Owino 2008). The huge diversity of melon fruits traits is also observed for ethylene production, earliness of ripening and ripening-associated traits, suggesting that a complex and polygenic inheritance underlies ripening behaviour (Pitrat 2016). For this reason, melon has become an alternative crop model for fruit ripening research, and also because of the great availability of genetic and genomic tools (Ezura and Owino 2008).

Ethylene biosynthesis and transduction in melon are probably very similar to those described in tomato, since orthologous genes in the melon genome have been found for almost all components (Yano and Ezura 2016). Two ACS, *CmACS1* and *CmACS5*, and one ACO, *CmACO1*, are responsible of the burst of ethylene at the onset of ripening, being up-regulated in the climacteric varieties (Saladié et al. 2015). A climacteric variety, "Védrantais", with suppressed expression of *CmACO1* showed a delay and a significantly lower ethylene peak when compared to the wild type, and the major part of the ripening-associated traits were also altered (Ayub et al. 1996).

Regarding the regulation of ethylene production and fruit ripening, several quantitative trait loci (QTL) have been described (Yano and Ezura 2016), and one of the underlying genes has been cloned (Rios et al. 2017). The QTL *ETHQV6.3* induces climacteric ripening in a non-climacteric background and a positional cloning strategy revealed that *CmNAC-NOR* is the orthologue of tomato NOR TF (Rios et al. 2017).

The response to ethylene varies slightly depending on the species. Ripening-associated traits in the model crop tomato have been described above, but in some cases the behavior in melon is different. The above-mentioned study of the anti-sense *CmACO1*cantaloupe-type melon, which does not produce ethylene, allowed to define whether ripening traits are or not dependent on ethylene (Ayub et al. 1996). Fruit abscission, chlorophyll degradation, aroma production and the major part of flesh softening are ethylene-dependent, while sugar and organic acid accumulation, carotenoid biosynthesis (which determines flesh color), and a minor fraction of flesh softening are ethylene-independent (Figure I.3) (Pech et al. 2008).

Concerning the ethylene-independent traits, the most noticeable could be the sugar and organic acid accumulation and the flesh color, which have already been described above (Figure I.3). Sugar and organic acid contents in melon, unlike other species, may vary greatly, leading to sweet dessert fruits very popular mainly in Europe and America, and

sour fruits consumed immature similarly to cucumber, grown in Africa and Asia (Gur et al. 2016). The range of sugar content covers from 3 to 18 ºBrix, concentrating the high-sugar varieties mainly in ssp. *melo*. This variability has been deeply explored and used in QTL mapping experiments and genome-wide association studies, proposing more than 10 QTLs affecting this trait. The sugar metabolism pathway in cucurbits, based on sucrose accumulation, is unique, since other species as tomato or grape mainly accumulate hexoses. The complex pathway involves around 20 enzymatic reactions, but surprisingly, any of the characterized genes encoding these enzymes is co-localizing with mapped QTLs for sugar content, reflecting the complexity of the trait. On the opposite side, a single major gene is controlling fruit acidity (or sourness) in melon, identified by a map-based cloning strategy (Cohen et al. 2014). The responsible gene (*MELO3C025264*) encodes a membrane transporter that had not been described before, contributing significantly to the understanding of fruit acidity.

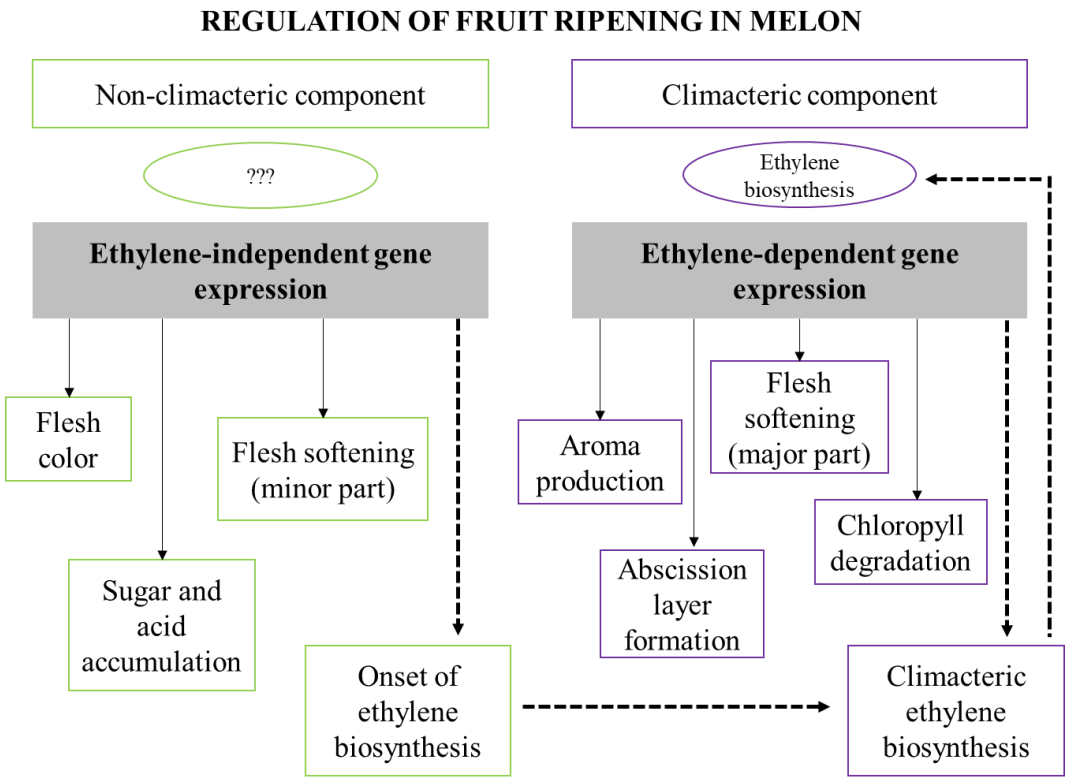

Figure I.3. Fruit traits associated to fruit ripening in melon and their relationship with ethylene. Adapted from Pech et al., (2008).

Another trait of great importance for melon consumers is flesh color. Flesh color in melon, unlike in tomato, is ethylene-independent (Figure I.3) (Pech et al. 2008). Its inheritance is controlled by two genes that act epistatically (Dogimont 2011). The first

gene, *green flesh* (*gf*), determines the presence or absence of orange color, due mainly to β-carotene accumulation, the orange color being dominant. The second gene, *white flesh* (*wf*), determines whether the fruit is green or white when the recessive allele of *gf* is present. The gene underlying *gf* is *CmOr*, the orthologue of the *BoOr* gene in cauliflower (Tzuri et al. 2015). *CmOr* is inducing the chromoplast biogenesis and β-carotene accumulation in a similar way that *BoOr* does in cauliflower and transgenic potato tubers. A non-synonymous SNP in a highly conserved region of the protein is responsible of the phenotype, being totally coincident in a panel of accessions representing melon diversity, where only these two main haplotypes were found. *Wf* has been mapped, using different populations, to chromosome VIII (Monforte et al. 2004; Cuevas et al. 2009), and a pentatricopeptide protein, *CmPPR1*, has been recently proposed as a candidate for *wf* (Galpaz et al. 2018). This protein is related to RNA processing in plastids and regulates the expression of a group of chloroplast-related genes; however, the segregating population used did not segregate for green and white flesh, only for orange intensity.

Concerning the ethylene-dependent traits, we could affirm that, in general, in melon they are analogous to the described in tomato, although much less is known. Probably the most studied trait would be the aroma production, since melon is very popular in some countries due to its strong, rich and sweet aroma (Gur et al. 2016). As climacteric and non-climacteric varieties coexist in the species, the volatile profile varies widely depending on the ripening behavior (Obando-Ulloa et al. 2008). Non-climacteric varieties have a low content of volatiles and the main contributors are alcohols and aldehydes. On the opposite side, climacteric varieties have a high content of volatiles from different biosynthetic origin and with diverse chemical structures; being esters one of the most typical compounds (Freilich et al. 2015). Nine enzymes have been described in melon that participate in all the biosynthetic pathways of volatiles (Gur et al. 2016; Galpaz et al. 2018).

References

Adams-Phillips L, Barry C, Kannan P, Leclercq J (2004) Evidence that CTR1-mediated ethylene signal transduction in tomato is encoded by a multigene family whose members display distinct regulatory features. Plant Mol Biol 54:387–404.

Argyris JM, Díaz A, Ruggieri V, et al (2017) QTL Analyses in Multiple Populations Employed for the Fine Mapping and Identification of Candidate Genes at a Locus Affecting Sugar Accumulation in Melon (*Cucumis melo* L.). Front Plant Sci 8:1–20.

Argyris JM, Ruiz-herrera A, Madriz-masis P, et al (2015) Use of targeted SNP selection for an improved anchoring of the melon (*Cucumis melo* L.) scaffold genome assembly. BMC Genomics 16:1–14.

Ayub R, Guis M, Ben Amor M, et al (1996) Expression of ACC oxidase antisense gene inhibits ripening of cantaloupe melon fruits. Nat Biotechnol 14:862–866.

Barry CS, Giovannoni JJ (2006) Ripening in the tomato *Green-ripe* mutant is inhibited by ectopic expression of a protein that disrupts ethylene signaling. Proc Natl Acad Sci U S A 103:7923–8.

Bemer M, Karlova R, Ballester AR, et al (2012) The Tomato FRUITFULL Homologs TDR4/FUL1 and Aspects of Fruit Ripening. Plant Cell 24:4437–4451.

Chai YM, Jia HF, Li CL, et al (2011) *FaPYR1* is involved in strawberry fruit ripening. J Exp Bot 62:5079–5089.

Cherian S, Figueroa CR, Nair H (2014) "Movers and shakers" in the regulation of fruit ripening: a cross-dissection of climacteric versus non-climacteric fruit. J Exp Bot 65:4705–4722.

Chung M-Y, Vrebalov J, Alba R, et al (2010) A tomato (*Solanum lycopersicum*) APETALA2/ERF gene, *SlAP2a*, is a negative regulator of fruit ripening. Plant J 64:936–947.

Cohen S, Itkin M, Yeselson Y, et al (2014) The PH gene determines fruit acidity and contributes to the evolution of sweet melons. Nat Commun 5:4026.

Corbacho J, Romojaro F, Pech J-C, et al (2013) Transcriptomic Events Involved in Melon Mature-Fruit Abscission Comprise the Sequential Induction of Cell- Wall Degrading Genes Coupled to a Stimulation of Endo and Exocytosis. PLoS One 8:58363.

Cuevas HE, Staub JE, Simon PW, Zalapa JE (2009) A consensus linkage map identifies genomic regions controlling fruit maturity and beta-carotene-associated flesh color in melon (*Cucumis melo* L.). Theor Appl Genet 119:741–756.

Dahmani-Mardas F, Troadec C, Boualem A, et al (2010) Engineering Melon Plants with Improved Fruit Shelf Life Using the TILLING Approach. PLoS One 5:e15776.

Daminato M, Guzzo F, Casadoro G (2013) A SHATTERPROOF-like gene controls ripening in non-climacteric strawberries, and auxin and abscisic acid antagonistically affect its expression. J Exp Bot 64:3775–3786.

Díaz A, Hernández M, Dolcet R, et al (2017) Quantitative trait loci analysis of melon (*Cucumis melo* L.) domestication-related traits. Theor Appl Genet 130:1837–1856.

Dogimont C (2011) 2011 Gene List for Melon. Cucurbit Genet Coop Rep 33–34:104–133.

Dong T, Chen G, Tian S, et al (2014) A non-climacteric fruit gene *CaMADS-RIN* regulates fruit ripening and ethylene biosynthesis in climacteric fruit. PLoS One 9:1–11.

Dong T, Hu Z, Deng L, et al (2013) A tomato MADS-box transcription factor, *SlMADS1*, acts as a negative regulator of fruit ripening. Plant Physiol 163:1026–36.

Eduardo I, Arús P, Monforte AJ, et al (2007) Estimating the Genetic Architecture of Fruit Quality Traits in Melon Using a Genomic Library of Near Isogenic Lines. J Amer Soc Hort Sci 132:80–89.

Elitzur T, Yakir E, Quansah L, et al (2016) Banana *MaMADS* Transcription Factors Are Necessary for Fruit Ripening and Molecular Tools to Promote Shelf-Life and Food Security. Plant Physiol 171:380–391.

Ezura H, Owino WO (2008) Melon, an alternative model plant for elucidating fruit ripening. Plant Sci 175:121–129.

FAO (2017) Statistics Division of Food and Agriculture Organization of the United Nations (FAOSTAT). In: http://faostat.fao.org/.

Feder A, Burger J, Gao S, et al (2015) A Kelch Domain-Containing F-Box Coding Gene Negatively Regulates Flavonoid Accumulation in Muskmelon. Plant Physiol 169:1714–1726.

Freilich S, Lev S, Gonda I, et al (2015) Systems approach for exploring the intricate associations between sweetness, color and aroma in melon fruits. BMC Plant Biol 15:71.

Fujisawa M, Nakano T, Shima Y, Ito Y (2013) A Large-Scale Identification of Direct Targets of the Tomato MADS Box Transcription Factor RIPENING INHIBITOR Reveals the Regulation of Fruit Ripening. Plant Cell 25:371–386.

Fujisawa M, Shima Y, Higuchi N, et al (2012) Direct targets of the tomato-ripening regulator RIN identified by transcriptome and chromatin immunoprecipitation analyses. Planta 235:1107–1122.

Galpaz N, Gonda I, Shem-Tov D, et al (2018) Deciphering genetic factors that determine melon fruit-quality traits using RNA-Seq-based high-resolution QTL and eQTL mapping. Plant J 94:169–191.

Gapper NE, McQuinn RP, Giovannoni JJ (2013) Molecular and genetic regulation of fruit ripening. Plant Mol Biol 82:575–91.

Garcia-Mas J, Benjak A, Sanseverino W, et al (2012) The genome of melon (*Cucumis melo* L.). Proc Natl Acad Sci USA 109:11872–7.

Giner A, Pascual L, Bourgeois M, et al (2017) A mutation in the melon Vacuolar Protein Sorting 41 prevents systemic infection of Cucumber mosaic virus. Sci Rep 7:1–12.

Giovannoni J, Nguyen C, Ampofo B, et al (2017) The Epigenome and Transcriptional Dynamics of Fruit Ripening. Annu Rev Plant Biol 68:61–84.

Giovannoni JJ (2007) Fruit ripening mutants yield insights into ripening control. Curr Opin Plant Biol 10:283–289.

González M, Xu M, Esteras C, et al (2011) Towards a TILLING platform for functional genomics in Piel de Sapo melons. BMC Res Notes 4:289. doi: 10.1186/1756-0500-4-289

Goulao LF, Oliveira CM (2008) Cell wall modifications during fruit ripening: when a fruit is not the fruit. Trends Food Sci Technol 19:4–25.

Guo J-E, Hu Z, Zhu M, et al (2017) The tomato histone deacetylase SlHDA1 contributes to the repression of fruit ripening and carotenoid accumulation. Sci Rep 7:7930.

Gur A, Gonda I, Portnoy V, et al (2016) Genomic Aspects of Melon Fruit Quality. In: Genetics and genomics of Cucurbitaceae.

Gur A, Tzuri G, Meir A, et al (2017) Genome-Wide Linkage- Disequilibrium Mapping to the Candidate Gene Level in Melon (*Cucumis melo*). Sci Rep 7:1–13.

Hu Z, Deng G, Mou H, et al (2018) A re-sequencing-based ultra-dense genetic map reveals a gummy stem blight resistance-associated gene in *Cucumis melo*. DNA Res 25:1–10.

Hu ZL, Deng L, Chen XQ, et al (2010) Co-suppression of the EIN2-homology gene *LeEIN2* inhibits fruit ripening and reduces ethylene sensitivity in tomato. Russ J Plant Physiol 57:554–559.

Ito Y, Kitagawa M, Ihashi N, et al (2008) DNA-binding specificity, transcriptional activation potential, and the *rin* mutation effect for the tomato fruit-ripening regulator RIN. Plant J 55:212–223.

Ito Y, Nakano T (2015) Development and regulation of pedicel abscission in tomato. Front Plant Sci 6:1–6.

Ito Y, Nishizawa-yokoi A, Endo M, et al (2017) Re-evaluation of the *rin* mutation and the role of RIN in the induction of tomato ripening. Nat Plants 3:866–874.

Jia HF, Chai YM, Li CL, et al (2011) Abscisic Acid Plays an Important Role in the Regulation of Strawberry Fruit Ripening. Plant Physiol 157:188–199.

Jia H, Wang Y, Sun M, et al (2013) Sucrose functions as a signal involved in the regulation of strawberry fruit development and ripening. New Phytol 453–465.

Ju C, Yoon GM, Shemansky JM, et al (2012) CTR1 phosphorylates the central regulator EIN2 to control ethylene hormone signaling from the ER membrane to the nucleus in *Arabidopsis*. Proc Natl Acad Sci 109:19486–19491.

Karlova R, Rosin FM, Busscher-Lange J, et al (2011) Transcriptome and Metabolite Profiling Show That APETALA2a Is a Major Regulator of Tomato Fruit Ripening. Plant Cell 23:923–941.

Kieber J, Rothenberg M, Roman G, et al (1993) CTR1, a negative regulator of the ethylene response pathway in *Arabidopsis*, encodes a member of the raf family of protein kinases. Cell 72:427–441.

Klee HJ (2010) Improving the flavor of fresh fruits: Genomics, biochemistry, and biotechnology. New Phytol 187:44–56.

Lang Z, Wang Y, Tang K, et al (2017) Critical roles of DNA demethylation in the activation of ripening-induced genes and inhibition of ripening-repressed genes in tomato fruit. Proc Natl Acad Sci USA 114:4511–4519.

Lelievre JM, Latche A, Jones B, et al (1997) Ethylene and fruit ripening. Physiol Plant 101:727–739.

Li C, Jia H, Chai Y, Shen Y (2011) Abscisic acid perception and signaling transduction in strawberry: A model for non-climacteric fruit ripening. Plant Signal Behav 6:1950–1953.

Lin Z, Hong Y, Yin M, et al (2008) A tomato HD-Zip homeobox protein, LeHB-1, plays an important role in floral organogenesis and ripening. Plant J 55:301–310.

Liu D, Wang D, Qin Z, et al (2014) The SEPALLATA MADS-box protein SLMBP21 forms protein complexes with JOINTLESS and MACROCALYX as a transcription activator for development of the tomato flower abscission zone. Plant J 77:284–296.

Liu R, How-kit A, Stammitti L, et al (2015) A DEMETER-like DNA demethylase governs tomato fruit ripening. Proc Natl Acad Sci USA 112:10804–10809.

Manning K, Tör M, Poole M, et al (2006) A naturally occurring epigenetic mutation in a gene encoding an SBP-box transcription factor inhibits tomato fruit ripening. Nat Genet 38:948–952.

Mao L, Begum D, Chuang H, et al (2000) JOINTLESS is a MADS-box gene controlling tomato flower abscission zone development. Nature 406:910–913.

Martel C, Vrebalov J, Tafelmeyer P, Giovannoni JJ (2011) The tomato MADS-box transcription factor RIPENING INHIBITOR interacts with promoters involved in numerous ripening processes in a COLORLESS NONRIPENING-dependent manner. Plant Physiol 157:1568–79.

Matsukura C (2016) Sugar Accumulation in Tomato Fruit and Its Modification Using Molecular Breeding Techniques. In: Functional genomics and biotechnology in Solanaceae and Cucurbitaceae crops. pp 141–154

McMurchie EJ, McGlasson WB, Eaks IL (1972) Treatment of Fruit with Propylene gives Information about the Biogenesis of Ethylene. Nature 237:235–236.

McQuinn RP, Giovannoni JJ, Pogson BJ (2015) More than meets the eye: from carotenoid biosynthesis, to new insights into apocarotenoid signaling. Curr Opin Plant Biol 27:172–179.

Meng C, Yang D, Ma X, et al (2016) Suppression of tomato SlNAC1 transcription factor delays fruit ripening. J Plant Physiol 193:88–96.

Monforte AJ, Oliver M, Gonzalo MJ, et al (2004) Identification of quantitative trait loci involved in fruit quality traits in melon (*Cucumis melo* L.). Theor Appl Genet 108:750–8.

Monforte AJ, Diaz A, Caño-Delgado A, Knaap E Van Der (2014) The genetic basis of fruit morphology in horticultural crops : lessons from tomato and melon. J Exp Bot 65:4625–4637.

Mu Q, Huang Z, Chakrabarti M, Illa-berenguer E (2017) Fruit weight is controlled by *Cell Size Regulator* encoding a novel protein that is expressed in maturing tomato fruits. PLoS Genet 13:e1006930.

Nakano T, Kimbara J, Fujisawa M, et al (2012) MACROCALYX and JOINTLESS Interact in the Transcriptional Regulation of Tomato Fruit Abscission Zone Development. Plant Physiol 158:439–450.

Nimmakayala P, Tomason YR, Abburi VL, et al (2016) Genome-Wide Differentiation of Various Melon Horticultural Groups for Use in GWAS for Fruit Firmness and Construction of a High Resolution Genetic Map. Front Plant Sci 7:1–15.

Obando-Ulloa JM, Moreno E, García-Mas J, et al (2008) Climacteric or non-climacteric behavior in melon fruit 1. Aroma volatiles. Postharvest Biol Technol 49:27–37.

Osorio S, Alba R, Damasceno CMB, et al (2011) Systems biology of tomato fruit development: combined transcript, protein, and metabolite analysis of tomato transcription factor (*nor*, *rin*) and ethylene receptor (*Nr*) mutants reveals novel regulatory interactions. Plant Physiol 157:405–25.

Osorio S, Fernie AR (2014) Fruit Ripening: Primary Metabolism. In: Fruit ripening: physiology, signaling and genomics. pp 15–27

Paris MK, Zalapa JE, McCreight JD, Staub JE (2008) Genetic dissection of fruit quality components in melon (*Cucumis melo* L.) using a RIL population derived from exotic x elite US Western Shipping germplasm. Mol Breed 22:405–419.

Pavan S, Marcotrigiano AR, Ciani E, et al (2017) Genotyping-by-sequencing of a melon (*Cucumis melo* L.) germplasm collection from a secondary center of diversity highlights patterns of genetic variation and genomic features of different gene pools. BMC Genomics 18:1–10.

Pech JC, Bouzayen M, Latché A (2008) Climacteric fruit ripening: Ethylene-dependent and independent regulation of ripening pathways in melon fruit. Plant Sci 175:114–120.

Pech JC, Bouzayen M, Latché A (2014) Cellular, metabolic and molecular aspects of chromoplast differentiation in ripening fruit. In: Fruit ripening: physiology, signaling and genomics. pp 28–47

Pitrat M (2016) Melon Genetic Resources: Phenotypic Diversity and Horticultural Taxonomy. Springer New York, New York, NY, pp 1–36

Pitrat M (2013) Phenotypic diversity in wild and cultivated melons (*Cucumis melo*). Plant Biotechnol 30:273–278.

Qin G, Wang Y, Cao B, et al (2012) Unraveling the regulatory network of the MADS box transcription factor RIN in fruit ripening. Plant J 70:243–55.

Raghavendra AS, Gonugunta VK, Christmann A, Grill E (2010) ABA perception and signalling. Trends Plant Sci 15:395–401.

Renner SS, Schaefer H (2016) Phylogeny and evolution of the *Cucurbitaceae*. In: Genetics and genomics of Cucurbitaceae. pp 17–23

Rios P, Argyris JM, Vegas J, et al (2017) *ETHQV6.3* is involved in melon climacteric fruit ripening and is encoded by a NAC domain transcription factor. Plant J 91:671–683.

Roldan Gomez MV, Périlleux C, Morin H, Huerga- S (2017) Natural and induced loss of function mutations in *SlMBP21* MADS-box gene led to jointless-2 phenotype in tomato. Sci Rep 7:1–10.

Ruggieri V, Alexiou KG, Morata J, et al. An improved assembly and annotation of the melon (Cucumis melo L.) reference genome. (under review in Sci Rep)

Rushton DL, Tripathi P, Rabara RC, et al (2012) WRKY transcription factors: Key components in abscisic acid signalling. Plant Biotechnol J 10:2–11.

Saladié M, Cañizares J, Phillips MA, et al (2015) Comparative transcriptional profiling analysis of developing melon (*Cucumis melo* L.) fruit from climacteric and non-climacteric varieties. BMC Genomics 16:1–20.

Sanseverino W, Hénaff E, Vives C, et al (2015) Transposon Insertions, Structural Variations, and SNPs Contribute to the Evolution of the Melon Genome. Mol Biol Evol 32:2760–2774.

Sebastian P, Schaefer H, Telford IRH, Renner SS (2010) Cucumber (*Cucumis sativus*) and melon (*C. melo*) have numerous wild relatives in Asia and Australia, and the sister species of melon is from Australia. Proc Natl Acad Sci U S A 107:14269–14273.

Seo M, Koshiba T (2002) Complex regulation of ABA biosynthesis in plants. Trends Plant Sci 7:41–48.

Seymour GB, Østergaard L, Chapman NH, et al (2013) Fruit Development and Ripening. Annu Rev Plant Biol 64:219–241.

Seymour GB, Ryder CD, Cevik V, et al (2011) A SEPALLATA gene is involved in the development and ripening of strawberry (*Fragaria* x *ananassa* Duch.) fruit, a non-climacteric tissue. J Exp Bot 62:1179–1188.

Solano R, Stepanova A, Chao Q, Ecker JR (1998) Nuclear events in ethylene signaling a transcriptional cascade mediated by ETHYLENE-INSENSITIVE3 and ETHYLENE-RESPONSE-FACTOR1. Genes Dev 12:3703–3714.

Tadmor Y, Burger J, Yaakov I, et al (2010) Genetics of flavonoid, carotenoid, and chlorophyll pigments in melon fruit rinds. J Agric Food Chem 58:10722–10728.

Tieman DM, Ciardi JA, Taylor MG, Klee HJ (2001) Members of the tomato *LeEIL* (EIN3-like) gene family are functionally redundant and regulate ethylene responses throughout plant development. Plant J 26:47–58.

Till BJ, Colbert T, Tompa R, et al (2003) High-Throughput TILLING for Functional Genomics. In: Grotewold E. (eds) Plant Functional Genomics. Methods in Molecular Biology™, vol 236. Humana Press

Tohge T, Alseekh S, Fernie AR (2014) On the regulation and function of secondary metabolism during fruit development and ripening. J Exp Bot 65:4599–4611.

Tucker ML (2014) Cell-wall metabolism and softening during ripening. In: Fruit ripening: physiology, signaling and genomics. pp 48–62

Tzuri G, Zhou X, Chayut N, et al (2015) A "golden" SNP in *CmOr* governs the fruit flesh color of melon (*Cucumis melo*). Plant J 82:267–279.

Uluisik S, Chapman NH, Smith R, et al (2016) Genetic improvement of tomato by targeted control of fruit softening. Nat Biotechnol 34:950–952.

Vegas J (2014) Estudio genético de la maduración del fruto en melón en la línea isogénica SC3-5-1. Dissertation, Autonomous University of Barcelona

Vrebalov J, Pan IL, Arroyo AJM, et al (2009) Fleshy fruit expansion and ripening are regulated by the Tomato SHATTERPROOF gene *TAGL1*. Plant Cell 21:3041–62.

Vrebalov J, Ruezinsky D, Padmanabhan V, et al (2002) A MADS-box gene necessary for fruit ripening at the tomato ripening-inhibitor (*rin*) locus. Science 296:343–346.

Wang D, Yeats TH, Uluisik S, et al (2018) Fruit Softening: Revisiting the Role of Pectin. Trends Plant Sci 23:302–310.

Wang L, Baldwin EA, Bai J (2016) Recent Advance in Aromatic Volatile Research in Tomato Fruit: The Metabolisms and Regulations. Food Bioprocess Technol 9:203–216. doi: 10.1007/s11947-015-1638-1

Xie Q, Hu Z, Zhu Z, et al (2014) Overexpression of a novel MADS-box gene *SlFYFL* delays senescence, fruit ripening and abscission in tomato. Sci Rep 4:1–10. doi: 10.1038/srep04367

Yano R, Ezura H (2016) Fruit ripening in melon. In: Genetics and genomics of Cucurbitaceae. pp 345–375

Zanor MI, Osorio S, Nunes-Nesi A, et al (2009) RNA Interference of LIN5 in Tomato Confirms Its Role in Controlling Brix Content, Uncovers the Influence of Sugars on the Levels of Fruit Hormones, and Demonstrates the Importance of Sucrose Cleavage for Normal Fruit Development and Fertility. Plant Physiol 150:1204–1218.

Zhang B, Chen K-S (2014) Aroma volatiles. In: Fruit ripening: physiology, signaling and genomics. pp 63–80

Zhong S, Fei Z, Chen Y, et al (2013) Single-base resolution methylomes of tomato fruit development reveal epigenome modifications associated with ripening. Nat Biotechnol 31:154–159.

Zhu M, Chen G, Zhou S, et al (2014) A New Tomato NAC (NAM/ATAF1/2/CUC2) Transcription Factor, SlNAC4, Functions as a Positive Regulator of Fruit Ripening and Carotenoid Accumulation. Plant Cell Physiol 55:119–35.

Objectives

The main objective of this PhD thesis is to study the genetic basis of fruit quality in melon, focusing on the ripening behaviour. To achieve this goal, three specific objectives were proposed:

1. QTL mapping of fruit quality traits in a "Védrantais" x "Piel de Sapo" RIL population using a high-density GBS-based genetic map.

2. Genetic dissection of climacteric ripening in melon.

    a. Development of a non-invasive method to measure ethylene production in attached fruits.
    b. QTL mapping of ethylene production and ripening-associated traits using the "Védrantais" x "Piel de Sapo" RIL population.
    c. Fine mapping of the QTL *ETHQB3.5* controlling climacteric ripening in the introgression line 8M35.

3. Development of two reciprocal introgression line collections using the climacteric "Védrantais" and the non-climacteric "Piel de Sapo" varieties.

Chapter 1

QTL mapping of melon fruit quality traits using a high-density GBS-based genetic map

QTL mapping of melon fruit quality traits using a high-density GBS-based genetic map

Pereira, L.[1], Ruggieri, V.[1,2], Pérez, S.[1], Alexiou, K. G.[1,2], Fernández, M.[3], Jahrmann, T.[3], Pujol, M.[1,2] and Garcia-Mas, J.[1,2*]

[1]Centre for Research in Agricultural Genomics (CRAG) CSIC-IRTA-UAB-UB, Campus UAB, Bellaterra, Barcelona, Spain

[2]IRTA (Institut de Recerca i Tecnologia Agroalimentàries), Barcelona, Spain

[3]Semillas Fitó S.A., Cabrera de Mar, Barcelona, Spain

[*]Corresponding author: Jordi Garcia-Mas, jordi.garcia@irta.cat, IRTA, Centre for Research in Agricultural Genomics CSIC-IRTA-UAB-UB, Edifici CRAG, Campus UAB, 08193 Cerdanyola, Barcelona, Spain. Phone: +34 935636600.

ORCID numbers: JGM (0000-0001-7101-9049); LP (0000-0001-5184-8587); MP (0000-0002-3595-5363); VR (0000-0001-6038-8703)

Submitted to BMC Plant Biology

Abstract

Melon shows a broad diversity in fruit morphology and quality, which is still underexploited in breeding programs. The knowledge of the genetic basis of fruit quality traits is important for identifying new alleles that may be introduced in elite material. In order to identify QTLs controlling fruit quality, a recombinant inbred line population was developed using as parental lines two commercial cultivars: "Védrantais", from the *cantalupensis* group, and "Piel de Sapo", from the *inodorus* group. Both types show desirable quality traits for the market, but their fruits differ in several traits such as rind and flesh color, sugar content, size and shape. We used a genotyping-by-sequencing strategy to construct a dense genetic map, which included around five thousand variants distributed in 824 bins. The RIL population was phenotyped for several quality and morphology traits, and we mapped 33 stable QTLs involved in sugar and carotenoid content, fruit and seed morphology and major genes controlling external color of immature fruit and mottled rind. The median confidence interval of the QTLs was 942 kb, suggesting that the high density of the genetic map helped in increasing the mapping resolution. Some of these intervals contained less than a hundred annotated genes, and an integrative strategy combining gene expression and resequencing data enabled to identify candidate genes for some of these traits.

Key message

Several QTLs controlling fruit quality traits in melon have been identified and delimited to narrow genomic intervals, using a RIL population and a GBS-based genetic map.

Keywords: Quantitative Trait Loci; Melon; Fruit quality; Fruit morphology; Genotyping-By-Sequencing; Genetic map

Introduction

Melon (*Cucumis melo* L.) is an important vegetable crop worldwide, with a production of more than 31 million tons in 2016 (FAO, 2017). The main producers are located in temperate regions, with China reaching around 50% of total production. Although until the last decade the origin of melon was placed in Africa, recent phylogenetic studies suggested that the species originated in Asia [2]. Traditionally, two subspecies have been described: *C. melo* ssp. *melo*, including most of the commercial varieties in European markets belonging to *cantalupensis* and *inodorus* botanical groups; and *C. melo* ssp. *agrestis*, which contains the major part of the Asian exotic landraces and accessions [3]. A high phenotypic and genetic variability is found between and within melon subspecies for diverse traits, including plant architecture, sex determination, yield and fruit characteristics [3]. Several mapping populations have been used to study this diversity, as F_2 [4,5], introgression lines (IL) [6,7] and recombinant inbred lines (RIL) [8–10]. Generally, the crosses used to develop these mapping populations have been obtained between exotic (*chinensis*, *conomon*, *makuwa* or *flexuosus* groups) and cultivated (*cantalupensis*, *reticulatus* or *inodorus* groups) melon types. To our knowledge, the variability between two commercial varieties that belong to different botanical groups has not been exploited yet through linkage mapping studies. Association studies using accession panels is another approach that has shown recently its potential to characterize important agronomic traits in melon [11,12].

In addition to the above-mentioned genetic tools, diverse genomic resources have been developed in melon during the past years. Melon is a diploid species with a small genome (450 Mb) and 12 chromosomes (2n = 24). The availability of a reference genome [13] and the fast advance in Next-Generation Sequencing (NGS) technologies have facilitated the use of genomic resources in order to better understand fruit morphology and quality, as RNA-seq [9] and Genotyping-By-Sequencing (GBS) [11,14,15]. GBS strategy is based on the reduction of genome complexity before sequencing, performed generally through restriction enzyme digestion; only a low percentage of the genome is sequenced but the fragments are normally well distributed across the genome [16]. Currently, the GBS approach has been widely used in many species [17–20] due to its simplicity, effectiveness and low-cost when compared to other high-throughput genotyping techniques. The availability of unlimited number of SNPs has increased the precision of Quantitative Trait Loci (QTL) mapping. Linkage maps have shown their effectiveness as

a tool to study the genetic architecture of both monogenic and complex traits [21]. Recently, high-density maps using hundreds [22] to thousands of markers [10,14,15] have been constructed for QTL mapping of fruit traits. It has been proven that a higher SNP density increases substantially the QTL mapping potential, affecting both the detection and the resolution of QTLs [10,15].

One of the most important aspects to the market is fruit quality. Fruits from the *cantalupensis* group are usually defined by medium fruit weight with round shape, climacteric ripening, orange flesh and white, ribbed and netted rind. In contrast, *inodorus* melons are characterized by non-climacteric ripening, high sugar content, generally big size and elliptical shape, green, mottled and smooth rind without ribs nor vein tracts [23]. Several bi-parental mapping and association analysis have been performed for most of these traits, which were integrated and reviewed by [21]. Some of these traits seem to be under monogenic or oligogenic control [24], as flesh and rind color, sutures and ribs. However, the most relevant traits related to fruit quality, as sugar content, fruit size and shape and climacteric ripening are complex and polygenic [10,25–27]. Extensive work has been done to dissect the genetic control of these traits, but generally using crosses between exotic and cultivated material types. Even they are very valuable, the introduction of exotic alleles in breeding programs is complicated due to linkage drag, which implies a high cost in removing undesired regions [28]. However, the variation between phylogenetically close commercial cultivars, but phenotypically different, has not been exploited before and can offer new tools easily implemented in breeding programs. The aim of this study was to identify QTLs and major genes related with fruit quality in narrow genomic intervals, using a high-density genetic map obtained using a RIL population from a *cantalupensis* x *inodorus* cross.

Materials and methods

Plant material

A RIL population was generated from two commercial varieties, “Védrantais” (Ved) (ssp. *melo*, *cantalupensis* group) and “Piel de Sapo” accession T111 (PS) (ssp. *melo*, *inodorus* group). Ved is a French variety from the group *cantalupensis* that produces medium-size fruits, rounded, the external color is white when immature and cream after ripening and

with orange flesh. PS is a Spanish variety from the group *inodorus* that presents large-size fruits, elongated and mottled, with dark green rind and white flesh. Both varieties show high soluble solid content since they are accepted in European markets.

The RIL population was developed at Cabrera de Mar (Barcelona) and Caldes de Montbui (Barcelona) in greenhouses through a strategy of single seed descent until F7-F8, starting from an F2 population obtained in 2008. The population was composed by 89 RILs, including 82 and 7 RILs in the F8 and F7 generations, respectively. A set of 48 polymorphic SNPs evenly distributed through the melon genome was used to confirm the homozygosity of the RILs, which was higher than 98% (not shown).

The RIL population was grown in Caldes de Montbui (Barcelona) under greenhouse conditions during the summers of 2015 (three blocks T1-T3) and 2016 (two blocks T4-T5). Plants were pruned weekly and each plant was allowed to set only a single fruit. Each block (T1-T5) contained a single individual per RIL and 1-3 individuals of the parental lines (Ved, PS) and the F1 (Hyb). Flowers were hand-pollinated and the date was recorded to register the total days of development of the fruit until harvest. According to the type of ripening of each RIL, the harvest date was recorded as follows: (1) the abscission date for climacteric fruits showing abscission, (2) seven days after the first symptom of climacteric ripening (aroma production, chlorophyll degradation or abscission layer formation) for climacteric fruits that did not show abscission and (3) 60 days after pollination for non-climacteric fruits.

Blocks T1-T3 (2015) were grown during the same season but each block separated by three weeks. Blocks T4-T5 (2016) were grown together. A mean of 8.6 lines per block were not evaluated due to problems related to seed germination, plant disease or fruit set; 60 out of 89 RILs (67%) were evaluated in the five blocks.

Phenotyping of fruit and seed traits

Fruit quality traits (Table 1.1) were recorded during the development of the fruit and at harvest. Mottled rind (MOT) and external color of immature fruit (ECOL) were phenotyped as qualitative traits, before the ripening onset, around 20-30 days after pollination (DAP). Data for these traits were merged by year, due to the low variability observed among blocks (>95% of the RILs showed the same phenotype across blocks).

After harvest, the fruit was weighted and cut in two longitudinal sections: the first one was scanned to perform the morphological analysis using the Tomato Analyzer 3.0 software [29,30] and the second section was used to measure SSC and total carotenoids (CAR). The morphology traits recorded were fruit weight (FW), diameter (FD), length (FL) and perimeter (FP) with the Tomato Analyzer 3.0 software and shape index (FS) was calculated as the ratio between FL and FD. To measure soluble solid content (SSC), four flesh samples of 1 cm diameter per melon were used; the juice was extracted and analyzed with a digital hand refractometer (Atago Co. Ltd., Tokyo, Japan). Total carotenoids analysis was performed by UV-VIS Spectroscopy [31] as described by [32], using the flesh from the first three blocks (T1-T3). The yellowing of mature rind (YELL) was recorded as a qualitative trait by visual inspection of ripe fruits. Fifteen dried seeds were used to estimate seed weight (SW) and seed number (SN) per fruit.

Table 1.1. Traits evaluated in the Ved x PS RIL population.

Trait	**Code**
Soluble solid content	SSC
Fruit weight	FW
Fruit diameter	FD
Fruit shape	FS
Fruit length	FL
Fruit perimeter	FP
Yellowing of mature rind	YELL
Mottled rind	MOT
External color of immature fruit	ECOL
Total carotenoid content	CAR
Seed weight	SW
Seed number	SN

Genotyping and linkage map construction

Young leaves from the RIL population and the parental lines Ved and PS were collected during the summer of 2015 and stored at -80°C. DNA extraction was performed following the CTAB protocol [33] with some modifications. Briefly, the isopropanol precipitation was followed by an incubation of 30 min at 4ºC and by a spinning of 10 min after adding the washing buffer. The extracted DNA was re-suspended in MilliQ water and PicoGreen

and electrophoresis in agarose gels were used to estimate the DNA concentration and quality.

GBS was performed at CNAG (Barcelona, Spain). *Ape*KI GBS libraries of the 89 RIL and the parental lines (PS and Ved) were prepared at CNAG and sequenced using Illumina HiSeq2000 (2 x 100 bp).

The Fast-GBS pipeline [34] and the melon v3.6.1 genome assembly (http://www.melonomics.net) were used for the identification of the variants (SNPs and INDELs). Fast-GBS uses the MEM (maximal exact matches) algorithm implemented in BWA to perform alignment of the reads and relies on the Platypus software [35] to perform the variant calling. The parameters applied were the following: minimum number of reads (NR) per locus (default = 2), mapping quality score of reads to call a variant (MQ ≥ 20), minimum base quality (20), multiple nucleotide polymorphisms (MNPs) distance (minFlank = 5), and maximum missing data (MaxMD) allowed (default ≤ 80%). As a preliminary check, the row data were cross-checked with a set of variants identified after the whole genome re-sequencing of the two parental lines PS and Ved [36] and the overlapping variants (SNPs and INDELs) were retained (pre-filtered variants) and used in the downstream analyses. Then, Vcftools [37] and in-house scripts were subsequently applied to retain only bi-allelic variants with a Minor Allele Count greater than 1, with at least one homozygous variant for marker, with a global quality greater than 100 and with missing values (MV) ≤ 60%. In addition, sparse heterozygous variants with a genotype depth (GDP) lower than 5 were converted to missing values.

Once variants were obtained and filtered, a chromosome-by-chromosome manual inspection was performed and variants showing highly distorted segregation and discrepancies with the genotyping of the parental lines were discarded. This final set of variants was used to define the bins. A bin was established as a group of variants with the same genotype for each RIL, meaning a region without any recombination breakpoint in any individual of the population. A single variant showing the minor number of missing data was selected to represent each bin. If missing data were present in this variant, they were imputed manually recovering the genotyping information from the other variants in the same bin. Finally, only bins with less than 30% of missing data were considered valid to generate the genetic map. Bins evidencing a discrepancy between genetic and physical maps but showing a proper segregation and reliable quality were included in the genetic map construction.

The genetic linkage map was constructed using the online software tool MSTmap [38]. Linkage groups (LG) were formed at minimum LOD=10 and we allowed the software to detect genotyping errors. Mapping size threshold was set to 2 and the distance threshold to 15 cM. The genetic distances were estimated using the Kosambi mapping function [39]. The graphical representation of the genetic map was obtained using MapChart version 2.2 [40].

QTL mapping

For quantitative traits we were aware that the environmental effects have usually a considerable influence in the phenotype. To test if the quantitative data of the blocks from the same year could be merged, creating only one dataset per year, we performed a Principal Component Analysis (PCA) (Figure 1.1a). We could not identify a pattern that distinguished the blocks according to the year, actually T1 and T5 were very similar even though they belong to different years. Considering these results, we decided to analyze the data using two different ways: one including the mean for each line after merging data from the five blocks, and another one including the individual data for each block.

The QTL mapping was performed with MapQTL6 [41] considering each block (T1-T5) and the mean across the blocks. We used the interval mapping procedure for all traits and for the monogenic or oligogenic traits, we performed a Kruskal-Wallis (KW) test. QTLs that appeared in the mapping experiment performed with the mean values with LOD>2.5 were considered significant. To evaluate their significance in the individual blocks we checked if they were located in the same position and with the same sign (positive or negative) of additive effect.

To code the identified QTL, we adopted the same terminology system described in [21], where the first letters represent the trait abbreviation, followed by a “Q” that stands for QTL, a letter to name the mapping experiment (“U”, in this case), a digit designating the linkage group (LG) to which the QTL maps, a dot and a final number to differentiate several QTL on the same LG.

Statistical analyses

All the statistical analyses and graphical representations were performed using the software R v3.2.3 [42] with the RStudio v1.0.143 interface [43].

The normality of distributions was tested using the Shapiro-Wilk test, assuming that the distribution was significantly different from a normal distribution when p-value<0.05.

The PCA was performed using R package "factoextra" with data from a random subset of 22 RILs from which we had no missing values in any block and a representative subset of 7 quantitative variables (SSC, FW, FL, FD, FS, SN and SW). We removed the effect of the line to observe only the effect of the block (environment) before the PCA, using the function "removeBatchEffect" from the R package "limma".

To obtain the correlation matrix among traits we calculated the Pearson coefficient with the R package "Hmisc" and the visualization of data was performed with "corrplot".

Results

Phenotyping of the RIL population

The RIL population and the parental lines were evaluated during the summers of 2015 (blocks T1-T3) and 2016 (blocks T4-T5). Several interesting traits related with fruit quality and morphology were segregating in the population (Table 1.1). Some of these traits were considered as qualitative (Table 1.2), although some variation in intensity could be observed for MOT, ECOL and YELL. These traits were evaluated for their segregation ratio in the RIL population (Table 1.2). A segregation of 1:1, expected for a monogenic trait, was observed for ECOL, where the white color of Ved was dominant over green color. For MOT, the segregation showed a deviation from the 1:1 expected for a monogenic trait, and the mottled pattern of PS was dominant over its absence. For YELL, a segregation of 3:1 (yellow: not yellow) was observed, in accordance with a dominant epistasis system, where the yellowing allele was dominant over its absence.

The phenotypic values for the quantitative traits are shown in Table 1.3. In each block, we included the parental lines (Ved, PS) and the Hyb as controls. As an example, fruit weight is lower and quite stable in Ved (771± 156 g) when compared to PS and Hyb (1,311 ± 428 and 1,148 ± 387 g, respectively), where some individuals weighted more than double than Ved but showing a higher dispersion (Figure 1.1b). The dispersion can be observed when looking at the standard deviation, which is high in complex traits with low heritability (e.g. SSC, FW) and low in more stable traits (e.g. FS) (Table 1.3 and Figure 1.S1). Transgressive segregation was observed for all traits analyzed.

The distribution of the data for each trait and block was represented with beanplots (Figure 1.1c and Figure 1.S2). The distribution was normal in all blocks for SSC, FL and FS but for FW, FD, FP, SW and SN at least one block was significantly deviated from a normal distribution. CAR was not normally distributed in any of the three blocks analyzed, presenting a higher density in high-carotenoid values (>5 µg/g FW).

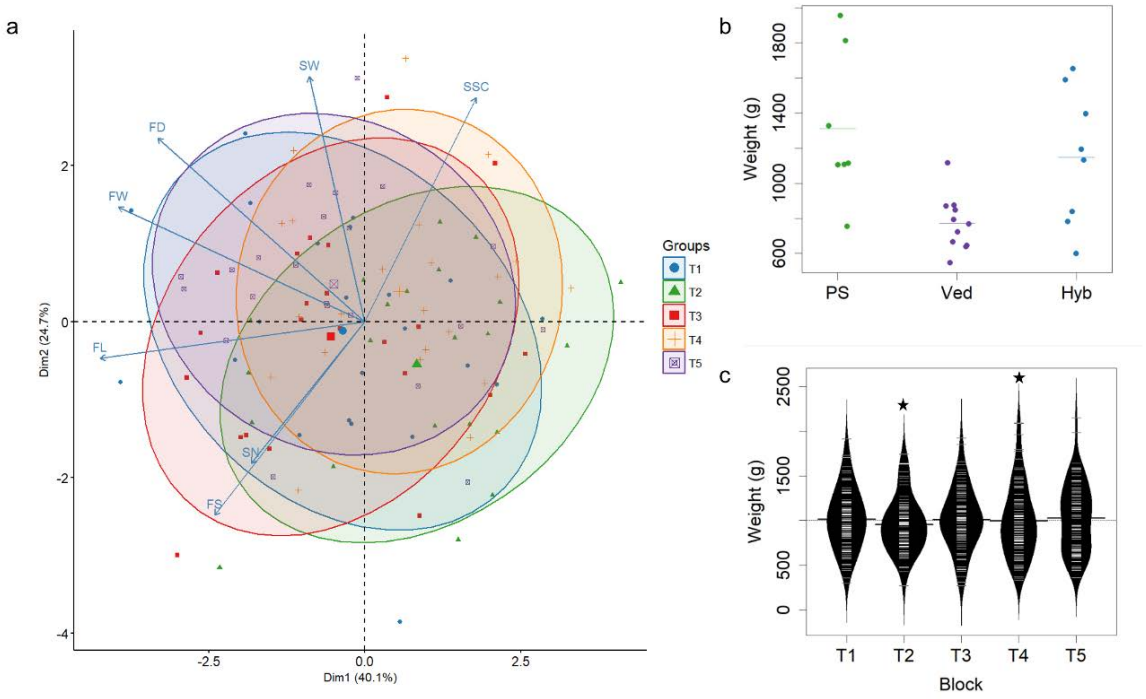

Figure 1.1. Phenotypic data in the RIL population and the parental lines. **a.** PCA showing the similarities between blocks T1 to T5. **b.** Distribution of fruit weight in the parental lines, merging data from all blocks. Each dot corresponds to an observation in any of the five blocks T1-T5. The mean for each line is displayed with a horizontal line. **c.** Distribution of fruit weight in the RIL population in each block T1-T5; black stars indicate significant deviations from normality.

Table 1.2. Mapping of qualitative traits in the Ved x PS RIL population.

Trait	PS	Ved	Hyb	Expected segregation	χ^2	Map position (cM)	Interval[1]	Gene (ref.)
External color of immature fruit (ECOL)	Green	White	White	1:1	1.39 ns	39.8	chr07_2707033-chr07_4345823	*Wi* [44]
Mottled rind (MOT)	Yes	No	Yes	1:1	6.22 *	127.7	chr02_26206397-end of chr02	*Mt-2* [45]
Yellowing of mature rind (YELL)	Yes	No	Yes	3:1	1.38 ns	34.1	chr10_3152004-chr10_4144573	*CmKFB* [46]
						125.1	chr05_28951742-chr05_29246933	This work

[1]According to version v3.6.1 of melon reference genome

Table 1.3. Mean and standard deviation of the parental lines and mean and range in the RIL population for each quantitative trait.

		Parental lines			**RIL population**	
Class	**Trait (unit)**	PS	Ved	Hyb	Mean	Range
Fruit quality	SSC (°Brix)	11.8 ± 1.3	10.7 ± 0.8	10.6 ± 1.7	10.4	5.6 - 14.0
Fruit morphology	Weight (FW) (g)	1311 ± 428	771 ± 156	1148 ± 387	994	345 - 1763
	Diameter (FD) (cm)	13.0 ± 1.3	11.7 ± 0.6	12.8 ± 1.3	12.0	8.3 - 14.8
	Shape (FS)	1.36 ± 0.21	1.02 ± 0.22	1.07 ± 0.06	1.2	0.9 - 1.6
	Length (FL) (cm)	17.8 ± 3.5	12.0 ± 2.8	13.8 ± 2.1	14.0	9.5 - 19.3
	Perimeter (FP) (cm)	51.5 ± 7.3	39.8 ± 4.9	45.1 ± 5.9	44.0	30.7 - 53.6
Flesh color	Carotenoid content (CAR) (µg/gFW)[1]	0.7 ± 0.2	18.4 ± 5.6	10.9 ± 1.4	8.8	0.4 - 30.6
Seed morphology	Seed weight (SW) (mg)	31 ± 4	30 ± 3	37 ± 9	32	18 - 45
	Seed number (SN)	249 ± 114	324 ± 108	408 ± 194	293	67 - 499

[1]Only blocks T1, T2 and T3 were analyzed.

The correlations between traits are presented in Figure 1.2. There was a clear relationship within morphometric measurements. As expected, correlation between fruit dimensions (FL, FD and FP) and FW was strong and positive. The correlation between FS and FL was higher than with FD, implying that the length is the major determinant of fruit shape in this population. A positive correlation was detected between seed (SN, SW) and some fruit morphometric traits (FP, FW, FD). ECOL correlated negatively with CAR and positively with FL, FP, FW and FD. YELL was negatively correlated with SSC.

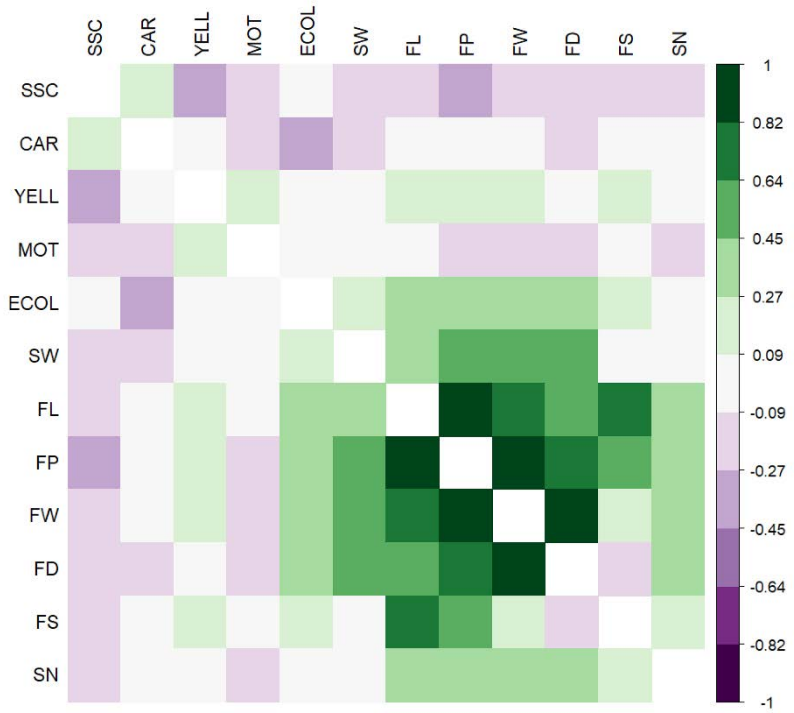

Figure 1.2. Correlation matrix between the measured traits. The scale represent the values of Pearson coefficient between the traits using the mean value across the blocks for each variable.

Construction of a genetic linkage map through Genotyping-By-Sequencing

Sequencing of 91 GBS libraries for the 89 RILs and the two parental lines yielded about 230 million raw reads, corresponding to an average of 2.5 million reads/sample. About 86% of the reads were successfully mapped onto the melon genome (version 3.6.1). A total of 125,465 raw GBS-polymorphisms were called with Fast-GBS. However, about 80% of them were removed due to a disagreement when compared to the variants coming from the published re-sequencing data of Ved and PS [36]. The remaining 24,988 pre-filtered variants were further reduced by applying additional filtering criteria (see Material and Methods). In particular, about 50% of the variants were filtered out due to

the stringent missing value threshold imposed (MV ≤ 60 %) and about 20% due to the other criteria imposed (at least one homozygous variant for marker, global quality >100, only bi-allelic variants). Among the 5,944 variants retained, 9.8% were INDEL and 90.2% were SNPs, supported by a medium coverage of 17.89. More transition-type SNPs (63.9%) were observed than transversion-type SNPs (36.1%) with a transition/ transversion (Ts/Tv) SNP ratio of 1.77. An average of 492 variants per chromosome was detected and chromosome six harbored the highest number (Table 1.4). A high correlation was observed between the number of variants per chromosome and their physical size. This highlighted that the variants were well distributed and covered quite uniformly all the chromosomes. The distribution of the markers along the 12 melon chromosomes and the unassembled scaffolds (chromosome 0) is reported in Table 1.S1a. Then, a further manual refinement of the marker dataset was carried out to ensure a high reliability for the genetic map construction and the QTL mapping analysis, discarding a total of 1,056 markers (Table 1.S1b and Table 1.4). The 4,888 retained GBS-markers were used to build individual bins (Table 1.S1c). Excluding the bins differing only because of the presence of heterozygous variants, we obtained a total of 824 GBS-derived bins that were used to build the genetic linkage map.

The genetic distance, the covered physical distance and the recombination rate of the genetic map are presented in Table 1.4. The map covered 1,519.4 cM, distributed in 13 linkage groups (LG) (Figure 1.3). Two of them belong to chromosome XI, which was split in two linkage groups LG XIa and LG XIb. The largest LG is LG IV, with 156.9 cM, and the smallest one, LG X, with 103.2 cM. In terms of physical distance, we calculated the covered region for each chromosome as the difference between the physical positions of the last and the first markers in the LG. The map covered 97% of the melon genome. LG I is the most covered with 98.97% of physical sequence covered by markers and the least covered is LG X, with only 87.72% of the sequence represented in the genetic map.

We included in the genetic map nine bins that mapped to chromosome 0, which may help in anchoring some additional scaffolds to pseudomolecules. These bins belong to LG I, LG II, LG III, LG V, LG VIII, LG IX and LG XII. We also detected a few inconsistencies between the physical and the genetic map: three bins from chromosomes 2 and 7 according to their physical position were inserted in LG X (not shown).

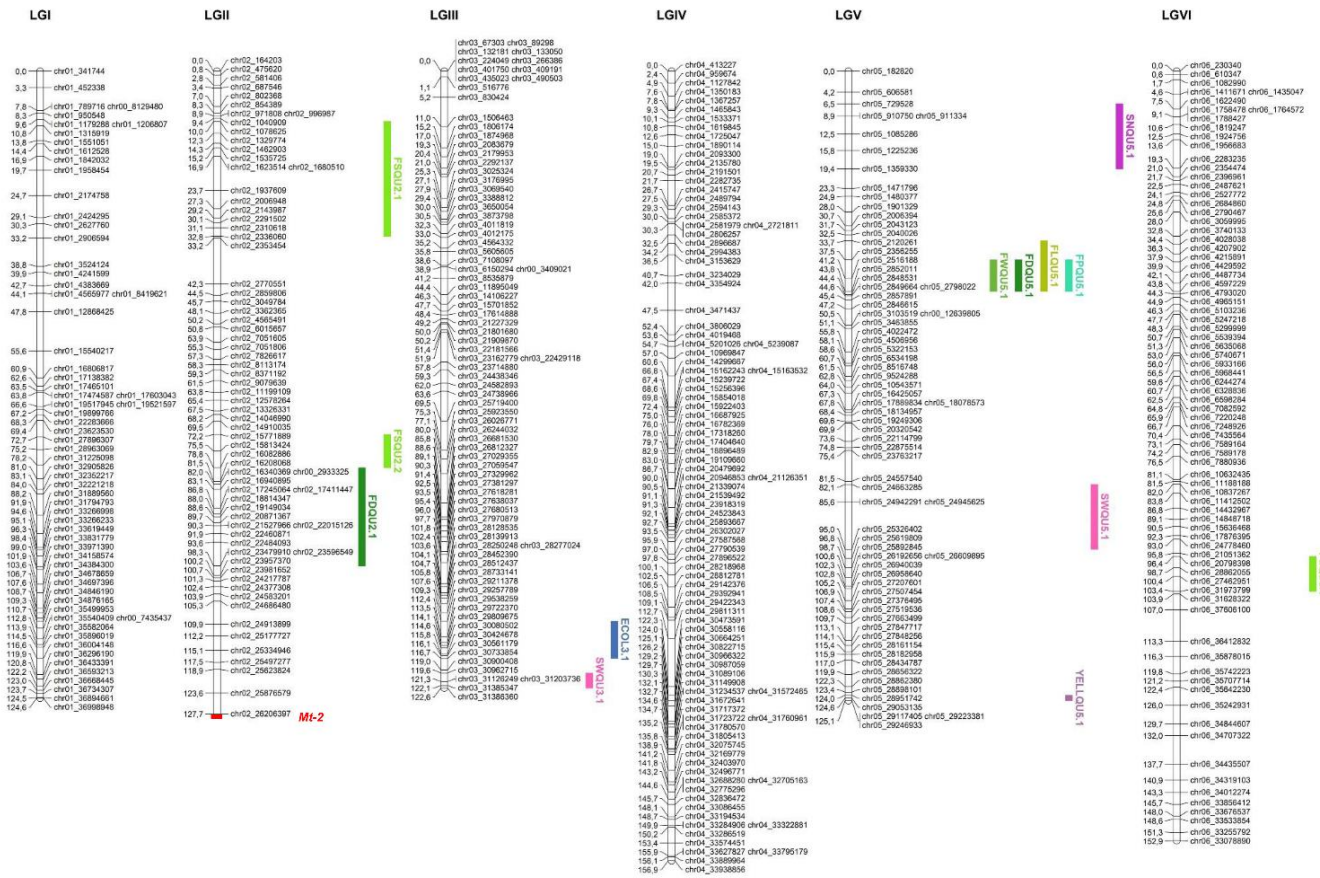

Figure 1.3. Genetic map containing detected QTLs and major genes. Major genes *Mt-2* (MOT) and *Wi* (ECOL) are placed in their physical position, indicated with a red line. Cloned genes *CmOr* and *CmKFB* are placed in their physical position, indicated with a black line. QTLs are represented as colored bars, using a 1-LOD confidence interval. Green tones for morphological QTLs (FP, FW, FS, FL and FD), pink tones for seed traits (SN and SW), dark blue for ECOL, light blue for SSC, red for CAR and purple for YELL.

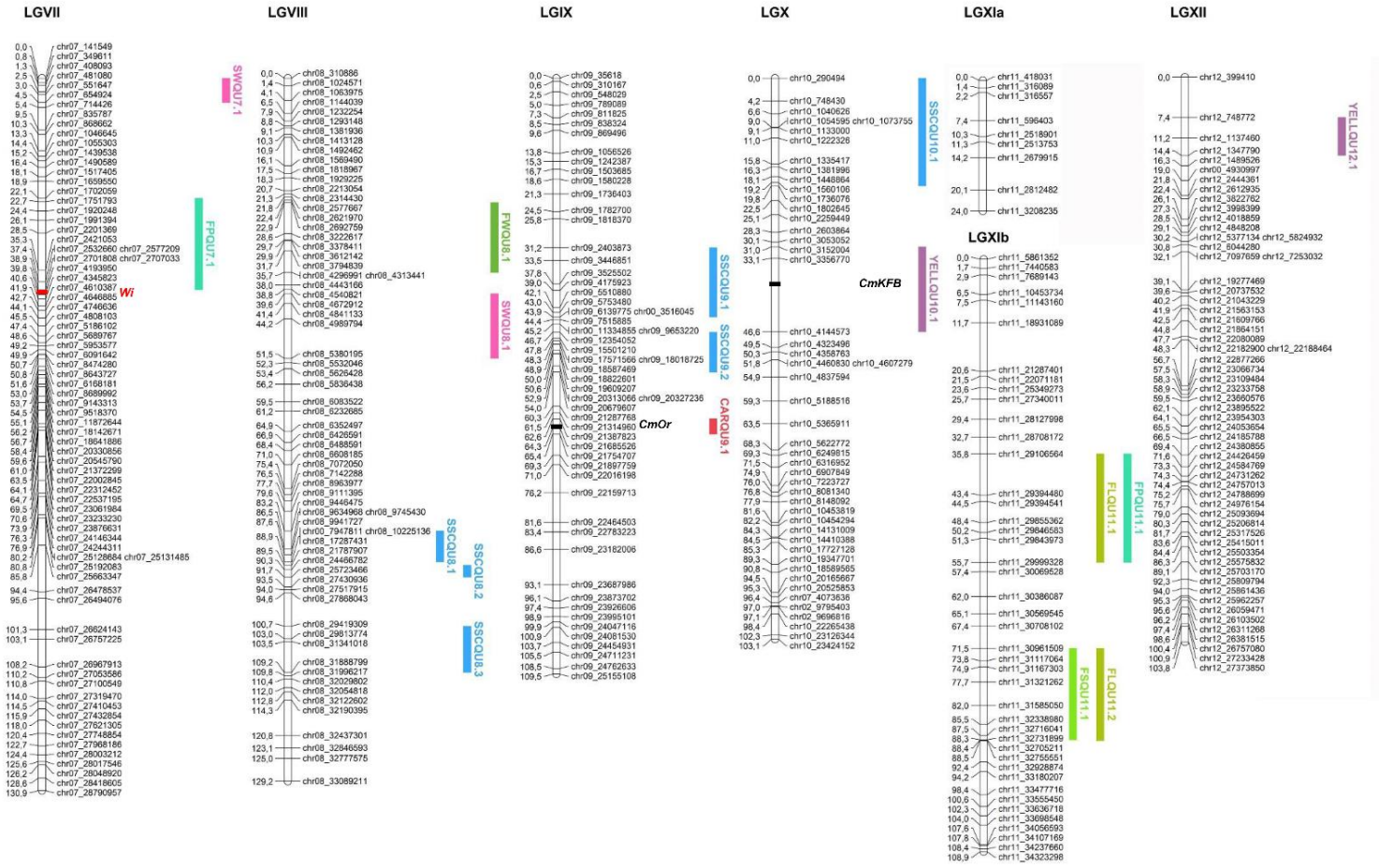

Figure 1.3. Genetic map containing detected QTLs and major genes (continued).

Table 1.4. Variants from the SNP calling and characteristics of the genetic map by chromosome

	Number of variants								
Chr[1]	**Raw data**	**Pre-filtered**	**Filtered**	**Genetic map**	**Nº bins**	**Genetic distance (cM)**	**Total physical distance (bp)[3]**	**Covered physical distance (bp)[4]**	**Recombination rate (cM/Mb)**
1	6,584	2,087	417	360	63	124.6	37,037,532	36,657,204	3.40
2	9,643	2,511	616	510	71	127.7	27,064,691	26,042,194	4.90
3	12,136	2,663	622	508	81	122.6	31,666,927	31,095,866	3.94
4	15,054	2,122	534	440	97	156.9	34,318,044	33,448,353	4.69
5	9,007	1,754	466	365	70	125.1	29,324,171	28,833,706	4.34
6	9,067	2,575	638	501	79	152.9	38,297,372	37,423,280	4.09
7	13,792	2,062	539	460	78	130.9	28,958,359	28,560,617	4.58
8	8,242	2,281	519	400	67	129.2	34,765,488	32,947,662	3.92
9	6,157	1,716	419	369	54	109.5	25,243,276	24,844,222	4.41
10	10,363	1,776	383	319	45	103.2	26,663,822	23,388,534	4.41
11	14,194	1,801	380	326	52	24 + 109[2]	34,457,057	33,905,267	3.92
12	11,226	1,640	360	310	58	103.8	27,563,660	26,974,440	3.85
0	-	-	51	20	9	-	-	-	-
Total	125,465	24,988	5,944	4,888	824	1,519.4	375,360,399	367,540,170	-

[1]Melon chromosome
[2]Chromosome XI is divided in two linkage groups
[3]Version 3.6.1 of the melon genome.
[4]Substraction between the first and the last positions covered by markers in the genetic map

Mapping of major genes and QTLs

Qualitative traits

For two of the three qualitative traits studied in our RIL population, MOT and ECOL, we detected one major gene controlling the phenotype in LGs II and VII, respectively. In the case of YELL, two minor QTLs in addition to a major gene were also observed. In Figure 4, we show the phenotypical differences between the two categorical classes for each trait and the association between the markers and the phenotype using the non-parametric KW test. In all cases, we also performed the interval mapping to confirm that the results were consistent using both methodologies.

According to the segregation data, ECOL showed a monogenic inheritance. This hypothesis was confirmed with the mapping experiments. The gene conferring the external color of immature fruit was located in LG VII, with a KW value of 81.02 at the position chr07_4193950 (Figure 1.4a). In the interval mapping, a major QTL with maximum LOD of 72.80 at 39.8 cM in LG VII, corresponding to the same physical position than KW, explained 97.7% of the variance and was delimited in a region of 1.6 Mb (Table 1.2). We detected a second QTL *ECOLQU3.1* with significant LOD score at 113.4 cM in LG III (Table 1.5), with an additive effect of 0.2 (greener skin when Ved allele was present); this QTL can also be observed in Figure 1.4a, although with a minor KW value.

The evaluation of MOT was difficult in some fruits. The allele that confers the mottled rind is from PS, but it is not easily detected due to the dark green color of the PS rind, which masks the darker spots (Figure 1.S3a). By contrast, the presence of dark spots in melons with white rind color is very striking (Figure 1.4b). Although the segregation was not following the expected 1:1 ratio for a monogenic trait (Table 1.2), the KW test and the interval mapping showed clearly a major gene in the distal part of LG II (Figure 1.4b). In fact, after analyzing the segregation of the markers in this region of the genetic map, we observed a segregation distortion ($\chi^2 = 6.40$ in the closest marker). The major gene is located at the end of the LG, being chr02_26206397 the last marker of the linkage group and the most associated to the phenotype, and showing a LOD=63.90 in the interval mapping. In the melon genome there is a region of approximately 0.8 Mb distal to chr02_26206397, not covered by markers in the genetic map, which was considered in the QTL interval (Table 1.2).

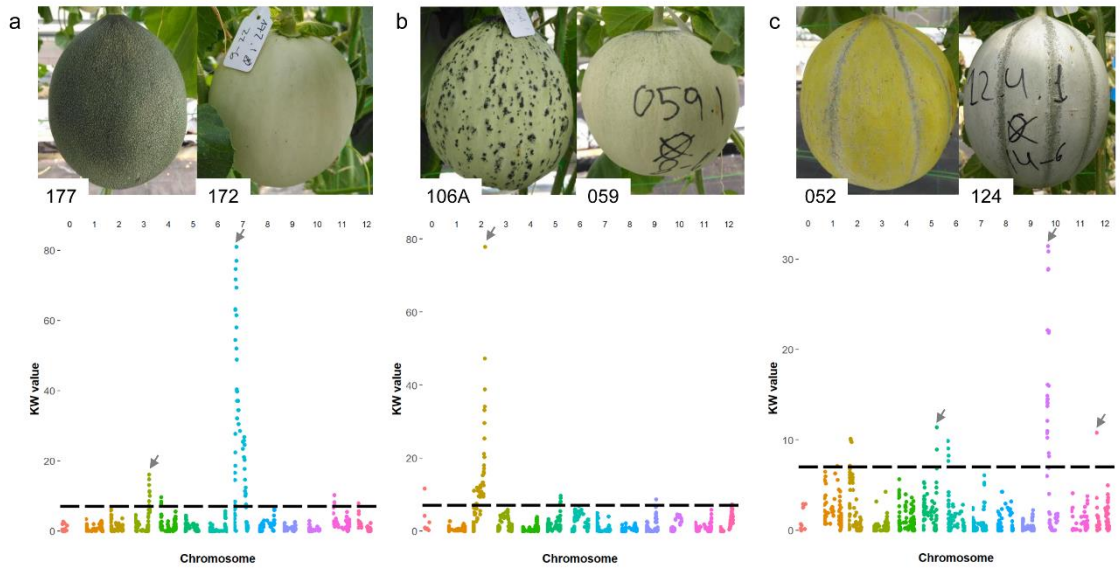

Figure 1.4. Kruskal-Wallis (KW) statistic test (significant threshold for $p < 0,01$) and pictures of fruits showing the two observed phenotypes for ECOL, MOT and YELL. Grey arrows indicate the most significant values. Chromosomes (0 to 12 from left to right) are represented with different colors. **a.** External color of immature fruit (ECOL) (RIL 177 green and RIL 172 white). **b.** Mottled rind (MOT) (RIL 106A presence and RIL 059 absence). **c.** Yellowing of mature rind (YELL) (RIL 052 presence and RIL 124 absence).

Another qualitative trait evaluated was the yellowing of mature rind (YELL). As the mottled rind, the yellow allele comes from PS and is partially masked by the dark green rind color, but a different tonality, leading to a greyish color, can be appreciated when the yellow allele is absent (Figure 1.S3b). The observed segregation suggested the hypothesis of two genes under dominant epistasis. The first and most important gene is located in LG X, in a region of approximately 1 Mb (Table 1.2 and Table 1.5) and was detected in the KW test (Figure 1.4c) and in the interval mapping with a LOD=8.79. Other two QTLs were detected: *YELLQU5.1* in LG V, explaining 15.1% of the variance with the Ved allele decreasing the yellow color; and the second one *YELLQU12.1* in LG XII, explaining 14.2% of the variance with the Ved allele increasing the yellow color. Both QTLs can also be observed in Figure 1.4a, although with minor KW values.

Quantitative traits

The QTL mapping was performed using the mean of five blocks and using each block individually (T1-T5) (Table 1.5, Figure 1.3). A QTL was considered significant with a LOD score higher than 2.5 in the mapping analysis that considered the mean phenotypic values. We also presented the LOD for the same QTL/position in the individual blocks. Thirty-three significant QTLs were detected for the 11 measured traits. The level of

consistency between blocks was different depending on the trait and the significance of the QTL. Although some QTLs seemed to be dependent on the year, for example *YELLQU12.1*, which presented higher LOD scores in both 2016 blocks than in the three 2015 blocks, this effect was not general.

Fruit quality traits

We evaluated SSC, an important trait concerning fruit quality in melon. Both parental lines are commercial types and the SSC is acceptable, but in PS is slightly higher than in Ved. In our evaluations, it ranges from 10.5 to 13.1 °Brix in PS and from 9.9 to 11.5 °Brix in Ved. The hybrid is similar to Ved (Table 1.3 and Figure 1.S1).

Six significant QTLs were detected for SSC (Table 1.5). Among them, *SSCQU8.3* was the most consistent, showing a LOD score above 3.5 in all the experiments; it explained 42.7% of the variance and the Ved allele presented reduced 1.3 °Brix. The QTL is located in LG VIII around 102.66 cM, in an interval of 2.5 Mb.

Although SSC content is higher in PS than in Ved, in three out of six QTLs the Ved allele had a positive effect, explaining the transgressive segregation observed in the RIL population. The percentage of the variance explained by each of them was around 13% and the additive effect of the Ved allele was 0.7 ºBrix.

Fruit morphology traits

We evaluated five traits related with fruit morphology: weight, diameter, shape, length and perimeter. In total, we detected 17 QTLs; some of them were exclusive for one trait (e.g. *FSQU2.1*) and others co-localized for several morphological traits (e.g. *FWQU5.1*, *FDQU5.1*, *FLQU5.1* and *FPQU5.1*) (Figure 1.3 and Table 1.5).

The most significant QTL for FW was *FWQU5.1* in LG V, explaining 28.3% of the variance; the allele of Ved increased fruit weight in 153.27 g. It was detected in the mean analysis with a LOD score of 6.42 and in T1 and T4 with LOD≥3. A QTL in the same interval was also detected with high LOD scores for FD, FL and FP, indicating an important effect in fruit size in this region. The best resolution for this QTL was obtained for *FWQU5.1*, *FDQU5.1* and *FPQU5.1*, which delimited it to a 500-kb interval.

FLQU6.1 in position 100.4 cM of LG VI, presented a LOD score of 5.78 in the mean analysis and it was significant in all blocks (T1-T5). It explained 25.9% of the variance

and the Ved allele decreased 1.1 cm the length of the fruit. The QTL was located in an interval of 10.6 Mb in the centromeric region of the chromosome.

Concerning FS, we described five QTLs and in all cases, the Ved allele decreased the shape index to produce rounder fruits. A QTL co-localizing with *FLQU6.1*, *FSQU6.1*, was the most significant and consistent. *FSQU2.1*, in a region of approximately 1.3 Mb in LG II, did not co-localize with any other morphological trait-associated QTL.

Flesh color traits

Although the gene determining orange flesh color, *CmOr*, was already described by [47], we decided to measure total carotenoids content in flesh of ripe fruit. We observed a transgressive segregation (Table 1.3), finding almost double of total carotenoids than the mean of Ved in some RILs. The QTL mapping revealed just one major QTL in LG IX with a LOD=16.82 explaining 58% of the variance (*CARQU9.1*, Figure 1.3). We did not detect any other minor QTL for this trait.

Seed traits

Although the mean values for the parental lines were similar, we detected four significant QTLs for seed weight (Table 1.5 and Figure 1.3). None of the QTLs for seed weight co-localized with fruit morphology QTLs. The most significant was *SWQU8.1*, with a LOD score of 4.29 and explaining 19.9% of the variance in the RIL population. The allele of Ved diminished the weight of seeds. *SWQU8.1* was located in a region of 636 kb. A single QTL *SNQU5.1* for seed number was detected in LG V, but with a lower LOD score.

Table 1.5. QTL analysis for the traits evaluated. QTLs with LOD > 2.5 using the mean of five blocks (maximum LOD in each block T1-T5 is also annotated)

QTL ID	LOD	R^2	Additive effect[1]	Chr	Genetic position (cM)	Physical position[2] (pb)	Flanking marker 1 respect 1-LOD CI	Flanking marker 2 respect to 1-LOD CI	LOD T1[3]	LOD T2[3]	LOD T3[3]	LOD T4[3]	LOD T5[3]
SSCQU8.1	9.96	40.3	-1.26	8	86.49	9,634,968	chr08_9446475	chr08_17287431	**6.3**	**8.0**	2.7	**5.8**	**4.4**
SSCQU8.2	9.83	39.9	-1.27	8	90.28	2,446,682	chr08_21787907	chr08_25723466	**5.7**	**8.9**	**3.0**	**5.9**	**4.7**
SSCQU8.3	10.76	42.7	-1.3	8	102.66	29,813,774	chr08_29419309	chr08_31888799	**8.2**	**6.2**	**3.8**	**6.9**	**5.9**
SSCQU9.1	2.78	13.4	0.711	9	33.49	3,446,851	chr09_2403873	chr09_6139775	1.6	**4.1**	1.4	2.7	2.5
SSCQU9.2	2.57	12.5	0.69	9	49.89	18,822,601	chr09_12354052	chr09_20679607	0.8	**4.6**	1.5	2.5	2.7
SSCQU10.1	3.3	15.7	0.77	10	18.06	1,448,864	chr10_290494	chr10_1736076	1.5	2.8	1.5	2.6	2.6
FWQU5.1	6.42	28.3	153.27	5	40.51	2,516,188	chr05_2356255	chr05_2852011	6.7	2.1	2.3	**3.0**	2.2
FWQU8.1	2.51	12.2	-92.38	8	31.73	3,794,839	chr08_2692759	chr08_4296991	0.8	0.3	1.7	2.5	2.8
FDQU2.1	3.29	15.6	0.47	2	88.58	19,149,034	chr02_16082886	chr02_23479910	1.4	1.4	1.7	**3.2**	2.4
FDQU5.1	4.92	22.5	0.6	5	41.22	2,516,188	chr05_2356255	chr05_2852011	**5.5**	1.8	2.3	2.0	1.5
FSQU2.1	2.96	14.2	-0.061	2	30.07	2,291,502	chr02_1078625	chr02_2336060	2.6	**3.0**	2.4	**3.6**	0.1
FSQU2.2	3.18	15.2	-0.064	2	75.52	15,813,424	chr02_15771889	chr02_16082886	**4.5**	2.0	0.3	1.5	1.4
FSQU6.1	7.7	32.9	-0.092	6	99.72	27,462,954	chr06_20798398	chr06_31973799	**4.1**	**4.9**	**6.9**	2.5	**5.7**
FSQU6.2	6.96	30.2	-0.087	6	106.99	37,606,100	chr06_31628322	chr06_36412832	**4.3**	**5.0**	**5.6**	2.9	**3.4**
FSQU11.1	3.34	15.9	-0.064	11b	81.68	31,585,050	chr11_30961509	chr11_32731899	2.1	2.8	**4.8**	2.1	1.1
FLQU5.1	5.29	24	1.16	5	40.51	2,516,188	chr05_2120261	chr05_2852011	**5.1**	2.3	2.0	**3.8**	2.9

FLQU6.1	5.78	25.9	-1.1	6	100.43	27,462,951	chr06_21051362	chr06_31628322	**3.2**	**4.5**	**3.8**	2.5	**4.6**
FLQU11.1	3.79	17.8	-0.96	11b	47.46	29,855,362	chr11_29106564	chr11_29999328	**3.7**	2.5	1.7	**3.1**	1.8
FLQU11.2	2.67	12.9	-0.81	11b	80.68	31,585,050	chr11_30961509	chr11_32755551	**4.7**	2.8	**4.4**	0.6	0.2
FPQU5.1	6.73	29.4	2.95	5	40.51	2,516,188	chr05_2356255	chr05_2852011	**7.7**	2.8	2.6	**3.2**	2.5
FPQU6.1	2.75	13.3	-1.81	6	100.43	27,462,951	chr06_11412502	chr06_36412832	1.5	**3.2**	1.6	1.7	2.0
FPQU7.1	2.54	12.3	-1.83	7	29.47	2,201,369	chr07_1702059	chr07_2701808	1.0	1.8	1.1	2.4	1.7
FPQU11.1	3.27	15.6	-2.03	11b	42.79	29,394,480	chr11_29106564	chr11_29999328	**3.5**	2.7	1.1	**3.0**	1.1
YELLQU5.1	3.15	15.1	-0.15	5	125.12	29,117,405	chr05_28951742	chr05_29246933	**3.8**	2.8	1.4	2.5	1.9
YELLQU10.1	8.79	36.6	-0.25	10	34.07	3,356,770	chr10_3152004	chr10_4144573	**8.1**	**5.9**	**4.2**	**6.6**	**6.7**
YELLQU12.1	2.96	14.2	0.15	12	11.21	1,137,460	chr12_748772	chr12_1347790	1.7	1.6	1.4	2.8	2.4
ECOLQU3.1	3.49	16.5	0.21	3	113.40	29,722,370	chr03_29257789	chr03_30733854		**3.5**[4]		**3.0**[4]	
CARQU9.1	16.82	58.5	5.6	9	64.32	21,685,526	chr09_21387823	chr09_21754707	**12.7**	**11.6**	**13.6**	-	-
SNQU5.1	2.73	13.2	33.43	5	14.46	1,225,236	chr05_729528	chr05_1359330	2.1	0.5	0.3	2.1	0.4
SWQU3.1	4.11	19.2	2.7	3	122.11	31,385,347	chr03_30962715	chr03_31386360	2.4	1.6	0.3	2.7	1.7
SWQU5.1	4.3	19.9	2.9	5	87.63	24,945,625	chr05_24663285	chr05_25326402	**3.0**	2.6	**3.2**	2.4	1.2
SWQU7.1	2.91	14.0	-2.2	7	0.78	349,611	chr07_141549	chr07_654924	0.9	1.4	1.5	0.9	2.0
SWQU8.1	4.29	19.9	-2.7	8	43.35	4,989,794	chr08_4672912	chr08_5308195	0.9	**6.9**	1.9	**3.1**	1.2

[1]Additive effect of the Ved allele.
[2]Physical position is relative to the melon genome sequence v3.6.1.
[3]Bold and highlight font for LOD scores above 3, highlight font for LOD scores between 2.5-3
[4]LOD scores for 2015 and 2016, respectively.

Discussion

The GBS approach applied in a biparental RIL population is highly effective for QTL mapping studies

Understanding the genetic control of important agronomic traits has been a challenge during the last decades. Different strategies have shown their effectiveness, being the most used the QTL mapping approach. Type and size of the population and map density are the main limiting factors that determine the detection of QTLs and their resolution. RIL populations present some advantages: the lines are fixed, so multiple evaluations in different years or environments are possible; each individual has potentially suffered multiple recombination events, increasing the mapping resolution; and the development of this type of population is simple and of low cost using a single-seed descent method without need of intermediate genotyping [48].

Until recently, the main limiting factor, in terms of work and cost, was marker discovery and genotyping. The first genetic maps used during the eighties and nineties included generally from tens to a few hundreds of markers, mainly including isoenzymes and RFLPs [49–51]. Due to the fast development of sequencing technologies and bioinformatics, genotyping is becoming more and more affordable and accessible to the scientific community. A reference genome sequence has already been published for many important crops, as maize [52], rice [53] and tomato [54], among others, facilitating the use of high-throughput genotyping methods based on NGS. The GBS strategy is by far the most widespread technique for high-throughput genotyping, allowing performing simultaneously the variant calling and the genotyping for thousands of SNPs and INDELs, and without the need of a reference genome. In melon, GBS was recently used to characterize collections of accessions [11,14,55] and biparental populations [14,15]. The number of variants we obtained (24,988 SNPs and INDELs) was comparable to those obtained in these previous studies, ranging from 13,756 to 99,263. Such a divergence in the number of variants is expected depending on different factors such as the diverse origin of the material, the sequencing technology used, the software chosen for the variant calling and the different filtering criteria applied. Also the possibility to impute or not the missing values could greatly affect the final size of the variants. Concerning the number of bins found in our Ved x PS linkage map (824), it was lower than in previous studies, 1,837 [14] and 2,493 [15]. This discrepancy was expected since in those studies the

founding cross for the RIL population was between *C. melo* spp. *melo* and a *C. melo* ssp. *agrestis* accessions, which represent wider diversity in comparison to our population.

Although many QTL mapping studies performed using less dense linkage maps have confirmed their effectivity, increasing the number of markers allows to fully exploiting the recombination events in the population, improving the resolution of the QTLs. In a RIL population, where multiple meiosis could derive in short bins, this effect could increase notably not only the resolution but also the power of detection, especially for minor QTLs [15]. The power of detection is not comparable among different populations, but the resolution in our QTL mapping had a median QTL confidence interval of 9.42 cM and 0.94 Mb in genetic and physical distances, respectively. These results are comparable with the 4.04 cM and 0.93 Mb obtained in [15] and more precise than in other recent studies performed using less dense maps, where the QTL genetic confidence interval ranged between 23 cM [5] and 28.6 cM [4].

To validate our QTL mapping results, we used as a proof of concept two fruit quality traits that are segregating in our population whose subjacent genes are already known, *CmOr* [47] and *CmKFB* [46] (Table 1.S2). *CmOr* is determining the orange flesh in ripe melon when the dominant allele is present, due to the high synthesis of β-carotene. We mapped a major QTL for CAR, *CARQU9.1*, at position 21,685,526 in chromosome IX, in a confidence interval of 366.8 Kb containing 47 genes according to the annotation version v4.0 of the melon genome [56] (Table 1.6). To observe the expression pattern of the candidate genes in this interval we used the atlas expression database Melonet-DB [57], developed using 30 different tissues from the *cantalupensis* variety "Harukei-3". We could reduce the number of candidate genes to 19 that were expressed in fruit flesh from 20 to 50 DAP, and only three of them presented sequence differences between Ved and PS causing a non-synonymous amino acid change. *CmOr* was included in this final group, and the maximum LOD position of the QTL was inside this gene (*MELO3C005449*, coordinates 21,683,406-21,690,712). *CmKFB* controls the biosynthesis of flavonoids in ripe melon rind, conferring the yellow external color typical of "Canary yellow" melons. We detected a major QTL for this trait in our RIL population, *YELLQU10.1*, at position 3,356,770 in chromosome X. The confidence interval of 992 Kb contained 156 genes (Table 1.6), of which 33 presented variations in our population causing a non-synonymous amino acid change. *CmKFB* was among them and the maximum LOD position was located approximately 100 kb upstream of this gene

(*MELO3C011980*, coordinates 3,475,283-3,476,416). Gene expression was not inspected in Melonet-DB in this case due to the absence of the dominant yellowing phenotype in the variety "Harukei-3", suggesting a lack of gene expression.

Table 1.6. Genomic intervals containing the identified QTLs for each trait and number of annotated genes in each interval.

Trait	Gene/QTL ID	QTL interval (cM)	QTL interval (pb)	Number of annotated genes[1]
SSC	*SSCQU8.1*	5.64	7,840,956	389
	SSCQU8.2	2.23	3,935,559	195
	SSCQU8.3	8.55	2,469,490	123
	SSCQU9.1	12.68	3,735,902	290
	SSCQU9.2	7.36	8,325,555	525
	SSCQU10.1	19.75	1,445,582	231
FW	*FWQU5.1*	6.28	495,756	48
	FWQU8.1	12.76	1,604,232	220
FD	*FDQU2.1*	19.51	7,397,024	501
	FDQU5.1	6.28	495,756	48
FS	*FSQU2.1*	22.77	1,257,435	136
	FSQU2.2	6.55	310,997	34
	FSQU6.1	6.98	11,175,401	545
	FSQU6.2	9.34	4,784,510	432
	FSQU11.1	16.77	1,770,390	221
FL	*FLQU5.1*	10.10	731,750	82
	FLQU6.1	8.11	10,576,960	505
	FLQU11.1	19.96	892,764	108
	FLQU11.2	16.99	1,794,042	224
FP	*FPQU5.1*	6.28	495,756	48
	FPQU6.1	29.43	25,000,330[1]	1444
	FPQU7.1	16.80	999,749	149
	FPQU11.1	19.96	892,764	108
YELL	*YELLQU5.1*	1.11	295,191	54

	YELLQU10.1 (*CmKFB*)	15.61	992,569	156
	YELLQU12.1	7.00	599,018	65
MOT	*Mt-2*	-	858,294	139
ECOL	*ECOLQU3.1*	7.37	1,476,065	238
	Wi	-	308,385+271,774[2]	41+19
CAR	*CARQU9.1* (*CmOr*)	2.77	366,884	47
SN	*SNQU5.1*	12.92	629,802	76
SW	*SWQU3.1*	2.99	423,645	73
	SWQU5.1	12.96	663,117	85
	SWQU7.1	4.48	513,375	90
	SWQU8.1	11.92	635,283	94
Median		9.42	942,667	130

[1]Annotation version v4.0 of the melon genome (http://www.melonomics.net)

[2]An inconsistency between the physical and the genetic map exists in this region.

Deciphering the genetic architecture of fruit quality and domestication traits in melon

Deciphering the genetic control of important traits in crops is one of the main objectives of modern research in agriculture. The knowledge of the responsible genes would offer the opportunity of exploring the functional mechanisms that control phenotypes, allowing to search and study the allelic diversity of cultivars and accessions and ultimately modifying crop behaviour. As a first step, our work has identified major genes and QTLs involved in important traits in melon.

Rind traits

External color of fruit is an important trait concerning fruit quality, since the appearance is one of the main determinants for consumer's choice in the market. The phenotype varies depending on the developmental stage and is settled mainly by the accumulation of different pigments as chlorophylls, carotenoids and flavonoids [58]. In our RIL population, at least two major traits are controlling rind color: ECOL, conferring white or green rind in immature fruit, and YELL, determining the yellowing of mature rind, probably involving biosynthesis of flavonoids.

The external color of immature fruit was previously described by [44] as a monogenic trait named *Wi*, but to our knowledge it has not been mapped. More recently, four loci involved in ECOL were identified in LGs III, VII, IX and X using two mapping populations derived from PS and PI 161375, suggesting an epistatic interaction between at least some of them [59]. Our RIL population shares one parental (PS) with this study, and *ECOLQU3.1* and *Wi* map in the same chromosomes as *ECOLQC3.5* and *ECOLQC7.2* [58], respectively, however their physical positions do not co-locate (Table 1.S2). This trait has been characterized in cucumber, leading to identify a candidate gene, a *two-component Response Regulator-like Protein* (*APRR2*) [60,61]. We could not find any *RRP* gene in the confidence interval containing *Wi*, however there is an inconsistency in the genome assembly in this region that could affect this result (Table 1.6). *ECOLQU3.1*, having a minor effect in comparison to *Wi*, could modify slightly the external color by affecting the same pathway or by another mechanism.

The yellowing of mature rind was described before, identifying the flavonoid naringenin chalcone as the principal pigment responsible for the yellow color in some melon cultivars as "Noy Amid" [57]. Lately, a Kelch domain-containing F-Box protein coding gene (*CmKFB*) was cloned by [46], showing that this transcription factor is the main regulator of the flavonoid biosynthetic pathway. In addition to naringenin chalcone, other downstream flavonoids were identified in yellow melon rinds. In other species, the complex of MYB-bHLH-WDR transcription factors has been shown to control flavonoid production [62,63]. The major QTL *YELLQU10.1* interval contains the gene *CmKFB*, as explained above. According to the observed segregation 3:1 for this trait (Table 1.2), *YELLQU5.1* could act epistatically with *CmKFB*, regulating the biosynthesis of naringenin chalcone or other flavonoids. Following this hypothesis, the yellow rind phenotype in our RIL population could be determined by PS alleles in any of the two genes. Inside the *YELLQU5.1* interval, which contains 54 annotated genes, we identified *MELO3C004621*, which is described as a "Ectonucleotide pyrophosphatase/ phosphodiesterase" and is implicated in the flavonoid pathway; additionally, this gene is highly expressed in fruit rind during the last steps of development in Melonet-DB [57] and is carrying a variant that produced an amino acid change in the protein. However, further experiments are necessary to demonstrate the identity of *YELLQU5.1*.

The presence or absence of a mottled pattern also influences the rind appearance; this trait (*Mt-2*) is controlled by a major gene in LG II previously described by [64] and [45],

probably the same one that has been mapped in our population (Figure 1.4b). Although this pattern can be observed also in other cucurbits, both the genetic control and the physiological mechanism remain unknown. We could hypothesize that the spots correspond to areas of the rind where the chlorophyll content is higher, due to an increased number and/or activity of chloroplasts. This hypothesis is supported by the observation of more intense yellow color in spots of mature rinds, when the allele for yellowing is present. *Mt-2* is located in an interval of 858 kb that contains 139 annotated genes, without any candidate gene by functional annotation.

The rind color of fruits in our RIL population should be determined by these three traits and modified by other important aspects of fruit development, such as the type of fruit ripening (climacteric or non-climacteric), where chlorophyll degradation can be involved [65].

Soluble solid content

Melon fruit is mainly consumed as a dessert, being a high content of sugars a desired characteristic with special importance in crop improvement. Ved and PS are both commercial varieties from the European market, with medium-high soluble solid content, so we did not expect to find major QTLs for this trait (Table 1.3).

Three QTLs were found in LG VIII with LOD > 9, between the physical positions 9,446,475 and 31,888,799 bp, explaining around 40% of the variance and the Ved allele decreasing 1.3 ºBrix. We detected three clear peaks even increasing the confidence interval of these QTLs (Figure 1.S4), but it could still be possible that there is a single QTL in this region and the low-LOD regions inside the interval were artefactual. The higher LOD value corresponds to *SSCQU8.3*, delimited in a region of 2.5 Mb that contains 123 genes (Table 1.6). In other studies, QTLs for SSC were also detected in LG VIII (Table 1.S2); [66] found two introgression lines (ILs) in the PS background containing introgressions from the exotic accession PI 161375 that covered the major part of chromosome VIII, including *SSCQU8.3*, with a significant different SSC content.

Other three QTLs were detected in LG IX and LG X, *SCCQU9.1*, *SSCQU9.2* and *SSCQU10.1*. Although having a lower effect in SSC, they are interesting because in all cases the Ved allele is increasing sugar content. However, they are unstable, showing significant LOD scores only in T2, T4 and T5. QTLs for SSC in LGs IX and X were previously described in similar positions to *SSCQU9.2* and *SSCQU10.1* (Table 1.S2).

Fruit morphology

Fruit morphology, including weight, size, length, diameter and shape, are key traits in the domestication process, enabling to discriminate between cultivated and wild accessions. According to their importance, they have been extensively studied in many species, especially in tomato, where several genes have been cloned (reviewed in [26]). The two principal genes involved in fruit size are *Cell Number Regulator*, *SlKLUH*, a cytochrome P450 A78 class, and *Cell Size Regulator* [67]. Fruit shape is mainly determined by the combination of different alleles of *FAS*, from the YABBY family; *SUN*, an IQ domain member; *LC*, a member of the WOX family, and *OVATE*. In melon, a sort of different populations have been used to perform QTL mapping studies that allowed to identify meta-QTLs implicated in fruit morphology [4,59,68]; unfortunately, none of the genes responsible for these QTLs have been cloned. All the QTLs described in the present work are supported by previous works that identified QTLs in the same LGs (Table 1.S2), except *FPQU7.1*. Although the physical positions associated to the QTLs are not always similar, it should be considered that only one marker was used to calculate the position of several QTLs described in Table 1.S2, which usually span the major part of the LG. For example, *SC5-2* was described by [7] using an introgression line that covers almost all LG V (0-20,855,850 bp).

A clear transgressive segregation was obtained for fruit weight, from a mean of 345 g in RIL 172 to 1,763 in RIL 140 (Figure 1.S5). Consistently, a QTL explaining 28.3% of the variation, *FWQU5.1*, increased the weight when the Ved allele was present. A QTL in the same chromosome was previously described using populations developed from a cross between PS and the exotic Korean accession PI 161375 (Table 1.S2). The 496-kb interval of *FWQU5.1* contains 48 genes, and among them only 23 were expressed following the expected pattern for fruit size regulators (ovary and young fruit) using the atlas expression database Melonet-DB [57]. Five of these genes carried variants in the sequence provoking a non-synonymous change between Ved and PS. One of these genes is *MELO3C014402*, described as FANTASTIC FOUR 2 in the annotation v4.0. These proteins are usually related with meristem development [69] and *Cell Size Regulator*, the gene underlying a recently cloned fruit weight QTL in tomato, contains a FANTASTIC FOUR domain [67].

FLQU6.1 and *FSQU6.1* are located in the same region in the centromere of chromosome VI, implying that the decrease in length caused by the Ved allele provokes a decrease in

the shape index. They are co-localizing with a QTL published recently for the same traits [68], which was mapped in an F2 population between PS and the Indian wild accession "Trigonus", and validated using introgression lines. In this case, the PS allele is also increasing fruit length and the percentage of variance explained is similar, around 20%. The segregation of this QTL in commercial varieties suggests that is not a domestication QTL but a diversification one, according to classical definitions.

Possibly, orthologs of the genes that regulate fruit size and shape in tomato could be implicated in the same process in melon, and thus be candidate genes underlying the detected QTLs. In order to evaluate whether they co-localize within the QTL intervals, we identified the potential fruit morphology orthologs in the melon genome (version 3.6.1 and annotation v4.0) (Table 1.S3a), which resulted in the identification of 89 genes. Twelve of them are contained in the intervals of *FSQU2.1*, *FDQU2.1*, *FSQU6.1*, *FSQU6.2*, *FWQU8.1* and *FSQU11.1* (Table 1.S3b). Among them, there are four genes (*MELO3C015418*, *MELO3C025343*, *MELO3C013751*, *MELO3C022253*) that showed the expected pattern of expression, being specific of ovaries and young fruit, according to the melon expression atlas [57]. In addition, *MELO3C015418* and *MELO3C025343* carried one and two non-synonymous polymorphisms between the parental lines, so they could be the candidate genes for *FSQU2.1* and *FDQU2.1*, respectively. Additional studies, as QTL fine mapping and differential expression analysis between Ved and PS, should be performed to confirm their involvement in fruit morphology.

Seed traits

Seeds are the most valuable part of the fruit in terms of evolution, so both seed weight and number are important fitness traits. Although this trait has been widely studied in crops in which grain is consumed, as rice [70–74] and soybean [75,76], in vegetable crops much less is known. Although seed is not consumed in many vegetable crops, it is the product that seed companies are commercializing. A higher seed production and better seed quality are interesting traits for both breeders and farmers.

In melon, seed size is considered a domestication trait, since wild accessions have smaller seeds than cultivated melons [3]. The genetic basis of this trait has not been well studied; a recent QTL mapping study, focused on domestication traits, evaluated seed weight, without the identification of any QTL [68], suggesting that a complex inheritance involving several minor QTLs could be the reason.

Surprisingly, in our RIL population, which is founded by two close commercial cultivars, we could identify four QTLs for seed weight. SW was positively correlated with FP, FW and FD, but SW QTLs did not co-localize with fruit morphology QTLs (Figure 1.2 and 1.3). Due to the high stability of the trait (Figure 1.S1), we could map these QTLs in narrow regions of the genome, spanning between 423 and 663 kb, containing in all cases less than 100 genes. The stability of seed size has been studied before in multiple crops, showing that this trait presented a low dispersion even in different environmental conditions, unlike seed number, which is a very plastic trait [77].

The QTL mapping performed using the RIL population Ved x PS has identified several QTLs and major genes that modify and modulate fruit quality, from the external appearance to the biochemical composition. The location of these QTLs in narrow genomic intervals could facilitate the cloning of the underlying genes and their use in breeding programs by marker-assisted selection. The introgression of favorable alleles into breeding lines could be performed easily, since the mapping population was developed from commercial cultivars, avoiding the negative consequences associated to linkage drag when using exotic material as donors. The reduced number of annotated genes in some of these intervals has allowed to propose potential candidate genes through an integrative strategy that included the analysis of gene expression and the predicted effect of variants using genomics databases.

Acknowledgements

We thank Pere Arús for helpful suggestions in the genetic map construction. This work was supported by the Spanish Ministry of Economy and Competitiveness grant AGL2015-64625-C2-1-R, Severo Ochoa Programme for Centres of Excellence in R&D 2016-2010 (SEV-2015-0533) and the CERCA Programme/Generalitat de Catalunya to JGM. LP was supported by a FPI grant from the Spanish Ministry of Economy and Competitiveness. VR was supported by the European Union's Horizon 2020 research and innovation programme under Marie Skłodowska-Curie grant agreement No 6655919.

Author Contributions

LP, MF and TJ obtained the RIL population. LP cultivated and phenotyped the RIL population with the contribution of SP. VR and KGA analyzed the GBS data. LP constructed the genetic map and performed the QTL analyses. MP and JGM conceived, designed and coordinated the study. LP, VR, MP and JGM drafted the manuscript.

Supplementary Material

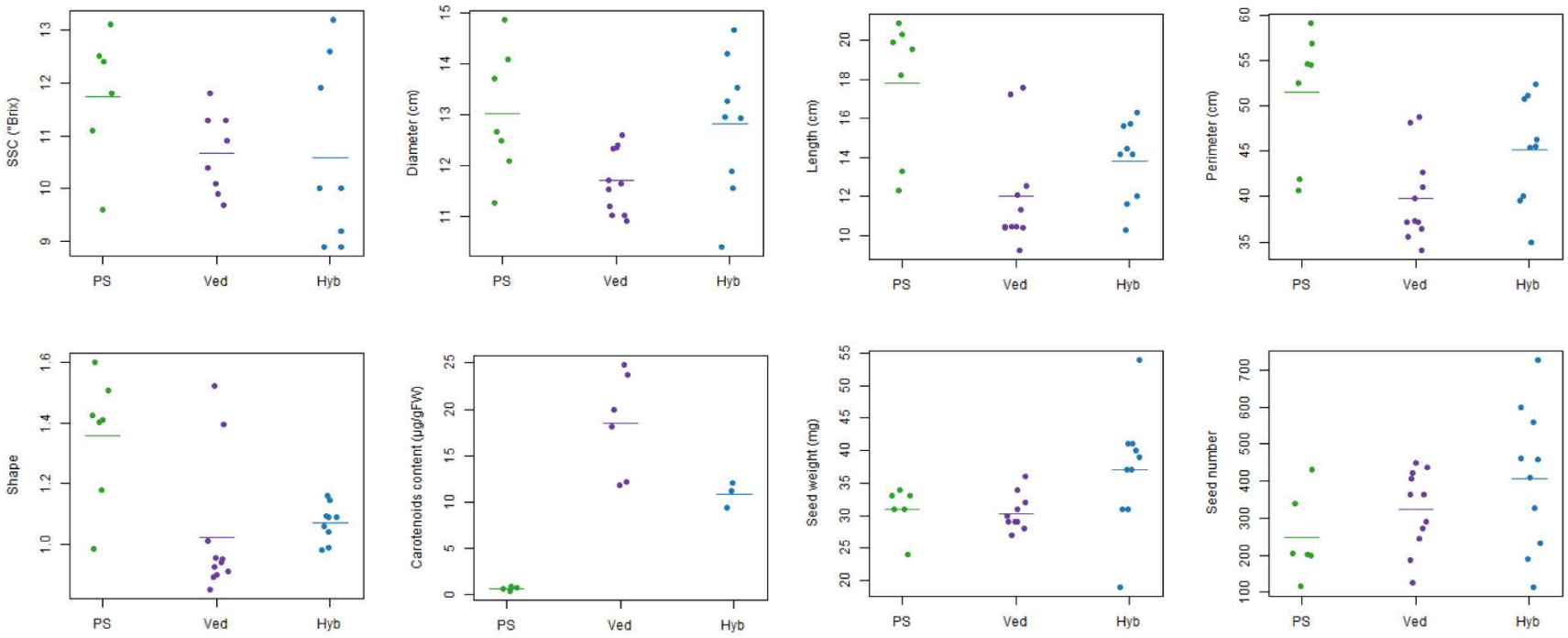

Figure 1.S1. Distribution of the quantitative traits evaluated in the parental lines PS, Ved and Hyb. Each dot corresponds to an observation in any of the five blocks T1-T5. The mean for each line is displayed with a horizontal line.

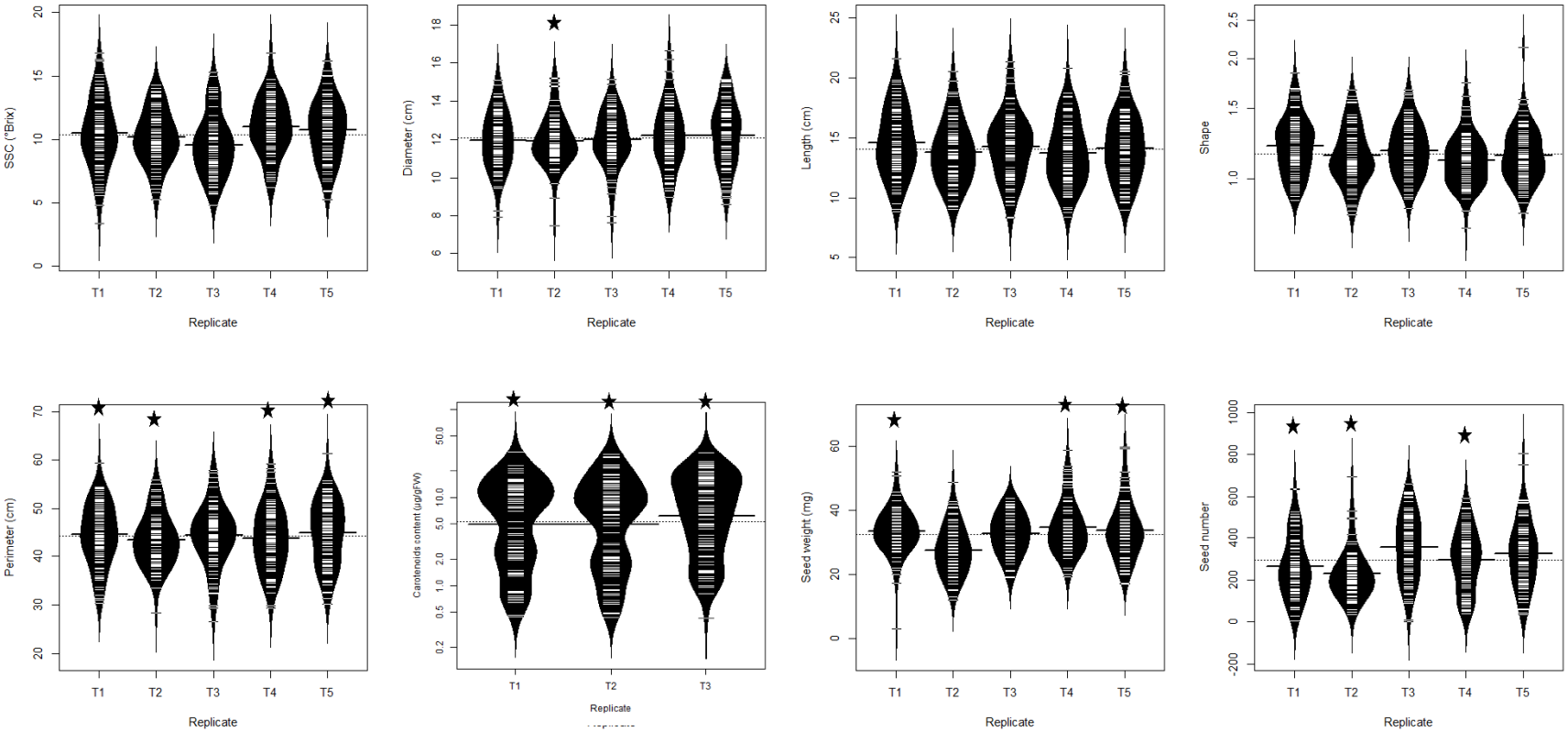

Figure 1.S2. Distribution of the quantitative traits evaluated in the RIL population for each block (T1-T5). Black stars indicate a significant deviation from normality.

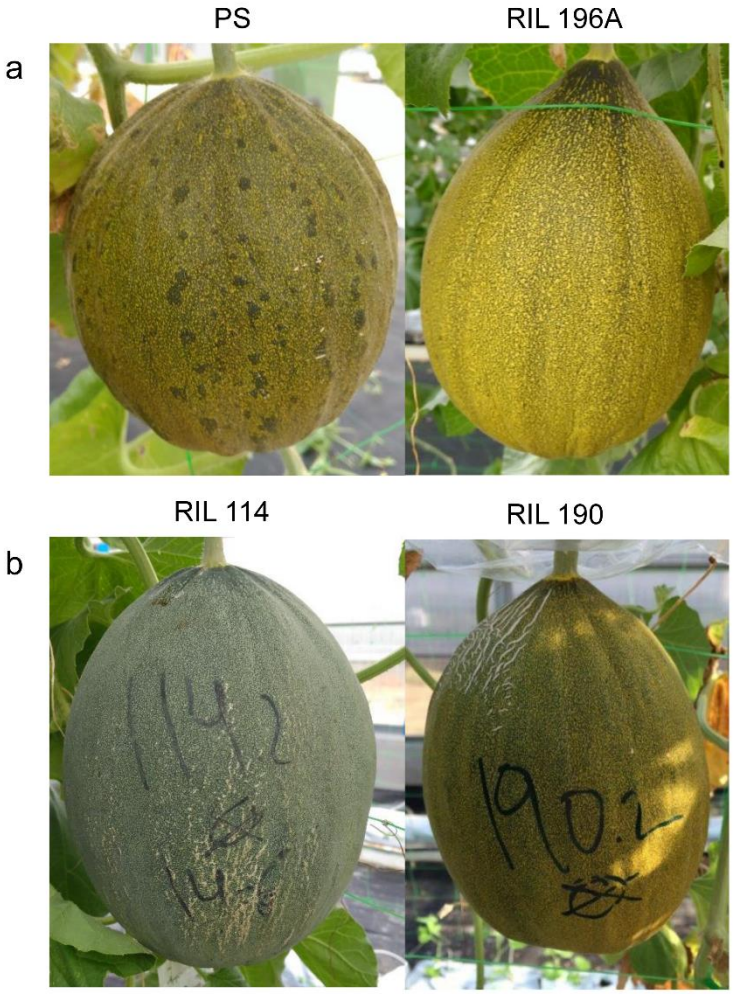

Figure 1.S3. Some examples of complicated cases to phenotype. **a.** Mottled rind (MOT) is partially masked in PS due to the dark green rind, but darker spots can be observed in comparison to RIL 196A. **b.** Yellowing of mature rind (YELL), present in RIL 190 and appreciable as a different tone in green rind.

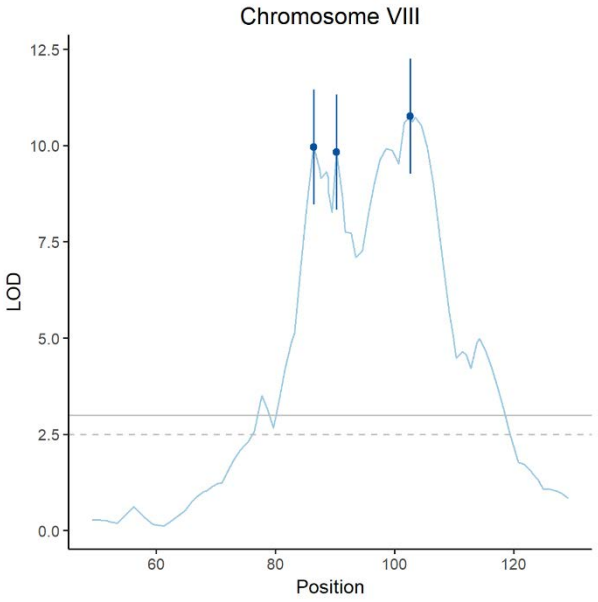

Figure 1.S4. LOD scores for SSC in the QTL mapping experiment using the mean values for a QTL region in LG VIII. The dots represent the LOD peak for each QTL (*SSCQU8.1*, *SSCQU8.2* and *SSCQU8.3* from left to right) and the bars the LOD peak ± 1.5.

Figure 1.S5. RILs 172 (**a)** and 140 (**b)** from 2016, showing transgressive segregation in fruit size in comparison with the parental lines PS (**c)** and Ved (**d)**. The white square represents 1cm^2.

Table 1.S2. Summary of QTLs described in other studies that map in similar intervals to those detected in our work.

Trait	QTL/gene ID	Plant material	Chr	Physical position[1] (pb)	Linked marker	Principal reference[2]	Other references
SSC	*SSC8.5*	"Top Mark" x USDA-846-1	8	-	OPAY1-831	[78]	[59,66]
	SSC9.7	"Top Mark" x USDA-846-1	9	24,516,921	CMATN22	[78]	[66]
	SC9-3	PS x SC	9	-	CMCT1b	[66]	
	SSC10.8	"Top Mark" x USDA-846-1	10	3,803,151	CMGA172	[78]	
FW	*FWQT8.1*	PS x TRI	8	4,310,341	CI_33-B09	[68]	[5,66]
	SC5-2	PS x SC	5	20,855,850	CMGAN3	[66]	[59]
FD	*FD.2*	MAK x VED	2	8,178,416	AI_14-H05	[6]	[5,78,79]
FS	*FSQT6.1*	PS x TRI	6	15,162,313	AI_19-F11	[68]	[5,11,59,66,78]
	FS.11	MAK x VED	11	29,558,732	PSI_41-B07	[6]	[11,59,78,79]
	FSH2.1	PI 414 x "Dulce"	2	900,871	CMAGN39	[22]	[5,11,78,79]
FL	*FLQT6.1*	PS x TRI	6	36,413,356	CMPSNP1021	[68]	[4,6,66]
	FL.11	MAK x VED	11	31,483,477	CMPSNP389	[6]	[21,66]
	FL5.1	VED x PI 414	5		M35_14	[79]	
YELL	*CmKFB*	NA x TVT	10	3,475,283	-	[46]	
ECOL	*ECOLQC3.5*	PS x SC	3	3,914,573	CSWCT10	[59]	[21]
	ECOLQC7.2	PS x SC	7	23,437,923	CMTCN30	[59]	[21]
CAR	*CmOr*	"Dulce" x "Tam Dew"	9	21,683,406	-	[47]	

Digital Supplementary Material

Table 1.S1. Markers obtained with GBS. a. All markers; b. Selected markers; c. All bins; d. Selected bins.

Table 1.S3. a. Candidate genes for fruit morphology in the melon genome annotation v4.0. b. Candidate genes for fruit morphology contained in the QTL intervals

References

1. FAO. Statistics Division of Food and Agriculture Organization of the United Nations (FAOSTAT). http://faostat.fao.org/.

2. Sebastian P, Schaefer H, Telford IRH, Renner SS. Cucumber (*Cucumis sativus*) and melon (*C. melo*) have numerous wild relatives in Asia and Australia, and the sister species of melon is from Australia. Proc. Natl. Acad. Sci. U.S.A. 2010;107:14269–14273.

3. Pitrat M. Phenotypic diversity in wild and cultivated melons (*Cucumis melo*). Plant Biotechnol. 2013;30:273–8.

4. Díaz A, Zarouri B, Fergany M, Eduardo I, Álvarez JM, Picó B, et al. Mapping and Introgression of QTL Involved in Fruit Shape Transgressive Segregation into "Piel de Sapo" Melon (*Cucumis melo* L.). PLoS One. 2014;9:e104188.

5. Ramamurthy RK, Waters BM. Identification of fruit quality and morphology QTLs in melon (*Cucumis melo*) using a population derived from *flexuosus* and *cantalupensis* botanical groups. Euphytica. 2015;204:163–77.

6. Perpiñá G, Esteras C, Gibon Y, Monforte AJ, Picó B. A new genomic library of melon introgression lines in a cantaloupe genetic background for dissecting desirable agronomical traits. BMC Plant Biol.2016;16:1–21.

7. Eduardo I, Arús P, Monforte AJ. Development of a genomic library of near isogenic lines (NILs) in melon (*Cucumis melo* L.) from the exotic accession PI161375. Theor. Appl. Genet. 2005;112:139–48.

8. Périn C, Gomez-Jimenez M, Hagen L, Dogimont C, Pech J, Latché A, et al. Molecular and Genetic Characterization of a Non- Climacteric Phenotype in Melon Reveals Two Loci Conferring Altered Ethylene Response in Fruit. Plant Physiol. 2002;129:300–9.

9. Freilich S, Lev S, Gonda I, Reuveni E, Portnoy V, Oren E, et al. Systems approach for exploring the intricate associations between sweetness, color and aroma in melon fruits. BMC Plant Biol. 2015;15:71.

10. Galpaz N, Gonda I, Shem-Tov D, Barad O, Tzuri G, Lev S, et al. Deciphering genetic factors that determine melon fruit-quality traits using RNA-Seq based high-resolution QTL and eQTL mapping. Plant J. doi:10.1111/tpj.13838

11. Gur A, Tzuri G, Meir A, Sa U, Portnoy V, Katzir N, et al. Genome-Wide Linkage-Disequilibrium Mapping to the Candidate Gene Level in Melon (*Cucumis melo*). Sci. Rep. 2017;7:1–13.

12. Leida C, Moser C, Esteras C, Sulpice R, Lunn JE, de Langen F, et al. Variability of candidate genes, genetic structure and association with sugar accumulation and climacteric behavior in a broad germplasm collection of melon (*Cucumis melo* L.). BMC Genet. 2015;16:28.

13. Garcia-Mas J, Benjak A, Sanseverino W, Bourgeois M, Mir G, González VM, et al. The genome of melon (*Cucumis melo* L.). Proc. Natl. Acad. Sci. U.S.A. 2012;109:11872–7.

14. Nimmakayala P, Tomason YR, Abburi VL, Alvarado A, Ronin Y, Garcia-Mas J, et al. Genome-Wide Differentiation of Various Melon Horticultural Groups for Use in GWAS for Fruit Firmness and Construction of a High Resolution Genetic Map. Front. Plant Sci. 2016;7:1–15.

15. Chang C, Wang Y, Tung C. Genome-Wide Single Nucleotide Polymorphism Discovery and the Construction of a High-Density Genetic Map for Melon (*Cucumis melo* L.) Using Genotyping-by-Sequencing. Front. Plant Sci. 2017;8:1–11.

16. Elshire RJ, Glaubitz JC, Sun Q, Poland J a, Kawamoto K, Buckler ES, et al. A robust, simple genotyping-by-sequencing (GBS) approach for high diversity species. PLoS One. 2011;6:e19379.

17. Huang Y, Poland JA, Wight CP, Jackson EW, Tinker NA. Using Genotyping-By-Sequencing (GBS) for Genomic Discovery in Cultivated Oat. PLoS One. 2014;9:e102448.

18. Liu H, Bayer M, Druka A, Russell JR, Hackett CA, Poland J, et al. An evaluation of genotyping by sequencing (GBS) to map the *Breviaristatum-e* (*ari-e*) locus in cultivated barley. BMC Genomics. 2014;15:1–11.

19. Celik I, Gurbuz N, Uncu AT, Frary A, Doganlar S. Genome-wide SNP discovery and QTL mapping for fruit quality traits in inbred backcross lines (IBLs) of *Solanum pimpinellifolium* using genotyping by sequencing. BMC Genomics. 2017;1–10.

20. Wei Q, Wang Y, Qin X, Zhang Y, Zhang Z, Wang J, et al. An SNP-based saturated genetic map and QTL analysis of fruit-related traits in cucumber using specific-length amplified fragment (SLAF) sequencing. BMC Genomics. 2014;15:1–10.

21. Diaz A, Fergany M, Formisano G, Ziarsolo P, Blanca J, Fei Z, et al. A consensus linkage map for molecular markers and quantitative trait loci associated with economically important traits in melon (*Cucumis melo* L.). BMC Plant Biol. 2011;11:111.

22. Harel-Beja R, Tzuri G, Portnoy V, Lotan-Pompan M, Lev S, Cohen S, et al. A genetic map of melon highly enriched with fruit quality QTLs and EST markers, including sugar and carotenoid metabolism genes. Theor. Appl. Genet. 2010;121:511–33.

23. Pitrat M. Melon Genetic Resources: Phenotypic Diversity and Horticultural Taxonomy. New York, NY: Springer New York; 2016. p. 1–36.

24. Dogimont C. 2011 Gene List for Melon. Cucurbit Genet. Coop. Rep. 2011;33–34:104–33.

25. Vegas J, Garcia-Mas J, Monforte AJ. Interaction between QTLs induces an advance in ethylene biosynthesis during melon fruit ripening. Theor. Appl. Genet. 2013;126:1531–44.

26. Monforte AJ, Diaz A, Caño-Delgado A, Van Der Knaap E. The genetic basis of fruit morphology in horticultural crops: lessons from tomato and melon. J. Exp. Bot. 2014;65:4625–37.

27. Argyris JM, Díaz A, Ruggieri V, Fernández M, Jahrmann T, Gibon Y, et al. QTL Analyses in Multiple Populations Employed for the Fine Mapping and Identification of Candidate Genes at a Locus Affecting Sugar Accumulation in Melon (*Cucumis melo* L.). Front. Plant Sci. 2017;8:1–20.

28. Zamir D. Improving plant breeding with exotic genetic libraries. Nat. Rev. Genet. 2001;2:3–10.

29. Brewer MT, Lang L, Fujimura K, Dujmovic N, Gray S, van der Knaap E. Development of a controlled vocabulary and software application to analyze fruit shape variation in tomato and other plant species. Plant Physiol. 2006;141:15–25.

30. Darrigues A, Hall J, Knaap E Van Der, Francis DM, Dujmovic N, Gray S. Tomato Analyzer-color Test : A New Tool for Efficient Digital Phenotyping. J. Am. Soc. Hortic. Sci. 2008;133:579–86.

31. Lichtenthaler H, Buschmann C. Chlorophylls and Carotenoids: Measurement and Characterization by UV-VIS Spectroscopy. Curr Protoc Food Anal. Chem. 2001;F4.3.1-F4.3.8.

32. Perelló C, Rodríguez-Concepción, M., Pulido P. Quantification of Plant Resistance to Isoprenoid Biosynthesis Inhibitors. In: Rodríguez-Concepción M., editor. Plant Isoprenoids. Methods in Molecular Biology (Methods and Protocols), vol 1153. Humana Press, New York, NY

33. Doyle J. DNA Protocols for Plants. In: Hewitt GM, Johnston AWB, Young JPW, editors. Mol. Tech. Taxon. Berlin, Heidelberg: Springer Berlin Heidelberg; 1991. p. 283–93.

34. Torkamaneh D, Laroche J, Bastien M, Abed A, Belzile F. Fast-GBS: a new pipeline for the efficient and highly accurate calling of SNPs from genotyping-by-sequencing data. BMC Bioinformatics. 2017;18:1–7.

35. Rimmer A, Phan H, Mathieson I, Iqbal Z, Twigg SRF, Consortium WGS, et al. Integrating mapping-, assembly- and haplotype-based approaches for calling variants in clinical sequencing applications. Nat. Genet. 2014;46:912–8.

36. Sanseverino W, Hénaff E, Vives C, Pinosio S, Burgos-Paz W, Morgante M, et al. Transposon Insertions, Structural Variations, and SNPs Contribute to the Evolution of the Melon Genome. Mol. Biol. Evol. 2015;32:2760–74.

37. Danecek P, Auton A, Abecasis G, Albers CA, Banks E, Depristo MA, et al. The variant call format and VCFtools. Bioinformatics. 2017;27:2156–8.

38. Wu Y, Bhat PR, Close TJ, Lonardi S. Efficient and accurate construction of genetic linkage maps from the minimum spanning tree of a graph. PLoS Genet. 2008;4.

39. Kosambi DD. The estimation of map distances from recombination values. Ann Eugen. 1944;12:172–5.

40. Voorrips RE. MapChart: software for the graphical presentation of linkage maps and QTLs. J. Hered. 2002;93:77–8.

41. Van Ooijen J, Maliepaard C. MapQTL Version 3.0: Software for the calculation of QTL positions on genetic maps. DLO-Centre Plant Breed. Reprod. Res. Wageningen, Netherlands. 1996.

42. R Core Team. R: A language and environment for statistical computing. Vienna, Austria: R Foundation for Statistical Computing; 2012. URL http://www.R-project.org/

43. RStudio. RStudio: Integrated development environment for R RStudio. Boston, MA, USA; 2012. URL http://www.rstudio.com/

44. Kubicki B. Inheritance of some characters in muskmelons (*Cucumis melo*). Genet. Pol. 1962;3:265–74.

45. Périn C, Dogimont C, Giovinazzo N, Besombes D, Guitton L, Hagen L, et al. Genetic Control and Linkages of Some Fruit Characters in Melon. Cucurbit Genet. Coop. Rep. 1999;22:16–8.

46. Feder A, Burger J, Gao S, Lewinsohn E, Katzir N, Schaffer AA, et al. A Kelch Domain-Containing F-Box Coding Gene Negatively Regulates Flavonoid Accumulation in Muskmelon. Plant Physiol. 2015;169:1714–26.

47. Tzuri G, Zhou X, Chayut N, Yuan H, Portnoy V, Meir A, et al. A "golden" SNP in *CmOr* governs the fruit flesh color of melon (*Cucumis melo*). Plant J. 2015;82:267–79.

48. Ferreira A, Flores da Silva M, Da costa e Silva L, Cruz CD. Estimating the effects of population size and type on the accuracy of genetic maps. Genet. Mol. Biol. 2006;29:187–92.

49. Chang C, Bowman JL, Dejohn AW, Landert ES, Meyerowitz EM. Restriction fragment length polymorphism linkage map for *Arabidopsis thaliana*. Proc. Natl. Acad. Sci. U.S.A. 1988;85:6856–60.

50. Tanksley SD, Medina-Filho H, Rick CM. Use of naturally-occurring enzyme variation to detect and map genes controlling quantitative traits in an interspecific backcross of tomato. Heredity. 1982;49:11–25.

51. Tanksley SD, Ganal MW, Prince JP, de Vicente MC, Bonierbale MW, Broun P, et al. High Density Molecular Linkage Maps of the Tomato and Potato Genomes. Genetics. 1992;132:1141–60.

52. June C, Page SEEL, Pasternak S, Liang C, Zhang J, Fulton L, et al. The B73 Maize Genome: Complexity, Diversity, and Dynamics. Science. 2012;326:1112–5.

53. Goff SA, Ricke D, Lan T, Presting G, Wang R, Dunn M, et al. A Draft Sequence of the Rice Genome (*Oryza sativa* L. ssp *japonica*). Science. 2005;296:92–100.

54. The Tomato Genome Consortium. The tomato genome sequence provides insights into fleshy fruit evolution. Nature. 2012;485:635–41.

55. Pavan S, Marcotrigiano AR, Ciani E, Mazzeo R, Zonno V, Ruggieri V, et al. Genotyping-by-sequencing of a melon (*Cucumis melo* L.) germplasm collection from a secondary center of diversity highlights patterns of genetic variation and genomic features of different gene pools. BMC Genomics. 2017;18:1–10.

56. Ruggieri V, Alexiou KG, Morata J, et al. An improved assembly and annotation of the melon (*Cucumis melo* L.) reference genome. (under review in Sci Rep)

57. Yano R, Nonaka S, Ezura H. Melonet-DB, A Grand RNA-seq Gene Expression Atlas in Melon (*Cucumis melo* L.). Plant cell Physiol. 2017;193.

58. Tadmor Y, Burger J, Yaakov I, Feder A, Libhaber SE, Portnoy V, et al. Genetics of flavonoid, carotenoid, and chlorophyll pigments in melon fruit rinds. J. Agric. Food Chem. 2010;58:10722–8.

59. Monforte AJ, Oliver M, Gonzalo MJ, Alvarez JM, Dolcet-Sanjuan R, Arús P. Identification of quantitative trait loci involved in fruit quality traits in melon (*Cucumis melo* L.). Theor. Appl. Genet. 2004;108:750–8.

60. Liu H, Meng H, Pan Y, Liang X, Jiao J, Li Y, et al. Fine genetic mapping of the white immature fruit color gene w to a 33.0-kb region in cucumber (*Cucumis sativus* L.). Theor. Appl. Genet. 2015;128:2375–85.

61. Liu H, Jiao J, Liang X, Liu J, Meng H, Chen S, et al. Map-based cloning, identification and characterization of the *w* gene controlling white immature fruit color in cucumber (*Cucumis sativus* L.). Theor. Appl. Genet. 2016;129:1247–56.

62. Xu W, Dubos C. Transcriptional control of flavonoid biosynthesis by MYB – bHLH – WDR complexes. Trends Plant Sci. 2015;20:176–85.

63. Xu W, Grain D, Bobet S. Complexity and robustness of the flavonoid transcriptional regulatory network revealed by comprehensive analyses of MYB – bHLH – WDR complexes and their targets in *Arabidopsis* seed. New Phytol. 2014;202:132–44.

64. Ganesan J. Genetic studies on certain characters of economic importance in muskmelon (*Cucumis melo* L.). Annamalai Univ. 1988.

65. Pech JC, Bouzayen M, Latché A. Climacteric fruit ripening: Ethylene-dependent and independent regulation of ripening pathways in melon fruit. Plant Sci. 2008;175:114–20.

66. Eduardo I, Arús P, Monforte AJ, Obando J, Fernández-Trujillo JP, Martínez JA, et al. Estimating the Genetic Architecture of Fruit Quality Traits in Melon Using a Genomic Library of Near Isogenic Lines. J. Amer. Soc. Hort. Sci. 2007;132:80–9.

67. Mu Q, Huang Z, Chakrabarti M, Illa-Berenguer E. Fruit weight is controlled by Cell Size Regulator encoding a novel protein that is expressed in maturing tomato fruits. PLoS Genet. 2017;13:e1006930.

68. Díaz A, Hernández M, Dolcet R, Garcés A, José C, Álvarez M, et al. Quantitative trait loci analysis of melon (*Cucumis melo* L.) domestication-related traits. Theor. Appl. Genet. 2017;130:1837–56.

69. Wahl V, Brand LH, Guo Y, Schmid M. The FANTASTIC FOUR proteins influence shoot meristem size in *Arabidopsis thaliana*. BMC Plant Biol. 2010;10:1–12.

70. Duan P, Xu J, Zeng D, Zhang B, Geng M, Zhang G, et al. Natural Variation in the Promoter of GSE5 Contributes to Grain Size Diversity in Rice. Mol. Plant. 2017;10:685–94.

71. Fan C, Xing ÆY, Mao ÆH. *GS3*, a major QTL for grain length and weight and minor QTL for grain width and thickness in rice, encodes a putative transmembrane protein. Theor. Appl. Genet. 2006;112:1164–71.

72. Shomura A, Izawa T, Ebana K, Ebitani T, Kanegae H, Konishi S, et al. Deletion in a gene associated with grain size increased yields during rice domestication. Nat. Genet. 2008;40:1023–8.

73. Song X, Huang W, Shi M, Zhu M, Lin H. A QTL for rice grain width and weight encodes a previously unknown RING-type E3 ubiquitin ligase. Nat. Genet. 2007;39:623–30.

74. Wang S, Wu K, Yuan Q, Liu X, Liu Z, Lin X, et al. Control of grain size, shape and quality by *OsSPL16* in rice. Nat. Genet. 2012;44:950–4.

75. Lu X, Xiong Q, Cheng T, Li Q, Liu X, Bi Y, et al. A PP2C-1 Allele Underlying a Quantitative Trait Locus Enhances Soybean 100-Seed Weight. Mol. Plant 2017;10:670–84.

76. Tang X, Su T, Han M, Wei L, Wang W, Yu Z, et al. Suppression of extracellular invertase inhibitor gene expression improves seed weight in soybean (*Glycine max*). J. Exp. Bot. 2017;68:469–82.

77. Fisher J, Bensal E, Zamir D. Bimodality of stable and plastic traits in plants. Theor. Appl. Genet. 2017;130:1915–26.

78. Paris MK, Zalapa JE, McCreight JD, Staub JE. Genetic dissection of fruit quality components in melon (*Cucumis melo* L.) using a RIL population derived from exotic x elite US Western Shipping germplasm. Mol. Breed. 2008;22:405–19.

79. Périn C, Hagen LS, Giovinazzo N, Besombes D, Dogimont C, Pitrat M. Genetic control of fruit shape acts prior to anthesis in melon (*Cucumis melo* L.). Mol. Genet. Genomics 2002 ;266:933–41.

Chapter 2

Non-invasive ethylene quantification in attached fruit headspace at 1 ppb by gas chromatography – mass spectrometry

Non-invasive ethylene quantification in attached fruit headspace at 1 ppb by gas chromatography – mass spectrometry

Lara Pereira[a], Marta Pujol[a], Jordi Garcia-Mas[a], Michael A. Phillips[b*]

(lara.pereira@cragenomica.es, marta.pujol@irta.cat, jordi.garcia@irta.cat, michaelandrew.phillips@utoronto.ca)

[a] IRTA, Center for Research in Agricultural Genomics (IRTA- CSIC- UAB-UB), Edifici CRAG, Bellaterra (Barcelona), Spain 08193

[b] Department of Biology, University of Toronto - Mississauga, Mississauga, Ontario, L5L 1C6, Canada

* To whom correspondence should be addressed: Michael A. Phillips, michaelandrew.phillips@utoronto.ca, Tel. 1-905-569-4848, Department of Biology, University of Toronto - Mississauga, 3359 Mississauga Rd, Mississauga, Ontario, L5L 1C6, Canada

The Plant Journal (2017) 91, 172–183. doi: 10.1111/tpj.13545

Abstract

Ethylene is a gaseous plant hormone involved in defense, adaptations to environmental stress, and fruit ripening. Its relevance to the latter makes its detection highly useful to physiologists interested in ripening onset. Produced as a sharp peak during the respiratory burst, ethylene is biologically active at tens of $nL \cdot L^{-1}$. Reliable quantification at such concentrations generally requires specialized instrumentation. Here we present a rapid, high sensitivity method for detecting ethylene in attached fruit using a conventional gas chromatography – mass spectrometry (GC-MS) system and *in situ* headspace collection chambers. We apply this method to melon (*Cucumis melo* L.), a unique species consisting of climacteric and non-climacteric varieties, with a high variation in the climacteric phenotype among climacteric types. Using a population of recombinant inbred lines (RILs) derived from highly climacteric ("Védrantais", *cantalupensis* type) and non-climacteric ("Piel de sapo", *inodorus* type) parental lines, we observed a significant variation for the intensity, onset, and duration of the ethylene burst during fruit ripening. Our method does not require concentration, sampling times over 1 h, or fruit harvest. We achieved a limit of detection of 0.41 ± 0.04 $nL \cdot L^{-1}$ and a limit of quantification of 1.37 ± 0.13 $nL \cdot L^{-1}$ with an analysis time of 2.6 min per sample. Validation of the analytical method indicated that linearity (>98%), precision (CV ≤ 2%), and sensitivity compared favorably with dedicated optical sensors. This study adds to evidence of the characteristic climacteric ethylene burst as a complex trait whose intensity in our RIL population lies along a continuum in addition to two extremes.

Significance statement

We present a rapid, non-invasive headspace assay that detects trace emissions of ethylene in attached, developing fruit without concentration and show its utility in dissecting climacteric fruit ripening in melon using a recombinant inbred line population. The short sampling and analysis times support high throughput workflows with a sensitivity of 1 part per billion using a conventional capillary gas chromatography – mass spectrometry system, a vital technique for plant biologists studying climacteric ripening mechanisms.

Keywords: Melon (*Cucumis melo*), volatile analysis, headspace analysis, climacteric fruit ripening, ethylene biosynthesis, phytohormone analysis, gas chromatography – mass spectrometry

Introduction

Sensitive, high throughput procedures for the trace analysis of plant hormones are increasingly familiar to plant researchers in an age of multidimensional metabolome analysis (Van Meulebroek et al. 2012; Tarkowská et al. 2014; Cajka and Fiehn 2016). Yet the detection of the gaseous phytohormone ethylene at physiological concentrations continues to present technical challenges for non-specialists. Techniques for measuring ethylene in plants, including their corresponding costs, sensitivities, and analysis times, have recently been reviewed (Cristescu et al. 2013). Traditionally, ethylene measurement has been accomplished by gas chromatography with a flame ionization detector (GC-FID) (Bassi and Spencer 1989; Kume et al. 2001; Pham-Tuan et al. 2000), but this technique generally lacks sufficient sensitivity to detect physiological concentrations (limits of quantification, LOQ, in the 100s of $nL \cdot L^{-1}$), necessitating the use of traps or concentrators or isolation of plant tissue. One group of alternatives consists of electrochemical sensors which function by amperometric (Jordan et al. 1997a), chemoresistive (Esser et al. 2012), capacitive (Balachandran et al. 2008), or other mechanisms (Zevenbergen et al. 2011; Lambertus et al. 2005; Jordan et al. 1997b). Electrochemical sensors offer sensitivity in the range of 10s of $nL \cdot L^{-1}$ but lack the robustness and reproducibility of traditional GC analysis. High sensitivity techniques utilizing dedicated optical sensors can detect physiologically relevant levels of ethylene (Cristescu et al. 2013; Xie et al. 2009; Weidmann et al. 2004; Wahl et al. 2006) but require greater technical knowledge and highly specialized and costly analytical equipment with additional maintenance needs. The highest current sensitivity for a commercially available laser sensor has a limit of detection (LOD) of 0.3 $nL \cdot L^{-1}$ and a fast response time (5 s) (ETD-300, Sensor Sense BV, Netherlands). High throughput, low cost alternatives are currently lacking for non-specialists, particularly when non-invasive sampling methods are required to study developmental processes such as the control of fruit ripening or stress-responsive roles of ethylene under native conditions.

Ethylene's role in initiating fruit ripening in certain species of plants has been known since the 1930s (Gane 1934), and more recent investigations have uncovered roles in plant responses to herbivore egg deposition (Schröder et al. 2007), pathogen infection (Díaz et al. 2002), circadian rhythm (Thain et al. 2004), oxygen deprivation (Vergara et al. 2012), and P and K availability (Borch et al. 1999; Jung et al. 2009). The net metabolic effect of ethylene biosynthesis on plant metabolism is dependent on the context in which it is synthesized and may have a synergistic or antagonistic effect on other phytohormone signals (Pieterse et al. 2009). Much uncertainty regarding ethylene's mode of action remains, and its biological function in the context of other hormones remains an active area of research. However, in agriculture, it is principally recognized for its importance as a hormonal signal for certain species which utilize ethylene to initiate their fruit ripening programs, including tomato, avocado, apple and banana (Giovannoni 2004). Such fruits are designated as climacteric, and their ripening process is accompanied by changes in fruit aroma, sweetness, acidity, and firmness (Yamaguchi et al. 1977). On the other hand, precocious or excessive ethylene production by fruits may lead to premature ripening, spoilage in fruit storage facilities and increased damage during transport (Fernández-Trujillo et al. 2008). Ethylene production has therefore long been of interest to agronomists working in post-harvest biology as well as experimental biologists studying the control mechanisms behind fruit ripening.

Melon (*Cucumis melo*) has been proposed as an alternative model system for understanding the role of ethylene in fruit ripening (Vegas et al. 2013; Saladié et al. 2015; Garcia-Mas et al. 2012; Pech et al. 2008; Ezura and Owino 2008) due to the unusual instance of both climacteric and non-climacteric varieties within the same species. This allows the production of segregating populations for this trait and provides an ideal system to dissect the genetics of climacteric ripening. Recent results suggest fruit ripening is complex (Argyris et al. 2015; Paul et al. 2012) and that our knowledge of its regulation is still fragmented. In general, ripening in climacteric melon is accompanied by a burst of ethylene production and a rise in respiration, a breakdown in cell wall integrity that leads to softening, the biosynthesis of aromatic volatiles, and fruit abscission (Pech et al. 1994; Ezura and Owino 2008). However, other ripening processes such as the biosynthesis of β-carotene, while characteristic of climacterics, are in fact independent of ethylene (Ayub et al. 1996). Ripening in non-climacteric varieties such as the *inodorus* type, on the other hand, does not involve

autocatalytic ethylene production or a rise in respiration, resulting in firmer fruit with less aroma and a lack of fruit abscission (Pratt et al. 1977). A recent transcriptomic comparison of climacteric and non-climacteric melon varieties revealed major differences in the expression of fruit quality genes, transcription factors, and genes related to sucrose catabolism (Saladié et al. 2015), but also identified varieties displaying intermediate fruit ripening behaviour between the classical climacteric and non-climacteric categories. We have established a recombinant inbred line population by crossing a typical climacteric variety from the *cantalupensis* type "Védrantais", which features orange flesh, a sweet aroma, and presence of an abscission layer, with the non-climacteric variety "Piel de Sapo" from the *inodorus* type, which has none of the above characteristics and possesses white flesh. The reproducible detection of ethylene in developing fruit of these lines is a fundamental metric to dissect the role of this hormone in climacteric vs. non-climacteric ripening programs. Without it, the measure of the climacteric phenotype by indirect traits such as fruit abscission, external color change or aroma production provides incomplete information.

In this report, we describe a GC mass spectrometry (GCMS) based method which non-invasively quantifies ethylene in the headspace of attached melon fruit. This technique relies on widely available analytical equipment and features a headspace sampling method devised to measure ethylene in attached climacteric fruits with short sampling time, in contrast with the routinely used method with detached fruits fitted in jars. We further demonstrate the broad applicability of this method to physiologists studying the role of ethylene in the ripening of other climacteric fruits such as tomato.

Materials and methods

Plant material

Melon (*Cucumis melo* L.) plants were cultivated under standard greenhouse conditions as described (Eduardo et al. 2005). Ethylene analysis was performed on individual melons from a RIL population obtained from a cross between Ved, a climacteric variety from the *cantalupensis* group, and PS line T111, a non-climacteric variety from the *inodorus* type. A

single flower on each plant was hand pollinated, and ethylene headspace measurements were performed periodically beginning 24-35 days after pollination (DAP). Commercial hybrid melons used in headspace collection time course were obtained from Semillas Fitó, S.A. (Barcelona, Spain).

Headspace sampling of attached melon fruit

The procedure for non-invasive ethylene sampling of attached melon fruits is demonstrated in Movie 2.S1. For an ethylene headspace assay, individual developing melon fruits were placed in polyamide-polyethylene bags of 3.4 or 6.2 L (Allfo Vakuumverpackung, Waltenhofen, Germany). A half meter length of 6 mm (i.d.) polyvinylchloride tubing was sealed to the pedicel using 5 g plumber's putty (Figure 2.1).

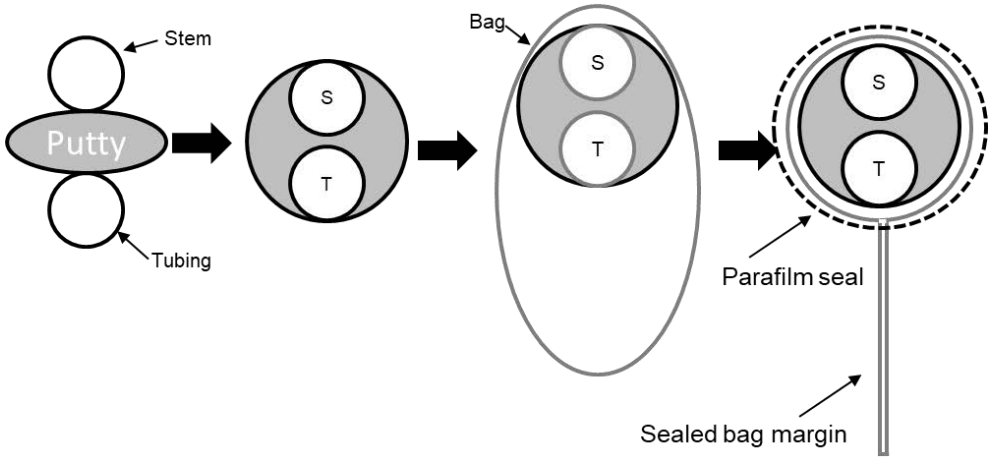

Figure 2.1. Diagram of the sealing method used to enclose ripening melon fruit in a temporary, *in situ* volatile collection chamber. Sealing the fruit within the chamber requires forming a cylindrical union consisting of the stem, tubing used to inflate a polyamide bag, and a malleable substance such as putty. This assembly is further sealed with parafilm (dotted line).

Teflon tape was applied to the point of attachment of stem and tubing to seal the enclosed headspace (Figure 2.2b), and control measurements using all of these components but lacking fruit were performed to confirm no ethylene was given off by any material used in this sampling procedure. The upper margin of the bag was sealed with a thermo-sealing iron (Shenzhen Deogra Electrical Co., model DG070) (Figure 2.2a). Once the seal was created, the external end of the tubing was fitted with a 2-way switch valve (Vitlab). A hand held electric pump was used to inflate the bags using ambient air (Figure 2.2c), and the atmosphere

within the bag was maintained by closing the switch valve. After 1 h, a 60 mL gas sample was withdrawn from the bag using a plastic syringe fitted with a needle (Figure 2.2d) and transferred to a 10 mL head space sample vial by slowing flushing out the vial with several volumes of sample before sealing it. Variables such as head space collection time, injection volume, and chromatographic conditions were optimized independently to reduce analysis time, maximize daily sample throughput, and maximize repeatability of measurements. In addition, the loss of ethylene from headspace vials during storage at different temperatures (25, 4, and -20 ^{0}C) for up to 48 hours was determined. Following the optimization of collection, storage, and analysis variables, this headspace method was then applied to the melon RIL population noted above. All collected headspace samples were analyzed within 12 hours of collection, and 5 and 20 ppm ethylene standards were prepared in triplicate along with ambient air controls for each day melon head space samples were collected. Standards, blanks, and samples were transported directly from the greenhouse to the laboratory for analysis. All samples were analyzed in less than 24 h from the moment of collection.

To evaluate this headspace sampling technique in other climacteric plant species, we adapted this method to sampling ethylene in a selection of commercial tomato varieties at the green, breaker, and ripe stages of development. Plants were obtained from Semillas Fitó, S.A. In some cases, racemes were pruned two days before sampling to reduce developmental variability. However, we also assayed unaltered racemes to detect possible effects of pruning on ethylene measurements. Sealed, inflated headspace bags were sampled after 1 h and analyzed exactly as described for melon headspace samples.

Figure 2.2. Static headspace sampling of ripening melon fruit for non-invasive ethylene measurements by GC-MS. **a.** Thermo-sealing of the bag along the top margin up to the pedicel. **b.** Hermetic seal with Teflon film around the pedicel. **c.** Bag is inflated with air using an electric pump and tubing sealed to the pedicel. Following inflation, a 2-way switch valve maintains the atmosphere. **d.** Collection of the headspace with a syringe, which is later transferred to a headspace vial for GC-MS analysis offsite.

GCMS analysis

GCMS analysis was performed with an Agilent 7890A gas chromatograph coupled to a 5975C mass selective detector. Using a CTC-PAL headspace sampler (Agilent Technologies), gas samples in 10 mL septum vials were incubated at 30 ^{0}C with shaking for 30 s, after which 100-500 µL was removed with a gas tight autosampler syringe heated to the same temperature. Injection was performed on a multi-mode injector in pulsed splitless mode at 100 ^{0}C with a 30 s pulse at 25 psi. The flow rate was otherwise held constant at 1 mL·min^{-1}. The relative detector responses of the same method run at 0.75, 1.0, and 2.0 mL·min^{-1} were

also compared. The column used was an HP-PLOT Al_2O_3/KCl (Agilent Technologies), 0.25 mm i.d. x 30 m, with 5 μm film thickness. The oven temperature program was as follows: 30 ^{0}C for 1.5 min, then 20 ^{0}C·min^{-1} to 50 ^{0}C with a 0.1 min hold time (total analysis time 2.6 min). After a solvent delay of 1.8 min to eliminate atmospheric nitrogen, electron impact energy was set to 70 eV with the detector operating in selected ion mode. Ions at *m/z* 26 and 27, representing the $[M-H]^+$ and $[M-2H]^+$ ethylene fragmentation products, were monitored with a dwell time of 100 ms each at high resolution. Resolution factor, *R*, of ethylene and nitrogen (determined with no solvent delay) was calculated using the formula $R = (t_E - t_N)/0.5(w_N + w_E)$, where *t* and *w* are the retention time and peak width of ethylene (E) and nitrogen (N) in min.

Quantitative real-time PCR (QPCR)

Developing fruit placed in polyamide-polyethylene bags and untreated controls from climacteric (Védrantais (Ved), RIL124, RIL 200 and the hybrid PS x Ved) and non-climacteric lines (PS, RIL021A and RIL033) were used in transcript profiling experiments. RNA from one (four RILs), two (PS, hybrid, Ved in bags) or three (Ved control) biological replicates was isolated from mesocarp of ripe fruit. RNA was isolated from 100 mg frozen sample and ground using the Spectrum Plant Total RNA kit (Sigma-Aldrich, USA). RNA quality was assessed as in Saladié et al. (2015). High-quality RNA samples were reverse transcribed into cDNA from 500 ng of total RNA with an oligo(dT)20 primer and a SuperScript™ III Reverse Transcriptase kit (Invitrogen, Carlsbad, CA) according to the manufacturer's instructions.

The genes investigated, *CmACS1* (1-aminocyclopropane-1-carboxylate synthase (EC 4.4.1.14), *CmACS5* and *CmACO1* (1-aminocyclopropane-1-carboxylate oxidase (EC1.14.17.4)), are known to be involved in the ethylene biosynthetic pathway during melon fruit ripening (Saladié et al. 2015). Gene expression analysis by QPCR was performed on a LightCycler® 480 Real-Time PCR System using SYBR® Green I Mix (Roche Applied Science, USA). The relative amounts of specific transcripts were determined using cyclophilin (*CmCYP7*) as a reference gene (Saladié et al., 2015) and then normalized to PS expression in controls (no headspace sampling). Primers were designed with Primer3 (http://primer3.wi.mit.edu/) and checked for the presence of secondary structures with

NetPrimer (http://www.premierbiosoft.com/netprimer/). Primer sequences are listed in Table 2.S3. Calculation of intra-assay variation, primer efficiencies, and amplification specificity of the PCR by melting curve analysis, were as described previously (Saladié et al., 2015).

Data analysis

Limits of detection (LOD) and quantification (LOQ) for ethylene were calculated by measuring the standard deviation (SD) of the background signal at the retention time of the analyte in blanks, or background measured before and after the elution of the analyte in standards or fruit headspace samples. All three methods gave nearly identical values. LOD was estimated as the SD/σ times 3, where σ is the slope of the standard curve. LOQ was obtained by multiplying the same value by 10. Ethylene concentrations in fruit head space samples were calculated from linear regression to the resulting standard curve, which typically featured an R^2 value of >0.99. Gas concentrations were combined with biometric fruit data (weight, length, width) to estimate effective head space volumes in collection bags (minus fruit volume) and ethylene emissions on a FW basis. Effective head space volumes (volume of bag – volume of melon) were calculated for each measurement taken as follows. Prior to fitting a melon for head space sampling, its volume was estimated by measuring the two principal axes of the fruit and modeling it as a prolate spheroid ($V = 4/3\pi \cdot a^2 \cdot c$, where a and c are the equatorial and polar radii, respectively). The fresh weight of each melon fruit was similarly recorded prior to head space sampling.

Results and discussion

In situ headspace collection enables non-invasive quantification of fruit volatiles

Traditional methods for the measurement of ethylene in developing climacteric fruit suffer from two principal drawbacks: the need to separate the fruit from the plant for measurement, effectively terminating its development, and the non-physiological nature of the sampling times and conditions. Since ethylene production occurs as a sharp peak that may last only a few days and trigger a distinct change in fruit metabolism, monitoring changes in ethylene

emission is fundamental to the task of understanding the process of fruit ripening at the molecular level. In order to track ethylene production over the ripening phase of individual melons, we have developed an assay suitable for detailed studies of the role of this hormone in fruit ripening that supports continuous, non-invasive sampling of fruit at arbitrary and repeated time points (Figure 2.1), an achievement which is not currently feasible given the sensitivity of standard ethylene quantification protocols (Cristescu et al. 2013) and the relatively low concentrations of ethylene at physiologically relevant concentrations.

Headspace collection was performed in an inflatable enclosure for 60 min (Figure 2.2 and Movie 2.S1), and ethylene can be immediately detected by GC-MS without further concentration under our analytical conditions. While ethylene production in climacteric and non-climacteric melon fruits is presented here as a proof of concept due to its significance for physiologists studying fruit ripening, this portable head space collection method can readily be applied to the non-invasive quantification of any volatile compound emitted by ripening fruit.

Following head space sampling, we observed no discoloration of the fruit, bruising of the pedicel, change in maturation time compared to untreated controls, or any other indication that this *in situ* head space sampling technique had a significant effect on the physiology of the fruit. Fruit head space was sampled periodically beginning 24-35 DAP until harvest with no apparent effect on fruit quality or development.

Possible effects on ethylene production or fruit physiology were further investigated by measuring the transcripts for ethylene biosynthetic genes in climacteric or non-climacteric fruits used in headspace sampling and comparing them to untreated controls at harvest. As judged by quantitative real-time PCR (QPCR), both 1-aminocyclopropane-1-carboxylate synthase (ACS) *CmACS1, CmACS5* and oxidase (ACO) *CmACO1* demonstrated significant differences in expression level when climacteric and non-climacteric fruits were compared, as expected (Figure 2.S1). However, when the expression of these same genes was compared between sampled (bagged) fruits and untreated controls (no bag), no obvious differences were observed (Figure 2.S1). This observation was corroborated by statistical tests for significance using the resulting QPCR data. Both Tukey and t-tests showed no significant differences in the expression of *ACS* or *ACO* as a result of our sampling procedure (Figure

2.S2 and Table 2.S1), consistent with the lack of difference in fruit coloration, pedicel bruising, and maturation time between the two groups. We therefore conclude that our headspace sampling technique has at most a negligible effect on fruit physiology and ethylene production.

Using this protocol, we estimate from the time required to fit a single melon with an *in situ* head space chamber, perform a 60 min incubation, and sample the chamber that two people can collect approximately 84 melon head space samples in a typical 8 h session. This places this technique in the medium throughput range of analytical methods and permitted us, in a typical season, to survey more than 80 melon lines, assuming 3 independent biological samples per line, a 100% pollination and survival rate, and continuous operation of a single GC-MS system. Given a total injection-to-injection time of approximately 5 min, and taking into consideration blanks and daily calibration curves, we estimate that a single GC-MS system could accommodate double this number of samples on a daily basis. Total sample throughput is currently limited by the time required for headspace collection. Shorter sampling times of 30-45 min may increase the number of daily headspace collections without saturating the capacity of a single GC-MS system, a modification which may be suitable for some applications given the exceptionally low LOQ for ethylene under our analytical conditions. However, while increasing the number of biological replicates would have obvious advantages for statistical analyses, the increased handing requirement would also necessitate additional workers available to carry out a higher number of headspace collections with shorter sampling times. Alternatively, the headspace collection segment of this procedure may be simplified by leaving the bag, seal, and inflation tubing assembly in place around the peduncle so that it can be reused without disassembly and reattachment. This alternative technique requires pre-marking the bag at discrete intervals so that it can be cut and opened following each headspace sampling and re-sealed with a known volume the next day. Optimization of this aspect of our headspace sampling technique is currently being developed.

Optimal sensitivity depends on monitoring m/z 26 and 27 fragments unique to ethylene

The detection of ethylene by GC-MS has received little experimental attention despite this technique being ostensibly more sensitive than GC-FID. This is largely due to the nominal molecular mass of ethylene coinciding with that of nitrogen gas, a highly abundant element which produces a high *m/z* 28 background at the comparatively low resolution of a quadrupole mass analyzer. The presence of nitrogen even at low concentrations in the analyzer (typically 1-3% of the PFTBA calibration gas) creates an unacceptably high level of background signal in a low mass discrimination instrument such as a quadrupole, which cannot distinguish the two based on differences in exact mass (elemental nitrogen has a monoisotopic mass of 28.0061 versus 28.0313 for ethylene). While this distinction could be made with a higher resolution instrument such as a time-of-flight mass spectrometer, we have focused on ethylene detection using the mass spectrometer type most commonly found in plant research laboratories.

Nitrogen gas, as the major component of air, is unavoidably co-injected with the sample, representing a large potential source of background noise. We achieved reasonable chromatographic separation of nitrogen present in the sample from ethylene using a Al_2O_3/KCl stationary phase, but persistent background levels of nitrogen continued to limit sensitivity of ethylene when monitoring *m/z* 28. However, apart from its molecular ion, which forms the base peak in its electron impact spectrum, the M-1 (*m/z* 27) and M-2 (*m/z* 26) ions resulting from successive $H^{\cdot}$ radical losses (or, alternatively, H_2 loss) are formed at 62.3% and 52.9% relative abundance, respectively (Figure 2.S3). We exploited these mass peaks, which were absent from the nitrogen spectrum, to reduce detector background noise. Selected ion monitoring (SIM) at *m/z* 26 - 27 yielded a >100-fold improvement in signal-to-noise ratio using a 5 ppm ethylene gas standard (Figure 2.3).

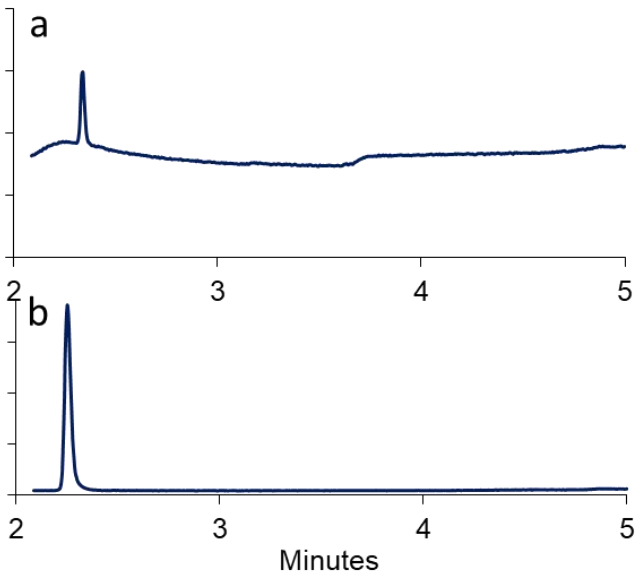

Figure 2.3. The effect of including (**a**) or excluding (**b**) m/z 28 on the signal to noise ratio of ethylene during GC-MS analysis in selected ion mode. High background associated with nitrogen gas is reduced when only m/z 26-27, representing ethylene fragmentation products not produced by nitrogen, are monitored.

Optimizing chromatographic and injection conditions for ethylene analysis

Despite this improvement in signal-to-noise afforded by a SIM method which excluded *m/z* 28, a broad nitrogen gas solvent front originating from the sample was still evident which partially overlapped with the ethylene peak. The appearance of nitrogen gas in this SIM method is not unexpected given incomplete *m/z* discrimination in the quadrupole, especially at the high nitrogen ion concentrations in a headspace sample, leading to partial overlap of the mass traces (i.e., low levels of nitrogen gas ions with a mass of 28 Da reach the detector monitoring *m*/z 26 – 27). This issue is worsened by the large sample injection volumes generally required to detect ethylene in unconcentrated headspace samples, a practice which also compromises the chromatographic separation of nitrogen from ethylene. We found that a pulsed splitless injection significantly improved this situation, resulting in a 2.5-fold increase in ethylene peak area compared to standard splitless injections under the same conditions. This injection technique did not produce a corresponding increase in the nitrogen gas signal. Pulsed splitless injection has been used mainly in pesticide or drug analysis to mitigate matrix effects (Godula et al. 1999) and to profile impurities in illicit drug analysis (Sasaki and Makino 2006), but its use in volatile analysis has been limited. It has, for

instance, been applied to the analysis of parmesan cheese headspace volatiles to identify individual components important for the aroma of the product (Qian and Reineccius 2003). The initial increase in column head pressure which occurs during pulsed splitless injection apparently favors introduction of ethylene gas onto the column. This improvement in ethylene detection may be a result of minimized sample loss through the septum purge valve which is more prominent without pulsed injection.

We achieved the best separation of nitrogen and ethylene under isocratic conditions at 30 ^{0}C in 1.5 min, followed by a steep gradient to 100 ^{0}C to eliminate any other volatile traces present. Under these conditions and using pulsed splitless injection, we calculated a resolution factor of 10.37 for these two gases (Figure 2.S4). A solvent delay of 1.8 min was sufficient to eliminate the nitrogen gas front, which we implemented for routine analysis to reduce wear on the filament. The complete analysis time was 2.6 min. Neither injection port temperature (30 ^{0}C to 150 ^{0}C) nor use of programmable temperature vaporization (PTV) had any effect on the sensitivity toward ethylene.

Head space collection time course using individual melons

Time course measurements were taken to establish the linear range of static ethylene accumulation in *in situ* headspace collection bags and to determine if this volatile collection technique had any observable effect on fruit metabolism or the kinetics of ethylene emission. Headspace incubations of 40 d old commercial hybrid melons showed that ethylene emission could be readily quantified in as little as 15 min of static headspace collection (Figure 2.4). Furthermore, ethylene emission was linear with respect to time over the 3 h time course surveyed (R^2 = 0.973 ±0.023; n = 6), indicating not only that measurements on this time scale were within the linear range of quantification but also that these short head space collection assays did not affect the rate of ethylene emission by the fruit. Static head space measurements of 60 min were routinely made to characterize melon RILs based on the observation that the accumulation of ethylene had no effect on emission rates from the fruit over this period of time. However, shorter sampling times could also be employed while still remaining in the quantifiable range.

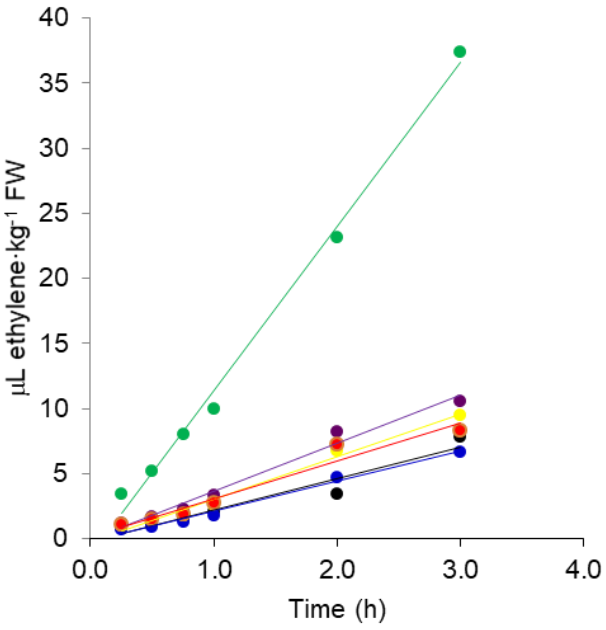

Figure 2.4. Ethylene accumulation time course in in situ headspace chambers containing individual, attached melon fruit. Six individual melons were sealed in headspace collection bags as described in methods. Aliquots were withdrawn from each bag at the time intervals shown and transferred to headspace vials for analysis by GCMS. Colors represent distinct individuals from the same commercial hybrid sampled repeatedly over the time course.

These ethylene emission time courses for individual melons also highlight the value of non-invasive sampling methods to study fruit ripening. We observed a considerable range in individual emission rates from this small sample, with values in the range of 2.29 to 12.6 µL ethylene·kg^{-1} FW·h^{-1} recorded (Table 2.S2). The average value of ethylene emission was 4.35 µL ethylene·kg^{-1} FW·h^{-1} ± 3.55 (coefficient of variance (COV): 0.82) for all melon samples. This implies a high degree of individual variation in ethylene emission rates, even for fruits derived from genetically identical individuals. However, when emission rates were calculated individually for each melon, the average COV within a single time course dropped to 0.20. This suggests that most of the experimental variation originates from biological differences between individuals rather than sampling errors. When time points are averaged from distinct individuals emitting ethylene at different rates, a corresponding increase in standard deviation of our measurements was observed. The capacity to re-sample the same individual melon on successive days and without harvesting, revealing individual variation in time course analyses, illustrates a principle advantage of this non-invasive technique.

Linearity of response with different injection volumes and ethylene concentrations

One of the drawbacks of headspace analysis is the relatively low concentration of analytes in the sample, which often necessitates a concentration step. This problem is exacerbated when multiple, short term headspace sampling experiments must be conducted in parallel in large scale experiments as these short incubation times further reduce analyte concentration. To offset these effects, we evaluated the ability to maintain a linear detector response with increasing injection volumes using ethylene standards. We observed a broad range of linearity with volumes ranging from 50 μL to 2.0 mL (Figure 2.5a) under pulsed splitless injection conditions. We chose 500 μL as the optimal injection volume which balances linearity with sensitivity. We next evaluated the linear range of total ethylene per analysis. We observed a strongly proportional signal between 0.125 nL and 20 nL ethylene (Figure 2.5b). However, the detector showed saturation above this amount. For particularly concentrated samples, the sample volume may be reduced, effectively extending the linear range of this analysis beyond the maximum levels of ethylene produced by ripening melon.

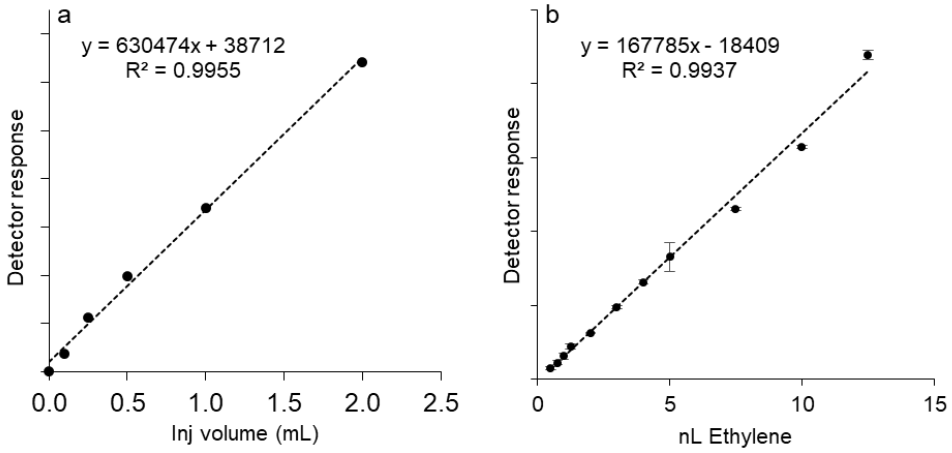

Figure 2.5. Optimization of instrument conditions for ethylene analysis by GCMS. The linear range of headspace injection volume and ethylene concentration were determined. **a.** different volumes of a 5 ppm ethylene standard were injected under identical analytical conditions and plotted against the integrated detector response. **b.** the absolute amount of ethylene gas producing a linear detector response was established using a narrow range of injection volumes of ethylene gas standards at 5, 20, or 50 ppm and plotted against the integrated detector response. Error bars show the standard error of 3 replicates per concentration.

LOD and LOQ of ethylene in fruit headspace samples using GCMS

The burst of ethylene synthesis and emission that characterizes climacteric ripening results in global changes in gene expression and metabolism. This volatile signal is active at concentrations as low as 0.2 $nL \cdot L^{-1}$ in etiolated Arabidopsis seedlings (Binder et al. 2004), but the minimum active concentrations in ripening fruit are not well established. Detection of ethylene at the lowest possible concentrations would offer clear advantages for studying fruit ripening. For example, the presence of ethylene in the headspace around a ripening fruit implies an equal or greater concentration in its interior. The kinetics of ethylene emission is linked to the diffusion rate from the site of biosynthesis inside the fruit to the peel, but this process has not been studied in detail. However, the sudden appearance of ethylene in the head space around the fruit may be taken as an indication that the autocatalytic ethylene production characteristic of climacteric ripening has recently started. In addition, ethylene-dependent and independent regulatory pathways co-exist in both climacteric and non-climacteric fruit (Lelièvre et al. 1997). The respiratory burst is the most marked metabolic and developmental event that characterizes climacteric ripening, but in order to distinguish between ethylene dependent and independent signaling events, the detection of ethylene at the earliest possible stage, and hence the lowest concentration in fruit head space, is desirable. Improvements in ethylene sensitivity are particularly relevant in light of the disappearance of the sharp distinction between climacteric and non-climacteric ripening programs. Lines once to thought to completely lack an ethylene burst may in fact exhibit a burst at trace levels with biological significance, and highly sensitive ethylene detection will assist in the characterization of such lines.

Given the utility of increasing sensitivity of ethylene analysis to address these biological questions, we evaluated the sensitivity of the method described herein by calculating the LOD and LOQ as 0.41 ± 0.04 $nL \cdot L^{-1}$ ($n = 18$) and 1.37 ± 0.13 $nL \cdot L^{-1}$, respectively ($n = 18$). The reproducibility of this analysis was examined by repeated sampling of reference and melon headspace samples, yielding a coefficient of variation of 0.019 ($n = 24$). This level of sensitivity is similar to that of laser based sensors (Cristescu et al. 2013), which are currently the most sensitive ethylene detectors available for commercial use. The high level of reproducibility reduces the number of technical replicates necessary for accurate

measurements, permitting a larger number of independent biological replicates to be analyzed in the same time frame.

Effect on storage time and temperature on ethylene recovery

One practical objective of the method described here is to maximize the number of individual fruits which can be analyzed in a single day to accommodate the high work flows typical of the pre-harvest period and increase the number of biological replicates needed to screen RIL populations. We determined that a key factor in maximizing sample throughout was to separate headspace sampling from the analysis phase so that a larger number of samples could be collected during the day, while automated analysis takes place throughout the night. Due to possible diurnal rhythms associated with ethylene emission, we restricted sample collection to a narrow period of the day, further necessitating the need to simplify sample collection during this period. Compared to hand held sensors which measure ethylene directly in the greenhouse, we estimate that the uncoupling of these two steps results in an approximately 2.5 fold gain in the number of samples processed. The continuous collection and analysis of headspace samples during the pre-harvest season using a single GCMS system requires that all sample analysis be completed within 24h of sample collection. To determine the stability of these headspace samples over this time interval and account for any potential loses during storage, we evaluated the effect of storage time and temperature on ethylene reference standards. Detectable ethylene in headspace vials decreased in a linear fashion over time and showed a strong temperature dependence (Figure 2.6). After 24h of storage at -20 ^{0}, the 5 ppm reference samples had lost an average of 50% while samples stored at 4 ^{0} and RT had lost 18 and 23%, respectively. After 48 h, those losses had increased to 71, 40 and 51% for the sample three storage temperatures. These data underscore the importance of preparing reference standards at the same time head space samples are collected and to store the calibration standards under identical conditions as the samples prior to analysis. The temperature dependence of ethylene recovery indicates that the best storage temperature for these headspace samples is 4°C. Samples stored at lower temperatures appear to suffer higher losses, possibly due to shrinkage of the septum seal at low temperatures.

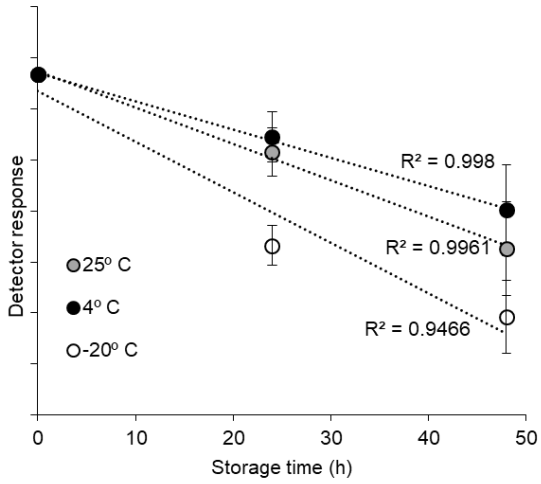

Figure 2.6. Effect on storage time and temperature on ethylene standard in headspace vials. Headspace samples obtained from ripening fruit are collected in the greenhouse and transported to the laboratory for analysis. Losses over time were estimated by preparing ethylene gas standards (5 ppm) in sealed headspace vials and analyzing by GC-MS after the indicated storage times at 25, 4, or -20 °C. Error bars represent the standard error of 5 independent measurements.

Ethylene emission in melon RILs shows variation in both intensity and duration

We applied this method to the quantification of ethylene emissions in the developing fruit of melon RILs derived from a cross of full climacteric ("Védrantais"; Ved) and non-climacteric (Piel de Sapo; PS) parental lines throughout their growing period (Figure 2.7a). Headspace samples of a single melon fruit from 11 RILs were monitored beginning 24-35 days after pollination (DAP) and ending after the characteristic peak of ethylene, around 35-53 DAP. In most cases, we observed a single sharp ethylene peak which reached its maximum between 32 and 51 DAP. Maximum peak amplitude varied over a more than 70-fold range among this representative groups of RILs, with lines peaking at as little as 3.3 μL ethylene·kg^{-1} FW·h^{-1} (line 190; Figure 2.7b) or as much as 239 μL·kg^{-1} FW·h^{-1} (line 203; Figure 2.7a). The parental lines of the population and the F1 hybrid derived from them were also monitored. The PS parental line did not produce detectable ethylene, consistent with its previous assignment as a non-climacteric line, while the Ved parental line emitted maximal ethylene concentrations of 87 μL ethylene·kg^{-1} FW·h^{-1}. The hybrid line produced intermediate levels of ethylene, peaking at 27 μL ethylene·kg^{-1} FW·h^{-}1 34 DAP. Surprisingly, two RILs, 203 and 116, produced ethylene levels greater than the Ved parental line. This indicated that crossing a

highly climacteric line with a non-climacteric one results in a transgressive segregation for this trait.

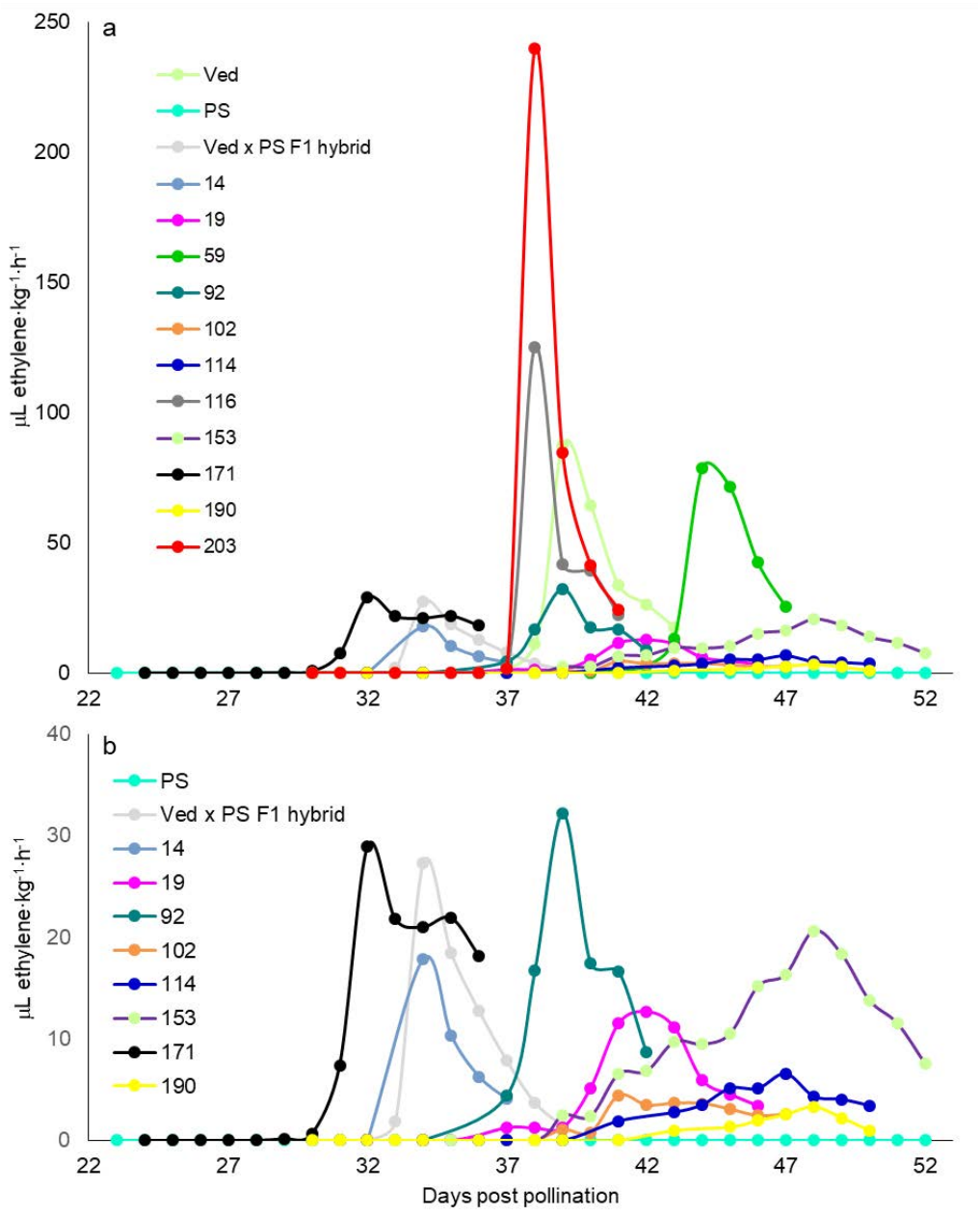

Figure 2.7. Ethylene emission time course of melon RILs obtained from a cross of a climacteric (Ved) and non-climacteric (PS) lineages. Among the higher emitting lines (**a**), the F1 hybrid (light grey) showed intermediate levels of ethylene emission between Ved and PS, while several RILs (203 in red and 116 in dark grey) surpassed the ethylene emission of the climacteric parent, Ved (light green). The ethylene emission profiles of RILs emitting lower levels of ethylene (shown in close up in **b** with higher emitting lines removed for clarity), display a broad range of intensity and duration of ethylene emission. For each line, a single melon was sampled on alternate days from approximately 23 to 52 DPA.

We also observed considerable variation in the duration of ethylene emission in our RILs and parental lines. In order to compare ethylene production between lines, we applied the chromatographic term peak width at half height ($W_{1/2}$) to describe the sharpness of the measured daily ethylene output as a function of time. Line 203, which displayed the highest peak of ethylene production, had a $W_{1/2}$ of approximately 2.5 days. The $W_{1/2}$ of Ved was similar, even though it displayed less than half the maximal ethylene emission. Line 19, whose maximal ethylene emission barely exceeded 12 μL ethylene·kg^{-1} FW·h^{-1}, showed a $W_{1/2}$ of about 4 days. Other lines, such as 153, showed a gradual rise and decline spanning nearly two weeks. Thus, both the intensity and duration of ethylene emission can vary substantially, leading to many intermediate patterns of ethylene production starting with two parental extremes. This proof of concept study demonstrates the efficacy of this method in characterizing members of a melon RIL population derived from two parents representing two poles of the climacteric ripening spectrum. The non-invasive detection of ethylene in these fruit is a powerful tool with which to dissect the genetic factors controlling ethylene-dependent ripening processes. The values obtained for the climacteric control in this experiment (Ved) are significantly higher than those reported in Saladié et al. (2015) in which ethylene was measured in headspace of detached fruit. One possible explanation is that detachment alters fruit development, resulting in an underestimation of true ethylene levels. This non-invasive method likely reflects the physiological state of ripening fruit in more realistic terms and thus provides more reliable measures of ethylene emissions.

Ethylene headspace analysis in other climacteric fruits: tomato

We further tested the applicability of this method in other climacteric species. Tomato represents a climacteric crop of major economic importance and is the model species for climacteric ripening studies. We therefore adapted our method to measuring ethylene in the headspace around ripening tomatoes leading up to and beyond the breaker stage (Figure 2.S5a-c). Fruit such as tomato which develop on racemes, versus single pedicels as in the case of melon, present special considerations for sampling headspace as the heterogeneity in developmental states within the same raceme could potentially dilute the accuracy of such measurements. We therefore pruned racemes to a single fruit and measured individuals as they developed from green to the breaker stage and again at the red ripe stage. In addition,

we assayed complete racemes with no pruning at the ripe stage to determine if any residual ethylene could be detected (Figure 2.S5, d). We observed that while considerable variation exists in absolute ethylene intensity among a random assortment of commercial tomato varieties, all showed the expected peak of ethylene production at the breaker stage, while far less (or none) was detected by the same fruits at the immature green or red ripe stages (Figure 2.S6). Trace detection of ethylene in individual green tomatoes may signify that the metabolic transition to the mature green or breaker stage has commenced before phenotypic changes are apparent, providing an independent means of detecting this transition when no visual clues are available. In contrast, residual ethylene detected in red tomatoes may indicate that the ripening process is not yet complete. Only trace levels were detected from red ripe fruit when racemes were left intact (not shown), consistent with our results using individual tomatoes, suggesting that assays on individual fruit following pruning did not alter ethylene emission in any obvious fashion. These results indicated that despite differences in plant architecture, this headspace sampling method could be applied to other climacteric species besides melon, although the implementation of cultivation methods specific to that species may be necessary to isolate individual fruits for measurement.

Conclusions

This method for ethylene analysis features several technical improvements that further improve sensitivity, putting GC-MS based analysis on par with dedicated optical sensors. This methodology, aimed at plant scientists with access to ordinary analytical instrumentation, has been applied here to the characterization of melon RILs. While the method we describe relies on an automated headspace sampler, manual injections with a gas tight syringe can also be performed using any single quadrupole GC-MS system, albeit with a reduction in throughput. We find that both the amplitude and duration of the ethylene burst typical of climacteric ripening can vary considerably. This further dispels the notion of climacteric ripening as an on/off process and provides experimental support for the possibility of fine gradations in ethylene production, which ultimately depend on a combination of wide ranging genetic factors. While we have applied this method to melon, it is equally applicable to similar studies of other climacteric fruit, including tomato, banana,

or apple. Such studies would also benefit from the non-invasive nature of this technique and permit the monitoring of individual fruits over the course of their ripening season. We are currently in the process of identifying new quantitative trait loci responsible for ethylene production and climacteric fruit ripening in this melon RIL population. Future work will continue to dissect the role of ethylene in directing this complex developmental process, which ultimately provides an important portion of the fresh produce in the diets of many people across the globe.

Acknowledgements

The authors wish to thank Jason Argyris for his assistance developing the headspace collection technique and in performing quantitative real-time PCR assays and Gerard Castro for filming the demonstration video. The authors also extend their gratitude to Semillas Fitó, S.A. for providing seeds and other plant materials and to Jordi Giné for assistance with ethylene detection. This work was supported in part by a grant from the Spanish Ministry of Science and Innovation (MICINN project GEN2006-27773-C2-1-E to JGM) and the University of Toronto Missisauga Research and Scholarly Activity Fund (to MAP). The authors declare no conflict of interest.

Supplementary Material

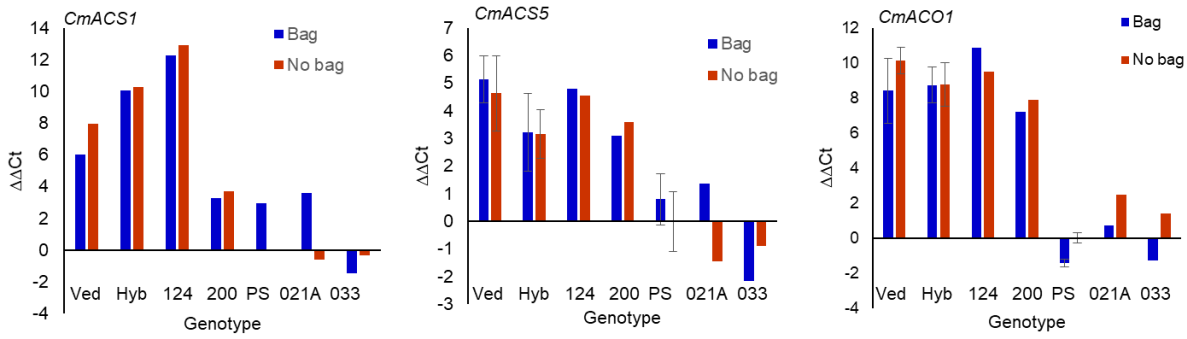

Figure 2.S1. Effect of headspace sampling in in situ collection chambers on the expression of melon ethylene biosynthetic genes. RNA from pure climacteric (Ved), hybrid (Hyb), non-climacteric (PS) or RILs derived from the climacteric *x* non-climacteric hybrid was extracted and converted to cDNA. Transcripts for the ethylene biosynthetic genes amino cyclopropane carboxylate synthase (*CmACS1, CmACS5*), and aminocyclopropane carboxylate oxidase (*CmACO1*) were quantified by QPCR using cyclophilin (*CmCYP7*) as a normalizer. No significant differences between fruits enclosed in headspace collection chambers and untreated control fruits were observed.

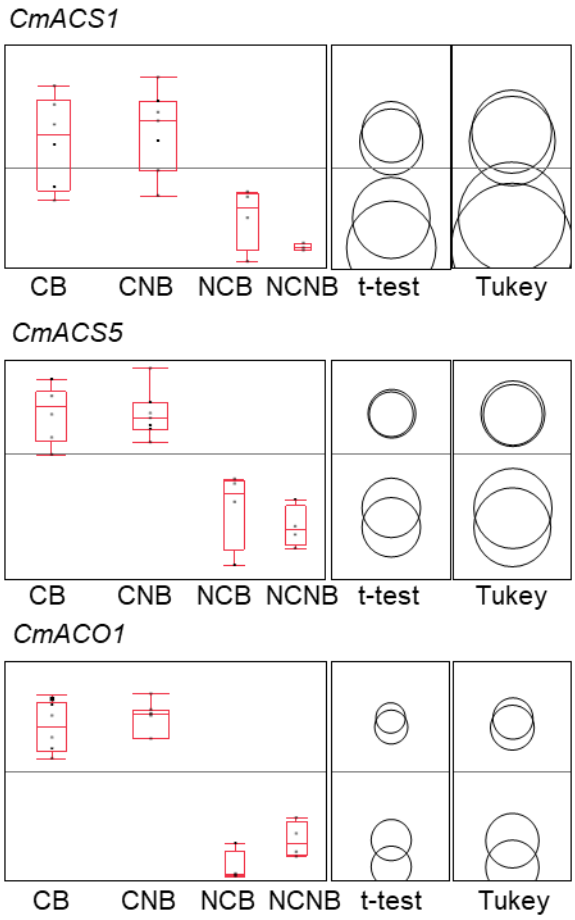

Figure 2.S2. Box plot analysis and tests for statistical significance of transcript levels of ethylene biosynthetic genes in treated or control melon fruit. Possible effects of the sampling technique on ethylene production were investigated by comparing the ethylene biosynthetic genes *CmACS1*, *CmACS5* and *CmACO1* from climacteric fruit enclosed in headspace sampling bags (CB), climacteric fruit with no headspace bag treatment (CNB), non-climacteric fruit enclosed in headspace bags (NCB), or non-climacteric fruit with no bag treatment (NCNB). Significant differences were observed between climacteric and non-climacteric fruits, but no differences were observed as a result of enclosure in headspace collection bags based on t-test and Tukey's test results. These data are summarized in table 2.S2.

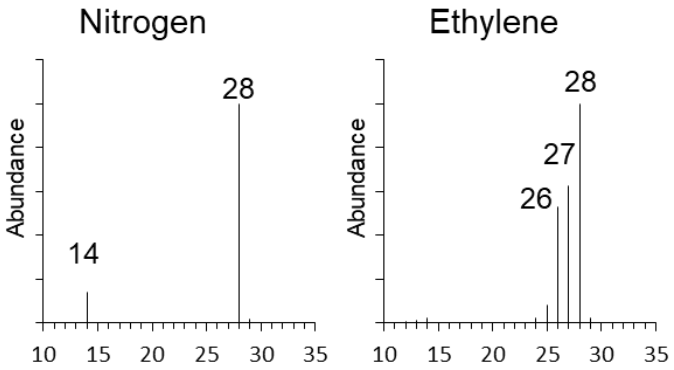

Figure 2.S3. Electron impact mass spectra of ethylene and nitrogen gas taken at 70 eV and full scan conditions. The ethylene spectrum features unique ions at m/z 26 and 27 resulting from successive hydrogen losses, or alternatively, loss of H2 directly. Selected ion monitoring of these two ions resulted in an improvement in the signal-to-noise ratio in the presence of nitrogen gas.

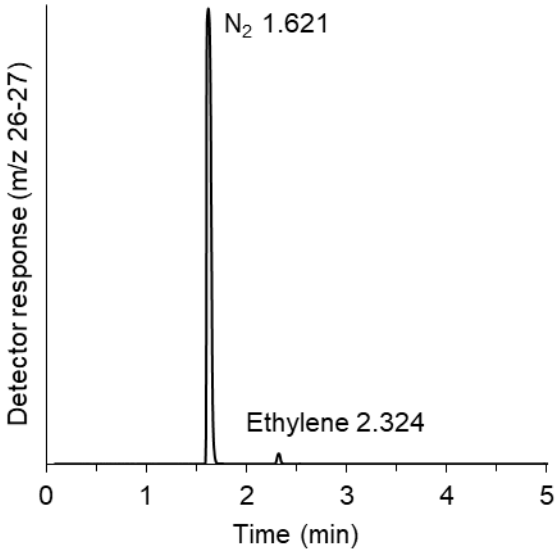

Figure 2.S4. Chromatographic separation of ethylene and nitrogen gas on an Al_2O_3/KCl capillary column using pulsed splitless injection and selected ion monitoring. We calculated the resolution factor, $R = (t_{R2}-t_{R1})/(0.5*(w_1+w_2)$, where t_R represents the retention time and *w* the peak width at baseline of these two analytes, and obtained a value of 10.37. Peaks widths for nitrogen and ethylene were measured as 0.076 and 0.060 min, respectively. Note the strong signal produced by nitrogen (MW = 28) when monitoring *m/z* 26-27 due to incomplete *m/z* discrimination in the quadrupole and high abundance of nitrogen ions in the sample.

Figure 2.S5. Ethylene headspace sampling in tomato at the green (a), breaker (b), and ripe (c) stages. The sealed, inflated polyamide bags were sampled following a 1 h incubation as for the melon samples and analyzed for ethylene content by GCMS as described in methods. In some cases, racemes were pruned to leave a single fruit to reduce the error incurred by sampling fruit at different stages. In others, untouched ripe racemes were sampled collectively (d).

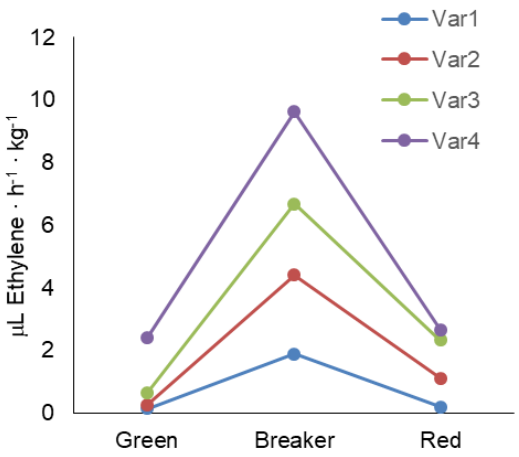

Figure 2.S6. Production of ethylene in single tomato fruits measured with a non-invasive headspace sampling technique at various stages of development. A selection of distinct varieties was chosen to illustrate that despite considerable variation in absolute ethylene emission levels, the peak of ethylene production associated with the breaker stage is conserved across lines.

Table 2.S1. Variation in ethylene headspace accumulation rates among individual melons

Melon	Linear regression	R^2
1	y = 2.42x - 0.216	0.935
2	y = 12.6x - 1.15	0.994
3	y = 2.29x - 0.177	0.988
4	y = 3.26x - 0.217	0.986
5	y = 3.68x - 0.019	0.981
6	y = 2.91x + 0.174	0.953

Table 2.S2. Test for statistically significant differences in ethylene biosynthetic gene expression in treated (bagged) or untreated control (non-bagged) melon fruit used in non-invasive headspace sampling.

Tukey method	*CmACO1*	*CmACS1*	*CmACS5*
Non-climacteric	0.2433	0.7445	0.6808
Climacteric	0.8407	0.9655	0.9745

T-test method	*CmACO1*	*CmACS1*	*CmACS5*
Non-climacteric	0.0673	0.3262	0.8762
Climacteric	0.4194	0.6476	0.9985

Digital Supplementary Material

Table 2.S3. Primer sequences used in this study.

Movie 2.S1. Non-invasive, *in situ* headspace collection of attached fruit.

References

Argyris J.M., Pujol M., Martín-Hernández A.M., Garcia-Mas J. (2015) Combined use of genetic and genomics resources to understand virus resistance and fruit quality traits in melon. *Physiologia Plantarum* **155**, 4-11.

Ayub R., Guis M., BenAmor M., Gillot L., Roustan J.P., Latche A., Bouzayen M., Pech J.C. (1996) Expression of ACC oxidase antisense gene inhibits ripening of cantaloupe melon fruits. *Nature Biotechnology* **14**, 862-866.

Balachandran M.D., Shrestha S., Agarwal M., Lvov Y., Varahramyan K. (2008) SnO_2 capacitive sensor integrated with microstrip patch antenna for passive wireless detection of ethylene gas. *Electronics Letters* **44**, 464-465.

Bassi P., Spencer M. (1989) Methods for the quantification of ethylene produced by plants. In: Linskens H, Jacksons J (eds) *Gases in plant and microbial cells. Modern methods of plant analysis.* vol 9. Springer, Berlin, pp 309-321

Binder B.M., Mortimore L.A., Stepanova A.N., Ecker J.R., Bleecker A.B. (2004) Short-Term Growth Responses to Ethylene in *Arabidopsis* Seedlings Are EIN3/EIL1 Independent. *Plant Physiology* **136**, 2921-2927.

Borch K., Bouma T.J., Lynch J.P., Brown K.M. (1999) Ethylene: a regulator of root architectural responses to soil phosphorus availability. *Plant, Cell & Environment* **22**, 425-431.

Cajka T., Fiehn O. (2016) Toward merging untargeted and targeted methods in mass spectrometry-based metabolomics and lipidomics. *Analytical Chemistry* **88**, 524-545.

Cristescu S.M., Mandon J., Arslanov D., De Pessemier J., Hermans C., Harren F.J.M. (2013) Current methods for detecting ethylene in plants. *Annals of Botany* **111**, 347-360.

Díaz J., ten Have A., van Kan J.A.L. (2002) The Role of ethylene and wound signaling in resistance of tomato to *Botrytis cinerea*. *Plant Physiology* **129**, 1341-1351.

Eduardo I., Arús P., Monforte A.J. (2005) Development of a genomic library of near isogenic lines (NILs) in melon (*Cucumis melo* L.) from the exotic accession PI161375. *Theoretical and Applied Genetics* **112**, 139-148

Esser B., Schnorr J.M., Swager T.M. (2012) Selective Detection of Ethylene Gas Using Carbon Nanotube-based Devices: Utility in Determination of Fruit Ripeness. *Angewandte Chemie-International* **51**, 5752-5756.

Ezura H., Owino W.O. (2008) Melon, an alternative model plant for elucidating fruit ripening. *Plant Science* **175**, 121-129.

Fernández-Trujillo J.P., Obando-Ulloa J.M., Martínez J.A., Moreno E., García-Mas J., Monforte A.J. (2008) Climacteric and non-climacteric behavior in melon fruit: 2. Linking climacteric pattern and main postharvest disorders and decay in a set of near-isogenic lines. *Postharvest Biology and Technology* **50**, 125-134.

Gane R. (1934) Production of ethylene by some ripening fruits. *Nature* **134**, 1008-1008.

Garcia-Mas J., Benjak A., Sanseverino W., *et al.* (2012) The genome of melon (*Cucumis melo* L.). *Proc Natl Acad Sci USA* **109**, 11872-11877.

Giovannoni J.J. (2004) Genetic Regulation of Fruit Development and Ripening. *The Plant Cell* **16** (suppl 1):S170-S180.

Godula M., Hajslova J., Alterova K. (1999) Pulsed splitless injection and the extent of matrix effects in the analysis of pesticides. *Journal of High resolution chromatography* **22**, 395-402

Jordan L.R., Hauser P.C., Dawson G.A. (1997a) Amperometric sensor for monitoring ethylene. *Analytical Chemistry* **69**, 558-562.

Jordan L.R., Hauser P.C., Dawson G.A. (1997b) Portable trap-sensor system for monitoring low levels of ethylene. *Analyst* **122**, 811-814.

Jung J.Y., Shin R., Schachtman D.P. (2009) Ethylene Mediates Response and Tolerance to Potassium Deprivation in *Arabidopsis*. *The Plant Cell* **21**, 607-621

Kume A., Tsuboi N., Nakatani N., Nakane K., Sakurai N., Nakagawa N., Sakugawa H. (2001) Measurement of ethylene emission from Japanese red pine (*Pinus densiflora*) under field conditions in NOx-polluted areas. *Environmental Pollution* **111**, 389-394.

Lambertus G.R., Fix C.S., Reidy S.M., Miller R.A., Wheeler D., Nazarov E., Sacks R. (2005) Silicon microfabricated column with microfabricated differential mobility spectrometer for GC analysis of volatile organic compounds. *Analytical Chemistry* **77**, 7563-7571.

Lelièvre J.M., Latchè A., Jones B., Bouzayen M., Pech J.C. (1997) Ethylene and fruit ripening. *Physiologia Plantarum* **101**, 727-739.

Paul V., Pandey R., Srivastava G.C. (2012) The fading distinctions between classical patterns of ripening in climacteric and non-climacteric fruit and the ubiquity of ethylene-An overview. *Journal of Food Science and Technology* **49**, 1-21.

Pech J.C., Balague C., Latche A., Bouzayen M. (1994) *Postharvest physiology of climacteric fruits : recent developments in the biosynthesis and action of ethylene*, vol 14. vol 1. Paris, France: Lavoisier

Pech J.C., Bouzayen M., Latche A. (2008) Climacteric fruit ripening: Ethylene-dependent and independent regulation of ripening pathways in melon fruit. *Plant Science* **175,** 114-120.

Pham-Tuan H., Vercammen J., Devos C., Sandra P. (2000) Automated capillary gas chromatographic system to monitor ethylene emitted from biological materials. *Journal of Chromatography A* **868**, 249-259.

Pieterse C.M.J., Leon-Reyes A., Van der Ent S., Van Wees S.C.M. (2009) Networking by small-molecule hormones in plant immunity. *Nat Chem Biol* **5,** 308-316

Pratt H., Goeschl J., Martin F. (1977) Fruit growth and development, ripening, and the role of ethylene in the "Honey Dew" muskmelon. *Journal American Society for Horticultural Science* **102**, 203–210.

Qian M., Reineccius G. (2003) Static Headspace and Aroma Extract Dilution Analysis of Parmigiano Reggiano Cheese. *Journal of Food Science* **68,** 794-798.

Saladié M., Cañizares J., Phillips M.A., Rodriguez-Concepcion M., Larrigaudière C., Gibon Y., Stitt M., Lunn J.E., Garcia-Mas J. (2015) Comparative transcriptional profiling analysis of developing melon (*Cucumis melo* L.) fruit from climacteric and non-climacteric varieties. *BMC Genomics* **16.**

Sasaki T., Makino Y. (2006) Effective injection in pulsed splitless mode for impurity profiling of methamphetamine crystal by GC or GC/MS. *Forensic Science International* **160**, 1-10

Schröder R., Cristescu S.M., Harren F.J.M., Hilker M. (2007) Reduction of ethylene emission from Scots pine elicited by insect egg secretion. *J Exp Bot* **58**, 1835-1842.

Tarkowská D., Novák O., Floková K., Tarkowski P., Turečková V., Grúz J., Rolčík J., Strnad M. (2014) Quo vadis plant hormone analysis? *Planta* **240**, 55-76

Thain S.C., Vandenbussche F., Laarhoven L.J.J., Dowson-Day M.J., Wang Z.Y., Tobin E.M., Harren F.J.M., Millar A.J., Van Der Straeten D. (2004) Circadian rhythms of ethylene emission in *Arabidopsis*. *Plant Physiology* **136**, 3751-3761.

Van Meulebroek L., Bussche J.V., Steppe K., Vanhaecke L. (2012) Ultra-high performance liquid chromatography coupled to high resolution Orbitrap mass spectrometry for metabolomic profiling of the endogenous phytohormonal status of the tomato plant. *Journal of Chromatography A* **1260**, 67-80.

Vegas J., Garcia-Mas J., Monforte A.J. (2013) Interaction between QTLs induces an advance in ethylene biosynthesis during melon fruit ripening. *Theor Appl Genet* **126**, 1531-1544.

Vergara R., Parada F., Rubio S., Pérez F.J. (2012) Hypoxia induces H2O2 production and activates antioxidant defence system in grapevine buds through mediation of H2O2 and ethylene. *J Exp Bot* **63**, 4123-4131

Wahl E.H., Tan S.M., Koulikov S., Kharlamov B., Rella C.R., Crosson E.R., Biswell D., Paldus B.A. (2006) Ultra-sensitive ethylene post-harvest monitor based on cavity ring-down spectroscopy. *Opt Express* **14**, 1673-1684.

Weidmann D., Kosterev A.A., Roller C., Curl R.F., Fraser M.P., Tittel F.K. (2004) Monitoring of ethylene by a pulsed quantum cascade laser. *Appl Opt* **43**, 3329-3334.

Xie L., Ying Y., Ying T. (2009) Rapid determination of ethylene content in tomatoes using visible and short-wave near-infrared spectroscopy and wavelength selection. *Chemometrics and Intelligent Laboratory Systems* **97**, 141-145.

Yamaguchi M., Hughes D.L., Yabumoto K., Jennings W.G. (1977) Quality of cantaloupe muskmelons: Variability and attributes. *Scientia Horticulturae* **6**, 59-70.

Zevenbergen M.A.G., Wouters D., Dam V.A.T., Brongersma S.H., Crego-Calama M. (2011) Electrochemical sensing of ethylene employing a thin ionic-liquid layer. *Analytical Chemistry* **83**, 6300-6307.

Chapter 3

Genetic dissection of fruit ripening behaviour and ethylene production in a melon RIL population

Genetic dissection of fruit ripening behaviour and ethylene production in a melon RIL population

Lara Pereira[1], Valentino Ruggieri[1,2], Jason Argyris[1,2], Michael A. Phillips[3], Marta Pujol[1,2], Jordi Garcia-Mas[1,2*]

[1]Centre for Research in Agricultural Genomics (CRAG) CSIC-IRTA-UAB-UB, Edifici CRAG, Campus UAB, 08193 Cerdanyola, Barcelona, Spain

[2]IRTA (Institut de Recerca i Tecnologia Agroalimentàries), Barcelona, Spain

[3]Department of Biology, University of Toronto–Mississauga, Mississauga, ON L5L 1C6, Canada

Lara Pereira: lara.pereira@cragenomica.es

Valentino Ruggieri: valentino.ruggieri@irta.cat

Jason Argyris: jason.argyris@irta.cat

Michael A Phillips: michaelandrew.phillips@utoronto.ca

Marta Pujol: marta.pujol@irta.cat

Jordi Garcia-Mas: jordi.garcia@irta.cat

Manuscript in preparation, to be submitted to Journal of Experimental Botany

Abstract

Fruit ripening is an important physiological process with major impact in fruit quality. Fleshy fruits are classified in climacteric or non-climacteric depending on the role of the hormone ethylene, although the genetic basis of ripening is not totally understood. Recently, melon has been proposed as an alternative model to study climacteric ripening due to the segregation of ripening behaviour within the species. Here we used a melon RIL population funded by a *cantalupensis* (highly climacteric) x *inodorus* (non-climacteric) cross. A QTL mapping experiment, using a GBS-based genetic map, allowed to identify several QTLs controlling ethylene production, earliness of climacteric ripening and diverse ripening-associated traits as aroma production, chlorophyll degradation and abscission layer formation. A major QTL, named *ETHQV8.1*, was detected for almost all the studied traits, including maximum ethylene production. Two families of introgression lines were used to validate the QTL and fine map it, leading to a narrow interval of 154 kb that contains 14 annotated genes. Other QTLs contributing to climacteric behaviour to a lesser extent were identified in other melon chromosomes, some of them in narrow intervals of 1 Mb containing around one hundred genes. Our work provides new insights into melon fruit ripening, proving that it is governed by polygenic inheritance and confirming that a continuum spectrum of climacteric behaviour exists, rather than two categorical classes.

Key words: climacteric ripening, QTL, melon, RIL, ethylene, genetic map

Introduction

Fleshy fruits are an important component of human diet as source of nutritional compounds and vitamins. Once fruit growth has been accomplished, fleshy fruits suffer a series of physiological and metabolic changes to become edible and attractive to animals, which is necessary for seed dispersal (Giovannoni *et al.*, 2017). Among these changes, sugar and organic acid accumulation, loss of firmness, color change and synthesis of volatiles commonly occur. Fleshy fruits are classified in two physiological groups depending on the involvement of the hormone ethylene during ripening: climacteric and non-climacteric. Climacteric fruits show a transient rise in respiration accompanied of autocatalytic synthesis of ethylene at the onset of ripening, leading to a

peak of this hormone that, by contrast, is absent in non-climacteric fruits (Lelievre *et al.*, 1997). It has been suggested that, at least partially, some overlapping exists between both types of ripening (Bemer *et al.*, 2012; Osorio *et al.*, 2012).

In climacteric fruits, the presence of ethylene is necessary to trigger multiple responses, among them the flesh softening, mediated by cell wall degrading enzymes; the accumulation of pigments as flavonoids and carotenes in parallel with chlorophyll degradation; the synthesis of sugars, organic acids and a diverse array of volatiles; and the formation of an abscission layer in the pedicel (Giovannoni, 2007). Tomato is considered the biological model to understand climacteric fruit ripening. Two enzymes of the biosynthetic pathway of ethylene, 1-aminocyclopropane-1-carboxylate (ACC) synthase and ACC oxidase, are regulated in a fine and complex way by transcription factors (TFs) as *RIN* (Vrebalov *et al.*, 2002), *NOR* (Giovannoni, 2007) and *CNR* (Manning *et al.*, 2006). In addition, other TFs modulating the initiation or evolution of fruit ripening have been characterized, as *FUL1/FUL2* (Bemer *et al.*, 2012; Shima *et al.*, 2014), *AP2a* (Chung *et al.*, 2010), *GLK2* (Powell *et al.*, 2012), *TAGL1* (Vrebalov *et al.*, 2009) and *HB-1* (Lin *et al.*, 2008). Mutations or overexpression of these TFs influence ethylene production and some of its downstream effects. Recently, several studies have proved that DNA demethylation has a major influence in controlling the onset of fruit ripening (Zhong *et al.*, 2013; Liu *et al.*, 2015; Lang *et al.*, 2017).

The use of mutants for some of the TFs described above has shown that several ripening responses are compromised if TFs are non-functional, giving rise to unripe fruits or fruits with a substantial delay in ripening when compared to wild type fruits. However, most of these processes are successfully achieved in non-climacteric fruits, probably through a combination of common mechanisms (Seymour *et al.*, 2011) and different hormonal pathways (Cherian *et al.*, 2014).

Although many advances have been achieved in understanding climacteric ripening in tomato, knowledge of the fruit ripening process in other crops is scarce (Mcatee *et al.*, 2015; Minas *et al.*, 2015; Elitzur *et al.*, 2016). Melon (*Cucumis melo* L.) has been proposed as an alternative model to understand fruit ripening due to the coexistence of climacteric and non-climacteric varieties within the same species (Ezura and Owino, 2008). Melons show a wide range of climacteric degree, from the typical climacteric varieties belonging to the *cantalupensis* group as the French cultivar cv. Védrantais to the

non-climacteric varieties from the *inodorus* group as cv. Piel de Sapo (Saladié *et al.*, 2015). The changes promoted by ethylene during melon fruit ripening are slightly different to those described in tomato. Silencing of *CmACO1* in a cv. Védrantais background allowed to determine which ripening processes were ethylene-dependent (Ayub *et al.*, 1996). Unlike in tomato, flesh carotenoid and sugar accumulation, acidity and, partially, flesh softening are ethylene-independent in melon (Pech *et al.*, 2008). QTLs controlling climacteric ripening and ethylene production have been described in segregating populations obtained from melon accessions showing different ripening behaviours (Périn *et al.*, 2002; Vegas *et al.*, 2013; Perpiñá *et al.*, 2016). So far only one of these QTLs, *ETHQV6.3*, has been cloned. An introgression of the non-climacteric accession PI 161375, containing *ETHQV6.3*, into the non-climacteric PS induced climacteric ripening (Vegas *et al.*, 2013). The *ETHQV6.3* underlying gene is *CmNAC-NOR*, the orthologue of the tomato *NOR* (Ríos *et al.*, 2017), suggesting that common mechanisms are involved in the control of climacteric ripening in both species.

A recombinant inbred line (RIL) population from a cross between cv. Védrantais (climacteric) and cv. Piel de Sapo (non-climacteric) has been developed and utilized to map QTLs related to fruit quality and morphology (Pereira *et al*., submitted). The aim of this work was to characterize the ethylene production and climacteric ripening behaviour in this RIL population to identify additional genetic factors that regulate this process in melon.

Materials and methods

Plant material

Plant material was grown in greenhouse at Caldes de Montbui (Barcelona). Plants were pruned weekly and pollinations were executed manually, allowing to develop only one fruit per plant. The harvest point was determined by the following criteria: a) abscission date when the fruit abscised; b) seven days after the appearance of any symptom of climacteric ripening in absence of abscission; c) at 60-62 days after pollination (DAP) when fruits were non-climacteric.

The RIL population used in this work was described in Pereira *et al*. (submitted). Briefly, the population was developed from a cross between cv. Védrantais (Ved) (ssp. *melo*,

cantalupensis group) and cv. Piel de Sapo T111 (PS) (ssp. *melo*, *inodorus* group) and contained 89 RILs. Five blocks (T1-T5), consisting in a unique fruit per RIL and 1-3 fruits per control line (Ved, PS and the F1 (Hyb)) were grown during the summers of 2015 and 2016 (Pereira *et al*., submitted).

The three blocks from 2015 (T1-T3) were sowed and planted with a delay between them of 20 days approximately. Although all the phenotypic evaluations were performed within the summer period (July-September) and the conditions in the greenhouse were partially controlled, we considered them as independent trials. The two blocks from 2016 (T4-T5) were planted at the same time, but were treated as independent trials to have a homogeneous design.

Two introgression line (IL) collections were obtained from the F1 of the Ved x PS cross after three backcrosses with the recurrent parentals Ved and PS, respectively (data not shown). Two families of ILs (720 and 414), containing introgressions in chromosome VIII of PS and Ved in the background of Ved and PS, respectively, were evaluated during the summer of 2016 (family 720, n=18 and family 414, n=12, respectively) and the progenies of two recombinant individuals of the 414 family (414.1, n=11 and 414.17, n= 15) during the autumn of 2017.

Phenotyping of climacteric ripening traits

Three ripening-related traits were evaluated as qualitative (production of aroma (ARO), chlorophyll degradation (CD) and abscission (ABS)) and six as quantitative (Table 3.1). Traits were divided in four different groups according to the physiological response to the production of ethylene: biosynthesis of volatiles leading to a sweet aroma (ARO and EARO), change of color mainly due to chlorophyll degradation (CD and ECD), abscission layer formation (ALF) in the pedicel of the fruit, provoking abscission in some cases (EALF, ABS, EABS and HAR) and softening of fruit flesh (FIR). The visual inspection of melon fruits, attached to the plant, was performed daily, from approximately 25 DAP until harvest. In addition, individual pictures of the fruits were obtained weekly. ARO and CD were recorded as 0 = absence and 1 = presence. ABS was recorded using an index from 0, no abscission layer formation; 1, subtle and/or partial ALF; 2, almost complete ALF with obvious scar; and 3, total ALF generally with fruit abscission. The earliness of ALF (EALF), abscission (EABS), aroma production (EARO) and chlorophyll degradation (ECD) were also recorded. The aroma production was evaluated each day by

smelling the fruits. Fruit flesh firmness was measured at harvest using a penetrometer (Fruit Test^{TM}, Wagner Instruments), in at least three regions of the fruit (distal, proximal and median), and the mean value was registered.

Table 3.1. Description and code of climacteric ripening traits and ethylene production evaluated in the RIL population.

Trait (units)	**Code**
Production of aroma	ARO
Earliness of production of aroma (DAP)	EARO
Chlorophyll degradation	CD
Earliness of chlorophyll degradation (DAP)	ECD
Earliness of abscission layer formation (DAP)	EALF
Abscission	ABS
Earliness of abscission (DAP)	EABS
Harvest date (DAP)	HAR
Flesh firmness ($kg \cdot cm^{-2}$)	FIR
Maximum ethylene production ($\mu L\ eth \cdot L^{-1} \cdot kg^{-1}$)	ETH
Earliness of ethylene production (DAP)	DAPE
Earliness of ethylene peak (DAP)	DAPP
Width of ethylene peak (days)	WEP

Ripening-related traits were phenotyped in the five blocks of the RIL population (T1-T5). The introgression lines (ILs) were evaluated in 2017 following the same criteria.

Ethylene production

Ethylene production in attached melon fruits was measured using gas chromatography – mass spectrometry (GC-MS) as described in Pereira *et al.* (2017) with minor modifications. Two blocks (T3 and T4) were evaluated for this trait. Ethylene production in attached fruits was measured in 66 RILs both years, in 17 RILs only one year and 6 RILs were excluded from the analysis due to infections or a wrong fruit set.

The ethylene peak was monitored during the ripening period customizing the design for each RIL. The first measurement before the onset of ripening was determined for each RIL based on previous evaluations, due to the segregation of earliness of ethylene production. For climacteric lines, the atmosphere of the chamber was measured every

other day while ethylene was undetectable, and every day after ethylene detection; the measurements were stopped when: a) fruit abscised from the plant or b) ethylene production decreased during at least two consecutive days. For non-climacteric lines, the atmosphere of the chamber was examined at least every three days, confirming that they did not produce any detectable amount of ethylene during fruit ripening.

To better characterize the ethylene peak, four traits were defined: maximum production of ethylene in the peak (ETH), earliness of ethylene production, representing the first day when ethylene was detectable (DAPE), earliness of the ethylene peak (DAPP) and width of ethylene peak (WEP), the latter calculated subtracting DAPP and DAPE (Table 3.1). For the non-climacteric lines, the earliness of the trait was considered as missing data.

DNA extraction and genotyping

DNA extractions were performed from young leaves following the CTAB protocol (Doyle, 1991) with some modifications (Pereira *et al*., submitted). IL families 720 and 414 were genotyped with SNPs using the KASPar SNP Genotyping System (KBiosciences, Herts, UK). KASPar assay primers were designed using Primer Picker (KBiosciences) and are presented in Table 3.S1A. The genotyping of SNPs across the genome was performed using the high-throughput genotyping system Biomark HD, based on Fluidigm technology, with 96x96 chips. Additional SNPs located within the flanking SNPs of *ETHQV8.1* (Table 3.S1B) were genotyped by qPCR in a LightCycler 480 instrument (Roche Diagnostics, Spain)using the universal KASPar MasterMix (LGC, England) following the technical instructions recommended by the supplier. All the SNPs used were obtained *in silico* from the re-sequencing of both parental lines (Sanseverino *et al.*, 2015).

Genetic map construction and QTL mapping

The genetic map, containing SNPs and INDELs obtained by genotyping-by-sequencing (GBS), was previously described in Pereira *et al*. (submitted). Phenotypic data was used to perform a QTL mapping analysis (Van Ooijen and Maliepaard, 1996) with the interval mapping procedure in each block individually, T1 to T5 for ripening-related traits and T3-T4 for ethylene traits. The threshold of significance was fixed at LOD>2.5 (Van Ooijen, 1999) and the 1-LOD confidence interval was used to locate the QTL interval.

QTLs were considered significant only when they were detected in similar positions and contributed to ripening in the same direction in at least three of the five blocks.

In order to increase the statistical power, a second interval mapping analysis was performed using the mean values for each RIL (LOD threshold = 3). A Principal Component Analysis (PCA) based on a subset of RILs and variables, evaluated in five blocks and without missing data, showed that, when extracting the effect of the line, the environmental effect was not associated with the year (Figure 3.S1).

To name the QTLs, the first letter corresponds to the trait code (Table 3.1), followed by a "Q", a letter identifying the experiment ("V", "W" and "X" in the mapping with the mean values, the subset VIII-VED and the subset VIII-PS, respectively), a number indicating the linkage group (LG), a dot and a digit to differentiate QTLs in the same LG (Diaz *et al.*, 2011).

Statistical analyses

All the statistical analyses and graphical representations were obtained using the software R v3.2.3 (R Core Team, 2012) with the RStudio v1.0.143 interface (RStudio, 2012).

The PCA was performed using R package "factoextra". To obtain the correlation matrix among traits we calculated the Pearson coefficient with the R package "Hmisc" and the visualization of data was performed with "corrplot". To compute these functions the data should not contain any missing data. In order to include in the analysis the non-climacteric lines without any phenotypic symptoms, EARO, ECD, EALF, EABS, DAPP and DAPE values were imputed with the latest harvest date value (62 DAP), and for WEP as the maximum value of this variable (8 days). The lines without any data for ethylene production were excluded of the PCA and correlation analysis.

Mean comparisons between the IL groups were performed with the function "pairwise.t.test" from the package "stats". To represent the EALF in the non-climacteric lines, we substituted the missing value by 62 DAP, as explained above.

Results

Ethylene production and climacteric ripening in the Ved x PS RIL population

The RIL population parents are Ved, a highly climacteric *cantalupensis* line, and PS, a non-climacteric *inodorus* type. Ved showed, as expected, a high climacteric behaviour starting around 34 DAP in all blocks: strong sweet aroma, slight change of color from white to cream and abscission layer formation with fruit abscission in most cases (Table 3.S2). PS did not show any symptom of climacteric ripening in any block. Hyb presented an intermediate phenotype between the parents, being always climacteric but showing some of the phenotypic effects later than Ved; however, flesh firmness in Hyb fruits was lower than in both parents. These phenotypes agree with the ethylene peaks obtained: Ved produced a high amount of ethylene (mean values of 72.6 and 224.9 $\mu L \cdot L^{-1} \cdot kg^{-1}$ in T3 and T4, respectively), PS did not produce ethylene and Hyb showed an intermediate peak (mean values of 33.3 and 37.7 $\mu L \cdot L^{-1} \cdot kg^{-1}$ in T3 and T4, respectively) (Figure 3.1A).

The statistics for climacteric traits in the RIL population are presented in Table 3.2, where segregation was observed for all of them. In qualitative terms, most of the RILs produced aromatic fruits that formed abscission layer, but only half of them changed their rind color during ripening.

Table 3.2. Basic statistics for climacteric ripening traits and ethylene production in the RIL population.

Trait	Mean	SD	Median	Range
ARO	0.69	0.34	0.75	0-1
EARO	43.05	6.68	41.67	30.6-60
CD	0.46	0.38	0.50	0-1
ABS	1.25	1.04	1.00	0-3
EABS	42.53	6.16	42.17	32-54
EALF	43.93	7.32	42.50	28-60
ECD	41.39	6.55	40.00	27,5-58
HAR	51.07	7.82	50.80	29,5-62
FIR	3.05	1.62	2.80	0,74-7,14
ETH	31.05	52.69	13.03	0-286,22
DAPP	42.21	5.89	42.00	32-58
WEP	3.71	1.82	3.50	0-9
DAPE	38.23	5.18	37.50	27,5-50

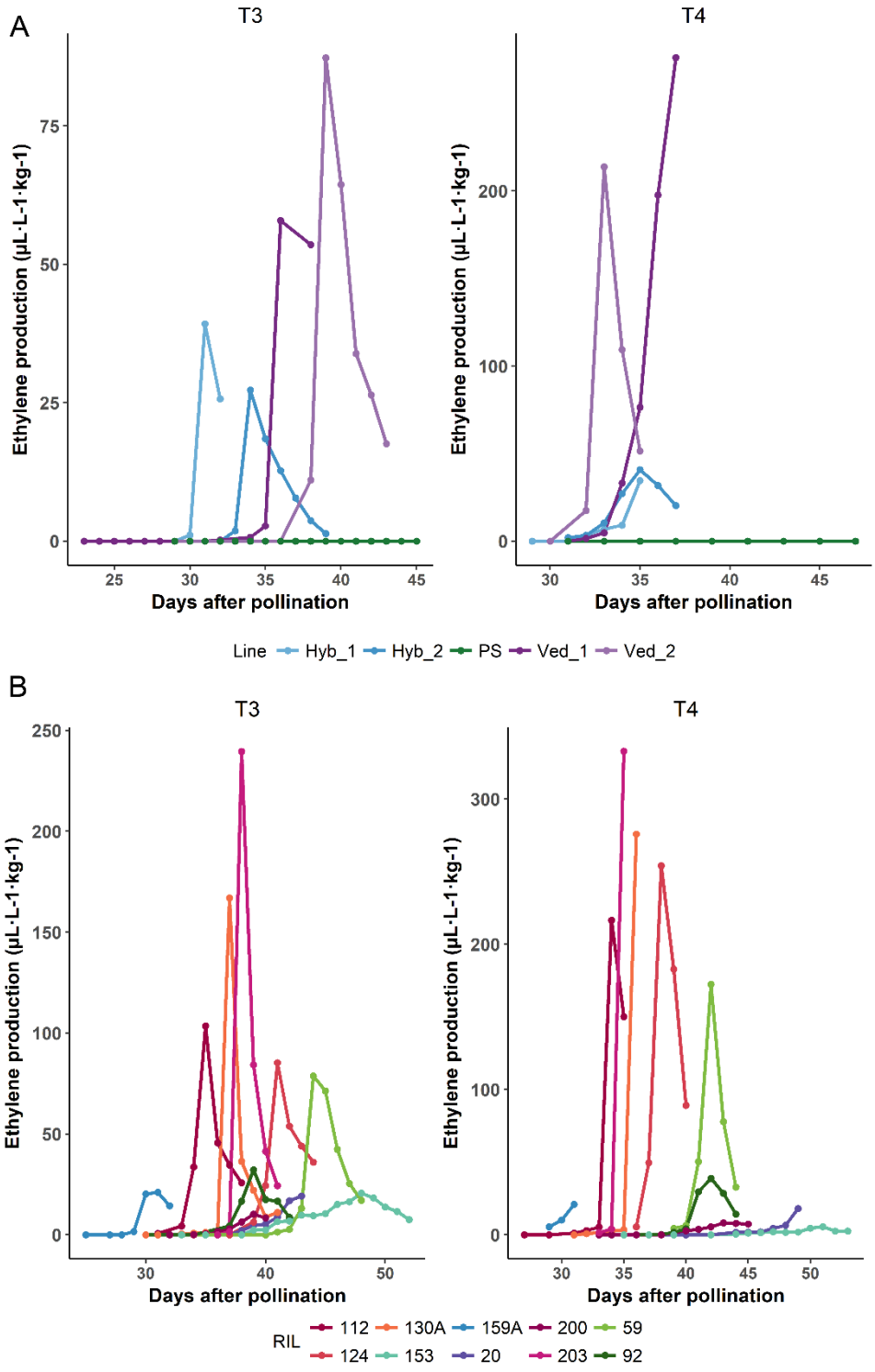

Figure 3.1. Ethylene production A) in the parental lines B) in 10 RILs representing the diverse phenotypes found.

The fruit rind change of color, mainly attributable to chlorophyll degradation, was differently manifested depending on the line. Some melons, with white rind when immature, turned to a cream-slight orange color when ripe (Figures 3.2D and 3.2E); the color change in these cases was subtle and the clearest effect was observed in the region

near the pedicel, where green color turned to yellow or slight orange. Other fruits were green when immature and during the ripening process became bright yellow (Figures 3.2C and 3.2F). In both cases, we observed a striking pattern in mottled rinds, where the spots changed color (Figures 3.2A, 3.2B and 3.2C).

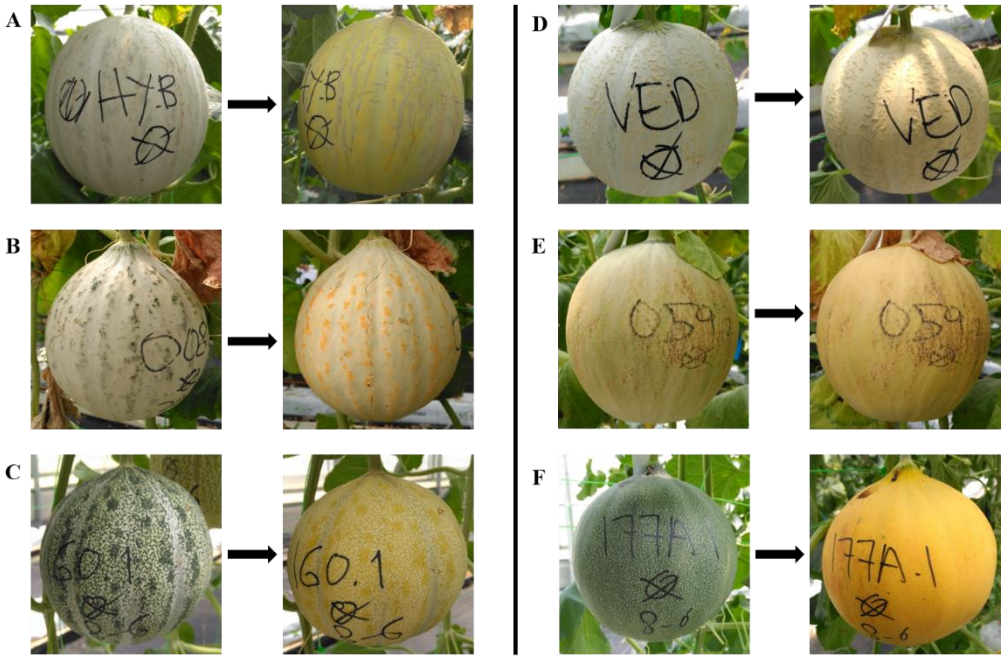

Figure 3.2. Change of rind color in ripe fruits, implicating chlorophyll degradation and synthesis of pigments as flavonoids. A) Hyb B) RIL 008 C) RIL 160 D) Ved E) RIL 059 F) RIL 177A.

Concerning the abscission layer formation, the RIL population included lines that did not abscise (Figure 3.3A), lines with complete fruit abscission (Figure 3.3D), lines with subtle and/or partial abscission layer formation (Figure 3.3B) and lines with marked scar in the abscission zone (Figure 3.3C). Only 31% of the climacteric lines presenting abscission layer fell from the plant, and even the controls Ved and Hyb did not always show abscission, a trait that may probably be highly dependent on the environment.

The ethylene peaks of a representative subset of RILs are presented in Figure 3.1B. Data for both years were treated separately due to the environmental effect affecting both ethylene production and earliness, however the general pattern was very similar. Earliness, height and shape of the ethylene peak segregated in the RIL population. We could observe an independent segregation, at least partially, between ETH and DAPE/DAPP. For example, RIL 159A presented an early ethylene peak but the maximum amount of ethylene was low in comparison with other lines; on the opposite side, RIL 59 showed a considerably high ethylene peak around 43 DAP, with a delay of 8-9 days compared to Ved (Figure 3.1A, 3.1B). Transgressive segregation was observed for ETH

in 3 RILs, which was consistent between years. Transgressive segregation was also found for DAPP and DAPE in both directions, i.e. RILs that ripe earlier or later than the climacteric parent Ved.

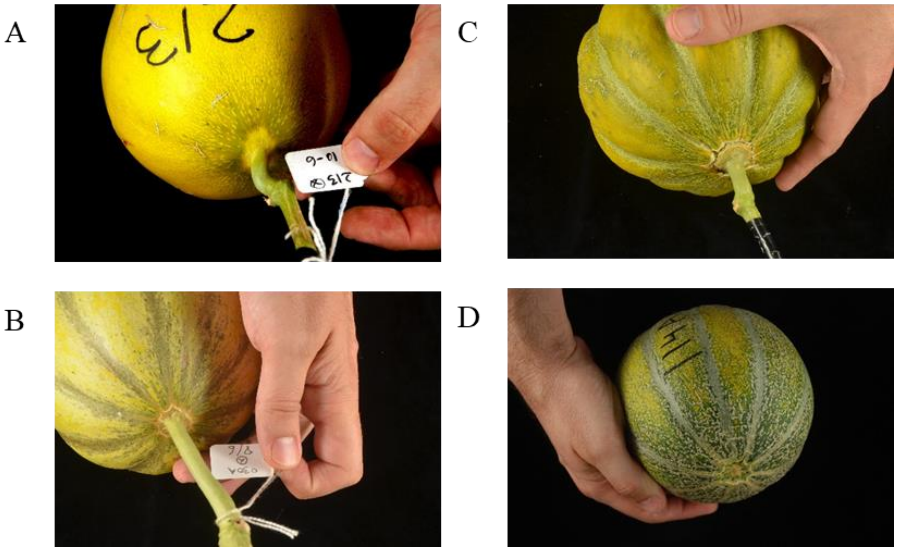

Figure 3.3. Fruit abscission (ABS) in ripe fruits: A) RIL 213, no abscission layer formation (ALF), score 0; B) RIL 030, partial and subtle ALF, score 1; C) RIL 047, almost complete ALF, score 2; D) RIL 114A, total ALF generally with abscission, score 3.

Generally, ethylene production is measured in detached fruits, precluding the precise phenotyping of other ripening-related traits. The method used in our study allows the fruit to follow the physiological process of ripening without any alterations and the phenotyping of downstream effects of ethylene *in planta*. The most common, and generally earliest climacteric symptom was the sweet aroma production, which appeared on average four days after the starting of ethylene production (DAPE) and in many RILs, before the ethylene peak was reached (DAPP). When a change of rind color was induced, it appeared almost simultaneously to ethylene production; the first or second day of detectable ethylene production, chlorophyll degradation started to be appreciable and in around three days the color change was complete. Commonly, the abscission layer formation was the latest symptom exhibited, around five days after the ethylene detection; however, we could observe that, depending on the RIL, the earliness and the penetrance of the phenotype varied, with some lines that fell from the plant the first or second day after ethylene production and others that remained with a subtle abscission layer during weeks.

Surprisingly, the correlation between ETH and the appearance and earliness of climacteric symptoms was not high (Figure 3.S2). EARO, DAPE, DAPP and HAR were

highly and positively correlated among them, in agreement with our observations. ARO was highly correlated with all the other phenotypic effects, positively with ABS and CD and negatively with FIR and with earliness of ripening (DAPP, DAPE, EARO, ECD, HAR), but slightly correlated to ETH.

QTL mapping

We performed two complementary mapping experiments, the first one for each individual block independently and the second one using the mean of all the blocks for each RIL. In the first experiment, we mapped 84 QTLs for all traits in almost all melon chromosomes (Table 3.S3A). QTLs with LOD >3 are represented in Figures 3.4 and 3.S3, indicating for each trait the LOD scores and the genetic position across the linkage groups (LG).

A major QTL, referred as *ETHQV8.1* hereafter, was mapped in LG VIII, with a maximum LOD around the position 86.49 cM. *ETHQV8.1* was detected for ETH, DAPE and DAPP in both years (T3 and T4) with significant LOD scores (e.g. 5.39 for ETH in T3 and 6.33 in T4 (Figure 3.4A)). Most of the other traits, in particular EARO, EALF and HAR, showed also significant QTLs in this region (Figure 3.4B). In all cases, the Ved allele increased the climacteric effect, meaning higher and earlier ethylene production and earlier aroma production, chlorophyll degradation and abscission layer formation. The impact of the QTL was more obvious for the earliness of climacteric symptoms rather than for their presence.

Other minor QTLs were observed in LGs II, III, VI, VII, X and XI. Ethylene production QTLs were only found in LGs II and XI. In some cases, QTLs were found in a certain genomic position for only one of the climacteric traits: the QTL in the center of LG VI affecting mostly CD, the QTL in the top of LG X influencing only FIR and the QTL at the top of LG XI for ABS.

In the second mapping experiment, we performed a QTL analysis with the mean values of the five blocks. The results (Table 3.3 and Figure 3.5) overlap to a high extent with the first mapping experiment, but are condensed in 29 QTLs instead of 84.

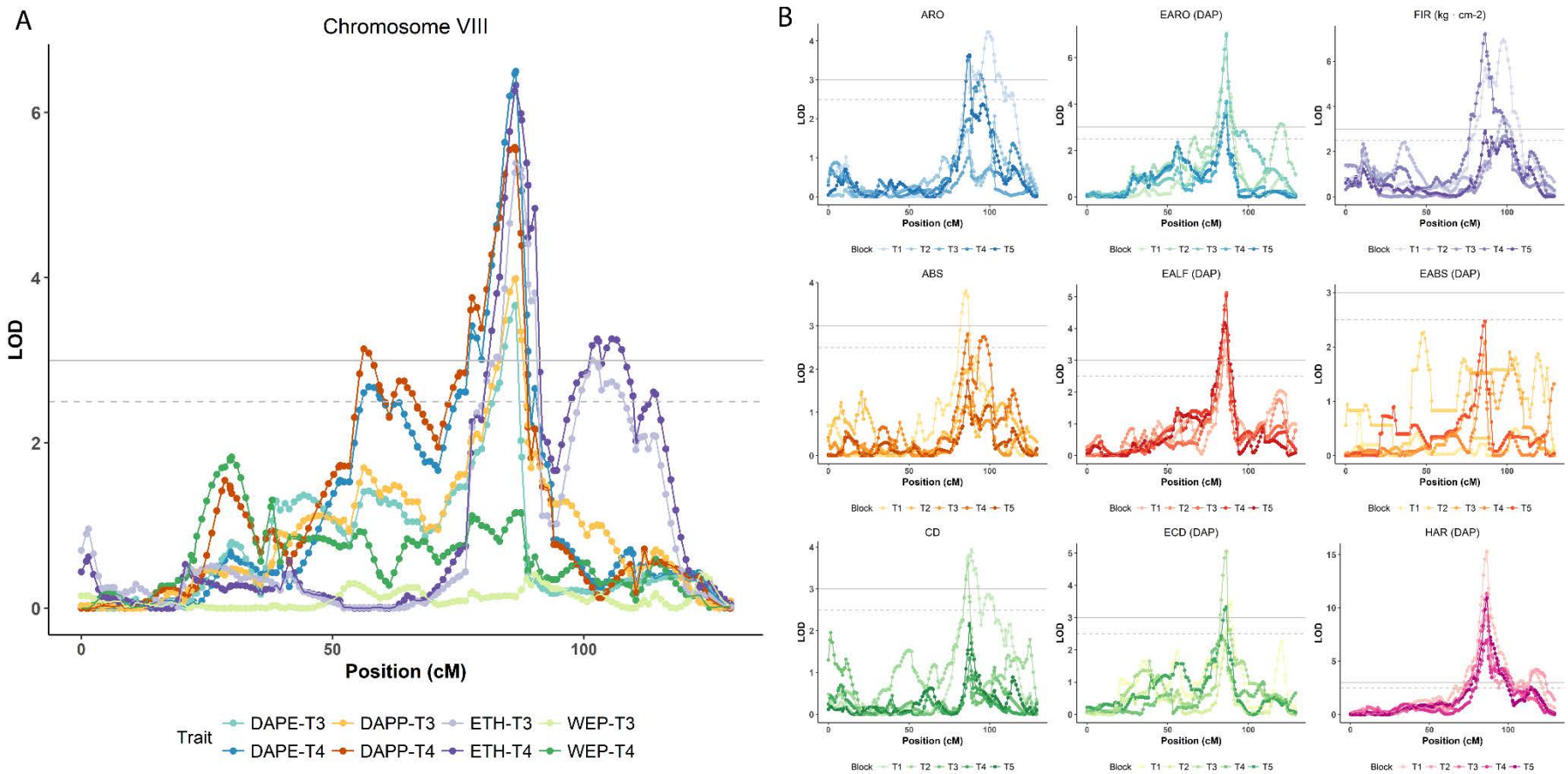

Figure 3.4. QTL mapping in chromosome VIII for: A) maximum ethylene production (ETH, purple), earliness of ethylene production (DAPE, blue), earliness of ethylene peak (DAPP, orange) and width of ethylene peak (WEP, green), in blocks T3 and T4. B) all traits related with climacteric ripening in the five analyzed blocks (T1-T5). The grey and dotted lines represent the thresholds of LOD = 3 and LOD = 2.5, respectively.

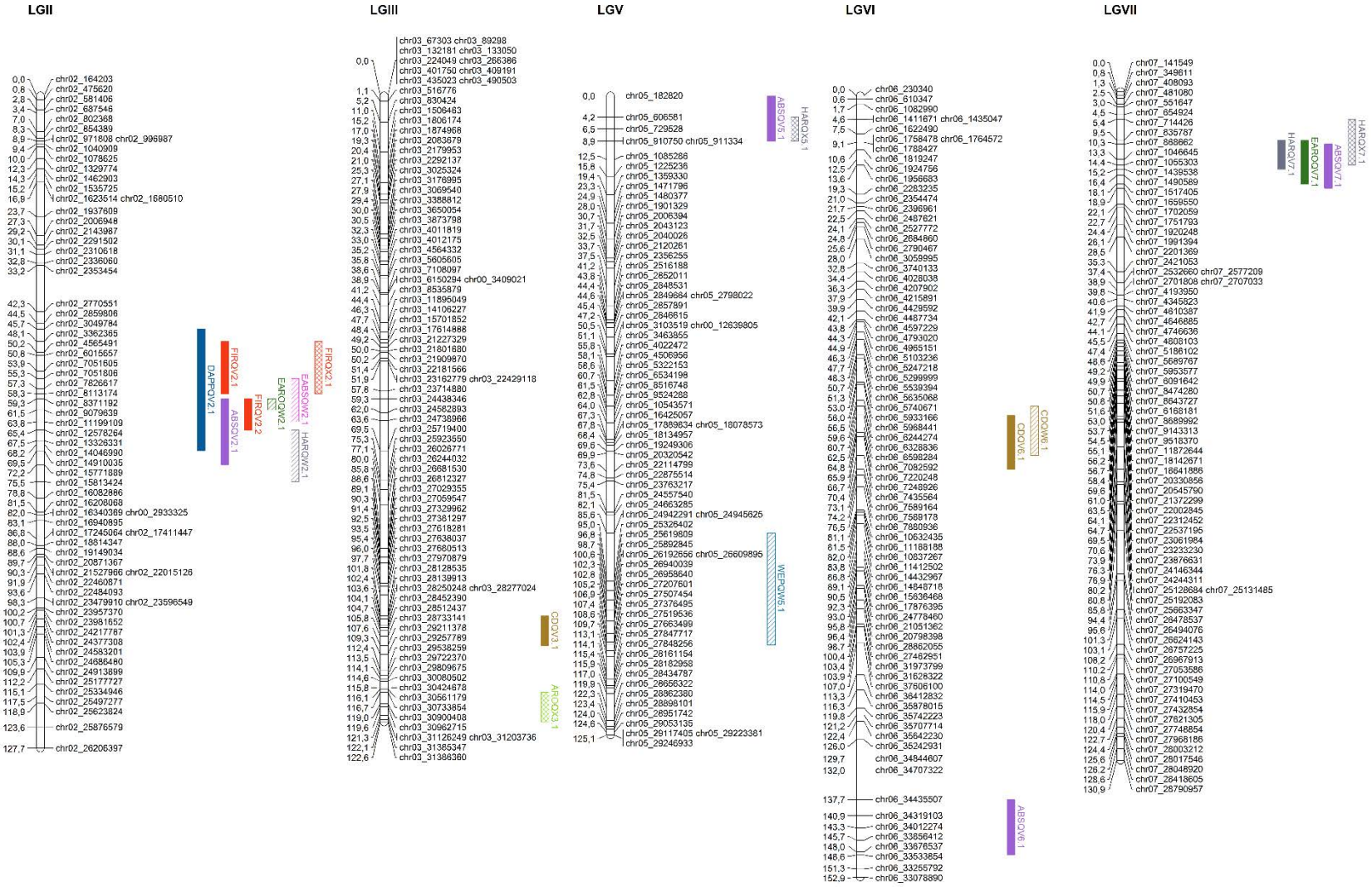
LGII
LGIII
LGV
LGVI
LGVII
DAFQV2.1
FIRQV2.1
ABSQV2.1
FIRQV2.2
E4RQW2.1
EABSQW2.1
HARQW2.1
FIRQX2.1
GDQV3.1
ARQQX3.1
WEPQW6.1
HARQX5.1
ABSQV5.1
CDQW6.1
CDQV6.1
ABSQV6.1
HARQV7.1
EARQQV7.1
ABSQV7.1
HARQX7.1

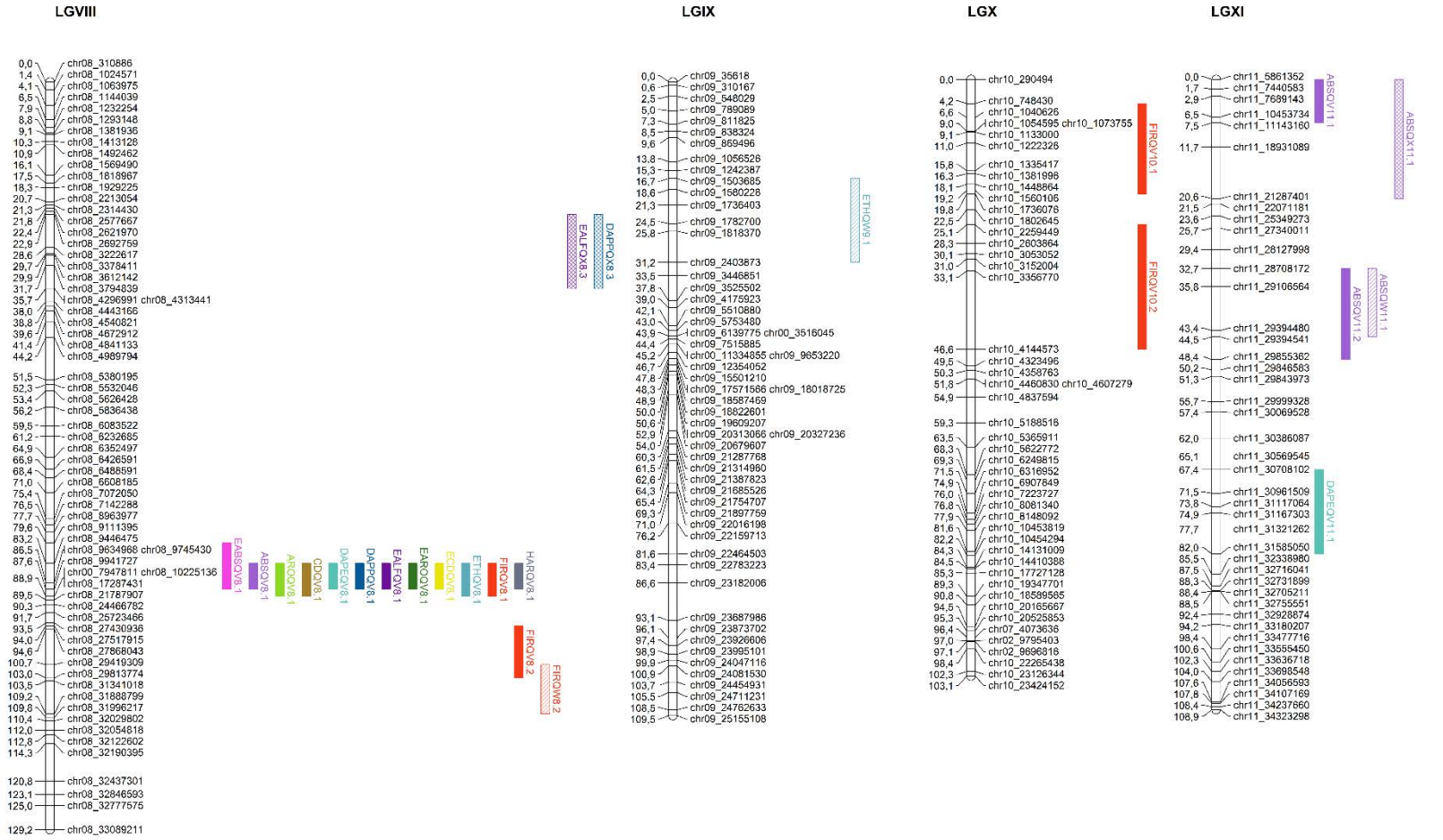

Figure 3.5. Genetic map of the RIL population showing the QTLs for ethylene production and climacteric ripening. Filled bars represent the QTLs mapped with the mean values, the striped bars the QTLs mapped using the subset VIII-Ved and the square bars the QTLs mapped using the subset VIII-PS. Light green, ARO; dark green, EARO; brown, CD; yellow, ECD; light purple, ABS; dark purple, EALF; pink, EABS; red, FIR; tones of blues, ETH, DAPP, DAPE and WEP; grey, HAR. LGs that did not contain any significant QTL were not represented.

Table 3.3. QTLs for climacteric ripening and ethylene production traits detected using the mean of phenotypic values for all the blocks.

Chr	QTL ID	LOD[a]	R^2	Additive effect[b]	Genetic position (cM)	Physical position[c] (pb)	Marker 1	Genetic position of marker 1	Marker 2	Genetic position of marker 2
2	DAPPQV2.1	2.4	14.8	2.41	58.28	8113174	chr02_3049784	45.69	chr02_14910035	69.54
	FIRQV2.1	5.0	22.9	0.81	51.84	6015657	chr02_3362365	48.11	chr02_8113174	58.28
	FIRQV2.2	5.0	22.7	0.80	63.53	11199109	chr02_8371192	59.28	chr02_12578264	65.4
	ABSQV2.1	2.9	13.9	-0.40	63.79	11199109	chr02_8371192	59.28	chr02_15771889	72.24
3	CDQV3.1	2.4	11.7	0.14	103.55	28250248	chr03_28128535	101.84	chr03_29211378	107.6
5	ABSQV5.1	2.7	12.8	-0.37	4.23	606581	chr05_182820	0	chr05_910750	8.89
6	CDQV6.1	3.8	17.8	0.17	68.66	7435564	chr06_6598284	62.51	chr06_7589164	73.06
	ABSQV6.1	2.7	13.2	0.38	145.7	33856412	chr06_34435507	137.68	chr06_33533854	148.56
7	HARQV7.1	2.8	13.5	-2.97	13.28	1046645	chr07_835787	9.54	chr07_1439538	15.16
	EAROQV7.1	2.8	15.1	-2.61	13.28	1046645	chr07_835787	9.55	chr07_1517405	18.09
	ABSQV7.1	2.7	13.2	0.38	13.28	1046645	chr07_868662	10.32	chr07_1657550	18.86
8	EABSQV8.1	3.3	36.2	-3.69	86.49	9634968	chr08_9111395	79.64	chr08_9941727	87.61
	EAROQV8.1	10.4	45.5	-4.51	86.49	9634968	chr08_9446475	83.23	chr08_9941727	87.61
	ABSQV8.1	4.4	20.2	0.48	86.49	9634968	chr08_9446475	83.23	chr08_9941727	87.61
	EALFQV8.1	10.2	50.5	-5.25	86.49	9634968	chr08_9446475	83.23	chr08_9941727	87.61
	ECDQV8.1	5.8	34.5	-3.80	86.49	9634968	chr08_9446475	83.23	chr08_9941727	87.61
	HARQV8.1	17.2	58.9	-6.20	86.49	9634968	chr08_9446475	83.23	chr08_9941727	87.61

	DAPPQV8.1	7.1	37.8	-3.59	86.49	9634968	chr08_9446475	83.23	chr08_9941727	87.61
	DAPEQV8.1	7.5	39.2	-3.19	86.49	9634968	chr08_9446475	83.23	chr08_9941727	87.61
	AROQV8.1	5.2	23.7	0.17	86.49	9634968	chr08_9446475	83.23	chr08_10225136	88.87
	CDQV8.1	4.5	20.9	0.18	87.49	9941727	chr08_9446475	83.23	chr08_10225136	88.87
	FIRQV8.1	6.1	27.2	-0.86	86.49	9634968	chr08_9446475	83.23	chr08_17287431	88.87
	ETHQV8.1	6.6	30.8	29.70	86.49	9634968	chr08_9446475	83.23	chr08_17287431	88.87
	FIRQV8.2	6.3	27.9	-0.92	97.6	27868043	chr08_27517915	94.04	chr08_29813774	102.97
10	FIRQV10.1	2.8	13.5	0.61	10.97	1222326	chr10_748430	4.24	chr10_1736076	19.75
	FIRQV10.2	2.7	13.0	0.60	33.07	3356770	chr10_2259449	25.07	chr10_4144573	46.6
11	ABSQV11.1	6.5	28.4	0.60	3.86	7689143	chr11_5861352	0	chr11_11143160	7.466
	ABSQV11.2	3.9	18.4	0.49	39.79	29394480	chr11_28708172	32.66	chr11_29855362	48.41
	DAPEQV11.1	2.5	15.3	2.00	77.68	31321262	chr11_30708102	67.35	chr11_31585050	81.97

[a] Presented the QTLs with LOD>2.4, and QTLs with a value of LOD>3 are shaded in grey
[b] Sign of the additive effect of the Ved allele
[c] Physical position in version v.3.6.1 of the melon genome

ETHQV8.1 was detected for all evaluated traits with LOD > 3, except for WEP, allowing to delimit a confidence interval of 4.3 cM spanning around 500 kb, with a maximum LOD score in the physical position 9,634,968 bp. In all cases, the Ved allele was increasing the climacteric behaviour, and an additive effect as high as 29.7 $\mu L \cdot L^{-1} \cdot kg^{-1}$ in ETH was observed. Other QTLs with high LOD scores (>3.5) were located in LG II, LG VI and LG XI. The first one (*FIRQV2.1*/*FIRQV2.2*) is mainly involved in FIR, although other two minor QTLs with lower significance were recorded in the same region for DAPP and ABS. The allele of Ved mitigated the climacteric behaviour, increasing FIR and reducing ABS. Using a conservative strategy, we could delimit the QTL in a region of around 28 cM, between physical positions 3,049,784 and 15,771,889 bp (Figure 3.5). The second QTL is associated principally with chlorophyll degradation, with the Ved allele triggering this symptom. *CDQV6.1* is located in a region of 11 cM, with the maximum LOD score at 7,435,564 bp. The third QTL is affecting ABS and is located in a region of 7 cM in chromosome XI. *ABSQV11.1* is explaining 28.4 of the variance, and the Ved allele increases the abscission layer formation. A second QTL *ABSQV11.2* for ABS was found 25 cM downstream from *ABSQV11.1*, being also the Ved allele the one that enhanced ABS. Other nine QTLs (in LG III, LG V, LG VI, LG VII, LG X and LG XI) with slight effects in different aspects of climacteric ripening were detected, although their LOD scores were slightly beyond the threshold of significance (2.4 < LOD < 3). All of them were detected also in some of the individual-block mapping experiments in similar positions and with the same direction of additive effect (Supplementary Table 3A).

Due to the high effect of *ETHQV8.1* in climacteric ripening, other minor QTLs could be masked and poorly detected in our analysis. To minimize this effect, we separated the RIL population in two subsets, each of them with *ETH8QV8.1* fixed for the Ved or the PS allele, respectively (VIII-Ved, n=34 and VIII-PS, n=55). For each subset, we did an interval mapping experiment using LOD>3 as threshold (Supplementary Table 3.3B) that revealed the same QTLs but with higher significance and some new potential QTLs. When the Ved allele is fixed for *ETHQV8.1*, all the RILs are climacteric to a greater or lesser degree, so we should increase our power of detection for QTLs that are modulating ethylene production or its physiological responses. The principal factors detected in the previous analysis and in the VIII-Ved subset were in LG II, LG VI, LG VIII and LG XI (Figure 3.5); other new potential QTLs were located in LG V and LG IX. For the subset VIII-PS, we observed non-climacteric and climacteric lines, but in any case the maximum

ethylene production overcame 50 $\mu L \cdot L^{-1} \cdot kg^{-1}$, suggesting that we were looking at QTLs that triggered the climacteric ripening with lower intensity. With this approach we detected again QTLs in LG II, LG III, LG V, LG VII and LG XI, and also a new one at the top of LG VIII (Figure 3.5).

Validation and fine mapping of ETHQV8.1

In order to validate *ETHQV8.1*, we used IL with the background of one of the parental lines, Ved or PS, and an introgression of the other parent in chromosome VIII. These lines belong to a collection of ILs still under development (data not shown). The two IL families used in this study (720 and 414) came from two BC3S1 segregating families that, besides the region of *ETHQV8.1*, still contain a few additional introgressions in other chromosomes (Table 3.S4A).

We evaluated the appearance and the earliness of climacteric symptoms for both families during the 2017 summer season. The 720 family, segregating for the introgression of PS in the genetic background of Ved, presented in all cases climacteric fruits, with presence of aroma, abscission layer and in most cases external change of color (Table 3.S4B). However, the earliness of the climacteric symptoms was delayed in the ILs carrying the PS allele of *ETHQV8.1*, either in heterozygosity or homozygosity. The evaluation of the 414 family, containing a Ved introgression in the genetic background of PS, showed clear differences between fruits carrying the Ved allele of *ETHQV8.1*, presenting various degrees of climacteric fruits, in comparison to those carrying the PS allele in homozygosis, which were non-climacteric (Table 3.S4B and Figure 3.6C). There is a clear association between the genotype of *ETHQV8.1* and EALF, with the Ved allele diminishing the number of DAP of appearance of the climacteric symptoms in both genetic backgrounds (Figures 3.6A and 3.6B). Statistically, the values were significantly different between PS and Ved (p-value of 0.001) for the 720 family, and between all the possible combinations for the 414 family (p-values 0.03 PS-Hyb, 0.007 Ved-Hyb and <0.001 PS-Ved).

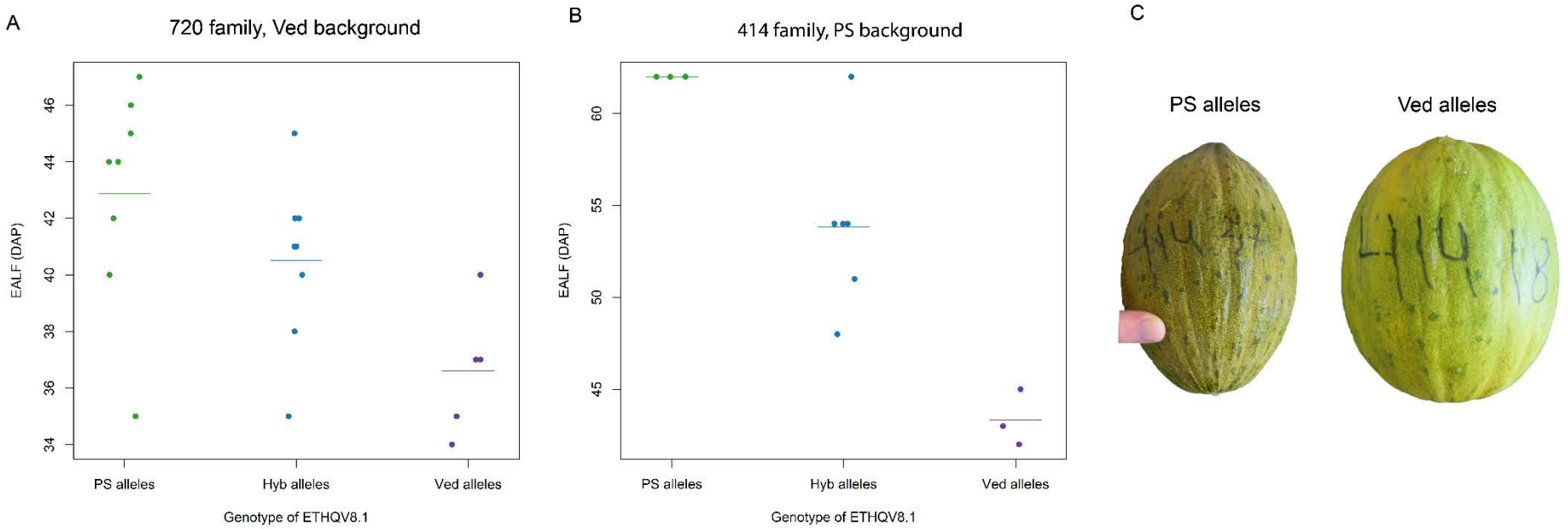

Figure 3.6. Phenotyping of individuals of the IL families 720 and 414 having distinct genotypes for *ETHQV8.1*. A) EALF values for the lines with Ved background and B) EALF values for the lines with PS background. C) fruits from two individuals from the 414 family, with PS and Ved alleles in homozygosity in the *ETHQV8.1* interval.

We increased the SNP density between the flanking markers of the *ETHQV8.1* interval (Supplementary Table 4A, flanking markers shaded in red). The most informative segregating ILs were genotyped and three of them had a recombination within the QTL interval (720.17, 414.1 and 414.17) (Table 3.S4C). Progeny seed of 414.1 and 414.17 was germinated and a subset of ILs were evaluated during the 2017 autumn season. None of the 11 plants of the 414.1 family showed abscission, although some fruits presented a subtle abscission layer around 55 DAP or later (Table 3.S4D). In contrast, nine from the 15 plants from the 414.17 family presented abscission between 44 and 52 DAP. The family 414.1 was segregating for a small introgression in chromosome VIII from 9,443,515 to 9,603,217 bp (Table 3.S4E and Figure 3.7); the phenotype of this family clearly discarded this interval for harboring *ETHQV8.1*. The family 414.17 segregated from 9,443,515 to 9,757,323, and both the earliness and the intensity of abscission were strongly associated with the genotype (Table 3.4E and Figure 3.7). Both families delimitate *ETHQV8.1* in a region of 154,106 bp, which contains the maximum LOD peak obtained in the QTL mapping.

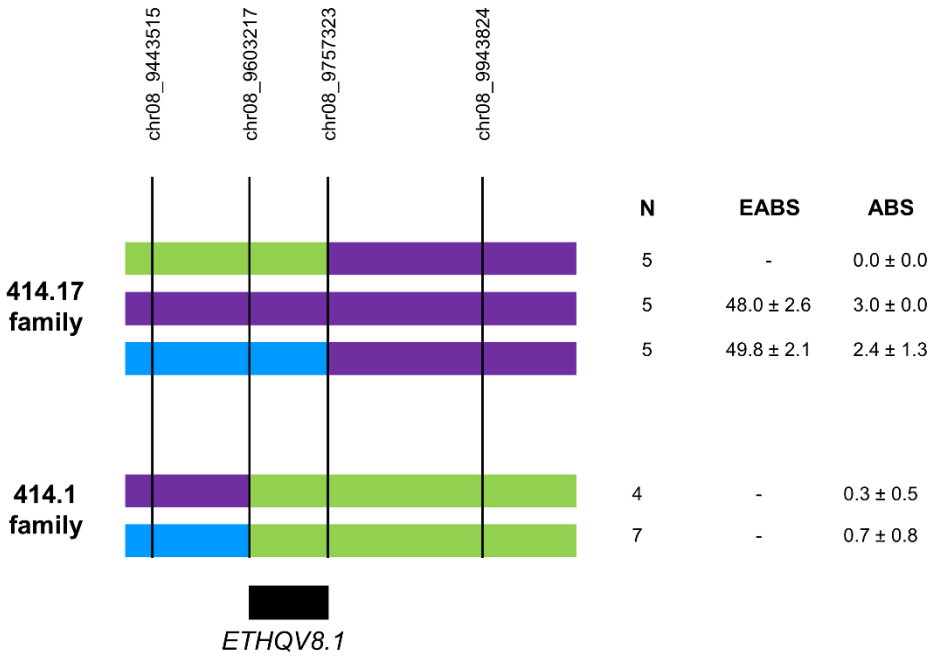

Figure 3.7. Fine mapping of *ETHQV8.1*. The colored bars represent the genotype in the QTL region in chromosome VIII: purple, homozygous for Ved; green, homozygous for PS; blue, heterozygous. The mean and standard deviation of phenotypic evaluation is presented on the side for each group.

Discussion

A continuum degree of climacteric ripening occurs in the Ved x PS RIL population

The main approach used to decipher the genetic control of climacteric fruit ripening has been the characterization of tomato ripening mutants; in these cases, the climacteric wild type is usually compared with the non-climacteric mutant (Giovannoni, 2007). As an essential part of phenotyping of ripening mutants, ethylene production is evaluated during the ripening process. Generally, the hormone is measured in detached fruits, which are collected when they acquire the competence to ripe but before the ripening process started. Although this strategy has been widely used and demonstrated its efficiency, it presents some disadvantages when applied to mapping populations containing many individuals, since it requires a lot of space to store containers for the fruits during all the ripening period. Previous knowledge of the ripening time of each line is also needed to adjust the harvest point. Additionally, as the *in planta* development is interrupted, it may lead to potential alterations in the ripening process. Our improved non-invasive method to monitor the ethylene peak allowed to observe the ethylene responses and the timing of their appearance *in planta* (Pereira *et al.*, 2017). The comprehensive evaluation of climacteric ripening in the Ved x PS RIL population has led to a complex and diverse group of phenotypes. From the two extreme phenotypes observed in the parental lines, the segregating RIL population displayed several combinations differing not only in quantity and earliness of ethylene production, but also in other ripening-associated phenotypes. Some ripening-associated phenotypes were not present in highly climacteric lines, e.g. RIL 124 presented high production of ethylene, very sweet aroma and abscission in all blocks, but it did not change external color, whereas RIL 213 showed medium levels of ethylene, aroma and a striking change of color to bright yellow without abscission layer formation.

Some RILs that are producing up to 5% of the ethylene produced by Ved (around 2 $\mu L \cdot L^{-1} \cdot kg^{-1}$) are phenotypically very similar, suggesting that a minimum threshold of the hormone may be necessary to trigger climacteric ripening. However, some common characteristics were observed in RILs producing low quantity of ethylene: they tended to ripe later; the ethylene peak was less sharp in comparison with lines producing higher levels of ethylene; and their phenotype was more dependent on the environment, showing

wider variation depending on the block. We can hypothesize that the amount of ethylene produced by these RILs is very close to a minimum threshold necessary to trigger the climacteric behaviour, so any environmental alteration that slightly reduces ethylene production may have a critical effect resulting in a non-climacteric fruit. Depending on the stability of the observed climacteric phenotypes among the RILs, we could identify three different ripening patterns: climacteric lines, which had at least one symptom of climacteric ripening in all blocks; unstable climacteric lines, showing an inconsistent behaviour throughout different blocks; and non-climacteric lines in all blocks. In general, unstable climacteric lines developed climacteric melons in some blocks, with detectable ethylene, aroma and abscission layer formation, but they were totally non-climacteric in other blocks. A PCA accurately grouped the RILs according to this classification and evidenced the high proportion of climacteric and unstable climacteric lines in comparison with non-climacteric ones in our population (Figure 3.S4).

The phenotypic distribution anticipated the existence of multiple QTLs with variable effects modulating climacteric ripening. Leida *et al.* (2015) classified a panel of melon accessions according to different degrees of climacteric ripening, using FIR and ABS as indicative traits. Although their phenotyping was not as extensive as in our work, they suggested a non-absolute classification of melon varieties according to this trait. The complex and polygenic nature of this trait was also demonstrated by previous works that characterized several QTLs for climacteric ripening or their associated effects. Périn *et al.* (2002) used a RIL population obtained from the cross between Ved and PI 161375, a non-climacteric accession, to identify two genes responsible for abscission layer formation, *Al-3* and *Al-4* in LGs VIII and IX, respectively, and four QTLs affecting the amount of ethylene production in LGs I, II, III and XI. An IL population founded by the same exotic parental, PI 161375, and PS, both non-climacteric, allowed to identify QTLs for climacteric ripening (*eth3.5*) and flesh firmness (*ff2.2*, *ff3.5*, *ff8.2*, *ff8.4* and *ff10.2*) (Moreno *et al.*, 2008). Another study implicating the same PI 161375 x PS population revealed a second QTL (*ETHQV6.3*) that also rescued the climacteric phenotype in the PS background when the exotic allele was present (Vegas *et al.*, 2013). The presence of the exotic allele in either *ETHQB3.5* or *ETHQV6.3* promoted climacteric ripening, but the combination of both conferred an earlier and more intense climacteric phenotype (Vegas *et al.*, 2013). Perpiñá *et al.* (2016) identified one QTL in LG X and possibly a second one in LG VII involved in climacteric ripening, using an IL population that

contained introgressions from the moderately climacteric Japanese "Ginsen makuwa" cultivar (*agrestis* ssp.), in the background of Ved. The present work has characterized several QTLs involved in different aspects of climacteric ripening in LGs II, III, V, VI, VII, VIII, IX, X and XI, using a combination of QTL mapping experiments. Several of these QTLs could be allelic to QTLs previously described (Table 3.S5), since they co-localize in the same LGs/physical positions. The minor effect of most of the described QTLs fits with the hypothesis of a complex trait with polygenic inheritance, displaying a continuum range of climacteric intensity. Surprisingly, the use of two phylogenetically close varieties as Ved and PS, both commercial and belonging to the spp. *melo*, allowed to identify several QTLs involved in climacteric ripening.

A major QTL, ETHQV8.1, is sufficient to trigger climacteric ripening

Among the identified QTLs in the RIL population, *ETHQV8.1* is by far showing the most important effect in both ethylene production and ripening-associated phenotypes. For all the recorded traits, except WEP, a highly significant QTL was mapped in an almost identical interval, around the physical position 9,634,968 bp of chromosome VIII. For all of these traits the Ved allele is causing a stronger climacteric phenotype, explaining between 20.2-58.9% of the variance. Furthermore, in the RIL subset Ved-VIII, which only contains the RILs with the Ved allele in the *ETHQV8.1* interval, none of them was non-climacteric. It is possible that *ETHQV8.1* is allelic to *Al-3*, a major gene described in the PI 161375 x Ved RIL population as essential to trigger fruit abscission and autocatalytic synthesis of ethylene (Périn *et al.*, 2002). However, the physical position of *Al-3* could not be determined as the genetic map used was exclusively based in AFLP markers, hampering the comparison of the physical positions from both QTLs.

In order to genetically validate *ETHQV8.1*, we generated ILs in the PS and Ved background containing Ved and PS introgressions in the *ETHQV8.1* interval, respectively. The evaluation of two families of ILs, 414 and 720, with PS and Ved background, respectively, proved the contribution of *ETHQV8.1* to the climacteric phenotype. According to the polygenic control of the trait, the ILs from family 720 were still climacteric, since they have a climacteric background and the introgression of the PS allele of *ETHQV8.1* did not eliminate completely the climacteric phenotype (Table 3.S4B). However, a significant delay of around seven days was observed in the appearance of aroma, abscission layer formation and chlorophyll degradation. This is

similar to the effect reported by Ríos *et al.* (2017) for mutants of the *CmNAC-NOR* (*ETHQV6.3*) in the "Charentais Mono" background, which also belongs to the *cantalupensis* group. On the other side, the ILs from family 414 showed a partial climacteric behaviour when the Ved allele was present in the *ETHQV8.1* region, either in homozygosity or heterozygosity; three ILs that contained the Ved allele in homozygosity in the PS background showed an intense climacteric phenotype, with sweet aroma, strong chlorophyll degradation and complete abscission layer formation, though these symptoms appeared later than in Ved (Table 3.S4B).

To fine map *ETHQV8.1* we selected two individuals from the 414 family, which had recombined inside the QTL interval, for a progeny test in autumn 2017. The climacteric behaviour of the control lines was less intense than the one observed during summer, as expected, since even under controlled conditions, fruit ripening is altered. The climacteric fruits did not change substantially their external color and did not produce aroma, nevertheless they produced abscission layer and fell from the plant, suggesting that in the PS background, fruit abscission is less environment-dependent. Therefore, the phenotyping of both recombinant progenies reduced *ETHQV8.1* to an interval between the positions 9,564,672 and 9,757,323 bp. In the melon genome annotation v4.0 (Ruggieri et al., under revision), 14 candidate genes are annotated inside the interval (Table 3.S6). Tentatively, three of them could be discarded because they are not expressed in fruit tissues in Melonet-DB (Yano *et al.*, 2018); by functional annotation, two genes could be related to *ETHQV8.1*, *MELO3C024520* and *MELO3C024518*, encoding an ethylene-responsive transcription factor ERF024 and a serine/threonine kinase CTR1-like, respectively. Ethylene-responsive transcription factors form a multigenic family that acts as the last step of ethylene signaling (Yano and Ezura, 2016). However, *MELO3C024520* has not sequence variants among PS and Ved causing changes in the protein, and its expression in fruit is low according to Yano *et al.* (2018). *MELO3C024518* has six non-synonymous variants between PS and Ved. CTR1 is a negative regulator of ripening that interacts physically with ethylene receptors (Kieber *et al.*, 1993). In the absence of ethylene, the ethylene receptor activates CTR1, which leads to inhibition of the downstream transduction pathway; when ethylene is present, the ethylene receptor terminates the activation of CTR1, thus releasing ethylene responses (Binder, 2008). In tomato, a multigene family is encoding CTR1 kinases and all of them complemented *A. thaliana* mutants, suggesting a redundant function (Leclercq *et al.*, 2002; Adams-Phillips

et al., 2004). In melon, two orthologues of CTR1 have been described (Yano and Ezura, 2016) and both of them are expressed in fruit tissues according to Yano *et al.* (2018). We may hypothesize that a loss of function in the CTR1 protein in the PS background could maintain its inhibitory activity even when ethylene is bound to the ethylene receptor. However, further experiments are needed to validate *MELO3C024518* as the gene underlying *ETHQV8.1*.

Other minor QTLs interact to modulate the climacteric response in the RIL population

In addition to *ETHQV8.1*, other genetic factors are implicated in the ripening process in our RIL population. In general, they are not affecting the amount of ethylene produced, but other traits as abscission or flesh firmness. Although some of them, as *FIRQV2.1*, *FIRQV2.2*, *CDQV6.1, ABSQV11.1* and *ABSQV11.2* presented high values of LOD scores (>3.5), in most cases they presented a limited effect in ripening, in contrast to *ETHQV8.1*.

Two regions in LGs II and VII seemed to be involved in fruit ripening, since QTLs for different traits co-located in them. In LG II, we identified two QTLs for FIR, which co-localize with QTLs for DAPP and ABS. Furthermore, other three QTLs for EARO, EABS and HAR were detected in the Ved-VIII subset and a forth one for FIR in the PS-VIII subset in this region. In all cases, the Ved allele was diminishing or delaying the climacteric response (Table 3.3 and Table 3.3B). We may hypothesize that a single QTL affecting the earliness of ethylene production is located between the physical positions 3,049,784-15,771,889 bp in chromosome II, which contains 670 genes. As we did not identify QTLs for the qualitative traits ARO and CD in the PS-VIII subset, we may suggest that *FIRQV2.1*/*FIRQV2.2* is incapable to trigger the autocatalytic ethylene production in a non-climacteric background. QTLs for FIR and ETH have been previously described in LG II (Table 3.S5), although their physical positions cannot be compared. In LG VII three QTLs for HAR, EARO and ABS co-located, with a maximum LOD of 2.8 in the physical position 1,046,645 bp, contributing positively to climacteric ripening and explaining around 15% of the variance (Table 3.3). A QTL in a similar position was mapped using the PS-VIII subset for HAR, with a LOD of 3.5, so this QTL may correspond to one of the factors that contribute to triggering climacteric ripening when *ETHQV8.1* is fixed for the PS alleles. The confidence interval of the QTL was delimited by the physical positions 835,787-1,657,550 bp and contains 129 genes. Among

them, *MELO3C016904* encodes a serine/threonine kinase CTR1-like. Although a QTL for climacteric ripening in chromosome VII has not been previously described, Perpiñá *et al.* (2016) reported an IL with an introgression of an exotic melon type in this region that was much less climacteric than the climacteric control; however, the presence of an additional introgression in LG X that also modified climacteric ripening made it difficult to evaluate the contribution of the QTL in LG VII.

In other regions of the genome, we mapped QTLs linked to single traits. Two QTLs for ABS were mapped in chromosome XI. *ABSQV11.1* presented a LOD = 6.5 and explained 28.4% of the variance, the Ved allele promoting ALF. *ABSQV11.1* is located in a region of 5.28 Mb that contains 316 genes with a maximum LOD in the position 7,689,143 bp. *ABSQV11.2*, a second QTL with LOD = 3.9, was located in an interval of 17 Mb downstream of *ABSQV11.1*. Interestingly, *ABSQV11.1* only modifies abscission layer formation, but not earliness or any other trait. This behaviour suggest that the gene underlying *ABSQV11.1* may be located downstream ethylene biosynthesis and may act in the abscission layer formation. The abscission mechanism has been widely studied in tomato, referred generally to flower abscission (Mao *et al.*, 2000; Liu *et al.*, 2014; Nakano *et al.*, 2014; Roldan Gomez *et al.*, 2017). The induction of abscission in tomato is controlled by multiple MADS-box proteins that form dimers to regulate the development of an abscission zone, leading to a drastic change of expression of TFs related with meristem functions and, later, of cell-wall hydrolysis enzymes (Ito and Nakano, 2015). The role of these TFs specifically in fruit abscission and ripening has been studied only for *SlFYFL*, suggesting that it affects both ethylene production and abscission zone development (Xie *et al.*, 2014). The transcriptomic pattern of early and late induction of fruit abscission in melon suggested that ethylene and ABA control the development of an abscission zone, altering the expression of cell-wall related enzymes (Corbacho *et al.*, 2013).

CDQV6.1 was also exclusively related to a single trait, the chlorophyll degradation that leads to a visible change of fruit color, showing a significant LOD (Table 3.3, Figure 3.S3C, and Table 3.S3B). The Ved allele increased CD in a climacteric background, as the QTL was significant in the Ved-VIII subset, but non-detectable it in the PS-VIII subset. Mutants with a similar phenotype have been characterized in tomato and pepper, identifying a STAY-GREEN protein as responsible of their inability to degrade chlorophyll at the onset of ripening (Oa *et al.*, 2008). *CDQV6.1* is located between the

physical positions 6,598,284 and 7,589,164 of chromosome VI and contains 106 genes. *CmNAC-NOR*, a QTL in chromosome VI that has been recently reported to control climacteric ripening in melon (Ríos *et al.*, 2017) does not map in this interval.

Regarding flesh firmness, additional QTLs in LG X and VIII were mapped (Table 3.3). *FIRQV10.1* and *FIRQV10.2*, located in LG X, increased FIR when the Ved allele was present. Since they are close to each other, we cannot rule out that they represent a single QTL in the interval 748,430-4,144,473 bp (Figure 3.S3E). This interval contains 530 genes. *FIRQV8.2* was mapped in chromosome VIII, around 10 Mb downstream *ETHQV8.1*, with a maximum LOD of 6.3 in the position 27,868,043 bp (Table 3.3). A QTL for FIR was detected in a similar position using the Ved-VIII subset, with a maximum LOD = 3.4 (Table 3.S3B). Fruit texture has been broadly studied in melon due to its great importance from the commercial perspective, as the market desires climacteric varieties that remain firm during the postharvest stage (Saladié *et al.*, 2015; Bianchi *et al.*, 2016; Perpiñá *et al.*, 2016). Unlike in tomato, the softening of fruit flesh in melon is partially controlled by ethylene, and non-climacteric melon types ripe displaying sugar accumulation and decrease of flesh firmness (Pech *et al.*, 2008). A comparative transcriptomic analysis of climacteric and non-climacteric varieties showed that the set of differentially expressed enzymes involved in modifying cell-wall metabolism was different in Ved (e.g. polygalacturonases, glucan endo-1,3-β-glucosidases and β-d-xylosidases) and PS (fasciclin-like arabinogalactanan protein) (Saladié *et al.*, 2015).

The mapping experiment that discriminated the RIL population depending on the haplotype for *ETHQV8.1* allowed to propose three new QTLs that were masked in the principal QTL mapping analysis and supported some of the minor QTLs already detected in the main mapping experiment (Figure 3.5). Using the Ved-VIII subset, we could detect two additional QTLs related with ethylene production, *WEPQW5.1* and *ETHQW9.1* (Table 3.S3B). *ETHQW9.1* could correspond to a major gene involved in fruit abscission (*Al-4*) in the distal part of LG IX (Table 3.S5), however the exact position of *Al-4* in the genome could not be deduced. *ETHQW9.1* was delimited within the positions 1,503,685-2,403,875 in chromosome IX, which contains 102 genes; among them, several transcription factors were found, highlighting a NAC-domain containing protein *MELO3C022002*. Using the PS-VIII subset, we detected two additional QTLs, *EALFQX8.3* and *DAPPQX8.3*. The Ved allele for these QTLs accelerated the climacteric

response. As QTLs for qualitative traits ARO and CD were not detected in this interval, *EALFQX8.3* and *DAPPQX8.3* are probably not sufficient to trigger ethylene production.

The characterization of ethylene production and climacteric ripening in a segregating melon population has led to identify several QTLs governing ethylene production and ripening-associated traits, as chlorophyll degradation, fruit firmness and abscission layer formation. Among them, *ETHQV8.1* has a major effect in both earliness and height of the ethylene peak that triggers climacteric ripening. *MELO3C024518*, encoding a CTR1 kinase, could be a strong candidate for *ETHQV8.1*, however further experiments should be performed to validate its involvement in climacteric fruit ripening. Our work supports the existence of a broad spectrum of climacteric behaviour in melon, which is under polygenic inheritance, and will contribute to decipher the genetic network controlling this important trait.

Supplementary material

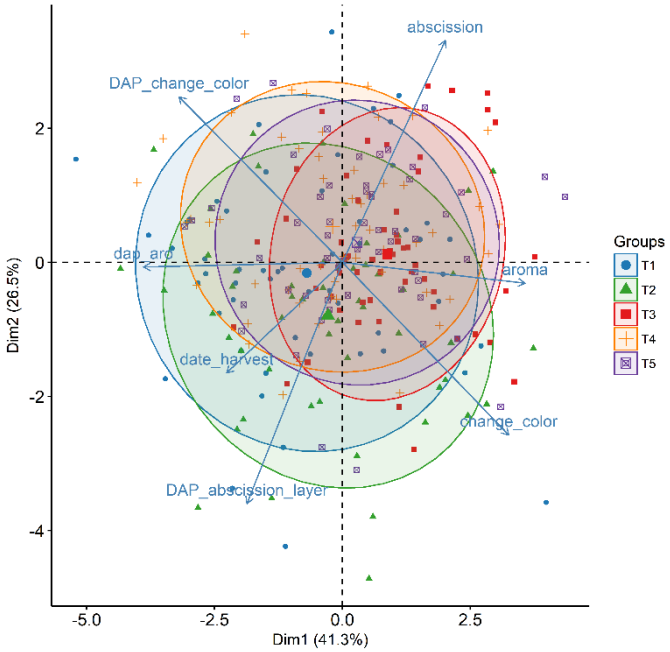

Figure 3.S1. PCA showing the variability in phenotypic data associated with environmental effects among blocks.

Table 3.S2. Basic statistics for climacteric ripening traits in the parental lines.

Trait	Line	Median	Mean	SD
ARO	Ved	1.00	1.00	0.00
	Hyb	1.00	1.00	0.00
	PS	0.00	0.00	0.00
EARO	Ved	34.00	34.67	2.27
	Hyb	34.00	35.22	3.03
	PS	-	-	-
CD	Ved	1.00	0.83	0.39
	Hyb	1.00	0.78	0.44
	PS	0.00	0.00	0.00
ABS	Ved	3.00	2.92	0.29
	Hyb	3.00	2.67	0.71
	PS	0.00	0.00	0.00
EABS	Ved	36.50	38.88	5.46
	Hyb	36.50	36.50	1.29
	PS	-	-	-
EALF	Ved	34.00	34.67	2.27
	Hyb	36.00	37.22	4.02
	PS	-	-	-
ECD	Ved	34.00	34.80	2.30
	Hyb	35.00	35.86	1.95
	PS	-	-	-

FIR	Ved	2.40	2.73	1.74
	Hyb	2.00	1.71	1.32
	PS	2.45	3.17	2.14
HAR	Ved	36.50	38.67	5.07
	Hyb	38.00	40.22	5.47
	PS	61.50	59.50	5.24

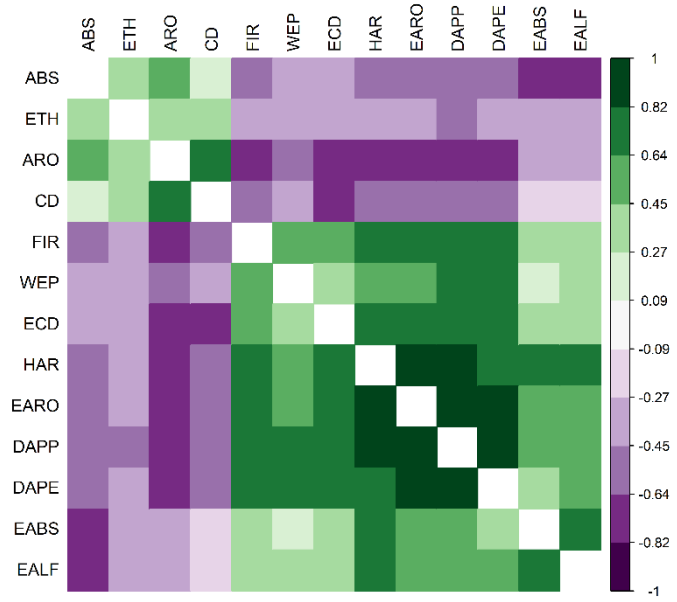

Figure 3.S2. Correlation matrix between traits, calculated with the mean values of all blocks.

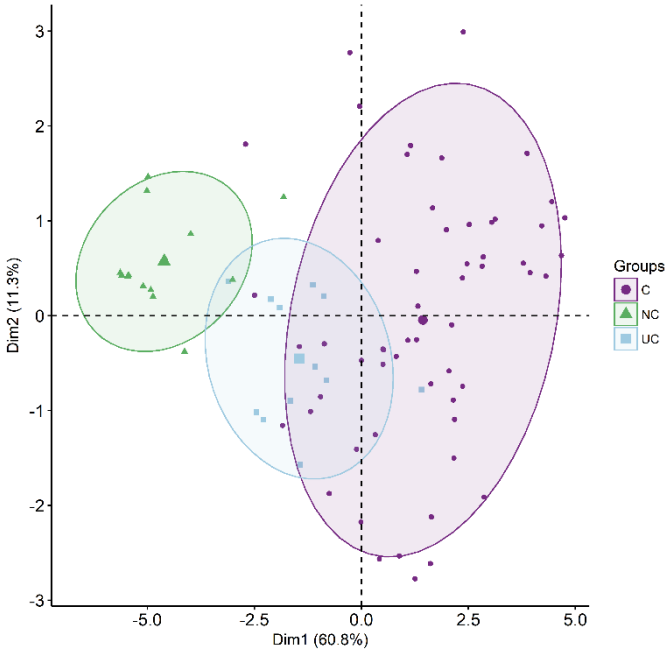

Figure 3.S4. PCA showing the grouping for climacteric (C, purple), unstable climacteric (UC, blue) and non-climacteric (NC, green) RILs.

Table 3.S5. Summary of QTLs described in other studies that map in similar intervals to those detected in our work.

Chr	Trait	QTL	Plant material	Physical position[1] (pb)	Linked marker	References
II	ETH	*eth2.1*	Ved x PI 161375	-	E39/M42_20	(Périn et al., 2002)
II	FIR	*ff2.2*	PS x PI 161375	-	CMGA36a	(Moreno et al., 2008)
III	ETH	*eth3.1*	Ved x PI 161375	-	E43/M44_20	(Périn et al., 2002)
III	ETH	*eth3.5*	PS x PI 161375	26,669,705	A_16-C12	(Vegas et al., 2013)
VIII	ABS	*Al-3*	Ved x PI 161375	-	H33/M43_21	(Périn et al., 2002)
VIII	FIR	*ff8.2*	PS x PI 161375	5,577,470	CMTC13	(Moreno et al., 2008)
VIII	FIR	*ff8.4*	PS x PI 161375	34,764,449	CMTCN56	(Moreno et al., 2008)
IX	ABS	*Al-4*	Ved x PI 161375	-	H36/M37_11a	(Périn et al., 2002)
X	FIR	*ff10.2*	PS x PI 161375	-	All LG	(Moreno et al., 2008)
X	ABS	*al.10*	Ved x Makuwa	1,722,720	CMPSNP528	(Perpiñá et al., 2016)
XI	FIR	-	Collection of accessions	29,559,098	PSI_41-B07	(Leida et al., 2015)
XI	ETH	*eth11.1*	Ved x PI 161375	-	E35/M35_8	(Périn et al., 2002)

Table 3.S6. List of potential candidate genes for *ETHQV8.1*.

Gene	Initial position	Final position	Description	Variants changing in the protein	Gene expression[1]				
					Fruit flesh DAP22	Fruit flesh DAP29	Fruit flesh DAP36	Fruit flesh DAP43	Fruit flesh DAP50
MELO3C024522	9603252	9605249	BnaAnng07340D protein	1	12.5	16.6	19.2	14.8	11.0
MELO3C024521	9623758	9626574	Histone-lysine N-methyltransferase SETD1B-like protein	2	0.0	0.0	0.0	0.0	0.1
MELO3C024520	9630393	9630993	ethylene-responsive transcription factor ERF024	0	0.0	0.6	1.1	3.3	10.0
MELO3C024519	9634048	9636531	Fructose-bisphosphate aldolase	0	125.4	71.5	103.4	93.7	72.9
MELO3C024518	9638990	9648937	serine/threonine-protein kinase CTR1-like	6	17.6	25.1	20.6	18.0	0.7
MELO3C024516	9653281	9675711	protein ROS1	10	3.0	11.1	6.4	3.1	0.2
MELO3C024515	9677903	9680982	splicing factor U2af small subunit B-like	1	68.1	82.1	86.2	99.5	45.5
MELO3C024514	9682886	9687564	enolase	0	339.8	401.2	417.8	527.5	241.3
MELO3C024513	9694722	9699966	glucomannan 4-beta-mannosyltransferase 9-like	0	59.3	2.7	3.6	4.8	1.5
MELO3C019311	9713031	9713408	glucomannan 4-beta-mannosyltransferase 9-like	0	0.0	0.0	0.0	0.0	0.0
MELO3C032937	9715540	9717395	glucomannan 4-beta-mannosyltransferase 9-like	0	-	-	-	-	-
MELO3C024511	9738405	9740144	Haloacid dehalogenase-like hydrolase superfamily protein	2	0.0	0.0	0.0	0.0	0.0
MELO3C024510	9741619	9745691	3-deoxy-d-manno-octulosonic-acid transferase	3	2.1	3.4	3.5	4.1	1.0
MELO3C024509	9754209	9761825	Pyruvate kinase	4	63.6	100.7	83.0	135.0	51.8

[1]According to the database Melonet-DB, generated from the cv. Harukei-3.

Digital Supplementary Material

Figure 3.S3. LOD scores for ethylene production and climacteric ripening traits showing minor QTLs. Only when at least one variable presented LOD>3 the chromosome is showed. The grey line showed the threshold of LOD=3 and the dotted line, LOD=2.5. A. chromosome II; B. chromosome III; C. chromosome VI; D. chromosome VII; E. chromosome X; F. chromosome XI.

Table 3.S1. Description of the SNPs used to A. select the IL families; B. genotype the QTL interval in the recombinant individuals and their progenies.

Table 3.S3. A. QTLs mapped using the phenotypic data from individual blocks (T1-T5); the significant QTLs (QTLs with LOD > 2.5 in three or more blocks co-localizing) are shaded in grey. B. QTLs mapped using the subsets VIII-Ved and VIII-PS.

Table 3.S4. A. Background genotyping of ILs from the families 720 and 414. B. Ripening-associated traits phenotyping of IL from the families 720 and 414, classified in base of the genotyping in the region of *ETHQV8.1*. C. Genotyping of additional internal SNPs for potential recombinants in the region of *ETHQV8.1*. D. Ripening-associated traits phenotyping of the progenies of two recombinant ILs from the family 414. E. Genotyping of additional internal SNPs within the interval of *ETHQV8.1* of the 414 recombinant progenies.

References

Adams-Phillips L, Barry C, Kannan P, Leclercq J. 2004. Evidence that CTR1-mediated ethylene signal transduction in tomato is encoded by a multigene family whose members display distinct regulatory features. Plant Molecular Biology **54**, 387–404.

Ayub R, Guis M, Ben Amor M, Gillot L, Roustan JP, Latché A, Bouzayen M, Pech JC. 1996. Expression of ACC oxidase antisense gene inhibits ripening of cantaloupe melon fruits. Nature Biotechnology **14**, 862–866.

Bemer M, Karlova R, Ballester AR, Tikunov YM, Bovy AG, Wolters-Arts M, de Barros Rossetto P, Angenent GC, de Maagd RA. 2012. The Tomato FRUITFULL Homologs TDR4 / FUL1 and Aspects of Fruit Ripening. The Plant Cell **24**, 4437–4451.

Bianchi T, Guerrero L, Gratacós-Cubarsí M, Claret A, Argyris J, Garcia-Mas J, Hortós M. 2016. Textural properties of different melon (*Cucumis melo* L.) fruit types : Sensory and physical-chemical evaluation. Scientia Horticulturae **201**, 46–56.

Binder BM. 2008. The ethylene receptors : Complex perception for a simple gas. Plant Science **175**, 8–17.

Cherian S, Figueroa CR, Nair H. 2014. 'Movers and shakers' in the regulation of fruit ripening: a cross-dissection of climacteric versus non-climacteric fruit. Journal of Experimental Botany **65**, 4705–4722.

Chung MY, Vrebalov J, Alba R, Lee J, McQuinn R, Chung J-D, Klein P, Giovannoni J. 2010. A tomato (*Solanum lycopersicum*) APETALA2/ERF gene, SlAP2a, is a negative regulator of fruit ripening. The Plant Journal **64**, 936–947.

Corbacho J, Romojaro F, Pech JC, Latche A, Gomez-jimenez MC. 2013. Transcriptomic Events Involved in Melon Mature-Fruit Abscission Comprise the Sequential Induction of Cell- Wall Degrading Genes Coupled to a Stimulation of Endo and Exocytosis. PloS one **8**, 58363.

Diaz A, Fergany M, Formisano G, *et al.* 2011. A consensus linkage map for molecular markers and quantitative trait loci associated with economically important traits in melon (*Cucumis melo* L.). BMC Plant Biology **11**, 111.

Doyle J. 1991. DNA Protocols for Plants. In: Hewitt GM,, In: Johnston AWB,, In:

Young JPW, eds. Molecular Techniques in Taxonomy. Berlin, Heidelberg: Springer Berlin Heidelberg, 283–293.

Elitzur T, Yakir E, Quansah L, Zhangjun F, Vrebalov J, Khayat E, Giovannoni JJ, Friedman H. 2016. Banana MaMADS Transcription Factors Are Necessary for Fruit Ripening and Molecular Tools to Promote Shelf-Life and Food Security. Plant Physiology **171**, 380–391.

Ezura H, Owino WO. 2008. Melon, an alternative model plant for elucidating fruit ripening. Plant Science **175**, 121–129.

Giovannoni JJ. 2007. Fruit ripening mutants yield insights into ripening control. Current Opinion in Plant Biology **10**, 283–289.

Giovannoni J, Nguyen C, Ampofo B, Zhong S, Fei Z. 2017. The Epigenome and Transcriptional Dynamics of Fruit Ripening. Annual Review of Plant Biology **68**, 61–84.

Ito Y, Nakano T. 2015. Development and regulation of pedicel abscission in tomato. Frontiers in Plant Science **6**, 1–6.

Kieber J, Rothenberg M, Roman G, Feldmann K, Ecker J. 1993. CTR1, a negative regulator of the ethylene response pathway in *Arabidopsis*, encodes a member of the raf family of protein kinases. Cell **72**, 427–441.

Lang Z, Wang Y, Tang K, Tang D, Datsenka T, Cheng J, Zhang Y, Handa AK, Zhu JK. 2017. Critical roles of DNA demethylation in the activation of ripening-induced genes and inhibition of ripening-repressed genes in tomato fruit. Proceedings of the National Academy of Sciences of the United States of America **114**, 4511–4519.

Leclercq J, Adams-phillips LC, Zegzouti H, Jones B, Latche A, Giovannoni JJ, Pech J, Bouzayen M. 2002. Ethylene Signaling Ability in *Arabidopsis* and Novel Expression Patterns in Tomato. Plant Physiology **130**, 1132–1142.

Leida C, Moser C, Esteras C, Sulpice R, Lunn JE, de Langen F, Monforte AJ, Picó B. 2015. Variability of candidate genes, genetic structure and association with sugar accumulation and climacteric behavior in a broad germplasm collection of melon (*Cucumis melo* L.). BMC Genetics **16**, 28.

Lelievre JM, Latche A, Jones B, Bouzayen M, Pech JC. 1997. Ethylene and fruit

ripening. Physiologia Plantarum **101**, 727–739.

Lin Z, Hong Y, Yin M, Li C, Zhang K, Grierson D. 2008. A tomato HD-Zip homeobox protein, LeHB-1, plays an important role in floral organogenesis and ripening. The Plant Journal **55**, 301–310.

Liu R, How-kit A, Stammitti L, *et al.* 2015. A DEMETER-like DNA demethylase governs tomato fruit ripening. Proceedings of the National Academy of Sciences of the United States of America **112**, 10804–10809.

Liu D, Wang D, Qin Z, Zhang D, Yin L, Wu L, Colasanti J, Li A. 2014. The SEPALLATA MADS-box protein SLMBP21 forms protein complexes with JOINTLESS and MACROCALYX as a transcription activator for development of the tomato flower abscission zone. The Plant Journal **77**, 284–296.

Manning K, Tör M, Poole M, Hong Y, Thompson AJ, King GJ, Giovannoni JJ, Seymour GB. 2006. A naturally occurring epigenetic mutation in a gene encoding an SBP-box transcription factor inhibits tomato fruit ripening. Nature Genetics **38**, 948–952.

Mao L, Begum D, Chuang H, Budiman MA, Szymkowiak EJ, Irish EE, Wing RA. 2000. *JOINTLESS* is a MADS-box gene controlling tomato flower abscission zone development. Nature **406**, 910–913.

Mcatee PA, Richardson AC, Nieuwenhuizen NJ, Gunaseelan K, Hoong L, Chen X, Atkinson RG, Burdon JN, David KM, Schaffer RJ. 2015. The hybrid non-ethylene and ethylene ripening response in kiwifruit (*Actinidia chinensis*) is associated with differential regulation of MADS -box transcription factors. BMC Plant Biology, 1–16.

Minas IS, Font C, Dangl GS, Gradziel TM. 2015. Discovery of non-climacteric and suppressed climacteric bud sport mutations originating from a climacteric Japanese plum cultivar (*Prunus salicina* Lindl.). Frontiers in Plant Science **6**, 1–16.

Moreno E, Obando JM, Dos-Santos N, Fernández-Trujillo JP, Monforte AJ, Garcia-Mas J. 2008. Candidate genes and QTLs for fruit ripening and softening in melon. Theoretical and Applied Genetics **116**, 589–602.

Nakano T, Fujisawa M, Shima Y, Ito Y. 2014. The AP2 / ERF transcription factor SlERF52 functions in flower pedicel abscission in tomato. Journal of Experimental

Botany **65**, 3111–3119.

Oa PW, Barry CS, Mcquinn RP, Chung M, Besuden A, Giovannoni JJ. 2008. Amino Acid Substitutions in Homologs of the STAY-GREEN Protein Are Responsible for the green-flesh and chlorophyll retainer Mutations of Tomato. Plant Physiology **147**, 179–187.

Osorio S, Alba R, Nikoloski Z, Kochevenko A, Fernie AR, Giovannoni JJ. 2012. Integrative Comparative Analyses of Transcript and Metabolite Pro fi les from Pepper and Tomato Ripening and Development Stages Uncovers Species-Specific Patterns of Network Regulatory Behavior. Plant Physiology **159**, 1713–1729.

Pech JC, Bouzayen M, Latché A. 2008. Climacteric fruit ripening: Ethylene-dependent and independent regulation of ripening pathways in melon fruit. Plant Science **175**, 114–120.

Pereira L, Pujol M, Garcia-mas J, Phillips MA. 2017. Non-invasive quantification of ethylene in attached fruit headspace at 1 p.p.b. by gas chromatography – mass spectrometry. The Plant Journal **91**, 172–183.

Pereira L, Ruggieri V, Pérez S, Alexiou KG, Fernández M, Jahrmann T, Pujol M and Garcia-Mas J. QTL mapping of melon fruit quality traits using a high-density GBS-based genetic map. (submitted)

Périn C, Gomez-Jimenez M, Hagen L, Dogimont C, Pech J, Latché A, Pitrat M, Lelièvre J. 2002. Molecular and Genetic Characterization of a Non-Climacteric Phenotype in Melon Reveals Two Loci Conferring Altered Ethylene Response in Fruit. Plant Physiology **129**, 300–309.

Perpiñá G, Esteras C, Gibon Y, Monforte AJ, Picó B. 2016. A new genomic library of melon introgression lines in a cantaloupe genetic background for dissecting desirable agronomical traits. BMC Plant Biology **16**, 1–21.

Powell ALT, Nguyen C V., Hill T, *et al.* 2012. Uniform ripening Encodes a Golden 2-like Transcription Factor Regulating Tomato Fruit Chloroplast Development. Science **336**, 1711–1715.

R Core Team. 2012. R: A language and environment for statistical computing. Vienna, Austria: R Foundation for Statistical Computing. URL http://www.R-project.org/

Rios P, Argyris JM, Vegas J, *et al.* 2017. *ETHQV6.3* is involved in melon climacteric fruit ripening and is encoded by a NAC domain transcription factor. The Plant Journal **91**, 671–683.

Roldan Gomez MV, Périlleux C, Morin H, Huerga S. 2017. Natural and induced loss of function mutations in SlMBP21 MADS-box gene led to jointless-2 phenotype in tomato. Scientific Reports **7**, 1–10.

RStudio. 2012. RStudio: Integrated development environment for R RStudio. Boston, MA, USA. URL http://www.rstudio.com/

Ruggieri V, Alexiou KG, Morata J, *et al.* An improved assembly and annotation of the melon (*Cucumis melo* L.) reference genome. (under review in Sci Rep)

Saladié M, Cañizares J, Phillips MA, Rodriguez-Concepcion M, Larrigaudière C, Gibon Y, Stitt M, Lunn JE, Garcia-Mas J. 2015. Comparative transcriptional profiling analysis of developing melon (*Cucumis melo* L.) fruit from climacteric and non-climacteric varieties. BMC Genomics **16**, 1–20.

Sanseverino W, Hénaff E, Vives C, Pinosio S, Burgos-Paz W, Morgante M, Ramos-Onsins SE, Garcia-Mas J, Casacuberta JM. 2015. Transposon Insertions, Structural Variations, and SNPs Contribute to the Evolution of the Melon Genome. Molecular Biology and Evolution **32**, 2760–2774.

Seymour GB, Ryder CD, Cevik V, Hammond JP, Popovich A, King GJ, Vrebalov J, Giovannoni JJ, Manning K. 2011. A SEPALLATA gene is involved in the development and ripening of strawberry (*Fragaria* x *ananassa* Duch.) fruit, a non-climacteric tissue. Journal of Experimental Botany **62**, 1179–1188.

Shima Y, Fujisawa M, Kitagawa M, Nakano T, Nakamura N, Shiina T, Sugiyama J, Kasumi T, Ito Y. 2014. Tomato FRUITFULL homologs regulate fruit ripening via ethylene biosynthesis. Bioscience, Biotechnology, and Biochemistry **78**, 231–237.

Van Ooijen JW. 1999. LOD significance thresholds for QTL analysis in experimental populations of diploid species. Heredity **83**, 613–624.

Van Ooijen J, Maliepaard C. 1996. MapQTL Version 3.0: Software for the calculation of QTL positions on genetic maps. DLO-Centre for Plant Breeding and Reproduction Research, Wageningen, The Netherlands.

Vegas J, Garcia-Mas J, Monforte AJ. 2013. Interaction between QTLs induces an advance in ethylene biosynthesis during melon fruit ripening. Theoretical and Applied Genetics **126**, 1531–1544.

Vrebalov J, Pan IL, Arroyo AJM, *et al.* 2009. Fleshy fruit expansion and ripening are regulated by the Tomato SHATTERPROOF gene *TAGL1*. The Plant Cell **21**, 3041–62.

Vrebalov J, Ruezinsky D, Padmanabhan V, White R, Medrano D, Drake R, Schuch W, Giovannoni J. 2002. A MADS-box gene necessary for fruit ripening at the tomato ripening-inhibitor (*rin*) locus. Science **296**, 343–346.

Xie Q, Hu Z, Zhu Z, Dong T, Zhao Z, Cui B, Chen G. 2014. Overexpression of a novel MADS-box gene *SlFYFL* delays senescence, fruit ripening and abscission in tomato. Scientific Reports **4**, 1–10.

Yano R, Ezura H. 2016. Fruit ripening in melon. Genetics and Genomics of Cucurbitaceae.345–375.

Yano R, Nonaka S, Ezura H. 2018. Melonet-DB, A Grand RNA-seq Gene Expression Atlas in Melon (*Cucumis melo* L.). Plant and Cell Physiology **59**, e(1-15).

Zhong S, Fei Z, Chen Y, *et al.* 2013. Single-base resolution methylomes of tomato fruit development reveal epigenome modifications associated with ripening. Nature Biotechnology **31**, 154–159.

Chapter 4

Fine mapping of *ETHQB3.5*, a QTL triggering climacteric ripening in the near isogenic line 8M35

Introduction

Fleshy fruits are a basic component of human diet, being a main source of sugars, antioxidants, vitamins and fiber. Fruit ripening is a complex physiological process with huge importance from the organoleptic and the nutritional perspectives. Once the fruit growth ends, a series of changes are triggered to become attractive for seed dispersal, as an increase in sugar content, changes in external and internal color and modifications in fruit texture, among others (Giovannoni et al. 2017). Classically, two types of ripening have been described, depending on the role of the hormone ethylene (Lelievre et al. 1997). In climacteric fruits, the onset of ripening is defined by an autocatalytic synthesis of ethylene accompanied by an increase in respiration, which provokes some specific processes as synthesis of volatiles that lead to a sweet aroma, chlorophyll degradation and abscission layer formation. On the other hand, non-climacteric fruits do not show an ethylene peak during ripening, although most of the changes associated to ripening also happen. Other hormones as abscisic acid (ABA) and auxin have also a role in the ripening process, especially in non-climacteric fruits (Cherian et al. 2014).

Fruit ripening has been largely studied using tomato, a climacteric species, as a model (Giovannoni et al. 2017). Several mutants have been characterized to identify the main regulators of the process: the MADS-box *RIN* (Vrebalov et al. 2002), the NAC factor *NOR* (Giovannoni 2007) and the SBP-box gene *CNR* (Manning et al. 2006), among others. Melon has recently emerged as an alternative model to study fruit ripening, due to the coexistence of climacteric and non-climacteric varieties within the species (Ezura and Owino 2008). Some recent work has attempted to characterize climacteric and non-climacteric ripening in melon, involving genetic, transcriptomic and metabolomics analyses of different varieties and segregating populations (Yano and Ezura 2016). An antisense transgenic line, where one of the genes encoding a main enzyme of ethylene biosynthesis, *CmACO1*, was silenced, has been very useful to determine the phenotypic effects that are ethylene dependent in melon; for example, the carotenoid accumulation of the fruit flesh is independent of ethylene, unlike in tomato (Ayub et al. 1996; Pech et al. 2008). Gene expression during fruit development and ripening varies greatly depending on the climacteric behavior of the line. Distinct patterns of transcription were observed for climacteric and non-climacteric varieties, involving the ethylene pathway and other phenotypic traits related with ripening as texture properties and sugar content (Saladié et al. 2015). In this study, they also observed that the Korean accession

"Songwhan Charmi" (SC), considered as non-climacteric, showed an intermediate profile. Recently, an expression atlas obtained in the climacteric variety "Harukei-3" has been used to observe the co-expression patterns of the main transcriptional regulators of fruit ripening (Yano et al. 2018).

A Near Isogenic Line (NIL) population developed from a cross between the exotic accession SC and the Spanish variety "Piel de Sapo" (PS), both non-climacteric, revealed two QTLs for climacteric ripening *ETHQB3.5* and *ETHQV6.3* in chromosomes III and VI, respectively (Moreno et al. 2008; Vegas et al. 2013). Both SC introgressions were capable of triggering the autocatalytic synthesis of ethylene independently, however the ethylene peak was higher and appeared earlier when both introgressions were carried together, showing an additive or epistatic interaction (Vegas et al. 2013). The NIL carrying both QTLs, 8M31, was highly climacteric, showing change of external fruit color from dark green to yellow, production of a sweet aroma and fruit abscission around 30-35 days after pollination (DAP). The NIL containing *ETHQV6.3*, 8M40, presented a less intense and delayed phenotype when compared to 8M31. The NIL containing *ETHQB3.5*, 8M35, showed an even weaker climacteric ripening, and generally very dependent on the environment. The positional cloning of *ETHQV6.3* revealed that the underlying gene is the orthologous of the tomato *NOR* gene (Ríos et al. 2017). Mutants of this gene in the highly climacteric "Charentais mono" background, showed a delay of around eight days in ripening, whereas the amount of ethylene produced was not affected.

8M35, carrying *ETHQB3.5*, and derived subNILs containing smaller introgressions have been previously studied, focusing especially on postharvest behavior and aroma production (Obando-Ulloa et al. 2008; Fernández-Trujillo et al. 2008; Obando-Ulloa et al. 2009; Obando-Ulloa et al. 2010). The volatile profile in melon varieties depends on the type of ripening; non-climacteric varieties present a scarce volatile content, mainly formed by alcohols and aldehydes, and the aroma is almost inexistent (so-called *inodorus*); climacteric varieties show a higher content of volatiles where the most characteristic are esters, conferring a strong sweet aroma (Gonda et al. 2016). The ethylene production and respiration rate of these 8M35-derived lines were also measured, allowing to classify them as climacteric or non-climacteric (Fernández-Trujillo et al. 2008). Nevertheless, an erratic behavior was observed in some of the subNILs in different years or environments, suggesting that *ETHQB3.5* may be highly environmental-dependent.

Although 8M35 and its derived subNILs have been previously studied, the gene underlying the QTL remains unknown. Therefore, the objective of the present work was to fine map *ETHQB3.5* and to identify a candidate gene as responsible of the climacteric phenotype.

Materials and methods

Plant material

The NIL 8M35, containing *ETHQB3.5*, and the Spanish cultivar "Piel de Sapo" (accession T111) were crossed to obtain a F2 segregating population. F2 seedlings were grown at CRAG greenhouses (Barcelona) and screened to select the informative individuals. An analogous process was followed with their progenies in subsequent years (Figure 4.1). A set of four subNILs developed before was used in 2014 (Obando-Ulloa et al. 2008).

The selected plant material was grown in Caldes de Montbui (Barcelona) in greenhouse conditions. Plants were pruned weekly and pollinations were executed manually, allowing to develop only one fruit per plant. The harvest point was determined by the following criteria: a) abscission date when the fruit abscised; b) after at least 60 DAP when fruits were non-climacteric. Due to the phenotypes observed in consecutive trials for some subNILs, the harvest date for non-climacteric fruits was increased to allow detecting delayed and slight climacteric phenotypes, leading to harvest fruits up to 75 DAP.

The number of biological replicates for each subNIL in each trial varied from 2 to 13, principally due to fruit set problems. In the main tables, graphical representations and statistical analysis, only the subNILs with $n \geq 3$ were used, although the subNILs with less replicates are presented in the supplementary material and referred occasionally in the text.

Phenotyping of climacteric ripening traits

Ripening-related traits were evaluated as qualitative (presence or absence) and quantitative, i.e. earliness of appearance of the trait in DAP. The studied ripening-related traits were biosynthesis of volatiles leading to a sweet aroma and earliness of aroma

production (ARO and EARO), change of external fruit color mainly due to chlorophyll degradation (CD) and abscission layer formation in the pedicel of the fruit, provoking abscission in some cases (EALF, ABS and EABS) (Table 4.1). The visual inspection of melon fruits, attached to the plant, was performed daily, from approximately 25 DAP until harvest. CD was recorded only when it was obvious in visual inspections. ARO was evaluated each other day by smelling the fruits. ABS was recorded using an index from 0, no abscission layer formation (ALF), 1, subtle and/or partial ALF, 2 almost complete ALF with obvious scar, and 3, total ALF, generally with fruit abscission. HAR was directly correlated with EABS, so in some trials it was used also as a climacteric-related phenotype.

Table 4.1. Description and code of climacteric ripening related traits evaluated.

Trait (units)	Code
Production of aroma	ARO
Earliness of aroma (DAP)	EARO
Chlorophyll degradation	CD
Earliness of abscission layer formation (DAP)	EALF
Grade of abscission	ABS
Earliness of abscission (DAP)	EABS
Harvest date (DAP)	HAR

DNA extraction and genotyping

DNA extractions were performed from young leaves following the CTAB protocol (Doyle 1991) with some modifications (Pereira et al. submitted).

The SNPs used were discovered and designed from resequencing data of the parental lines (PS and SC) and the positions are referred in all cases to the melon reference genome v3.6.1 (Ruggieri et al., under review, http://www.melonomics.net). SNPs are described in Table 4.S1. Plants were genotyped with SNPs using Custom TaqMan SNP Genotyping Assays (Thermo Fisher Scientific, USA) and the KASPar SNP Genotyping System (KBiosciences, Herts, UK). Both Taqman probes and KASPar primers were designed using specific tools provided by the suppliers. Taqman assays were used to screen progenies in search of recombinants and for subNILs development. The genotyping was done by qPCR in a LightCycler 480 instrument (Roche Diagnostics, Spain) using the universal LightCycler MasterMix following the technical instructions recommended by the supplier. KASPar assays were used to increase the SNP density in the region of the

introgression with selected individuals, and the genotyping was performed using the high-throughput genotyping system Biomark HD, based on Fluidigm technology, with 48x48 chips.

Identification of recombinants and subNIL development

In order to identify individuals that had recombined within the *ETHQB3.5* interval, we developed an F2 population from the 8M35 x PS cross (Figure 4.1) and we screened 500 seedlings with the flanking SNPs CMPSNP64 and CMPSNP4583 using Custom Taqman SNP Genotyping Assays. Due to the large number of recombinant individuals detected and the impossibility of growing all the plants because of logistic reasons, we performed a second screening with the internal SNP Cm0306 using the KASPar system to select the most interesting recombinants. The chosen recombinant individuals were grown in the greenhouse, self-pollinated and their progenies were screened again with the flanking SNPs to select the target subNILs (Figure 4.1). Once in the greenhouse, young leaves were collected to extract DNA and they were genotyped again using SNP chips containing flanking and internal SNPs.

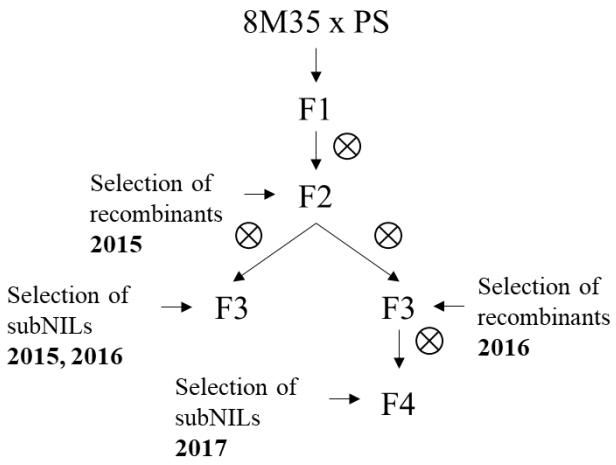

Figure 4.1. Breeding scheme representing the crosses performed to obtain the subNILs derived from 8M35.

An analogous procedure was followed with F3 seedlings from self-pollinated recombinants with a heterozygous haplotype in the most informative regions within the *ETHQB3.5* interval (Figure 4.1). 200 seedlings of the R87 progeny and 400 seedlings of the R34 and R154 progenies were used to obtain new recombinants. Two additional Taqman assays were designed to perform the genotyping experiments for SNPs chr3_24479823 and sca14_2983462 (Table 4.S1).

Genetic map construction and QTL mapping

The genetic map was obtained with the software JoinMap v4.1 (Van Ooijen 2006). The phenotypic data from recombinants and subNILs of 2015 (Table 4.S2a and 4.S2b, respectively) were used to perform a QTL mapping analysis (Van Ooijen and Maliepaard 1996) using the interval mapping algorithm.

Statistical analyses

All the statistical analyses and graphical representations were obtained using the software R v3.2.3 (R Core Team 2012) with the RStudio v1.0.143 interface (RStudio 2012).

In order to include the non-climacteric individuals in the visualization of the data when the fruits did not form abscission layer, EALF was imputed as the latest harvest date in the trial. The statistical tests used to compare the subNILs were Kruskal Wallis and Wilcox tests, due to the non-normal distribution of the data.

Results

Fine mapping of ETHQB3.5

A map-based cloning strategy was implemented to fine map *ETHQB3.5*, contained in the NIL 8M35, which carries an original introgression of 5.02 Mb in chromosome III. Several trials were done during four consecutive summers using F2 plants that had suffered a recombination within the *ETHQB3.5* interval and subNILs derived from the original NIL 8M35 carrying narrower introgressions.

2014 subNILs trial

A set of subNILs previously developed were evaluated for climacteric ripening in 2014 (Obando-Ulloa et al. 2008). After genotyping, four subNILs carrying different homozygous introgressions were identified (SC7, SC11, SC12 and SC13; Figure 4.2b), besides one segregating progeny from subNIL SC3 (Table 4.S3). Other two subNILs, SC8 and SC14, were found to be identical to SC7 and SC13 respectively after the genotyping, so they were included in the analysis as SC7 and SC13. Surprisingly, in this trial most of the phenotypes associated with climacteric ripening, as chlorophyll degradation and aroma production, were not clearly appreciated in any fruit, even for the

climacteric control line 8M35. However, an evident pattern was observed for fruit abscission. 8M35 and subNILs SC11, SC12 and SC13 were totally climacteric according to this trait, with all the individuals presenting abscission around 46 DAP (Table 4.2). In contrast, SC7 presented an intermediate phenotype, with 29% of the individuals showing fruit abscission, but later than the climacteric control line. None of the subNILs was totally non-climacteric as the PS parental. HAR allowed the differentiation of three behaviors: totally non-climacteric, only displayed by the PS parental line, an intermediate phenotype slightly climacteric in SC7, and a stronger climacteric phenotype as in the 8M35 parental line (Figure 4.2a). Using the Wilcox test, we determined that SC7 was significantly different from the climacteric NILs (8M35 and the rest of subNILs) but also different from PS (Table 4.3). This result suggested that two different QTLs could be involved in the phenotype observed in 8M35, one of them located within the physical interval 21,660,674 bp -26,421,885 bp (named *ETHQB3.5.1*) and the second one delimitated by the positions 28,352,817 bp - 28,841,908 bp (named *ETHQB3.5.2*). Although the progeny of SC3 was not included in the main analysis, because a part of the introgression was segregating, two individuals, SC3.5 and SC3.6, were fixed for PS alleles and they carried an introgression containing only *ETHQB3.5.1*. One of them, SC3.6 showed fruit abscission at 56 DAP, supporting our hypothesis of two QTLs with additive effect inside *ETHQB3.5* (Table 4.S3).

Table 4.3. Wilcox test p-values for HAR among the lines used in the 2014 subNILs trial.

Wilcox test	PS	8M35	SC7	SC11	SC12
8M35	0.016[1]	-	-	-	-
SC7	0.021	0.001	-	-	-
SC11	0.021	0.571	0.002	-	-
SC12	0.016	0.951	0.001	0.571	-
SC13	0.012	0.061	0.000	0.108	0.064

[1]Gray shading for significant differences

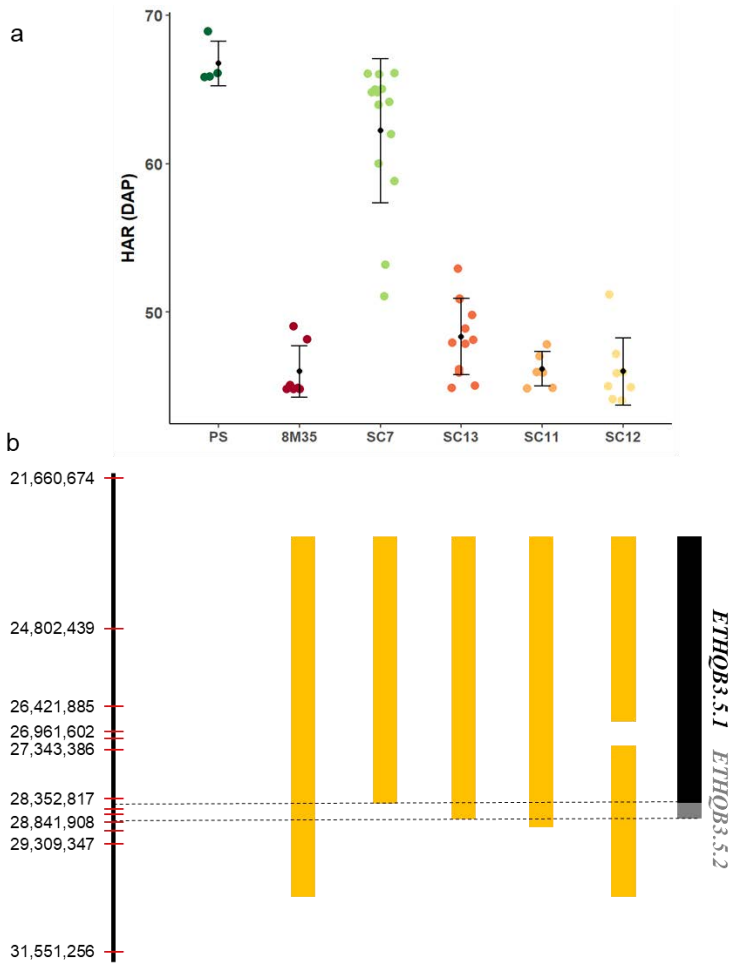

Figure 4.2. Evaluation of the original set of subNILs in the 2014 trial. a. HAR phenotype for the parental lines and the four subNILs, corresponding to EABS when the fruit presented abscission. b. Graphical representation of the introgressions according to the genotyping of the lines; the bar at the left represents the region of chromosome III containing *ETHQB3.5* and each red line corresponds to a genotyped SNP at its physical position (v3.6.1).

Table 4.2. Genotyping of the region of *ETHQB3.5* and phenotyping (mean and standard deviation) of the parental lines and the subNILs in the 2014 trial.

Line	CMPSNP31	CMPSNP661	CMPSNP641	CMPSNP979	Cm0306	CMPSNP8	CMPSNP4624	sca14_3312863	SFMe041	sca14_2983462	CMPSNP4583	CMPSNP6471	CMPSNP651	n2	ABS	EABS	HAR
8M35	B	B	A	A	A	A	A	A	A	A	A	A	B	8	3 ± 0	46.0 ± 1.7	46.0 ± 1.7
T111	B	B	B	B	B	B	B	B	B	B	B	B	B	4	0 ± 0	-	66.0 ± 0
SC7	B	B	A	A	A	A	A	A	B	B	B	B	B	14	1 ± 1	57.5 ± 6.9	62.2 ± 4.9
SC13	B	B	A	A	A	A	A	A	A	A	B	B	B	12	3 ± 0	48.3 ± 2.6	48.3 ± 2.6
SC11	-	-	A	A	A	A	A	A	A	A	A	B	B	6	3 ± 0	46.2 ± 1.2	46.2 ± 1.2
SC12	-	-	A	A	B	B	A	A	A	A	A	A	B	8	3 ± 0	46.0 ± 2.3	46.0 ± 2.3

ETHQB3.5.1 *ETHQB3.5.2*

[1]Flanking SNPs delimiting the introgression of 8M35 and ETHQB3.5.

[2]Number of replicates per line

2015 recombinants trial

The screening of 500 F2 seedlings with flanking markers identified 213 recombinant individuals within the interval region of *ETHQB3.5*. As the previous 2014 subNILs trial suggested the existence of two QTLs in this region, we genotyped one internal SNP (Cm0306) to specifically select more plants that had recombined in the distal region of the introgression, where *ETHQB3.5.2* is located. A total of 100 plants, 25 recombinants in the *ETHQB3.5.1* region and 75 in the *ETHQB3.5.2* region, were planted in the greenhouse and self-pollinated to phenotype and obtain their progenies. The recombinants were genotyped with a set of SNPs, including 38 internal SNPs and 4 external SNPs, in addition to the flanking markers, resulting in at least one recombinant for almost all the possible recombination points (Table 4.S1 and Table 4.S2a). We could obtain melons from 79 out of 100 recombinants but only 45 were successfully phenotyped for ripening traits, due to fungal infections and bad fruit development. A genetic map in the region was constructed, yielding a total genetic distance of 63 cM. A QTL interval mapping experiment revealed LOD scores > 3 for the four variables studied (ABS, ARO, CD and HAR) in almost the entire interval of the introgression, but two different peaks were observed, with LOD peaks around the physical positions 27,343,386 bp and 28,053,902 bp (Figure 4.3a). These positions are not exactly inside the intervals of *ETHQB3.5.1* and *ETHQB3.5.2*, but near them.

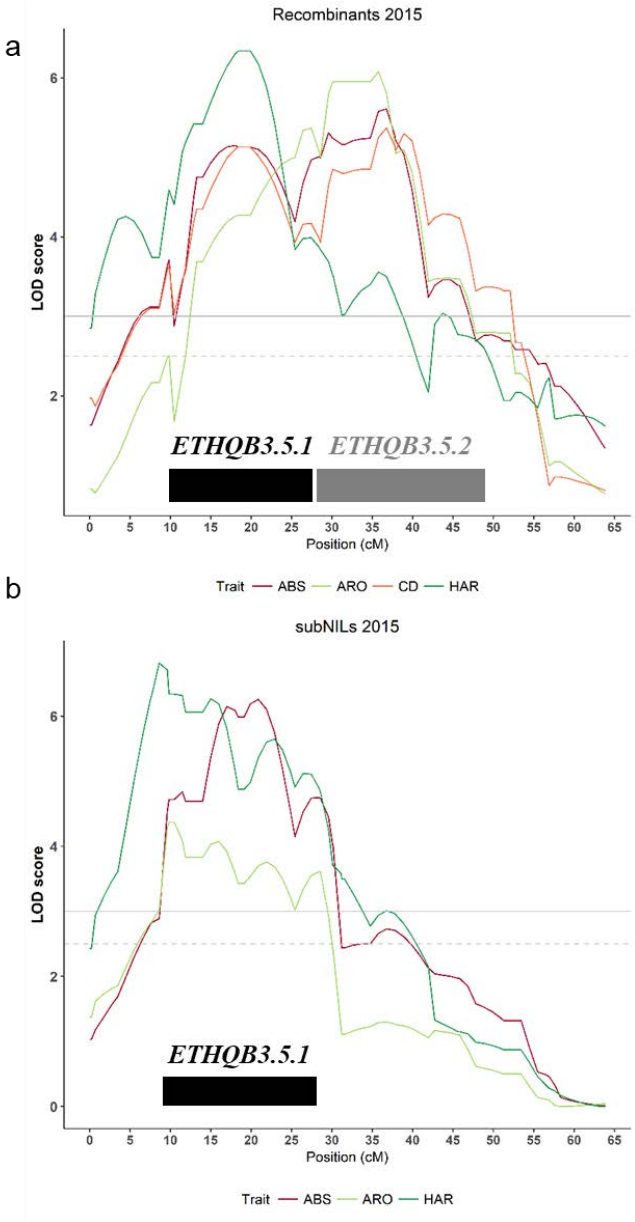

Figure 4.3. LOD scores obtained in the QTL mapping experiment for the recombinants (a) and subNILs (b) in 2015.

2015 subNILs trial

Twenty-one homozygous subNILs carrying different introgressions were selected from the progenies of the recombinants using the flanking SNPs (Table 4.S2b). Due to the low temperatures and high humidity, some plants presented fruit set problems and fungal infections, reducing the number of biological replicates available per subNIL. Besides, after genotyping with the internal SNPs, we detected additional recombinations within the expected introgressions, which also decreased the number of useful biological replicates (Table 4.S2b). The phenotypes and genotypes of the nine subNILs with n≥3

are presented in Figure 4.4 and Table 4.4. All the fruits from the climacteric control 8M35 showed aroma and abscised from the plant around 52 DAP (Figure 4.4a, c and d). The only subNIL presenting a phenotype very similar to the parental line 8M35 was R76, whose introgression covered the interval 25,961,864 bp -29,309,347 bp and could potentially carry both QTLs. The other subNILs presented intermediate phenotypes, with a variable proportion of fruits that produced aroma (from 100% in R90, R76 and R98 to 33% in R140 and R183) (Figure 4.4c) or abscission (from 100% in R76 and R98 to 25% in R145) (Figure 4.4d). The four subNILs (R183, R140, R149 and R145) that carried only the distal part of the introgression, corresponding to *ETHQB3.5.2*, produced aromatic fruits with abscission layer formation in around 50% of the cases, but these climacteric symptoms were delayed around 10 days when compared to 8M35 and R76. A similar behavior was observed for the three subNILs (R164, R137 and R90) carrying only the proximal region of the introgression, which contained *ETHQB3.5.1*, but the climacteric effects seemed slightly stronger and less delayed than the controls. None of the lines was totally non-climacteric, except PS.

The complete set of data, including the lines containing additional recombinations (Table 4.S2b), were used to perform a QTL mapping analysis. In this case, only one significant QTL was detected in the proximal region of the introgression, partially overlapping with *ETHQB3.5.1* (Figure 4.3b), in accordance with the stronger climacteric behavior observed in this group of subNILs.

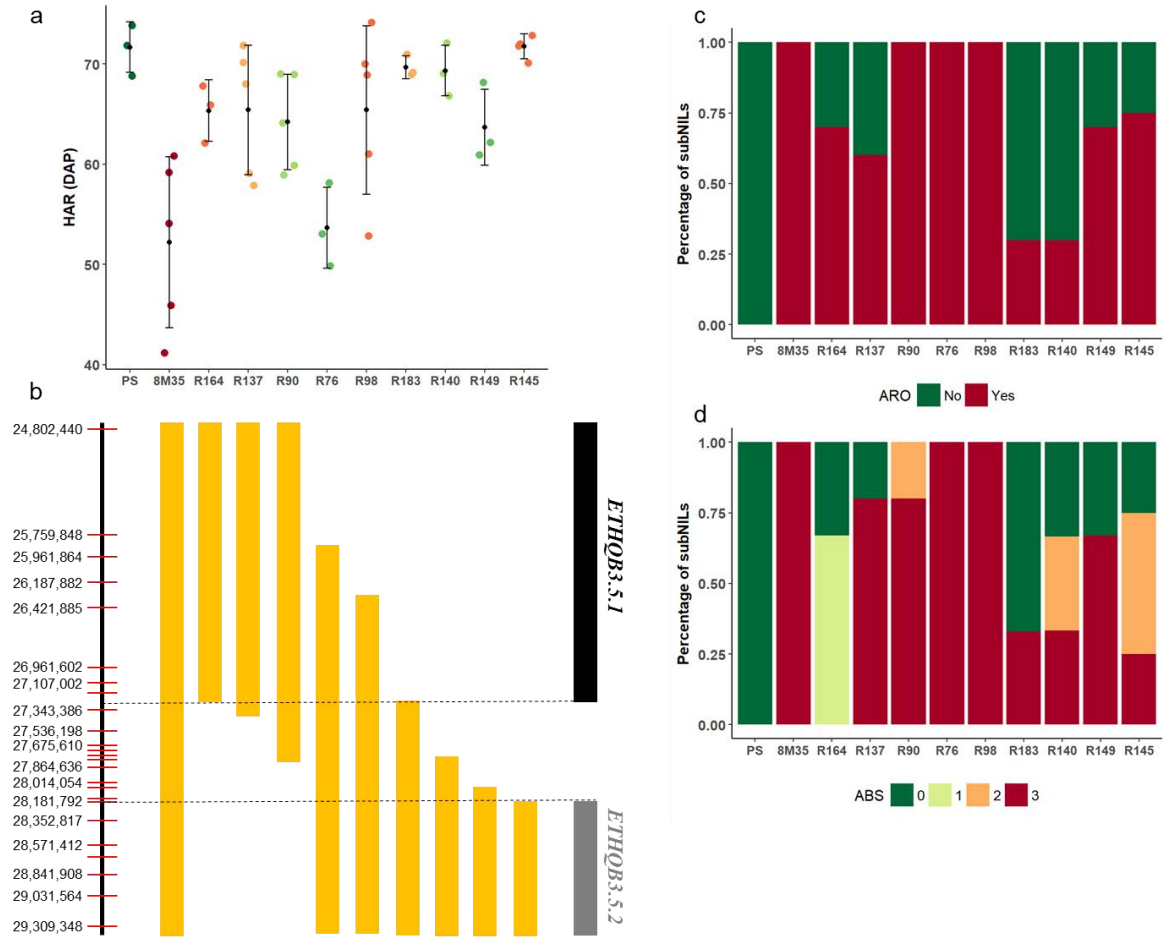

Figure 4.4. Evaluation of subNILs in the 2015 trial. a. HAR phenotype for the parental lines and the subNILs, corresponding to EABS when the fruit presented abscission. b. Graphical representation of the introgressions according to the genotyping of the lines; the bar at the left represents the region of chromosome III and each red line corresponds to a genotyped SNP at its physical position (v3.6.1). c. Evaluation of ARO at harvest. d. Evaluation of ABS at harvest.

Table 4.4. Genotyping of the region of *ETHQB3.5* and phenotyping (mean and standard deviation) of the parental lines and the subNILs in the 2015 trial.

Line	CMPSNP661	CMPSNP64[1]	chr3_23482128	chr3_23684230	chr3_23910349	CMPSNP979	chr3_24912205	CMPSNP4624	CMPSNP374	sca14_3989717	sca14_3950458	CMPSNP4618	sca14_3868153	sca14_3800747	sca14_3651269	sca14_3611423	sca14_3509329	sca14_3483884	CMPSNP4583[1]	CMPSNP651	n[2]	ARO	ABS	EABS	HAR
8M35	B	A	A	A	A	A	A	A	A	A	A	A	A	A	A	A	A	A	A	B	5	1.0 ± 0.0	3.0 ± 0.0	52.2 ± 8.5	52.2 ± 8.5
T111	B	B	B	B	B	B	B	B	B	B	B	B	B	B	B	B	B	B	B	B	3	0.0 ± 0.0	0.0 ± 0.0	-	71.7 ± 5.5
R164	B	A	A	A	A	A	A	B	B	B	B	B	B	B	B	B	B	B	B	B	3	0.7 ± 0.6	0.7 ± 0.6	-	65.3 ± 3.1
R137	B	A	A	A	A	A	A	A	A	B	B	B	B	B	B	B	B	B	B	B	5	0.6 ± 0.6	2.4 ± 1.3	61.7 ± 5.5	65.4 ± 6.5
R90	B	A	A	A	A	A	A	A	A	A	A	A	A	B	B	B	B	B	B	B	5	1.0 ± 0.0	2.8 ± 0.5	60.0 ± 0.0	64.2 ± 4.8
R76	B	B	B	A	A	A	A	A	A	A	A	A	A	A	A	A	A	A	A	B	3	1.0 ± 0.0	3.0 ± 0.0	53.7 ± 4.0	53.7 ± 4.0
R98	B	B	B	B	B	A	A	A	A	A	A	A	A	A	A	A	A	A	A	B	5	1.0 ± 0.0	3.0 ± 0.0	57.0 ± 6.7	65.4 ± 8.4
R183	B	B	B	B	B	B	B	A	A	A	A	A	A	A	A	A	A	A	A	B	3	0.3 ± 0.6	1.0 ± 1.7	-	69.7 ± 1.2
R140	B	B	B	B	B	B	B	B	B	B	B	A	A	A	A	A	A	A	A	B	3	0.3 ± 0.6	1.3 ± 1.5	67.0 ± 0.0	69.3 ± 2.5
R149	B	B	B	B	B	B	B	B	B	B	B	B	B	B	B	A	A	A	A	B	3	0.7 ± 0.6	2.0 ± 1.7	61.5 ± 0.7	63.7 ± 3.8
R145	B	B	B	B	B	B	B	B	B	B	B	B	B	B	B	B	B	A	A	B	4	0.8 ± 0.5	1.8 ± 1.3	-	71.8 ± 1.3

ETHQB3.5.1 *ETHQB3.5.2*

[1]SNPs shaded in red are the flanking markers of *ETHQB3.5*

[2]Number of replicates for each line

2016 recombinants trial

In order to increase the resolution of the fine mapping, we searched for additional individuals that presented a recombination breakpoint within the target regions containing both QTLs. To isolate the effect of *ETHQB3.5.1* and *ETHQB3.5.2*, we used the F3 recombinants that carried only one of these regions in heterozygosity, instead of the F2 recombinants. The total number of lines selected were twenty-two and eight individuals containing recombinations within the intervals that delimited *ETHQB3.5.1* (24,802,439 bp – 26,757,471 bp) and *ETHQB3.5.2* (28,682,613 bp – 28,841,908 bp), respectively (Table 4.S4). The major part of individuals carrying regions of *ETHQB3.5.1* were climacteric, presenting ARO and ALF between 45 and 73 DAP; however, some non-climacteric individuals were also founded. The individuals recombining within the interval of *ETHQB3.5.2* were non-climacteric or only slightly climacteric. Although the results are not conclusive due to the absence of replicates, the climacteric effect was minor in the recombinants carrying *ETHQB3.5.2* and more intense in the ones carrying *ETHQB3.5.1*.

2016 subNILs trial

A similar subset of eleven subNILs, including F3 and F4 families derived from the initial recombinant individuals (Figure 4.1), was phenotyped in the summer of 2016. The earliness of abscission layer formation (EALF) was used as a representative trait of climacteric ripening from now on because we considered that it could be slightly more precise than HAR. Again, the subNIL R76 and the parental line 8M35 displayed high climacteric behavior, with EALF values around 40 DAP and presenting ARO and ALF in all the replicates (Figure 4.5 and Table 4.5). The same phenotype was observed for the line M145, which presented the two potential QTLs fixed for the SC alleles, but containing PS alleles in the central region of the introgression. The remaining subNILs supported the hypothesis of two QTLs and highlighted the effect of *ETHQB3.5.1* in comparison with *ETHQB3.5.2*, since R18 presented a much stronger climacteric ripening (ALF and ARO in all replicates) in comparison with either R34, R131 and R82 (ALF and ARO presented partially and EABS > 60 DAP, when appeared).

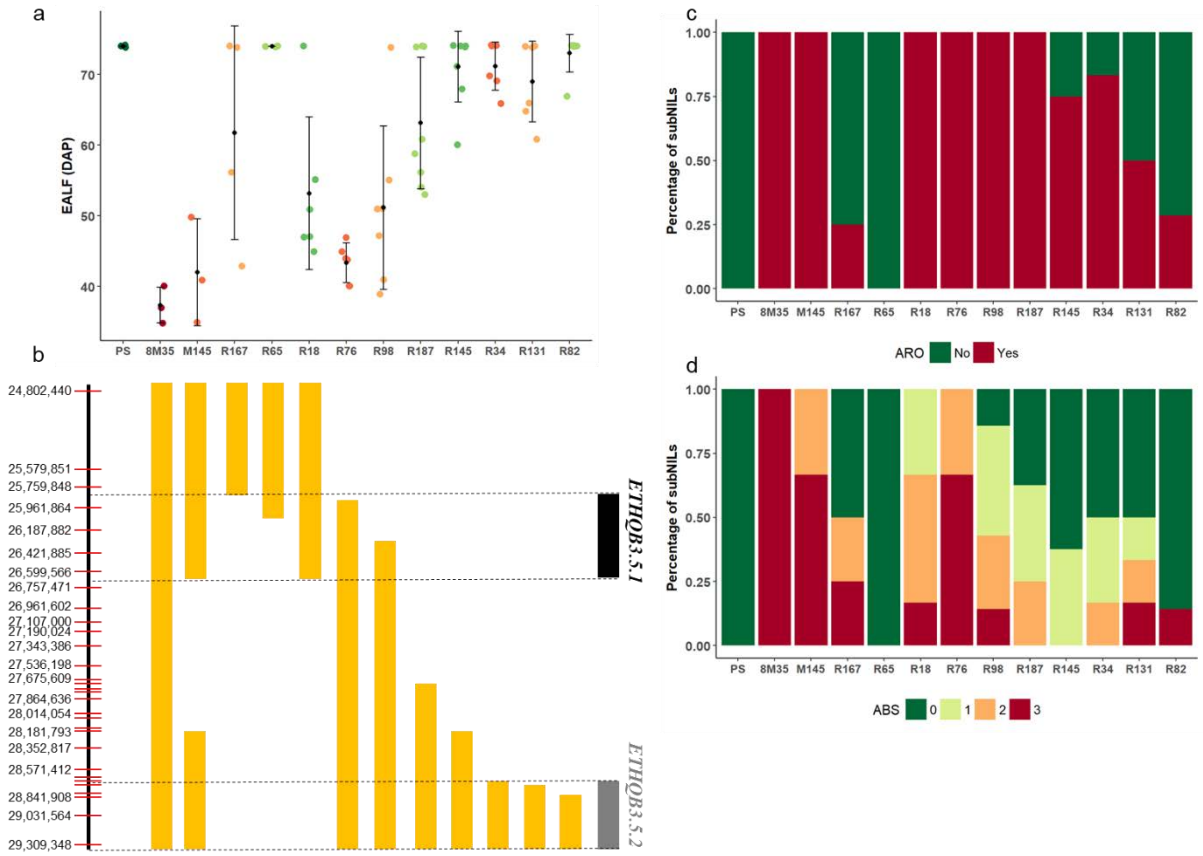

Figure 4.5. Evaluation of subNILs in the 2016 trial. a. EALF phenotype for the parental lines and the subNILs. b. Graphical representation of the introgressions according to the genotyping of the lines; the bar at the left represents the region of chromosome III and each red line corresponds to a genotyped SNP at its physical position (v3.6.1). c. Evaluation of ARO at harvest. d. Evaluation of ABS at harvest.

Table 4.5. Genotyping of the region of *ETHQB3.5* and phenotyping (mean and standard deviation) of the parental lines and the subNILs in the 2016 trial.

Line	CMPSNP661	CMPSNP64[1]	chr3_23482128	chr3_23684230	chr3_23910349	CMPSNP979	chr3_24322158	chr3_24479823[1]	Cm0306	sca14_3989717	sca14_3950458	sca14_3509329	sca14_3483884	chr3_26363822	sca14_29834622	chr3_26440980	chr3_26521963	CMPSNP45832	CMPSNP651	n[3]	ARO	EARO	EALF	ABS	EABS	HAR
8M35	B	A	A	A	A	A	A	A	A	A	A	A	A	A	A	A	A	A	B	3	1.0 ± 0.0	38 ± 3.6	37 ± 2.5	3.0 ± 0.0	43 ± 7.1	43 ± 7.1
PS	B	B	B	B	B	B	B	B	B	B	B	B	B	B	B	B	B	B	B	3	0.0 ± 0.0	-	-	0.0 ± 0.0	-	75 ± 4.7
M145	B	A	A	A	A	A	A	B	B	B	B	B	A	A	A	A	A	A	B	3	1.0 ± 0.0	43 ± 5.7	42 ± 7.6	2.7 ± 0.6	61 ± 9.2	60 ± 2.8
R167	B	A	A	B	B	B	B	B	B	B	B	B	B	B	B	B	B	B	B	4	0.3 ± 0.5	41 ± 0.0	49 ± 9.2	1.3 ± 1.5	62 ± 0.0	67 ± 4.1
R65	B	A	A	A	B	B	B	B	B	B	B	B	B	B	B	B	B	B	B	3	0.0 ± 0.0	-	-	0.0 ± 0.0	-	60 ± 11.0
R18.5	B	A	A	A	A	A	A	B	B	B	B	B	B	B	B	B	B	B	B	6	1.0 ± 0.0	48 ± 3.6	49 ± 4.0	2.0 ± 0.7	49 ± 0.0	63 ± 12.1
R76.5	B	B	B	A	A	A	A	A	A	A	A	A	A	A	A	A	A	A	B	6	1.0 ± 0.0	43 ± 2.4	43 ± 2.8	2.7 ± 0.5	51 ± 6.1	55 ± 7.5
R98.6	B	B	B	B	B	A	A	A	A	A	A	A	A	A	A	A	A	A	B	7	1.0 ± 0.0	45 ± 4.5	47 ± 6.3	1.4 ± 1.0	52 ± 0.0	65 ± 6.4
R187.2	B	B	B	B	B	B	B	B	B	B	A	A	A	A	A	A	A	A	B	8	1.0 ± 0.0	52 ± 4.1	56 ± 3.4	0.9 ± 0.8	-	67 ± 1.6
R145.2	B	B	B	B	B	B	B	B	B	B	B	B	A	A	A	A	A	A	B	8	0.8 ± 0.5	50 ± 5.0	66 ± 5.7	0.4 ± 0.5	-	70 ± 2.1
R34.2	B	B	B	B	B	B	B	B	B	B	B	B	B	B	A	A	A	A	B	6	0.8 ± 0.4	64 ± 4.9	68 ± 2.1	0.7 ± 0.8	-	70 ± 1.4
R131.4	B	B	B	B	B	B	B	B	B	B	B	B	B	B	B	A	A	A	B	6	0.5 ± 0.6	61 ± 0.6	64 ± 2.7	1.0 ± 1.3	68 ± 0.0	73 ± 4.9
R82.4	B	B	B	B	B	B	B	B	B	B	B	B	B	B	B	B	B	A	B	7	0.3 ± 0.5	67 ± 0.0	67 ± 0.0	0.4 ± 1.1	67 ± 0.0	71 ± 4.0

ETHQB3.5.1 *ETHQB3.5.2*

[1]SNPs shaded in red are the flanking markers of *ETHQB3.5.1*

[2]SNPs shaded in blue are the flanking markers of *ETHQB3.5.2*

[3]Number of replicates per line

2017 subNILs trial

Since the effect of *ETHQB3.5.2* in climacteric ripening seemed to be minor, we decided to focus on *ETHQB3.5.1* in our last trial, which was conducted during the summer of 2017 (Figure 4.6 and Table 4.6). Four subNILs that had been evaluated before (R7, R18, R65 and R167) were phenotyped again and showed concordant results in comparison with prior tests. Other five subNILs (R87.6, R87.9, R87.14, R154.1 and R154.6) obtained from the recombinants of 2016 were evaluated for the first time. The line R18 is clearly climacteric, presenting EALF values around 44 DAP, chlorophyll degradation (Figure 4.7a), presence of ARO in all the replicates and abscission in 75% of them (Figure 4.6d and Table 4.6). However, the three lines that carry the proximal region of the introgression (R7, R167 and R65) were totally non-climacteric, indicating that the distal region of the introgression was triggering the climacteric ripening. According to this result, the only subNIL that showed a clearly climacteric phenotype, with EALF around 50 DAP in all the replicates and presenting ARO in 70% of them was R87.6, carrying a fraction of R18's introgression (Figures 4.6a, 4.6c, 4.7a and 4.7b). In addition, the totally non-climacteric phenotype of R87.14, which did not present ARO, CD and ALF in any of the replicates (Table 4.6 and Figures 4.7a and 4.7b), allowed to narrow down the interval of *ETHQB3.5.1* to the positions 26,000,631 bp – 26,512,654 bp.

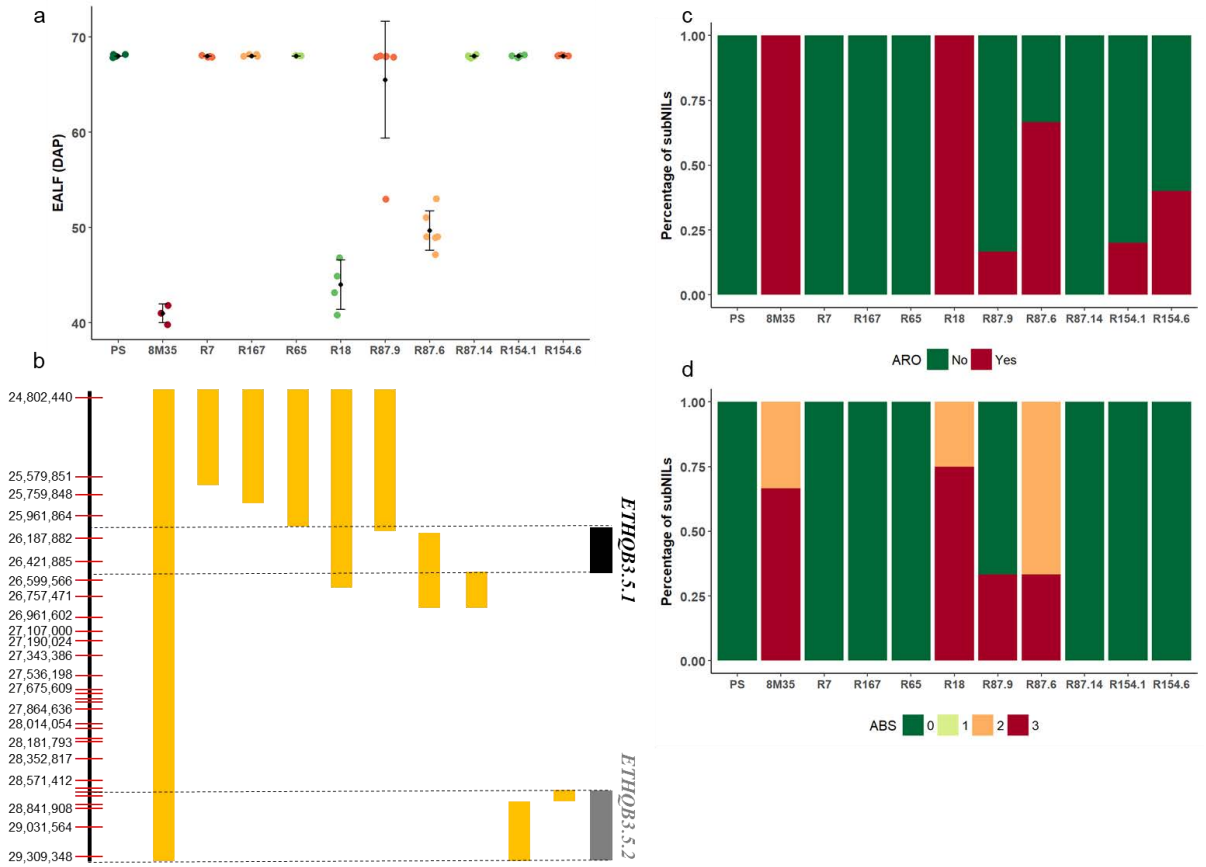

Figure 4.6. Evaluation of subNILs in the 2017 trial. a. EALF phenotype for the parental lines and the subNILs. b. Graphical representation of the introgressions according to the genotyping of the lines; the bar at the left represents the region of chromosome III and each red line corresponds to a genotyped SNP at its physical position (v3.6.1). c. Evaluation of ARO at harvest. d. Evaluation of ABS at harvest.

Table 4.6. Genotyping of the region of *ETHQB3.5* and phenotyping (mean and standard deviation) of the parental lines and the subNILs in the 2017 trial.

Line	CMPSNP661	CMPSNP64[1]	chr3_23302124	chr3_23482128	chr03_26000631	chr03_26089780	chr03_26359839	CMPSNP979	chr03_26512654	chr3_24322158	chr3_24479823[1]	Cm0306	chr3_26363822	sca14_2983462[2]	chr03_28742247	chr3_26480841	CMPSNP4583[2]	CMPSNP651	n[3]	ARO	EARO	EALF	ABS	EABS	HAR
8M35	B	A	A	A	A	A	A	A	A	A	A	A	A	A	A	A	A	B	3	1.0 ± 0.0	40 ± 0.6	41 ± 1.0	2.7 ± 0.6	41 ± 0.7	42 ± 2.1
PS	B	B	B	B	B	B	B	B	B	B	B	B	B	B	B	B	B	B	4	0.0 ± 0.0	-	-	0.0 ± 0.0	-	72 ± 11.9
R7	B	A	A	B	B	B	B	B	B	B	B	B	B	B	B	B	B	B	4	0.0 ± 0.0	-	-	0.0 ± 0.0	-	79 ± 1.7
R167	B	A	A	A	-	B	B	B	B	B	B	B	B	B	B	B	B	B	5	0.0 ± 0.0	-	-	0.0 ± 0.0	-	72 ± 8.7
R87.9	B	A	A	A	A	B	B	B	B	B	B	B	B	B	B	B	B	B	6	0.2 ± 0.4	67 ± 0.0	60 ± 10.6	1.0 ± 1.6	67 ± 0.7	73 ± 4.9
R65	B	A	A	A	A	A	B	B	B	B	B	B	B	B	B	B	B	B	3	0.0 ± 0.0	-	-	0.0 ± 0.0	-	66 ± 9.8
R18	B	A	A	A	A	A	A	A	A	A	B	B	B	B	B	B	B	B	4	1.0 ± 0.0	44 ± 3.3	44 ± 2.6	2.8 ± 0.5	46 ± 5.1	47 ± 4.4
R87.6	B	B	B	B	B	A	A	A	A	A	A	B	B	B	B	B	B	B	6	0.7 ± 0.5	55 ± 9.7	49 ± 2.1	2.3 ± 0.5	50 ± 2.1	56 ± 7.2
R87.14	B	B	B	B	B	B	B	B	A	A	A	B	B	B	B	B	B	B	5	0.0 ± 0.0	-	-	0.0 ± 0.0	-	78 ± 1.7
R154.6	B	B	B	B	B	B	B	B	B	B	B	B	B	A	A	B	B	B	5	0.4 ± 0.6	77 ± 1.4	-	0.0 ± 0.0	-	75 ± 7.0
R154.1	B	B	B	B	B	B	B	B	B	B	B	B	B	B	B	A	A	B	5	0.2 ± 0.5	52 ± 0.0	-	0.0 ± 0.0	-	72 ± 8.3

ETHQB3.5.1 *ETHQB3.5.2*

[1]SNPs shaded in red are the flanking markers of *ETHQB3.5.1*

[2]SNPs shaded in blue are the flanking markers of *ETHQB3.5.2*

[3]Number of replicates per line

Figure 4.7. Images showing a. the change of color due to chlorophyll degradation from light green/yellow in R18 and R87.6 (left) to dark green in R167 and R87.14 (right) b. the different levels of abscission layer formation: 0 in R87.14 (right), 2 in R87.6 (center) and 3 in R87.6 (left).

Concerning *ETHQB3.5.2*, two new subNILs, R154.1 and R154.6, presented a very slight climacteric behavior, without ALF but showing ARO in some of the replicates (Figures 4.6c and 4.6d). However, the results are non-conclusive about the location of the gene underlying *ETHQB3.5.2*, since both subNILs presented similar climacteric symptoms.

Candidate genes for ETHQB3.5.1

The interval of *ETHQB3.5.1*, of 512,023 pb, contains 63 genes according to the most recent version of the melon genome annotation v3.6.1 (www.melonomics.net) (Table 4.S5). Recently, the transcriptome of the NIL containing *ETHQB3.5* (8M35) and the non-climacteric parental PS in three developmental stages of the fruit (pre-ripe, transition to ripening and ripe) has been generated (Argyris et al. unpublished). According to this work, only 49 of the 63 genes in the *ETHQB3.5.1* interval were expressed in 8M35, 8M31 or PS (Trimmed Mean of M-values > 5 in at least one sample), reducing our potential candidate gene list. To determine the best candidates, we looked at both the differential expression between the climacteric NILs and PS, and the sequence variants between PS and SC.

The differential expression between the climacteric NIL carrying *ETHQB3.5* (8M35) and the non-climacteric parental PS at the stages “transition to ripening” and “ripe” was

analyzed. The first stage "transition to ripening" was determined depending on the ripening behavior of the NILs, corresponding with the onset of ripening, which matches the start of autocatalytic synthesis of ethylene in climacteric lines. Theoretically, the gene underlying *ETHQB3.5.1* could be up or downregulated in 8M35 during this stage. Although most likely at harvest the ripening reprogramming should be already determined, we also analyzed the differential expressed genes between 8M35 and PS at the "ripe" stage. Only the genes showing a two-fold change and significant p-value (<0.05) were considered as differential expressed genes. Sixteen genes were differentially expressed between 8M35 and PS (Table 4.7). Among them, the most differentially expressed were *MELO3C011413*, encoding a cytochrome P450 78A5; *MELO3C030290*, encoding an unknown protein; and *MELO3C011424*, encoding an alpha/beta-hydrolases superfamily protein. The former was down-regulated and the two latter were up-regulated in 8M35, respectively. Besides, these differences were also statistically significant at harvest.

According to the sequence variants between SC, the donor of the introgression, and PS, the recurrent parental, we could select the most probable candidates based on the estimated effect of the variants found in the protein. A detailed list of all the sequence variants among PS and SC within the candidate genes is presented in Table 4.S6. Among the 49 expressed candidate genes, 32 presented at least one genomic variant causing a non-synonymous amino acid change in the protein comparing SC and PS. In addition, six genes carried at least one variant causing a probable deleterious effect, either by changing the frameshift or by generating a truncated protein due to a lost start codon or an early stop codon (Table 4.8).

None of the candidate genes was evidently related to fruit ripening according to their functional annotation.

Table 4.7. Candidate genes for *ETHQB3.5.1* presenting a differential expression between PS and 8M35.

		Transition to ripening			Harvest		
Gene ID	**Gene description**	**8M35[1]**	**PS[1]**	**p-value**	**8M35[1]**	**PS[1]**	**p-value**
MELO3C011387	Nudix hydrolase	46.1	133.1	0.007	200.1	125.6	0.156
MELO3C011388	Transcription factor TGA2-like	2778.5	6057.7	0.002	2127.3	4381.4	0.002
MELO3C011392	Subtilisin-like protease	15605.3	7578.1	0.220	33338.3	1309.1	0.000
MELO3C011393	Thioredoxin-like protein CITRX, chloroplastic	58.9	22.4	0.028	151.5	25.2	0.000
MELO3C011397	Phosphatidylinositol 4-kinase gamma 7	4130.1	3388.1	0.467	1916.3	4907.9	0.000
MELO3C011401	18S pre-ribosomal assembly protein gar2-like protein	3268.8	1109.1	0.012	1892.0	1388.2	0.342
MELO3C011402	D-aminoacyl-tRNA deacylase	2115.6	1510.6	0.256	4841.3	2048.4	0.002
MELO3C011413	Cytochrome P450 78A5	10.1	5897.9	0.000	17.8	20370.8	0.000
MELO3C011421	14-3-3 protein, putative	6.5	4.0	0.460	39.6	4.8	0.000
MELO3C011423	Plasmodesmata callose-binding protein 3	736.7	843.8	0.495	1198.1	541.3	0.000
MELO3C011424	Alpha/beta-Hydrolases superfamily protein	22.8	7.3	0.051	95.8	22.0	0.003
MELO3C011430	Beta-glucosidase, putative	95.7	133.1	0.305	46.8	206.4	0.000
MELO3C011432	WRKY family transcription factor	317.9	531.0	0.110	249.5	1162.2	0.000
MELO3C011435	ABC transporter G family member 29-like	206.1	82.0	0.035	186.2	121.9	0.222
MELO3C030290	Unknown protein	137.9	10.0	0.000	165.3	8.1	0.000
MELO3C030294	Transmembrane protein, putative	364.7	174.9	0.003	281.2	225.1	0.221

[1]TMM, Trimmed Mean of M-values (Argyris et al. unpublished).

Table 4.8. Candidate genes for *ETHQB3.5.1* according to the sequence variants between PS and 8M35.

Gene ID	Gene description	Moderate effect	High effect	Frameshift
MELO3C011378	phosphopantothenate--cysteine ligase 2-like	1	0	0
MELO3C011379	Chaperone protein dnaJ	1	0	0
MELO3C011383	DNA-directed RNA polymerase subunit beta	5	0	0
MELO3C011384	ARM repeat superfamily protein	1	1	1
MELO3C011385	vacuolar protein sorting-associated protein 36	1	0	0
MELO3C011389	Alpha/beta-Hydrolases superfamily protein	2	0	0
MELO3C011391	CRS1/YhbY (CRM) domain protein	3	0	0
MELO3C011392	Subtilisin-like protease	1	0	0
MELO3C011393	thioredoxin-like protein CITRX, chloroplastic	2	0	1
MELO3C011394	RING-type E3 ubiquitin transferase	0	0	1
MELO3C011397	phosphatidylinositol 4-kinase gamma 7	2	0	0
MELO3C011399	transcription factor BIM2	5	0	3
MELO3C011401	18S pre-ribosomal assembly protein gar2-like protein	3	0	0
MELO3C011406	Chaperone DnaJ-domain superfamily protein	3	0	0
MELO3C011408	nucleolar protein 14 isoform X2	5	0	0
MELO3C011413	cytochrome P450 78A5	1	0	0
MELO3C011414	Glycine-rich RNA-binding protein, putative	1	0	0
MELO3C011415	cytochrome b5	1	0	0
MELO3C011419	Purple acid phosphatase	1	0	0
MELO3C011420	Protein root UVB sensitive 3	2	0	0
MELO3C011421	14-3-3 protein, putative	1	0	0
MELO3C011422	Pentatricopeptide repeat-containing protein	2	0	0
MELO3C011426	Pentatricopeptide repeat-containing family protein	1	0	0
MELO3C011427	Protein KTI12 like	4	1	1
MELO3C011430	Beta-glucosidase, putative	1	0	0
MELO3C011431	UDP-glucose 6-dehydrogenase	1	0	0
MELO3C011432	WRKY family transcription factor	2	0	0
MELO3C011433	DNA-directed RNA polymerase subunit beta	2	0	0
MELO3C011434	F-box only protein 21	1	0	0
MELO3C011435	ABC transporter G family member 29-like	1	0	0
MELO3C030293	Unknown protein	0	1	0
MELO3C030294	Transmembrane protein, putative	1	0	0

Discussion

Fruit ripening is a complex trait controlled by polygenic inheritance and partially modified by the environmental conditions, as humidity, hours of light and temperature. In this work, we have used a positional cloning strategy to decipher the genetics

controlling climacteric ripening in the NIL 8M35, carrying *ETHQB3.5*. 8M35 presented a weak climacteric behavior across several years and environments, with low ethylene production compared to typical climacteric varieties and a variable penetrance in other ripening-related traits as change of external color, aroma production and abscission layer formation (Obando-Ulloa et al. 2008; Vegas et al. 2013).

In this work, several trials were performed across four years, including a diverse panel of subNILs derived from the original NIL 8M35 that covered different regions of the introgression. Surprisingly, instead of two phenotypes related to climacteric and non-climacteric ripening classes, we obtained an unexpected range of climacteric behaviours of different intensity and penetrance. We may hypothesize that, in part, this variance can be explained by the low levels of ethylene produced by these lines, which could be just bordering the necessary threshold to trigger the physiological response. When the fruit does not have the optimal growing conditions, a decrease in ethylene production could avoid reaching a minimum threshold that cannot drive the changes associated with climacteric ripening. This hypothesis could explain why some of the replicates of weak climacteric lines did not ripe as expected.

SubNILs carrying non-overlapping introgressions were often climacteric, but showed a less intense phenotype than the parental 8M35. This behavior was consistent for most of the lines across more than one trial. Furthermore, a similar performance was observed in a different set of subNILs, which had been already used to study fruit quality and postharvest behavior; some subNILs with non-overlapping introgressions were classified as climacteric as well, using phenotypic data related with ethylene production and aroma profiles (Fernández-Trujillo et al. 2008). The most likely explanation would be the existence of more than one QTL within the introgression affecting climacteric ripening, which we named *ETHQB3.5.1* and *ETHQB3.5.2* (Figure 4.3).

The phenotype caused by *ETHQB3.5.2* alone was minor, since the subNILs carrying exclusively this interval showed a partial phenotype, generally producing aroma but without abscission nor change of external color. In addition, *ETHQB3.5.2* presented a low penetrance (only a low proportion of replicates displayed the phenotypes). Nonetheless, *ETHQB3.5.2* seemed to be necessary to achieve the complete ripening phenotype of 8M35, since the lines that did not carry the complete introgression showed a less intense climacteric ripening behaviour. An analogous result was obtained in a previous study with a similar set of subNILs derived from 8M31, were the NILs carrying only the distal region

of the introgression (5M9 and 5M10) produced ethylene but ALF was less evident than in other lines (Fernández-Trujillo et al. 2008).

ETHQB3.5.1 presented a stronger phenotype, represented in the subNIL R18 in the 2016 and 2017 trials. All the R18 replicates produced aroma, changed their color to light-green, formed an abscission layer, and most of them abscised from the plant around 49 and 46 DAP in 2016 and 2017, respectively. A very similar behaviour was observed in the subNIL R87.6, which was evaluated in 2017, although the effect was slightly weaker and delayed (Figure 4.6). This difference could be attributable to environmental effects. Since other lines carrying other intervals, covering partially the introgression contained in R18, were non-climacteric, we finally delimited *ETHQB3.5.1* to an interval of 512 kb between the positions 26,000,631 bp – 26,512,654 bp.

This interval contains 63 annotated genes, and using expression data in three stages of fruit development from 8M35 and PS we could discard 14 of them, which were not expressed in fruit tissues. From the potential 49 candidate genes, we used an integrative strategy to narrow down the list to the most probable candidates. Using the expression atlas Melonet-DB (Yano et al. 2018), we could identify 23 genes, predominantly expressed in fruit tissues, that are expected to have an important role in fruit development or ripening (Table 4.S5). Taking into account the sequence variants between SC and PS and the differential expression between 8M35 and PS during the "transition to ripening" stage (35 DAP), 37 genes were highlighted as candidates, since we expect that the phenotype may be caused by either a different transcript abundance or an altered sequence of the protein.

The most differentially expressed gene between 8M35 and PS was *MELO3C011413*, annotated as a cytochrome P450 78A5. Cytochrome P450 78A5 (*KLUH*) has been shown to control leaf, petal and sepal size in *Arabidopsis* (Anastasiou et al. 2007; Eriksson et al. 2010). A similar function has been proven in tomato, where KLUH orthologous control fruit size by increasing cell number (Chakrabarti et al. 2013). Interestingly, down-regulation of *SlKLUH* in tomato, in addition to lead to fruits with reduced size, provoked a faster ripening when compared to the control. *SlKLUH* is one of the orthologs of *MELO3C011413*, from a group of six genes (Proost et al. 2009; Van Bel et al. 2018). We could hypothesized that *MELO3C011413* may be involved in a similar mechanism in melon accelerating ripening when it is down-regulated in the climacteric NILs.

Additionally, other types of cytochrome P450 have been shown to be involved in ripening in avocado, a climacteric species (Bozak et al. 1990).

The gene *MELO3C011397* encodes a phosphatidylinositol 4-kinase. Phosphoinositides are a kind of membrane phospholipids involved in signal transduction in plants and have been related with hormone transduction (Antignani et al. 2015; Tang et al. 2016; Pak Dek et al. 2017b). A recent study suggested that in tomato, phosphatidylinositol kinases are essential for normal ripening and act downstream ethylene receptors (Pak Dek et al. 2017b). Transgenic lines both over-expressing and silencing a phosphatidylinositol 3-kinase proved the involvement of these enzyme in ethylene transduction, affecting both the biosynthesis and the phenotypic effects of the hormone (Pak Dek et al. 2017a). However, phosphatidylinositol 3-kinases seemed to be more important in fruit ripening than phosphatidylinositol 4-kinases. When comparing the *MELO3C011397* expression in 8M35 and PS, it was down-regulated in 8M35 at harvest, but no significant differences were observed during the transition to ripening. In the above-mentioned studies the over-expression of the enzyme increased ethylene production, and its inactivation blocked the hormone effects, being the opposite phenomena observed in 8M35 and PS. Two non-synonymous changes predicted in the protein could affect its performance and cause the phenotype observed in melon.

Another interesting gene within the interval is *MELO3C011421*, encoding a 14-3-3 protein. These proteins form a highly conserved family with regulatory functions in multiple physiological processes via phosphorylation (Dougherty 2004). Recently, this protein has been proved to increase the stability of one of the main enzymes in the biosynthetic pathway of ethylene, 1-aminocyclopropane-1-carboxylic acid synthase (ACS), in *Arabidopsis thaliana* (Yoon and Kieber 2013), rice (Yao et al. 2007) and banana (Li et al. 2012). In pear it has also been related with ethylene synthesis and fruit ripening (Shi and Zhang 2014). *MELO3C011421* is the orthologous of 14-3-3ι type of Arabidopsis (http://phylomedb.org/), which interacts directly with ACS5 and with ETO1, increasing the stability of the enzyme by both ways (Yoon and Kieber 2013). *MELO3C011421* was up-regulated in 8M35 when compared to PS at harvest and presented one non-synonymous change in the protein. Although its functional validation has not been performed in tomato and the knowledge of the implication of 14-3-3 proteins in fruit ripening is scarce, its implication in ethylene biosynthesis suggests *MELO3C011421* as a strong candidate for *ETHQB3.5.1*.

Other possible candidate gene, carrying three sequence variants with important predicted effects but without differential expression between 8M35 and PS, was *MELO3C011384*, encoding an ARM repeat superfamily protein. The predicted protein is formed by 187 amino acids and it contains an importin-beta domain (Finn et al. 2016), whose function is related with protein transport to the nucleus. An ARM repeat protein, ARIA, has been described in *Arabidopsis thaliana* as a signaling component of the abscisic acid pathway (Kim et al. 2004). However, *MELO3C011384* is not the ARIA orthologue and the length and structure of the protein is notably different. Therefore, it is unlikely that the melon protein could have the same function as the one described in *A. thaliana*.

As a summary, the fine mapping of *ETHQB3.5* showed that more than one factor is causing the phenotype observed in 8M35, obtaining less intense phenotypes when we narrowed down the original introgression to smaller regions. Two QTLs, *ETHQB3.5.1* and *ETHQB3.5.2*, were delimited within the region of ETHQB3.5. The *ETHQB3.5.2* presented a weak phenotype and high environmental effect, causing difficulties to fine map it and determine the candidate genes underlying the QTL. On the opposite side, the *ETHQB3.5.1*, main responsible for the phenotype, was fine mapped and located within the positions 26,000,631 bp – 26,512,654 bp of chromosome III. A list of 63 candidate genes was deeply explored using an integrative strategy and a reduced number of candidates were proposed, highlighting their function in hormone regulation and signaling and fruit development in other studies. Two genes, *MELO3C011413* and *MELO3C011421*, encoding for a cytochrome P450 78A5 and a 14-3-3 protein, respectively, seem to be the most likely candidates for *ETHQB3.5.1* according to the available information. However, additional experiments are necessary to identify and validate the candidate gene for *ETHQB3.5.1*.

Digital Supplementary Material

Table 4.S1. List of used SNPs.

Table 4.S2. Genotype and phenotype of **a.** 2015 recombinants **b**. 2015 subNILs individuals. A (yellow) represents SC genotype, B (green) PS genotype, and H (blue) heterozygous. The flanking SNPs of *ETHQB3.5* are shaded in red and the additional internal SNP screened, in blue.

Table 4.S3. Genotype and phenotype of the 2014 subNILs, including all the biological replicates. A (yellow) represents SC genotype, B (green) PS genotype and H (blue) heterozygous.

Table 4.S4. Genotype and phenotype of the 2016 recombinants. A (yellow) represents SC genotype, B (green) PS genotype and H (blue) heterozygous. The flanking SNPs of *ETHQB3.5.1* are shaded in red and the ones of *ETHQB3.5.2* in blue.

Table 4.S5. Genes contained in the *ETHQB3.5.1* interval and whether they are expressed in fruit tissues in 8M35 and PS (Argyris et al. unpublished) and whether they are predominantly expressed in fruit tissues in "Harukei-3" (Yano et al. 2018).

Table 4.S6. Detailed description of the sequence variants between 8M35 and PS in the candidate genes.

References

Anastasiou E, Kenz S, Gerstung M, et al (2007) Control of Plant Organ Size by *KLUH/CYP78A5*-Dependent Intercellular Signaling. Dev Cell 13:843–856.

Antignani V, Klocko AL, Bak G, et al (2015) Recruitment of PLANT U-BOX13 and the PI4Kβ1/β2 Phosphatidylinositol-4 Kinases by the Small GTPase RabA4B Plays Important Roles during Salicylic Acid-Mediated Plant Defense Signaling in *Arabidopsis*. Plant Cell 27:243–261.

Ayub R, Guis M, Ben Amor M, et al (1996) Expression of ACC oxidase antisense gene inhibits ripening of cantaloupe melon fruits. Nat Biotechnol 14:862–866.

Bozak KR, Yu H, Sirevåg R, Christoffersen RE (1990) Sequence analysis of ripening-related cytochrome P-450 cDNAs from avocado fruit. Proc Natl Acad Sci USA 87:3904–3908.

Chakrabarti M, Zhang N, Sauvage C, et al (2013) A cytochrome P450 regulates a domestication trait in cultivated tomato. Proc Natl Acad Sci 110:17125–17130.

Cherian S, Figueroa CR, Nair H (2014) "Movers and shakers" in the regulation of fruit ripening: a cross-dissection of climacteric versus non-climacteric fruit. J Exp Bot 65:4705–4722.

Dougherty MK (2004) Unlocking the code of 14-3-3. J Cell Sci 117:1875–1884.

Doyle J (1991) DNA Protocols for Plants. In: Hewitt GM, Johnston AWB, Young JPW (eds) Molecular Techniques in Taxonomy. Springer Berlin Heidelberg, Berlin, Heidelberg, pp 283–293

Eriksson S, Stransfeld L, Adamski NM, et al (2010) *KLUH/CYP78A5*-Dependent Growth Signaling Coordinates Floral Organ Growth in *Arabidopsis*. Curr Biol 20:527–532.

Ezura H, Owino WO (2008) Melon, an alternative model plant for elucidating fruit ripening. Plant Sci 175:121–129.

Fernández-Trujillo JP, Obando-Ulloa JM, Martínez J a., et al (2008) Climacteric and non-climacteric behavior in melon fruit. Postharvest Biol Technol 50:125–134.

Finn RD, Coggill P, Eberhardt RY, et al (2016) The Pfam protein families database: Towards a more sustainable future. Nucleic Acids Res 44:D279–D285.

Giovannoni J, Nguyen C, Ampofo B, et al (2017) The Epigenome and Transcriptional Dynamics of Fruit Ripening. Annu Rev Plant Biol 68:61–84.

Giovannoni JJ (2007) Fruit ripening mutants yield insights into ripening control. Curr Opin Plant Biol 10:283–289.

Gonda I, Burger Y, Schaffer AA (2016) Biosynthesis and perception of melon aroma. In: Havkin-Frenkel D, Dudai N (eds) Biotechnology in flavor production, 2nd edn. John Wiley & Sons, Ltd, pp 281–306

Kim S, Choi H, Ryu H-J, et al (2004) ARIA, an *Arabidopsis* Arm Repeat Protein Interacting with a Transcriptional Regulator of Abscisic Acid-Responsive Gene Expression, Is a Novel Abscisic Acid Signaling Component. Plant Physiol 136:3639–3648.

Lelievre JM, Latche A, Jones B, et al (1997) Ethylene and fruit ripening. Physiol Plant 101:727–739.

Li MY, Xu BY, Liu JH, et al (2012) Identification and expression analysis of four 14-3-3 genes during fruit ripening in banana (*Musa acuminata* L. AAA group, cv. Brazilian). Plant Cell Rep 31:369–378.

Manning K, Tör M, Poole M, et al (2006) A naturally occurring epigenetic mutation in a gene encoding an SBP-box transcription factor inhibits tomato fruit ripening. Nat Genet 38:948–952.

Moreno E, Obando JM, Dos-Santos N, et al (2008) Candidate genes and QTLs for fruit ripening and softening in melon. Theor Appl Genet 116:589–602.

Obando-Ulloa JM, Moreno E, García-Mas J, et al (2008) Climacteric or non-climacteric behavior in melon fruit 1. Aroma volatiles. Postharvest Biol Technol 49:27–37.

Obando-Ulloa JM, Nicolai B, Lammertyn J, et al (2009) Aroma volatiles associated with the senescence of climacteric or non-climacteric melon fruit. Postharvest Biol Technol 52:146–155.

Obando-Ulloa JM, Ruiz J, Monforte AJ, Fernández-Trujillo JP (2010) Aroma profile of a collection of near-isogenic lines of melon (*Cucumis melo* L.). Food Chem 118:815–822.

Pak Dek MS, Padmanabhan P, Sherif S, et al (2017a) Upregulation of phosphatidylinositol 3-kinase (Pi3k) enhances ethylene biosynthesis and accelerates flower senescence in transgenic *Nicotiana tabacum* L. Int J Mol Sci 18:1–15.

Pak Dek MS, Padmanabhan P, Subramanian J (2017b) Inhibition of tomato (*Solanum lycopersicum* L.) fruit ripening by 1-MCP, wortmannin and hexanal is associated with a decrease in transcript levels of phospholipase D and other ripening related genes. Postharvest Biol Technol 140:1–20.

Pech JC, Bouzayen M, Latché A (2008) Climacteric fruit ripening: Ethylene-dependent and independent regulation of ripening pathways in melon fruit. Plant Sci 175:114–120.

Pereira L, Ruggieri V, Perez S, et al. QTL mapping of melon fruit quality traits using a high-density GBS-based genetic map. (submitted).

Proost S, Van Bel M, Sterck L, et al (2009) PLAZA: A Comparative Genomics Resource to Study Gene and Genome Evolution in Plants. Plant Cell 21:3718–3731.

R Core Team. R: A language and environment for statistical computing. Vienna, Austria: R Foundation for Statistical Computing; 2012. URL http://www.R-project.org/

Rios P, Argyris JM, Vegas J, et al (2017) *ETHQV6.3* is involved in melon climacteric fruit ripening and is encoded by a NAC domain transcription factor. Plant J 91:671–683.

RStudio. RStudio: Integrated development environment for R RStudio. Boston, MA, USA; 2012. URL http://www.rstudio.com/

Ruggieri V, Alexiou KG, Morata J, et al. An improved assembly and annotation of the melon (*Cucumis melo* L.) reference genome. (under review in Sci Rep).

Saladié M, Cañizares J, Phillips MA, et al (2015) Comparative transcriptional profiling analysis of developing melon (*Cucumis melo* L.) fruit from climacteric and non-climacteric varieties. BMC Genomics 16:1–20.

Shi H, Zhang Y (2014) Pear 14-3-3a gene (*Pp14-3-3a*) is regulated during fruit ripening and senescense, and involved in response to salicylic acid and ethylene signalling. J Genet 93:747–753.

Tang Y, Zhao CY, Tan ST, Xue HW (2016) *Arabidopsis* Type II Phosphatidylinositol 4-Kinase PI4Kγ5 Regulates Auxin Biosynthesis and Leaf Margin Development through Interacting with Membrane-Bound Transcription Factor ANAC078. PLoS Genet 12:1–22.

Van Bel M, Diels T, Vancaester E, et al (2018) PLAZA 4.0: An integrative resource for functional, evolutionary and comparative plant genomics. Nucleic Acids Res 46:D1190–D1196.

Van Ooijen J, Maliepaard C (1996) MapQTL Version 3.0: Software for the calculation of QTL positions on genetic maps.

Van Ooijen JW (2006) JoinMap® 4.0: software for the calculation of genetic linkage maps in experimental population. Kyazma BV.

Vegas J, Garcia-Mas J, Monforte AJ (2013) Interaction between QTLs induces an advance in ethylene biosynthesis during melon fruit ripening. Theor Appl Genet 126:1531–1544.

Vrebalov J, Ruezinsky D, Padmanabhan V, et al (2002) A MADS-box gene necessary for fruit ripening at the tomato ripening-inhibitor (*rin*) locus. Science 296:343–346.

Yano R, Ezura H (2016) Fruit ripening in melon. In: Genetics and genomics of Cucurbitaceae. pp 345–375

Yano R, Nonaka S, Ezura H (2018) Melonet-DB, A Grand RNA-seq Gene Expression Atlas in Melon (Cucumis melo L.). Plant cell Physiol 59:e(1-15).

Yao Y, Du Y, Jiang L, Liu JY (2007) Interaction between ACC synthase 1 and 14-3-3 proteins in rice: a new insight. Biochem 72:1003–1007.

Yoon GM, Kieber JJ (2013) 14-3-3 Regulates 1-Aminocyclopropane-1-Carboxylate Synthase Protein Turnover in *Arabidopsis*. Plant Cell 25:1016–1028.

Chapter 5

Development of two reciprocal IL collections using “Védrantais”, a *cantalupensis* climacteric variety, and “Piel de Sapo”, an *inodorus* non-climacteric variety

Introduction

Understanding the genetics that relies beyond interesting traits, from human diseases to crop yield, has been one of the main goals of modern science. Genetic variation, e.g. diversity within a species, is studied and correlated with the phenotypic effects of interest, identifying the genomic regions that control them. In plants, due to the versatile possibilities of crossing, many types of populations can be developed depending on the desired cost in time and resources and the objectives of the research. In heterozygous species with large juvenile periods, as grapevine or peach, F1, F2 or BC1 populations are commonly used to perform QTL mapping studies (Doligez et al. 2002; Serra et al. 2017). In species with shorter generation periods, as cereals and vegetable crops, other populations with an increased complexity are usually developed, as Recombinant Inbred Line (Harel-Beja et al. 2010), Nested Association Mapping (McMullen et al. 2009), Multi-parent Advanced Generation Intercrosses (Huang et al. 2015) and Introgression Line (IL) (Eduardo et al. 2005; Barrantes et al. 2014) populations. Some of the desired advantages sought in segregating populations are a high resolution, obtained in populations that need a higher number of generations, leading to more recombination breakpoints; immortality of the lines, allowing multiple replicates and experiments under different environmental conditions; and increased allele diversity due to multiple parental lines. Particularly, IL collections are based on lines that share a high proportion of genetic background from a recurrent parental, differing only in a specific region of the genome (introgression), inherited from the donor parental. All the genome of the donor parental is covered by the different ILs that form the collection. They are considered a powerful resource since they allow not only performing QTL mapping experiments, but subsequent specific studies as QTL validation (Díaz et al. 2017), QTL interactions (Lin et al. 2000; Monforte et al. 2001) and fine mapping (Rios et al. 2017).

IL populations (also referred as Near Isogenic Lines, NILs) have been used as genetic resources in multiple species since several decades (Briggle 1969; Suge 1972; Pegg and Cronshaw 1976), from model plants as *Arabidopsis thaliana* (Keurentjes et al. 2007), rice (Li et al. 2005) and tomato (Bernacchi et al. 1998) to less studied and even orphan crops, as strawberry (Urrutia et al. 2015), peach (Serra et al. 2016) and groundnut (Foncéka et al. 2009). They have proven their efficiency to map and characterize different traits related with disease resistance, plant architecture and fruit morphology and quality. Furthermore, they have been commonly used in breeding programs to introduce desired

exotic alleles from the donor parental, where the recurrent parental is generally an elite line.

The development of ILs is performed using molecular markers, and the rapid increase in marker availability and high-throughput genotyping techniques have changed the methods used to develop these populations. Recently, the tendency has been to minimize the number of backcrosses needed by increasing the size of the initial screened populations and the number of markers, in order to decrease the number of non-desired contaminations in narrow non-genotyped regions of the genome (Barrantes et al. 2014; Urrutia et al. 2015; Serra et al. 2016).

IL populations have been developed and widely used throughout the last years in melon (Eduardo et al. 2005; Perpiñá et al. 2016; Eduardo et al. 2007; Obando-Ulloa et al. 2010; Vegas et al. 2013; Rios et al. 2017). Melon is a diploid species with a relatively small genome (450 Mb) and 2n=2x=24 (Garcia-Mas et al. 2012). Melon has become an alternative model species to study certain traits, as climacteric ripening (Ezura and Owino 2008) and sex determination (Martin et al. 2009). The first use of ILs in melon was reported in 1979 to study a fungus resistance, although only covering the desired region of the genome (Netzer et al. 1979). A complete IL collection was developed using as recurrent parental an *inodorus* type from the *melo* spp., and as donor parental an exotic Korean line from the *agrestis* spp. (Eduardo et al. 2005). An extensive phenotyping of the population lead to identify QTLs controlling fruit shape and size, sugar content, fruit ripening and virus resistance, among others. Some ILs of this collection have been used to fine map and clone two genes controlling climacteric ripening (Rios et al. 2017) and resistance to *Cucumber Mosaic Virus* (Giner et al. 2017). Pyramidization of multiple QTLs controlling or modulating the same trait allowed to detect the potential interactions between them; e.g., the already mentioned cloned gene involved in climacteric ripening (*ETHQB6.3*) (Chapter 4) interacts with a second QTL (*ETHQV5.3*), leading to a more intense climacteric phenotype when both introgressions are combined in the same IL (Vegas et al. 2013).

Most of the populations developed in melon have been funded by a cross between an elite cultivar and an exotic accession. A recent study using a RIL population between two European cultivars, “Védrantais” (Ved), a typical French variety belonging to the *cantalupensis* group, and “Piel de Sapo” (PS), a Spanish variety from the *inodorus* group, showed segregation for important agronomic traits related with fruit quality and

climacteric ripening (Pereira et al. submitted). Due to the above-mentioned advantages of IL collections, the goal of this work has been to develop two reciprocal IL collections that covered the whole melon genome, carrying Ved background with PS introgressions and vice versa.

Materials and methods

Plant material and breeding scheme

Seedlings were planted in fertilpots and maintained in controlled conditions in an indoor greenhouse facility (CRAG, Barcelona) during approximately three weeks. After this period, selected plants were grown in a greenhouse in Caldes de Montbui (Barcelona) during spring and summer seasons (April-October). Plants were pruned weekly and pollinations were executed manually, allowing to develop only one fruit per plant.

IL collections were funded by a cross between two commercial varieties, Ved, a French melon from the *cantalupensis* group, and PS, a Spanish melon from the *inodorus* group. Pollen from the F1 plants was used to pollinate female flowers from both parental lines, obtaining BC1 seed with the cytoplasm from the recurrent parental in each collection. After BC1, the recurrent parental was used generally as the male parent and the pre-IL as the female parent. Seedlings of the BC1 progenies were screened and a subset of plants for each collection was selected following these hierarchical criteria: 1) the complete genome of the donor parental should be contained at least twice in the selected individuals; 2) the lines should carry the lowest possible number of introgressions; 3) the lines should contain the highest possible percentage of the recurrent parental genome. The chosen individuals were backcrossed again with the recurrent parental to obtain the BC2. Analogous cycles of screening and selection were performed for the subsequent progenies (Figure 5.1). When the lines contained three or less introgressions, they were self-pollinated to identify a unique introgression in homozygosity within the progeny. Depending on the introgression line, three or four backcrosses followed by one or two self-pollinations were needed to obtain the target introgression line without additional introgressions in other chromosomes. In fact, the IL collections still contain some lines with more than one introgression or target introgressions in heterozygosis, which will be subjected to another cycle of screening and selection during the summer of 2018.

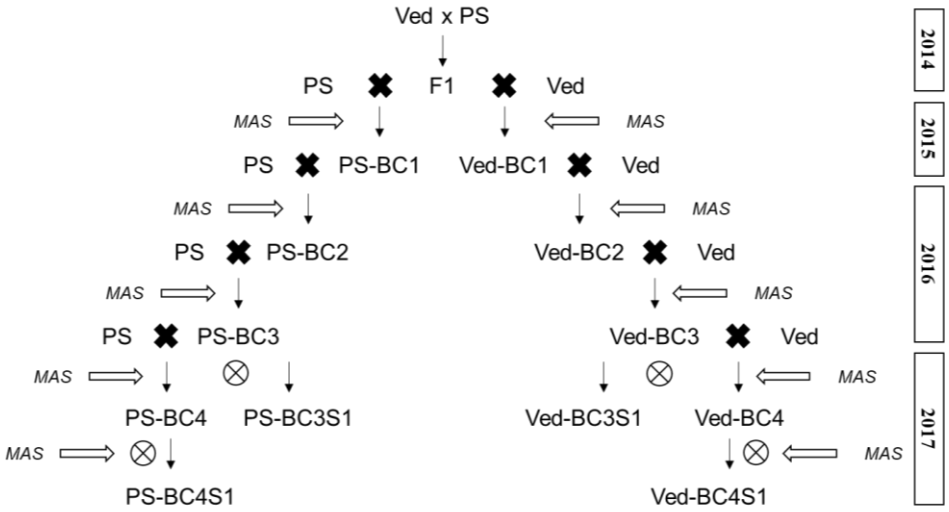

Figure 5.1. Breeding scheme used to develop the IL collections. MAS, marker-assisted selection.

DNA extraction and genotyping

DNA extractions were performed from young leaves following the CTAB protocol (Doyle 1991) with some modifications (Pereira et al. submitted).

The progenies of BC1, BC2 and most part of the BC3 seedlings were analyzed with an initial set of 48 SNPs (set 1) homogeneously distributed within the 12 melon chromosomes (Table 5.S1a). The selected plants from BC2 and BC3 generations were subsequently genotyped with an additional set of 48 SNPs (set 2) (Table 5.S1b). SNPs were discovered and designed from resequencing data of both parental lines and their positions are referred to the melon reference genome v3.6.1 (http://www.melonomics.net). SNPs producing sub-optimal genotypes were substituted by other SNPs located nearby. The progenies of BC3S1, BC4, BC3S2 and BC4S1, screened in 2017, were genotyped with the complete set of SNPs (Table 5.S1c). Plants were genotyped with SNPs using the KASPar SNP Genotyping System (KBiosciences, Herts, UK). KASPar primers were designed using Primer Picker, a specific tool provided by the supplier. The genotyping was performed using the high-throughput genotyping system Biomark HD, based on the Fluidigm technology, with 48x48 (2015 and 2016) and 96x96 (2017) chips. In the last phases of screening and selection, when most part of the genome was already fixed for the recurrent parental alleles, only SNPs contained in the known introgressions were genotyped with the same KASPar primers but using qPCR in a LightCycler 480 Real-time PCR System, using the technical instructions provided by the supplier (Roche Diagnostics, Spain).

To calculate the size of the introgressions, two assumptions were done; we supposed that the haplotypes of the non-genotyped extremes of the chromosome were the same than the first or last SNP genotyped; and we used the intermediate position between two genotyped SNPs as the virtual recombination breakpoint. The approximate genetic size of the introgressions was calculated using as a reference a genetic map obtained from a Ved x PS RIL population (Pereira et al. submitted).

Phenotyping of fruit quality and climacteric ripening traits

Although the IL collections are not totally finished, a preliminary phenotyping of the pre-ILs was performed in the last generations. Qualitative traits related with fruit appearance (external color of immature fruit, presence of sutures) were visually inspected and recorded as presence or absence (Table 5.1). Flesh color of mature fruits was recorded as orange, white or green. All fruits were photographed at harvest.

Ripening-related traits were evaluated as qualitative (presence or absence) or quantitative (earliness of appearance of the trait in days after pollination, DAP). The visual inspection of melon fruits attached to the plant was performed daily, from approximately 25 DAP until harvest. Chlorophyll degradation (CD) and its earliness (ECD) were recorded only when they were obvious in visual inspections. Aroma production (ARO) and its earliness (EARO) were evaluated each other day by smelling the fruits. Abscission (ABS) was recorded using an index from 0, no abscission layer formation (AFL); 1, subtle and/or partial ALF; 2, almost complete AFL with obvious scar; and 3, total AFL generally with fruit abscission.

Table 5.1. Description of the evaluated traits in the IL populations.

Trait	**Code**
Presence of sutures	*S-2*
External color of immature fruit	ECOL
Flesh color	FCOL
Chlorophyll degradation	CD
Earliness of chlorophyll degradation	ECD
Aroma production	ARO
Earliness of aroma production	EARO
Abscission	ABS

Results

Development of the Ved IL collection

For the IL collection carrying introgressions of PS in the Ved background, 321 BC1 seedlings were genotyped in 2015. The number of introgressions ranged from 4 to 17 introgressions per line, with a mean of 11.5 and a median of 12. The percentage of Ved genome ranged from 13.0 to 80.1%, with an average of 48.7%. The observed heterozygosity was $H_0 = 0.46$ and 16 SNPs showed significant segregation distortion. The highest segregation distortion was observed in the centromeric region of chromosome XII for SNP Cm0198 ($\chi^2 = 43.3$), which presented a minimum observed heterozygosity of 0.31. In fact, the observed heterozygosity was lower than the average for the four SNPs of chromosome XII, where the Ved alleles were overrepresented. A set of 25 BC1 plants (7.8%) were selected, presenting a mean of 8 introgressions and 62.2% of Ved background genome.

In the spring season of 2016, the BC2 progenies of 11 BC1 families were analyzed, using a number of individuals between 15 and 45 per family depending on the number of introgressions carried by the BC1 mother plant. A total of 321 BC2 seedlings were genotyped with the set 1 of SNPs (Table 5.S1a), 89 were subjected to a second round of genotyping with the set 2 of SNPs (Table 5.S1b) and 49 of them (15.3% of the total) were selected and backcrossed again with Ved to obtain the BC3. The selected individuals presented an average of 5 introgressions and 80.6% of Ved genome.

A total of 357 BC3 seedlings belonging to 20 BC2 families were screened with the set 1 of SNPs (Table 5.S1a) during the summer season of 2016. A set of 64 plants (17.9%) was selected and genotyped with the set 2 of SNPs (Table 5.S1b). They presented a mean of 2.6 introgressions and 85.7% of Ved genome. Either backcross or self-pollinations were performed depending on the number of introgressions that the BC3 plants carried, as described in Materials and Methods.

In the spring season of 2017, 590 seedlings were screened with the complete set of 96 SNPs (Table 5.S1c), belonging to 23 BC3S1 families and two BC4 families. The number of genotyped individuals per family ranged from 6 to 45 seedlings. A set of 100 plants were selected, carrying 1.8 introgressions and 88.3% of Ved genome on average. Six of them were already the desired ILs (Table 5.S2a), with homozygous introgressions from

PS in regions of chromosomes II, III, IV, VII, and XI. IL 74.37, in addition to the desired introgression in chromosome IV, presents a small contamination in chromosome I (Table 5.S2a). The other lines either contained more than one introgression or the target introgression in heterozygosity. Their progenies were screened during the summer season of 2017, following a different strategy due to the low number of introgressions presented by each family. For 26 progenies (25 BC3S2 and one BC4S1), a specific combination of SNPs was designed for each family, using exclusively the required SNPs to monitor the known introgressions, since most part of the background genome was already fixed for the Ved alleles. A total of 356 plants, with a median of eight plants per family, were screened with 1-4 SNPs located in the introgressions; ILs obtained in the previous generation (Table 5.S2a) were also germinated and genotyped to confirm that the introgression was fixed, and grown in the greenhouse to perform a preliminary phenotyping and seed multiplication. In addition, 165 seedlings that belonged to eight families containing additional or larger introgressions were genotyped with the complete set of 96 SNPs (Table 5.S1c). From these two screenings, 21 new target ILs were obtained (Table 5.S2b), mainly covering chromosomes I, II, IV, V, VI, VII, VIII, IX and XII. Besides the 27 ILs described before (6 BC3S1 and 21 BC3S2/BC4S1), a set of 13 advanced lines (Table 5.S2c) with two or less introgressions were developed and self-pollinated, and their progenies are now available to select the target ILs. Furthermore, other five ILs (Table 5.S2d), not specifically sought, were obtained and their progenies were conserved as potentially useful in the future. We considered a set of 38 selected lines as the basic IL collection (Figure 5.2 and Table 5.S3a), although an extended collection of 45 lines (Table 5.S3b), including additional redundant ILs, and a reduced collection (Table 5.S3c), are presented. The latter was formed by 33 ILs that covered the same proportion of PS genome that the basic collection, but with a maximum of three ILs per chromosome.

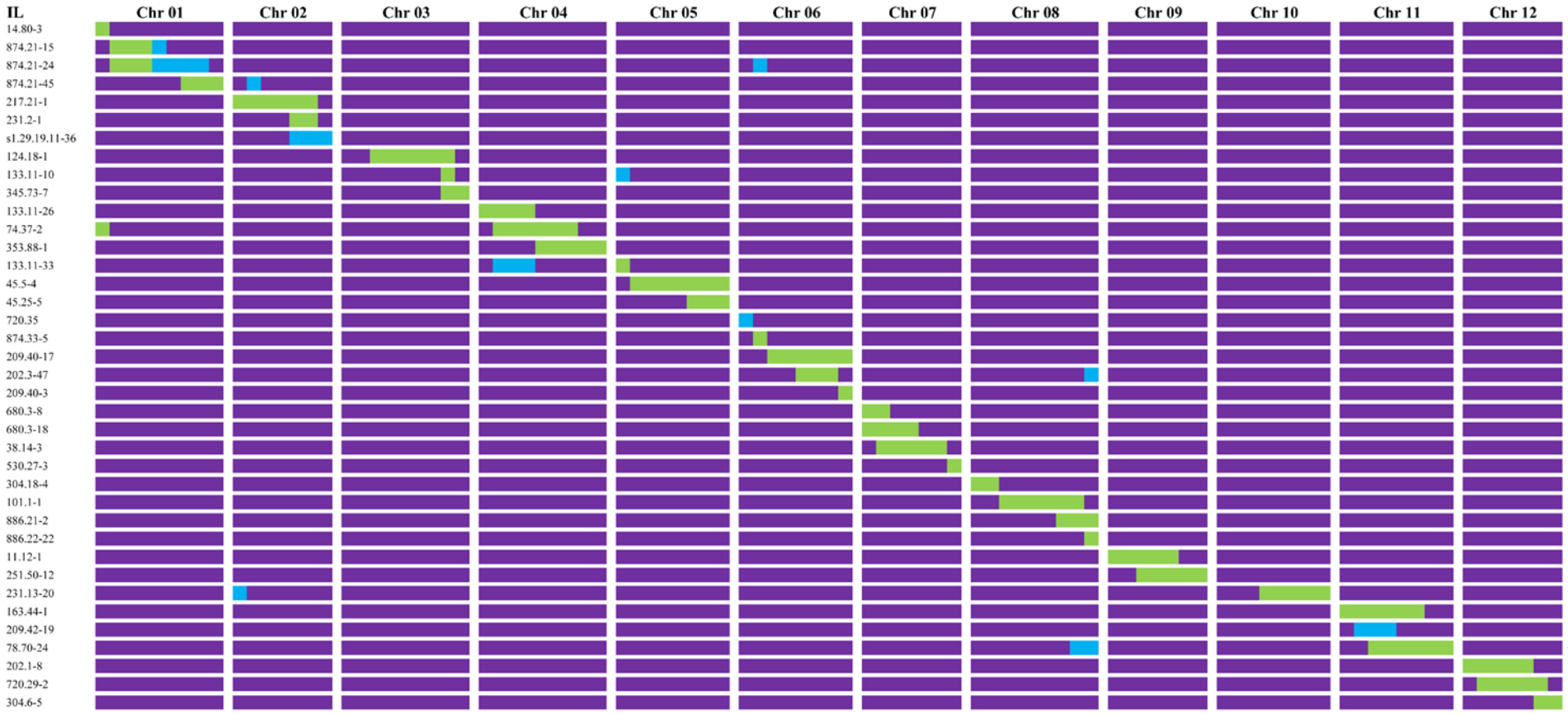

Figure 5.2. Diagram representing the basic Ved IL collection. The lines are represented in the horizontal axis and the chromosomes in the vertical axis. The length of each bar is proportional to the physical position of the used SNPs described in Table 5.S1c. Purple, homozygous for Ved allele; blue, heterozygous; green, homozygous for PS allele.

The basic IL collection almost covered the complete genome of PS, but three regions remained uncovered, mainly due to bad fruit set or inadequate performance of some SNPs in earlier generations (Table 5.2). These regions were located in chromosome II, from 22,518,306 bp to the end of the chromosome; in chromosome III, from the beginning of the chromosome to 8,125,561 bp; and in chromosome X, from the beginning of the chromosome to 9,527,106 bp. Furthermore, some of the ILs did not overlap, based on the information obtained from the analyzed SNPs. To detect whether they overlapped, additional SNPs (Table 5.S1d) were developed in the uncertain regions and genotyped in the lines that could potentially overlap. After the genotyping, we could determine that in chromosomes V and VIII the introgressions are overlapping (not shown). However, in other chromosomes putative gaps remained (Table 5.2).

Table 5.2. Putative detected gaps in the basic Ved IL collection.

Chr	Maximum size (Mb)	Initial position (Mb)	Final position (Mb)	Detection	Covered by existing pre-ILs
II	4.5	22.51	27.06	Absent alleles	Yes
III	8.1	0	8.13	Absent alleles	Yes
X	9.5	0	9.53	Absent alleles	Yes
I	3.3	0.22	3.53	No overlapping SNPs	Yes
VI	1.8	1.82	3.60	No overlapping SNPs	Yes

Although the non-represented intervals represent a very low proportion (6%) of the melon genome, we intended to cover them, so we recovered seeds from previous generations, specifically four BC1 and three BC2 progenies. The procedure followed was analogous to the one described above, and one or two cycles of selection were performed in 2017 depending on the family. One of these lines contained only one introgression in heterozygosity and was considered advanced material and included in the final IL collection (Figure 5.2), covering the above-mentioned gap in chromosome II. Another 10 pre-ILs (Table 5.S2e), with a mean of 4.8 introgressions and 80.1% of Ved genome, will allow to cover all the mentioned gaps in one or two more cycles of selection.

At the moment, the basic Ved IL collection covers the 95% of the Ved genome, and the remaining 5% will be achieved during the next year. The collection is composed by 26

ILs carrying only one homozygous introgression, four ILs with a heterozygous introgression, seven lines carrying the target introgression in homozygosity and an additional one in heterozygosity and one line carrying two introgressions in homozygosity. A mean of 3.2 ILs per chromosome was obtained, with a large range of introgressions length from 2,430,563 to 33,016,562 bp (Table 5.3). The size in genetic distance units ranged from 21.88 to 116.37 cM, with an average of 57.91 cM.

Table 5.3. Composition of the basic Ved IL collection.

Chr	ILs[1]	Introgression size (Mb)[2]	Introgression size (cM)[2]
I	4	16.09	50.23
II	3	14.59	63.83
III	3	11.34	51.15
IV	3	19.71	79.11
V	3	12.45	59.25
VI	5	12.77	42.28
VII	4	12.20	52.78
VIII	4	18.91	67.47
IX	2	20.08	63.58
X	1	16.57	23.54
XI	3	24.94	80.70
XII	3	17.11	59.09
Mean	3.2	16.23	57.91
Max	5.0	33.02	116.37
Min	1.0	2.43	21.88

[1]Number of ILs covering the chromosome
[2]Average using all the introgressions covering the chromosome

Development of the PS IL collection

To obtain the IL collection carrying introgressions of Ved in the PS background, 270 BC1 seedlings were screened in 2015 with the set 1 of SNPs (Table 5.S1a). The number of introgressions ranged from 5 to 17, with 11.8 introgressions on average (median of 12 introgressions). The percentage of PS genome varied from 10.6 to 76.6%, and the mean recurrent parental background was 50.2%. The mean observed heterozygosity was H_0 = 0.48 and 10 SNPs showed segregation distortion, but the distortion was lower than in the

Ved BC1. The highest distortion was $\chi^2 = 18$ and was observed for SNP chr7_16723157, belonging to chromosome VII and located in the position 18,255,891 bp; it showed $H_0 = 0.63$, predominating the Ved allele. For the other SNPs showing segregation distortion, the observed heterozygosity was below the mean and ranged from 0.41 to 0.44. A set of 20 plants (7.4% of the total) was selected to backcross with PS; these plants carried on average 8.3 introgressions and 65.6% of their genome was from the recurrent parental.

The BC2 progenies of 11 BC1 families were screened, using between 16 and 43 individuals per family, during the spring of 2016. A total of 295 BC2 seedlings were genotyped with the set 1 of SNPs (Table 5.S1a), 65 were subjected to a second round of genotyping with the set 2 of SNPs (Table 5.S1b) and 46 of them (15.6% of the total) were selected and backcrossed again with PS to obtain the BC3. The selected individuals presented an average of 5.3 introgressions and 77.3% of PS genome.

A total of 313 BC3 seedlings belonging to 19 BC3 families were screened with the set 1 of SNPs (Table 5.S1a) during the summer season of 2016. A set of 55 plants (17.6%) was selected and genotyped with the set 2 of SNPs (Table 5.S1b). They presented a mean of 3.4 introgressions and 82.4% of PS genome.

In the spring season of 2017, 475 seedlings were screened with the complete set of 96 SNPs (Table 5.S1c), belonging to 15 BC3S1 families and five BC4 families. The number of genotyped individuals ranged from 5 to 47 seedlings per family. A set of 92 plants were selected, carrying 2.2 introgressions and 89.7% of PS genome, on average. At the beginning of 2017, the pre-IL collection had some missing regions in chromosomes II, III, VI and VIII, mainly due to bad fruit set and germination problems. As explained for the Ved collection, some BC2 and BC3 families from previous generations were recovered in order to cover the gaps. A total of 169 seedlings belonging to seven BC3 families were added to the above explained families, and 27 of them were selected.

Five ILs of the selected set were already carrying the target introgressions from Ved in homozygosity (Tables 5.S4a and 5.S4d), however most of the lines contained more than one introgression. Useful progenies were germinated and genotyped with the complete set of SNPs, or a custom combination of them as explained for the Ved collection, during the summer season of 2017. Including the recovered families from previous generations, 312 seedlings from 18 families with multiple or larger introgressions were genotyped with 96 SNPs and another 226 plants from 16 progenies were screened with a specific set

of 1-4 SNPs, including 13 BC3S2, two BC3S1 and one BC4. The described analysis lead to 18 new ILs (Table 5.S4b) and 24 advanced lines (Table 5.S4c) with two or less introgressions. As performed in the Ved collection, a basic IL collection of 38 ILs (Table 5.S5a) was obtained, including ILs in both homozygosity and heterozygosity and advanced lines. An extended collection of 47 ILs (Table 5.S5b), including 9 additional ILs and advanced lines, and a reduced collection containing 31 ILs (Table 5.S5c) were also selected.

The basic PS IL collection is formed by 38 lines, including 17 ILs with a unique target introgression in homozygosity, six ILs carrying a heterozygous target introgression and 15 advanced lines with two introgressions (Figure 5.3). Each chromosome is covered by 3.2 ILs on average, with a maximum of 5 in chromosome I and a minimum of 2 in chromosomes VIII and XII (Table 5.4). The mean introgression size is 15.6 Mb in physical distance (range 2.3-34.5 Mb) and 58.25 cM in genetic distance (range 8.53-109.51 cM).

Table 5.4. Composition of the basic PS IL collection.

Chr	**ILs[1]**	**Introgression size (Mb)[2]**	**Introgression size (cM)[2]**
I	5	15.81	40.86
II	3	10.08	42.57
III	3	16.05	54.99
IV	4	16.01	64.42
V	4	11.40	48.38
VI	3	14.05	51.77
VII	3	17.44	69.34
VIII	2	15.95	75.63
IX	3	18.13	85.06
X	3	12.07	49.71
XI	3	25.35	75.49
XII	2	16.50	60.05
Mean	3.2	15.61	58.25
Max	5.0	34.46	109.51
Min	2.0	2.29	8.53

The basic PS IL collection covers 90.9% of the Ved genome, but some gaps are still remaining (Table 5.5) and the necessary lines to rescue these regions will be used during following generations. Although we describe all the putative gaps in Table 5.5, some of them could still be covered, since we did not genotype the uncovered region between SNPs. During next generations, additional SNPs (Table 5.S1d), and others if necessary, should be genotyped in all the ILs and pre-ILs in order to confirm these gaps.

Table 5.5. Putative detected gaps in the basic PS IL collection.

Chr	Maximum size (Mb)	Initial position (Mb)	Final position (Mb)	Detection	Covered by existing pre-ILs
II	3.5	0.73	4.25	No overlapping SNPs	No
II	5	22.52	27.02	No overlapping SNPs	Yes
III	8.4	22.44	30.85	Absent alleles	Yes
V	5.6	23.72	29.32	No overlapping SNPs	No
VI	4.6	0	4.67	Absent alleles	Yes
VI	4	-[1]	-[1]	No overlapping SNPs	Yes
VII	5.5	23.20	28.76	No overlapping SNPs	No
VIII	12.7	22.07	34.77	Absent alleles	Yes

[1]Inconsistency on physical positions according to the genetic map (Pereira et al. submitted)

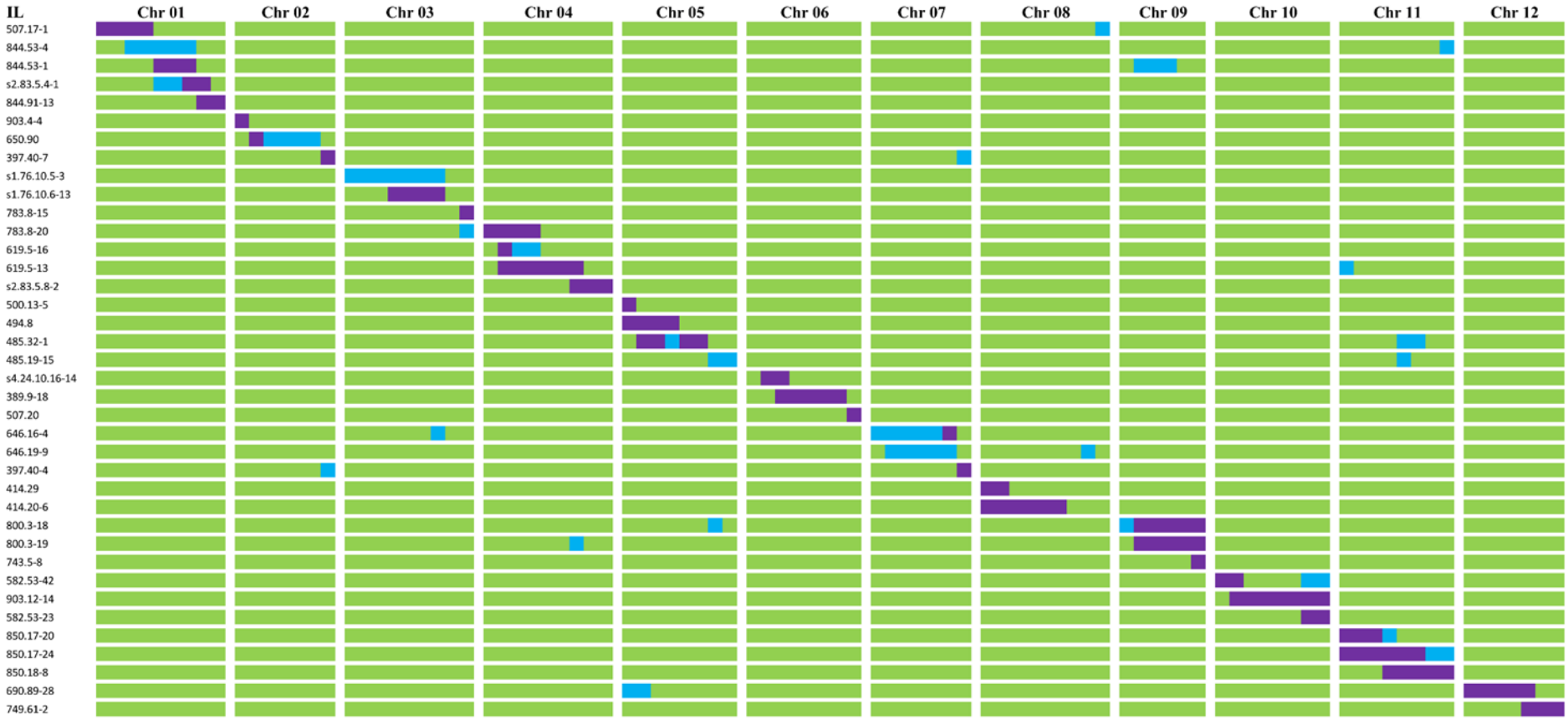

Figure 5.3. Diagram representing the basic PS IL collection. The lines are represented in the horizontal axis and the chromosomes in the vertical axis. The length of each bar is proportional to the physical position of the used SNPs described in Table 5.S1c. Purple, homozygous for Ved allele; blue, heterozygous; green, homozygous for PS allele

Preliminary phenotyping and QTL mapping

Although the IL collections are not totally finalized and the number of replicates for each IL was low, we performed a first preliminary phenotyping during the summer-autumn season of 2017, which included the obtained ILs and advanced lines.

Segregation for fruit quality traits in the IL collections

The IL collections showed a high level of segregation for different traits related to plant architecture and vigour, flowering time, fruit set rate, and specially fruit quality and ripening behaviour. Focusing on fruit traits, we could identify a wide range of phenotypes from almost identical to completely different fruits when comparing the ILs to the parental lines.

Most of the fruits in the Ved collection were very similar to Ved, such as 231.13-9 and 321.2-2 (Figure 5.4), presenting white/cream rind with slight netting and presence of sutures, medium size, round shape and orange flesh. The rind color of mature fruits was diverse in the IL collection, ranging from dark green (680.3-8) to different intensities of yellow and cream (38.10-5 and 163.44-1). Some fruits presented also dense netting (680.3-8) or mottled rind (s1.29.19.11-36). Flesh color was generally orange, although the intensity of the orange color varied, and even some green flesh melons were obtained (251.50-12). All the lines were climacteric, showing most of the ethylene-dependent symptoms as change of external color due to chlorophyll degradation, abscission layer formation and aroma production. But the intensity and the earliness of the traits associated with climacteric ripening differed in some ILs.

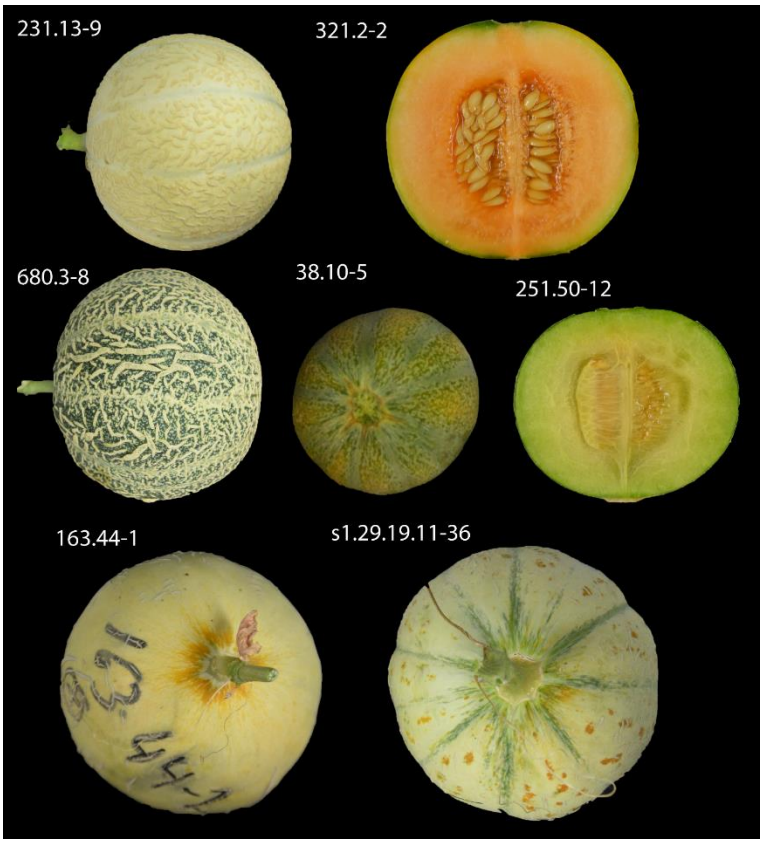

Figure 5.4. ILs representing the phenotypic segregation in the Ved IL collection.

In the PS collection, IL 507.17-3 presented a phenotype very similar to PS, with bright green and mottled fruit, large size, ellipsoid shape, and white/cream flesh color (Figure 5.5). Depending on the Ved introgression, other lines presented dark green (582.53-14) or yellow (646.16-9) rind in ripe fruits, presence of sutures (850.18-6) or orange flesh color (785.8-5). The size and shape also varied from small and almost round (850.18-6) to large and elongated (785.8-5) fruits. As for ripening behaviour, most of the lines were non-climacteric as PS, but some of them showed slight climacteric symptoms, specially related with abscission layer formation.

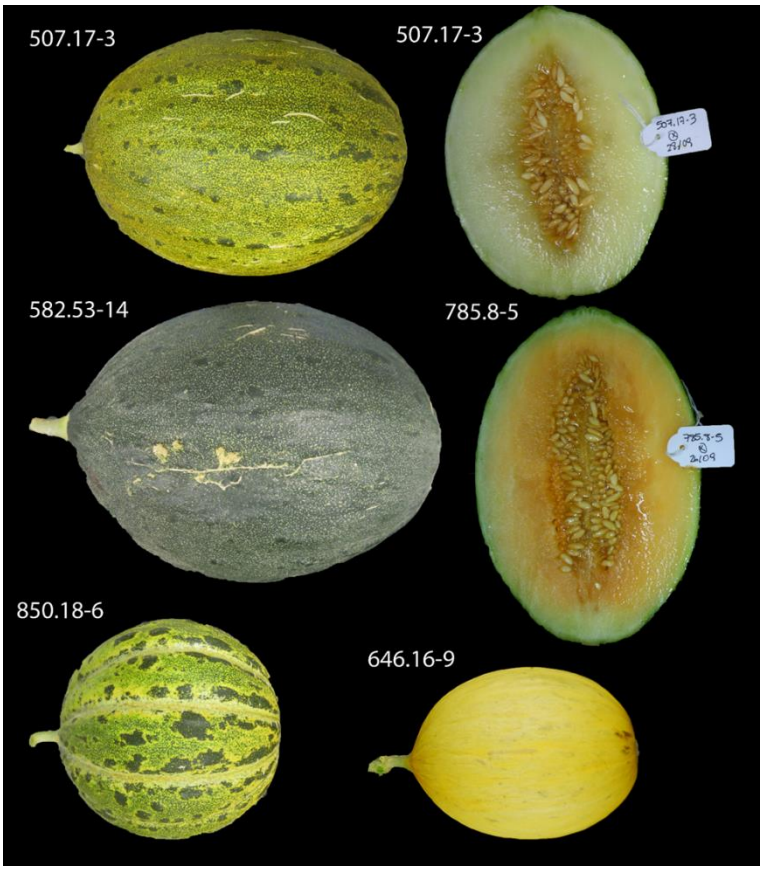

Figure 5.5. ILs representing the phenotypic segregation in the PS IL collection.

Mapping of major genes

Some of the interesting traits that are segregating in the IL collections are monogenic, showing a complete or almost complete association with a region of the genome. The ease of phenotyping and low environmental effect in these monogenic traits allowed to map them with high confidence even using a reduced number of replicates.

One of these traits is the development of sutures in the rind of the fruit, a characteristic that is present in Ved and absent in PS. The absence of sutures is dominant over their presence. In the summer season of 2017, we could phenotype ILs or pre-ILs carrying introgressions in chromosome XI in both backgrounds (Figure 5.6). The lines with the PS background and Ved introgressions in chromosome XI had marked sutures of grey-white color when the introgression was in homozygosity (n=7, 485.19-6). When it was in heterozygosity, a slight indentation with minor change of color from dark to light green could be observed in 4 of the 10 heterozygous ILs, as in the line 850.17-10. In the Ved collection, the lines with a PS introgression in chromosome XI, either homozygous (n=7, 163.44-2) or heterozygous (n=4, s1.53-30), showed smooth melons with no sutures.

Flanking SNPs outside of the introgression carried by the line 485.19-6 allowed to delimit the major gene to an interval of around 14 Mb between positions 17,337,052 and 31,744,823 bp in chromosome XI.

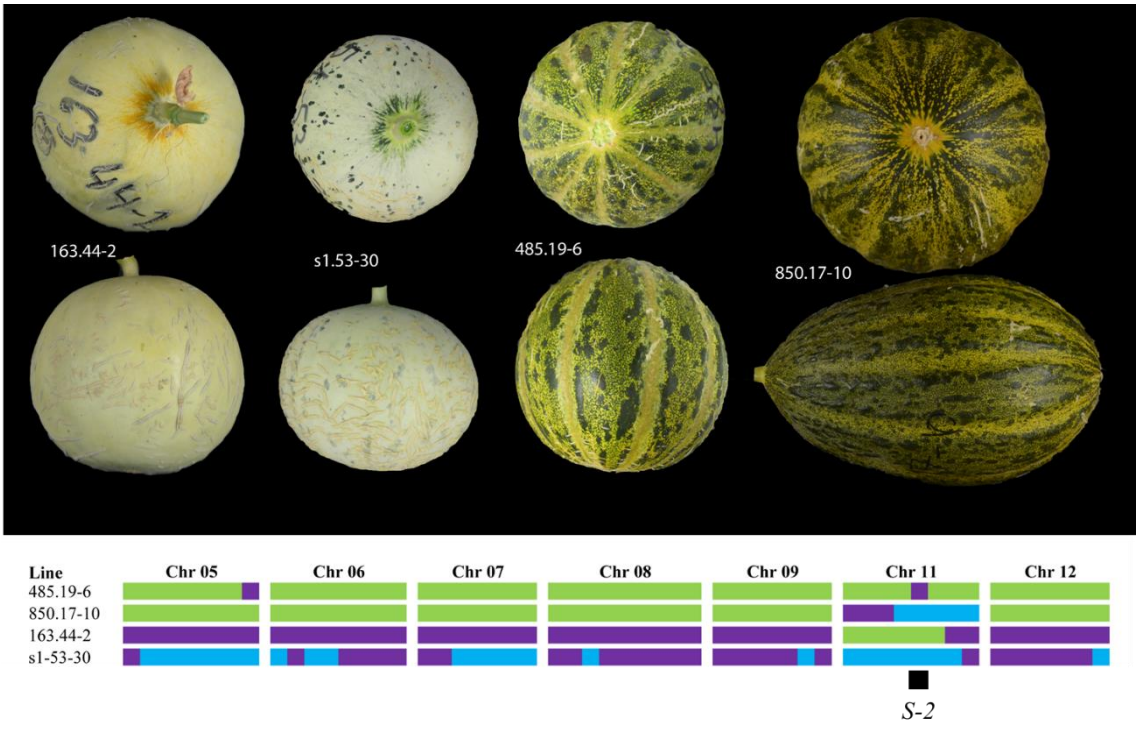

Figure 5.6. ILs and pre-ILs showing the segregation for sutures. 163.44-2 and s1.53-30 are lines with the Ved background without sutures and 485.19-6 and 850.17-10 are lines with the PS background with sutures. The genotype of the lines is presented in the diagram, showing only the chromosomes that carried an introgression from the donor parental in at least one plant.

Another important quality trait showing oligogenic inheritance is flesh color of ripe fruits. Three phenotypes, orange, white and green flesh, can be observed depending on the allelic combination of two genes that act epistatically. A dominant gene in chromosome IX already cloned, *Gf* or *CmOr* (Tzuri et al. 2015), is controlling the presence of orange color, conferred by a high content of carotenoids. The non-orange allele, which is the recessive one, permits the manifestation of the second gene, called *Wf*, to control white (dominant) or green (recessive) color (Monforte et al. 2004; Cuevas et al. 2009; Galpaz et al. 2017). In our Ved IL collection, if the chromosome IX had at least one Ved allele, the flesh color of these melons was orange (Figure 5.7, 251.50-44); but when a homozygous PS introgression was present in chromosome IX, the flesh became green (Figure 5.7, 251.50-12). In the PS background, we could observe the analogous effect in lines carrying Ved introgressions in chromosome IX and also the effect conferred by the second gene, located in chromosome VIII. We could observe the three possible

categories: orange if the Ved allele was present in chromosome IX (783.8-5 and 800.3-2); when the chromosome XI was fixed for PS alleles, the flesh was green when a homozygous Ved introgression was carried in chromosome VIII (s2.13.38.2-5); and white when the introgression was in heterozygosity for chromosome VIII (s2.13.38.2-9). The previously described inheritance and the locations of the genes *CmOr* and *Wf* fitted perfectly in our IL populations.

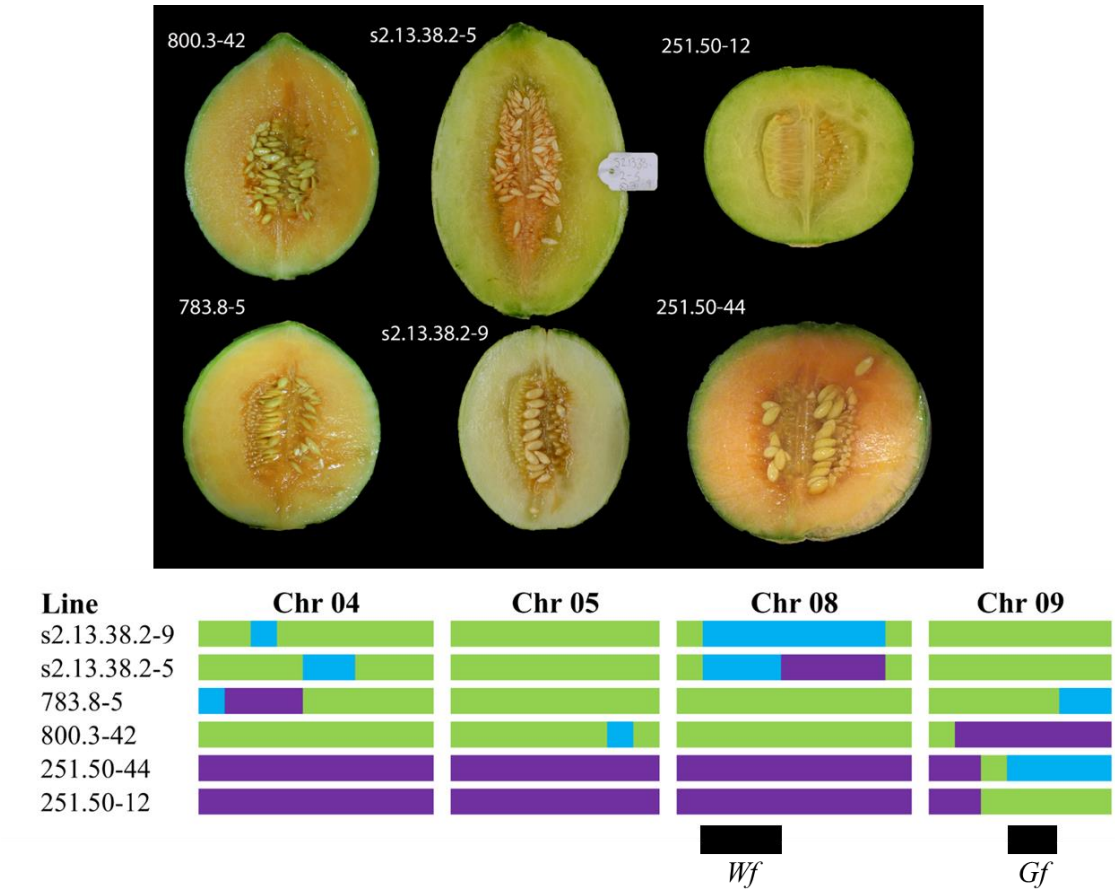

Figure 5.7. ILs and pre-ILs showing the segregation of flesh color. 800.3-42, 783.8-5, s2.13.38.2-5 and s2.13.38.2-9 are lines with the PS background and 251.50-12 and 251.50-44 are lines with the Ved background. The genotype of the lines is presented in the diagram, showing only the chromosomes that carried an introgression from the donor parental in at least one line.

Other qualitative monogenic traits as external color of immature fruit, mottled rind and yellowing of the ripe rind, identified and described in Pereira et al. (submitted) with a RIL population developed from the same parental lines, were also confirmed in the same locations using the IL collections (not shown).

QTL mapping

Most of the traits determining fruit quality are quantitative and controlled by a polygenic inheritance. QTL mapping for these traits should be performed using multiple replicates and environments, so we could not determine with enough confidence stable QTLs in our preliminary phenotyping. Nevertheless the phenotype of some lines allowed us to identify interesting phenotypes to be confirmed in future studies.

Two QTLs related to fruit ripening could be mapped in a reliable way using the Ved IL collection. The first one, referred as *CDQV7.1*, mainly caused a loss of chlorophyll degradation and was located at the beginning of chromosome VII. A major gene determining whether the external fruit color is white (Ved allele, dominant) or dark green (PS allele, recessive) mapped in Pereira et al. (manuscript in preparation) is co-segregating with the ripening-related QTL *CDQV7.1*. Thus the Ved ILs carrying an introgression of PS in chromosome VII are dark green when immature, provoking that the change of color observed during climacteric ripening becomes more evident. Two groups of ILs were compared, the lines coming from the plant BC3 680, with an introgression covering the proximal part of chromosome VII (Figure 5.8) and the lines derived from the plant BC3 38, carrying a very similar introgression but lacking the first 4.6 Mb of the chromosome. The three individuals from 680 were dark green at harvest, unlike the ones from 38 progeny, which presented a yellow color due mainly to chlorophyll degradation (Figure 5.8). In addition, the lines from the 680 family presented no or slight aroma, although the abscission layer formation was not affected, neither the earliness of climacteric ripening (not shown). These results indicate that a QTL controlling or modulating climacteric fruit ripening is located within the first 4.6 Mb of chromosome VII, although more phenotyping tests should be performed to confirm it.

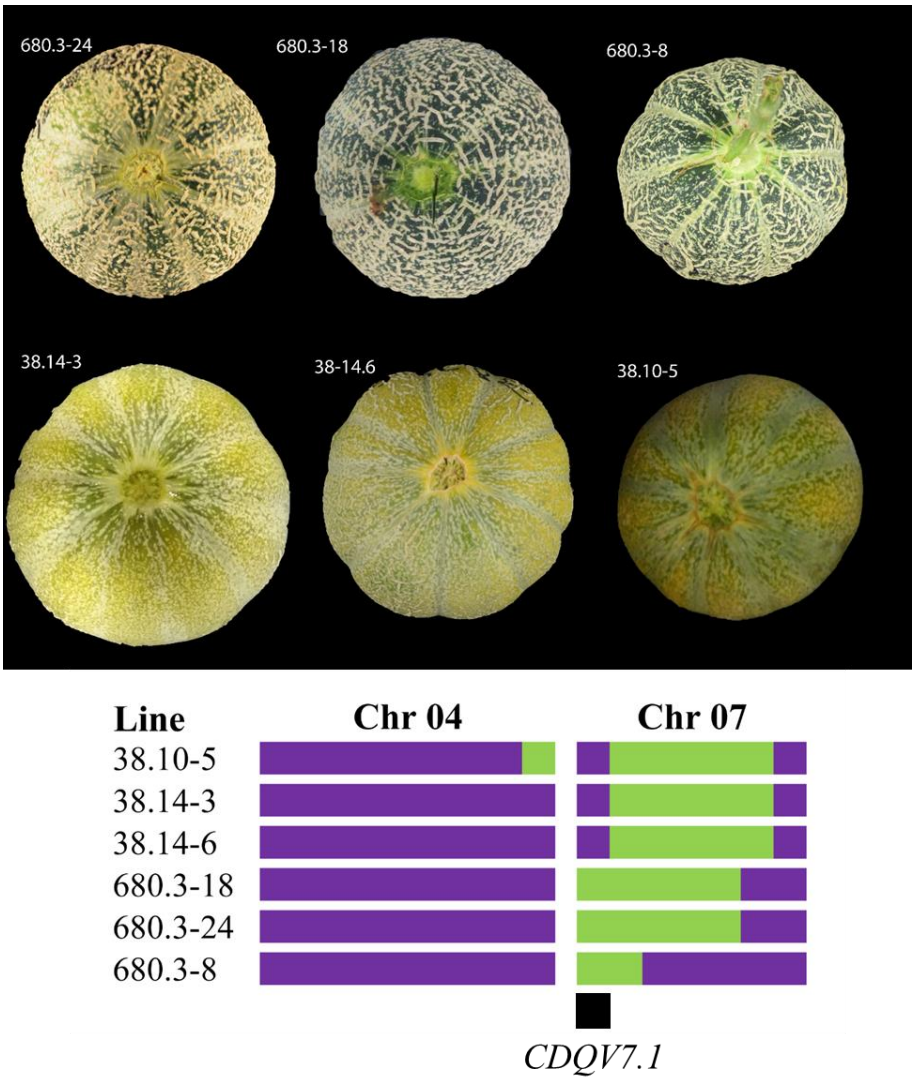

Figure 5.8. ILs and pre-ILs showing different ripening behaviour. The family 680 remained green after harvest, unlike the family 38.14 that degraded chlorophyll as part of an intense climacteric ripening. The genotype of the lines is presented in the diagram, showing only the chromosomes that carried an introgression from the donor parental (PS) in at least one line.

The second QTL seemed to be controlling fruit abscission after ethylene production. We show three representative lines from two families, 163.44 and 78.70, that bear PS introgressions in chromosome XI in the Ved background (Figure 5.9). Both of them ripe normally, showing a strong sweet aroma, chlorophyll degradation and getting a cream color similarly to Ved, but the family 163.44 did not form abscission layer or did it substantially later than all the other lines of the population. However, the family 78.70 showed a similar phenotype but including abscission layer formation and fruit abscission in some cases. The PS introgression of the family 163.44 covered a region at the beginning of chromosome XI not contained in the family 78.70 that is presumably

responsible of the phenotype. So we suggest that a QTL, *ABSQV11.1*, necessary for fruit abscission in a climacteric background, is located between the positions 0-10.9 Mb of chromosome XI. Two ILs with the PS background that carried a Ved introgression in this interval of chromosome XI showed a slight abscission layer formation.

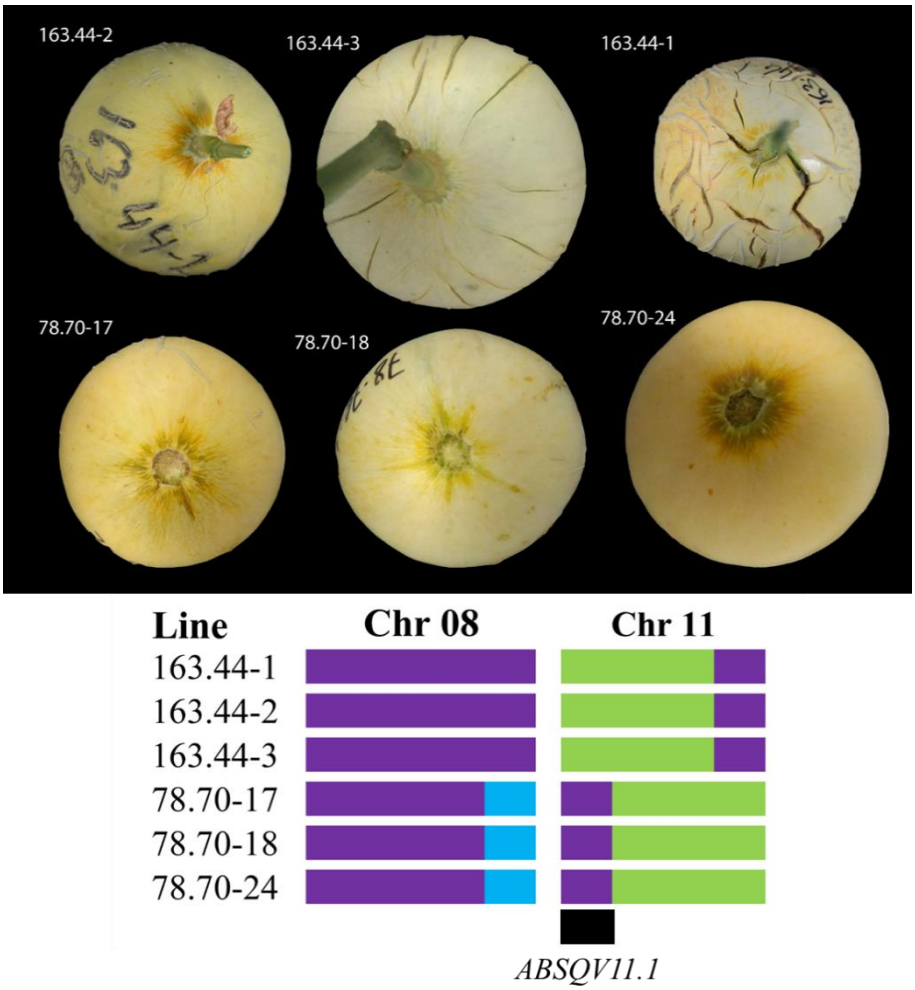

Figure 5.9. ILs and pre-ILs showing presence or absence of abscission layer formation. The family 163.44 did not form abscission layer during climacteric ripening, unlike the family 78.70. The genotype of the lines is presented in the diagram, showing only the chromosomes that carried an introgression from the donor parental in at least one line.

Discussion

IL collections are a highly valuable resource for both research and breeding, although their development is more complex and expensive than other populations. In the last years, many IL collections have been described for different species, including melon, which have been successfully used to map and characterize QTLs (Barrantes et al. 2016; Argyris et al. 2017; Urrutia et al. 2017). The most remarkable parameters for an IL population are the number of ILs per chromosome, which is directly correlated with the resolution and with the required resources for phenotyping, and the number of generations needed to obtain the ILs, which is related with undesired introgressions in non-target regions. In both of our IL populations, the mean number of ILs per chromosome was 3.2 (Table 5.3 and Table 5.4). In comparison to other IL collections, this is an intermediate size, below the 6 ILs per chromosome obtained in a strawberry IL collection (Urrutia et al. 2015) but substantially higher than the 1.3 ILs per chromosome from another recently described melon IL collection (Perpiñá et al. 2016) (Table 5.6). However, if more resolution is desired, we also described extended IL collections for both backgrounds (Table 5.S3b and Table 5.S5b), with a larger population size (45 ILs for Ved and 47 ILs for PS), presenting 3.8 and 3.9 ILs per chromosome for Ved and PS, respectively. Likewise, a reduced IL collection (Table 5.S3c and Table 5.S5c) with a smaller population size (33 ILs for Ved and 31 for PS) but covering virtually the same proportion of donor parental is also proposed. In this case, the phenotyping would require less effort at the beginning, and the desired regions could be inspected more carefully later adding additional ILs. The number of generations used to obtain the ILs in our work was generally six (BC3S2 and BC4S1), as in most other IL collections (Table 5.6). The percentage of covered donor genome is around the mean for the Ved collection (95%) and slightly below the mean for the PS collection (90.9%), but other pre-ILs will be used in the near future to recover the existing gaps, trying to cover practically 100% of the donor parental lines in the IL collections.

Table 5.6. General description of other recent IL collections

Species	Donor parental	Needed generations[1]	ILs/ chr	First MAS-generation	Reference
Tomato	*S. pimpinellifolium*	6	4.6	BC2	(Barrantes et al. 2014)
Melon	"Songwhan Charmi"	6	4.75	BC1	(Eduardo et al. 2005)
Strawberry	*Fragaria bucharica*	4	6	BC1	(Urrutia et al. 2015)
Melon	"Ginsen Makuwa"	6	1.3	BC2	(Perpiñá et al. 2016)
Peach	Almond, "Texas"	3	3.5[2]	BC1	(Serra et al. 2016)
Eggplant	*S. incanum*	7	2.1	BC1	(Gramazio et al. 2017)

[1]The number of generations needed in the major part of the population

[2]Only the homozygous ILs were considered

The first backcross obtained in both directions presented a mean of 12 introgressions per line, implying that on average one recombination per chromosome and meiosis had occurred. The use of marker-assisted selection in the first BC generation reduced substantially the risk of carrying non-detected contaminations. Thereafter, the number of introgressions found in our BC2 and BC3 populations, 6 and 2.7 respectively, were similar to other IL populations obtained in melon and tomato (2n=24) (Eduardo et al. 2005; Barrantes et al. 2014; Perpiñá et al. 2016). The size of the introgressions was around 16 Mb and 58 cM on average in both populations, which are slightly higher than the genetic distance value obtained in other IL collections (mean of 38.7 cM), but similar in physical distance (Eduardo et al. 2005; Barrantes et al. 2014; Urrutia et al. 2015; Perpiñá et al. 2016). This discordance could be attributed to the strategy used to select the SNPs for the marker-assisted selection, which was mainly based on physical distances (markers homogeneously distributed across the chromosomes). Since in melon it is known that the recombination frequency is higher in the telomeric regions and much lower in the large pericentromeric regions (Argyris et al. 2015; Sanseverino et al. 2015), we wanted to avoid obtaining ILs with very narrow introgressions in the telomeric regions and large

introgressions in the centromeres, as it has been observed in other IL collections (Barrantes et al. 2014; Urrutia 2015). We partially achieved our goal (Figure 5.2 and Figure 5.3), although the introgressions still presented a range of physical sizes (Table 5.2 and Table 5.3).

A preliminary phenotyping of the ILs showed a huge potential for QTL mapping. Both parental lines are commercial varieties with acceptable agricultural performance and high fruit quality, but they differ in many important traits such as fruit color, size and shape, external appearance and ripening behaviour (Pereira et al. submitted; Pereira et al. in preparation). These IL populations may allow better understanding their inheritance and facilitate QTL cloning. We observed segregation in several external appearance traits as external color of immature and ripe fruit, mottled rind, sutures and netting. Most of these traits have been phenotyped and mapped in a RIL population derived from the same parentals (Pereira et al. submitted), and the ILs confirmed these major genes. We focused on two traits, sutures and flesh color, which were not described in Pereira et al (submitted). The presence of sutures (*s-2*, sometimes erroneously called ribs or stripes) was previously mapped to chromosome XI (Périn et al. 1999; Harel-Beja et al. 2010; Ramamurthy and Waters 2015), but the underlying gene remains unknown. In our IL collections, the hypothesis of monogenic inheritance controlled by a major gene located in chromosome XI fits perfectly. Although the absence of sutures is dominant, in some plants we could differentiate between the heterozygous and the dominant homozygous, the former presenting an intermediate phenotype (Figure 5.6). The penetrance of the trait when the major gene is in heterozygosity may be modified by other minor QTLs or by the environment. The same trait has been studied in other cucurbits, especially in *Cucurbita pepo* (Esteras et al. 2012), but the biological process causing the sutures has not been yet described. Concerning flesh color, we observed the three expected phenotypes depending on the allelic combination in both the *CmOr* and *Wf* genes, located in chromosomes IX and VIII, respectively (Figure 5.7). *CmOr* has already been cloned (Tzuri et al. 2015) and is located in the position 21,683,406 bp of chromosome IX (version v3.6.1 of the melon genome); *Wf* has been mapped using several populations to a region of around 5 Mb of chromosome VIII (Monforte et al. 2004; Cuevas et al. 2009), and a candidate gene has been proposed recently (Galpaz et al. 2017). Using our ILs, we mapped these genes to the same locations already described, although the resolution is lower due to the large size of the introgressions. However, they represent useful material

to generate segregating populations to fine map *s-2* and *Wf*, since other minor QTLs affecting the traits have been proposed and may complicate the phenotyping when using other types of mapping populations.

Besides fruit quality traits, as the ones described above, and other traits as sugar content and fruit morphology, these IL populations are attractive because the ripening behaviour of the parental lines is opposite: PS is a non-climacteric variety and Ved is highly climacteric and produces a large amount of ethylene at the onset of ripening (Périn et al. 2002; Saladié et al. 2015). A quantitative composition of climacteric ripening, with the ethylene production and associated phenotypes varying in a continuum spectrum rather than a qualitative presence-absence hypothesis is gaining relevance in recent studies (Leida et al. 2015; Rios et al. 2017). Several QTLs related to climacteric ripening have been already mapped in melon (Périn et al. 2002; Vegas et al. 2013; Perpiñá et al. 2016). In the Ved x PS RIL population, several QTLs controlling or modulating ethylene production and/or climacteric traits as aroma production, fruit abscission and chlorophyll degradation have been identified (Pereira et al. manuscript in preparation). A preliminary phenotyping performed in 2017 with the IL collections allowed to validate two of them, located in chromosomes VII and XI. The first one, *HARQV7.1*/*EAROQV7.1*, was mapped in an interval of 0.68 Mb (835,787-1,517,405 bp) of chromosome VII, with the Ved allele increasing the climacteric behaviour (less DAP to aroma production and harvest) (Pereira et al. manuscript in preparation). Two families from the Ved IL collection allowed to map a QTL in the same region, called *CDQV7.1*, showing an analogous effect: when the PS allele was present, fruits did not lose chlorophyll during ripening (Figure 5.8). Other ripening-related phenotypes did not seem to be affected by *CDQV7.1* in the Ved ILs; however, in the RIL population the QTL was involved in other ripening-associated traits as aroma; the low number of replicates analyzed for the ILs or the QTL interactions, present in the RIL population and absent in the ILs, could explain the different behaviour. The second validated QTL, named *ABSQV11.1*, was located between the positions 5,861,352-11,146,160 bp of chromosome XI and was controlling abscission layer formation and fruit abscission in the RIL population (Pereira et al. manuscript in preparation). The Ved IL collection confirmed this QTL, since a Ved IL family carrying the region containing *ABSQV11.1* in homozygosity did not present abscission layer formation (Figure 5.9).

We have developed two reciprocal IL collections, using as parental lines the elite European cultivars Ved and PS. To our knowledge, this is the first time that the same varieties are used in parallel as donor and recurrent parental lines to obtain IL collections. A RIL population derived from the same parental lines has proven its effectiveness to perform QTL mapping experiments (Pereira et al. submitted). The IL collections will allow to improve the mapping resolution of polygenic traits, due to the reduction of QTL x QTL interactions. The availability of reciprocal collections also increases the power of detection, since some QTLs can be detected only in specific backgrounds. In addition, the QTL characterization can be performed in both IL populations, and the most suitable genetic background can be selected to carry on with the QTL cloning. Both IL populations segregate for several interesting traits for both fundamental research and breeding, and may be a valuable resource in either objectives.

Digital Supplementary Material

Table 5.S1. List of SNPs used in the screenings during the development of the IL collections. a. set 1 of SNPs; b. set 2 of SNPs; c. complete set of SNPs; d. additional SNPs genotyped in the putative gaps.

Table 5.S2. Genotyping of the material developed for the Ved IL collection. a. ILs obtained during the spring of 2017; b. ILs obtained during the summer of 2017; c. advanced lines obtained in 2017 with a maximum of two introgressions; d. additional redundant ILs; e. pre-ILs with more than two introgressions, developed in order to cover the putative gaps.

Table 5.S3. Genotyping of the Ved IL collection. a. basic IL collection; b. extended IL collection; c. reduced IL collection.

Table 5.S4. Genotyping of the material developed for the PS IL collection. a. ILs obtained during the spring of 2017; b. ILs obtained during the summer of 2017; c. advanced lines obtained in 2017 with a maximum of two introgressions; d. additional redundant ILs; e. pre-ILs with more than two introgressions, developed in order to cover the putative gaps.;

Table 5.S5. Genotyping of the PS IL collection. a. basic IL collection b. extended IL collection; c. reduced IL collection.

References

Argyris JM, Díaz A, Ruggieri V, et al (2017) QTL Analyses in Multiple Populations Employed for the Fine Mapping and Identification of Candidate Genes at a Locus Affecting Sugar Accumulation in Melon (*Cucumis melo* L.). Front Plant Sci 8:1–20.

Argyris JM, Ruiz-herrera A, Madriz-masis P, et al (2015) Use of targeted SNP selection for an improved anchoring of the melon (*Cucumis melo* L.) scaffold genome assembly. BMC Genomics 16:1–14.

Barrantes W, Fernández-del-Carmen A, López-Casado G, et al (2014) Highly efficient genomics-assisted development of a library of introgression lines of *Solanum pimpinellifolium*. Mol Breed 34:1817–1831.

Barrantes W, López-Casado G, García-Martínez S, et al (2016) Exploring New Alleles Involved in Tomato Fruit Quality in an Introgression Line Library of *Solanum pimpinellifolium*. Front Plant Sci 7:1–12.

Bernacchi D, Beck-Bunn T, Emmatty D, et al (1998) Advanced backcross QTL analysis of tomato. II. Evaluation of near-isogenic lines carrying single-donor introgressions for desirable wild QTL-alleles derived from *Lycopersicon hirsutum* and *L. pimpinellifolium*. Theor Appl Genet 97:170–180.

Briggle LW (1969) Near-Isogenic Lines of Wheat with Genes for Resistance to *Erysiphe graminis* f. sp. *tritici*. Crop Sci 9:70–72.

Cuevas HE, Staub JE, Simon PW, Zalapa JE (2009) A consensus linkage map identifies genomic regions controlling fruit maturity and beta-carotene-associated flesh color in melon (*Cucumis melo* L.). Theor Appl Genet 119:741–756.

Díaz A, Hernández M, Dolcet R, et al (2017) Quantitative trait loci analysis of melon (*Cucumis melo* L.) domestication - related traits. Theor Appl Genet 130:1837–1856.

Doligez A, Bouquet A, Danglot Y, et al (2002) Genetic mapping of grapevine (*Vitis vinifera* L.) applied to the detection of QTLs for seedlessness and berry weight. Theor Appl Genet 105:780–795.

Doyle J (1991) DNA Protocols for Plants. In: Hewitt GM, Johnston AWB, Young JPW (eds) Molecular Techniques in Taxonomy. Springer Berlin Heidelberg, Berlin, Heidelberg, pp 283–293.

Eduardo I, Arús P, Monforte AJ (2005) Development of a genomic library of near isogenic lines (NILs) in melon (*Cucumis melo* L.) from the exotic accession PI161375. Theor Appl Genet 112:139–148.

Eduardo I, Arús P, Monforte AJ, et al (2007) Estimating the Genetic Architecture of Fruit Quality Traits in Melon Using a Genomic Library of Near Isogenic Lines. J Amer Soc Hort Sci 132:80–89.

Esteras C, Gomez P, Monforte AJ, et al (2012) High-throughput SNP genotyping in *Cucurbita pepo* for map construction and quantitative trait loci mapping. BMC Genomics 13:80.

Ezura H, Owino WO (2008) Melon, an alternative model plant for elucidating fruit ripening. Plant Sci 175:121–129.

Foncéka D, Hodo-Abalo T, Rivallan R, et al (2009) Genetic mapping of wild introgressions into cultivated peanut: A way toward enlarging the genetic basis of a recent allotetraploid. BMC Plant Biol 9:1–13.

Galpaz N, Gonda I, Shem-Tov D, et al (2017) Deciphering genetic factors that determine melon fruit-quality traits using RNA-Seq based high-resolution QTL and eQTL mapping. ARPN J Eng Appl Sci 12:3218–3221.

Garcia-Mas J, Benjak A, Sanseverino W, et al (2012) The genome of melon (*Cucumis melo* L.). Proc Natl Acad Sci U S A 109:11872–7.

Giner A, Pascual L, Bourgeois M, et al (2017) A mutation in the melon Vacuolar Protein Sorting 41 prevents systemic infection of Cucumber mosaic virus. Sci Rep 7:1–12.

Gramazio P, Prohens J, Plazas M, et al (2017) Development and Genetic Characterization of Advanced Backcross Materials and An Introgression Line Population of *Solanum incanum* in a *S. melongena* Background. Front Plant Sci 8:1–15.

Harel-Beja R, Tzuri G, Portnoy V, et al (2010) A genetic map of melon highly enriched with fruit quality QTLs and EST markers, including sugar and carotenoid metabolism genes. Theor Appl Genet 121:511–33.

Huang BE, Verbyla KL, Verbyla AP, et al (2015) MAGIC populations in crops: current status and future prospects. Theor Appl Genet 128:999–1017.

Keurentjes JJB, Bentsink L, Alonso-Blanco C, et al (2007) Development of a near-isogenic line population of *Arabidopsis thaliana* and comparison of mapping power with a recombinant inbred line population. Genetics 175:891–905.

Leida C, Moser C, Esteras C, et al (2015) Variability of candidate genes, genetic structure and association with sugar accumulation and climacteric behavior in a broad germplasm collection of melon (*Cucumis melo* L.). BMC Genet 16:28.

Li ZK, Fu BY, Gao YM, et al (2005) Genome-wide introgression lines and their use in genetic and molecular dissection of complex phenotypes in rice (*Oryza sativa* L.). Plant Mol Biol 59:33–52.

Lin HX, Yamamoto T, Sasaki T, Yano M (2000) Characterization and detection of epistatic interactions of 3 QTLs, *Hd1*, *Hd2*, and *Hd3*, controlling heading date in rice using nearly isogenic lines. Theor Appl Genet 101:1021–1028.

Martin A, Troadec C, Boualem A, et al (2009) A transposon-induced epigenetic change leads to sex determination in melon. Nature 461:1135–1138.

McMullen MD, Kresovich S, Villeda HS, et al (2009) Supporting online material for: Genetic Properties of the Maize Nested Association Mapping Population. Science 325:737–741.

Monforte AJ, Oliver M, Gonzalo MJ, et al (2004) Identification of quantitative trait loci involved in fruit quality traits in melon (*Cucumis melo* L.). Theor Appl Genet 108:750–8.

Monforte AJ, Friedman E, Zamir D, Tanksley SD (2001) Comparison of a set of allelic QTL-NILs for chromosome 4 of tomato: Deductions about natural variation and implications for germplasm utilization. Theor Appl Genet 102:572–590.

Netzer D, Kritzman G, Chet I (1979) β-(1,3) glucanase activity and quantity of fungus in relation to *Fusarium wilt* in resistant and susceptible near-isogenic lines of muskmelon. Physiol Plant Pathol 14:47–55.

Obando-Ulloa JM, Ruiz J, Monforte AJ, Fernández-Trujillo JP (2010) Aroma profile of a collection of near-isogenic lines of melon (*Cucumis melo* L.). Food Chem 118:815–822.

Pegg GF, Cronshaw DK (1976) Ethylene production in tomato plants infected with

Verticillium albo-atrum. Physiol Plant Pathol 8:279–295.

Pereira L, Ruggieri V, Perez S, et al. QTL mapping of melon fruit quality traits using a high-density GBS-based genetic map (submitted).

Pereira L, Ruggieri V, Argyris J, et al. Genetic dissection of fruit ripening behavior and ethylene production in a melon RIL population. (manuscript in preparation).

Périn C, Dogimont C, Giovinazzo N, et al (1999) Genetic Control and Linkages of Some Fruit Characters in Melon. Cucurbit Genet Coop Rep 22:16–18.

Périn C, Gomez-Jimenez M, Hagen L, et al (2002) Molecular and Genetic Characterization of a Non- Climacteric Phenotype in Melon Reveals Two *Loci* Conferring Altered Ethylene Response in Fruit. Plant Physiol 129:300–309.

Perpiñá G, Esteras C, Gibon Y, et al (2016) A new genomic library of melon introgression lines in a cantaloupe genetic background for dissecting desirable agronomical traits. BMC Plant Biol 16:1–21.

Ramamurthy RK, Waters BM (2015) Identification of fruit quality and morphology QTLs in melon (*Cucumis melo*) using a population derived from *flexuosus* and *cantalupensis* botanical groups. Euphytica 204:163–177.

Rios P, Argyris JM, Vegas J, et al (2017) *ETHQV6.3* is involved in melon climacteric fruit ripening and is encoded by a NAC domain transcription factor. Plant J 91:671–683.

Saladié M, Cañizares J, Phillips MA, et al (2015) Comparative transcriptional profiling analysis of developing melon (*Cucumis melo* L.) fruit from climacteric and non-climacteric varieties. BMC Genomics 16:1–20.

Sanseverino W, Hénaff E, Vives C, et al (2015) Transposon Insertions, Structural Variations, and SNPs Contribute to the Evolution of the Melon Genome. Mol Biol Evol 32:2760–2774.

Serra O, Donoso JM, Picañol R, et al (2016) Marker-assisted introgression (MAI) of almond genes into the peach background: a fast method to mine and integrate novel variation from exotic sources in long intergeneration species. Tree Genet Genomes 12:96.

Serra O, Giné-Bordonaba J, Eduardo I, et al (2017) Genetic analysis of the slow-melting flesh character in peach. Tree Genet Genomes 13:77.

Suge H (1972) Effect of *uzu* (*uz*) gene on the level of endogenous gibberellins in barley. Japanese J Genet 47:423–430.

Tzuri G, Zhou X, Chayut N, et al (2015) A "golden" SNP in *CmOr* governs the fruit flesh color of melon (*Cucumis melo*). Plant J 82:267–279.

Urrutia M (2015) *Fragaria vesca* NIL collection: Development and Genetic Characterization of Agronomical, Nutritional and Organoleptic traits. Dissertation, Autonomous University of Barcelona

Urrutia M, Bonet J, Arús P, Monfort A (2015) A near-isogenic line (NIL) collection in diploid strawberry and its use in the genetic analysis of morphologic, phenotypic and nutritional characters. Theor Appl Genet 128:1261–1275.

Urrutia M, Rambla JL, Alexiou KG, et al (2017) Genetic analysis of the wild strawberry (*Fragaria vesca*) volatile composition. Plant Physiol Biochem 121:99–117.

Vegas J, Garcia-Mas J, Monforte AJ (2013) Interaction between QTLs induces an advance in ethylene biosynthesis during melon fruit ripening. Theor Appl Genet 126:1531–1544.

Main discussion

Fruit ripening in melon

Fruit ripening is, as already discussed above, a complex process of main importance for both commercial and research purposes. The genetic and epigenetic basis controlling climacteric ripening have been deeply studied in the model crop tomato, although the process is not fully understood yet. It has been proposed that epigenetics is involved in the acquisition of ripening competence and a transcription factor network fine tunes the autocatalytic biosynthesis of the hormone ethylene, which triggers the physiological changes required for the fruit to become edible (Giovannoni et al. 2017).

However, the knowledge about the molecular basis of fruit ripening in other species, especially in non-climacteric fruits, is scarce. During the last years, melon has been considered an interesting model to investigate ripening behaviour, due to the coexistence of climacteric and non-climacteric varieties within the species, which simplifies performing genetic studies (Ezura and Owino 2008). Among the different botanical groups described in melon, a high diversity in ripening-associated traits is found. Four ripening-associated traits are used as descriptors to classify melon accessions: presence of aroma, fruit abscission (or abscission layer formation), rind color at maturity and shelf life (Pitrat 2016). In the *melo* subspecies, accessions with different ripening behaviour coexist, from very climacteric (e.g. the *cantalupensis* group) to totally non-climacteric (e.g. the *inodorus* group). However, in wild and exotic melons the most common behaviour is an intermediate climacteric phenotype; for example, some accessions from the *kachri* group present long shelf life and no aroma with fruit abscission and an evident change of color at maturity (Pitrat 2016). Another exotic accession, PI 161375, from the *conomon* group, presents an intermediate expression of genes encoding ethylene pathway components, suggesting a low degree of climacteric behaviour (Saladié et al. 2015). The two varieties used in this thesis, Ved and PS, are representative of both extremes concerning ethylene production, with exceptionally high values in Ved and undetectable values in PS.

The use of mapping populations and collections of accessions allowed to identify several QTLs involved in fruit ripening (Périn et al. 2002; Vegas et al. 2013; Leida et al. 2015; Perpiñá et al. 2016), showing that climacteric ripening in melon is a complex process controlled by polygenic inheritance. This polygenic inheritance explains the continuum spectrum of climacteric ripening observed among melon groups and suggests that this

trait should be treated as quantitative rather than qualitative. Then, we could hypothesize that, although in wild and exotic varieties the most common is to find an intermediate climacteric behaviour, in some market types as *cantalupensis*, breeding programs have selected the favorable alleles for multiple genes involved in climacteric ripening, leading to highly climacteric varieties. The opposite selection would lead to other market types as *inodorus*, which are totally non-climacteric. The later groups may be described as mutants in multiple genes affecting ripening behaviour.

The present work has contributed to further understanding the genetic basis of climacteric ripening in melon. On one side, the Ved x PS RIL population allowed to detect 15 QTLs related to ethylene production and ripening-associated traits, in nine of the twelve melon chromosomes. Some of the identified QTLs were already described before, confirming their effect in different genetic backgrounds, and others have been reported here for the first time. We suggest that several genetic factors are involved in different aspects of climacteric ripening, affecting the earliness of ethylene production or the maximum amount of ethylene production. Other factors only affect downstream traits associated to ripening, as abscission and chlorophyll degradation. Furthermore, we hypothesize that some of these QTLs are sufficient to trigger the autocatalytic biosynthesis of ethylene by themselves, whereas others are just modifying the process. We observed that, when we isolated the effect of the major QTL *ETHQV8.1* by sub-setting according to the haplotype of the *ETHQV8.1* region, new minor QTLs controlling ripening and ethylene production appeared in both the Ved-VIII and PS-VIII subsets.

On the other side, we have fine mapped *ETHQB3.5* using a positional cloning strategy to identify potential candidate genes for the QTL. This QTL was previously described as sufficient to trigger climacteric ripening in a non-climacteric PS background (Moreno et al. 2008; Vegas et al. 2013). A NIL containing the haplotype of the exotic accession PI 161375 in homozygosity in the *ETHQB3.5* region, named 8M35, was used to generate subNILs carrying different portions of the original introgression. Several trials performed through four seasons showed that the behaviour of *ETHQB3.5* is complex and cannot be explained by the action of a unique gene. Somehow, the climacteric effect was partially lost when the original introgression was reduced, only obtaining a strong climacteric phenotype in the original NIL 8M35, and a less intense effect when we recovered narrow regions of PS. Two independent regions of the introgression were defined as carrying independent QTLs named *ETHQB3.5.1* and *ETHQB3.5.2*, although the former was

responsible for the major part of the phenotypic variation. Some candidate genes were identified within the interval of *ETHQB3.5.1*, among them *MELO3C011421*, encoding a 14-3-3 protein that could be involved in regulating the stability of *CmACS1* via phosphorylation.

Another hypothesis to explain the loss of climacteric behaviour in the subNILs derived from 8M35 could be that the introgression of an exotic DNA altered the expression of nearby genes located outside the introgression, by epigenetic alterations; similar processes have been described in other species (Liu et al. 2004; Zhang et al. 2008; Doerfler 2011). *CmACS1* is located 1.3 Mb downstream the end of the introgression contained in 8M35, so if the introgression was modifying its expression the ripening process would be altered. However, we lack proven evidence to support this mechanism and in order to explore it, it would be necessary to study the ethylene production, the *CmACS1* gene expression and the epigenetic modifications in an adequate subset of subNILs, including 8M35 and PS as controls.

Moreover, we have to take into account that the low amount of ethylene produced in 8M35 may be near a minimum threshold necessary to trigger climacteric ripening. So subNILs carrying fragments of the region may behave as climacteric or non-climacteric depending on the quantity of ethylene produced, which in some fruits may be not enough to trigger climacteric behaviour.

Climacteric and non-climacteric ripening

Ripening is a hormone-controlled process in both climacteric and non-climacteric species, being ethylene and ABA, respectively, the main hormones involved. Melon is an unusual case where we could find both types of ripening behaviour within the species; however, it is not the only one, since climacteric varieties have been reported in pepper (Gross et al. 1986), considered a non-climacteric species, and non-climacteric varieties in plum (Abdi et al. 1997), considered a climacteric species. In pear, European varieties are generally climacteric but the majority of the Chinese and Japanese varieties are non-climacteric (Paul et al. 2012). This behaviour found in some species could reinforce the idea of climacteric ripening being a qualitative trait that can vary in a wide range from

non-climacteric to totally climacteric varieties, depending on the allele combination in ripening genes carried by each variety or accession.

In addition, some authors have reported a peak of ethylene, accompanied by a change of color, in species categorized traditionally as non-climacteric, as grape (Chervin et al. 2004), strawberry (Iannetta et al. 2006), cucumber (Saltveit and Mcfeeters 1980) and pepper (Villavicencio 1999; Villavicencio et al. 2001). The values of maximum ethylene production were considerably lower than the values found in species classically categorized as climacteric. For example, in tomato the fruit produces, depending on the study, from 6 to15 nl · g^{-1} · h^{-1} of ethylene in detached (Chung et al. 2010; Shima et al. 2014; Ito et al. 2017) and attached (Pereira et al. 2017) fruits. In melon attached fruits, the quantities in climacteric varieties are much higher, around 200 nl · g^{-1} · h^{-1} but lower values around 2 nl · g^{-1} · h^{-1} are sufficient to trigger the climacteric response. Although the employed units are different in each study, in general the quantity of ethylene in non-climacteric fruits is very low; in strawberry, around 300 pl · $berry^{-1}$ · h^{-1} of ethylene (Iannetta et al. 2006), 0.5-1 nl · g^{-1} · h^{-1} in pepper (Villavicencio 1999) and approximately 157 pl · g^{-1} in grape (Chervin et al. 2004). An especial situation was reported in orange, in which only the young fruitlets seem to behave as climacteric, producing an ethylene peak barely simultaneously to change of color and abscission layer formation (Katz et al. 2004). In other non-climacteric species as eggplant and watermelon, ethylene has proven to have a role in postharvest behaviour (Mao et al. 2004; Concellón et al. 2005). The development of a new, highly sensitive and non-invasive method to monitor ethylene during ripening in attached fruits, may facilitate the research in species with low ethylene production that have classically been considered as non-climacteric (Pereira et al. 2017).

On the other hand, some studies suggest that ABA has a major role during ripening not only in non-climacteric but also in climacteric fruits (Leng et al. 2014). The pattern of ABA production in grape, non-climacteric, and peach, climacteric, is very similar, showing a peak that coincides with ripening symptoms in both species, and slightly before the beginning of ethylene production in peach (Zhang et al. 2009a). In tomato, fruits treated with fluridone, an abscisic acid inhibitor, reduced significantly ethylene production and showed deficiencies in ripening (Zhang et al. 2009b). Also in banana, a climacteric species, ABA-treated fruits showed a significant advance in ripening; the effects in ripening of different treatments, combining several doses of ethylene and ABA, suggested that ABA regulates ethylene sensitivity in fruit (Jiang et al. 2000). Similar

experiments have been performed in other climacteric species as avocado and mango (Chernys and Zeevaart 2000; Zaharah et al. 2013).

These insights in fruit ripening in different species, including the results observed in melon during this thesis, may suggest that the traditional classification into two qualitative types of fruits may be reconsidered.

Genetic control of melon fruit quality

Although the main focus of this PhD thesis was to decipher the genetics of fruit ripening, the Ved x PS RIL population was a very powerful resource to study other aspects of fruit quality. Fruit quality is a wide concept including diverse traits related to different aspects of fruit development, as internal and external color, ribbing and netting, sugar content, acidity and fruit morphology. Ved and PS are two elite varieties from the European market, and both of them present good quality, but they differ in all the above-mentioned traits. It is expected that lines derived from these RILs may have an easy introduction to the market.

In the RIL population, we observed a wide segregation for fruit quality traits, with some fruits presenting a totally different appearance when compared to the parental lines. For example, RIL 172 presented a smooth, white and elongated fruit of approximately 350 g, with high sugar content and slightly climacteric behaviour, since it produced aroma but with long shelf life and firm flesh. These characteristics could be interesting for the market, offering a melon with the size of an apple, with good organoleptic quality and long shelf life. Innovative and differentiated varieties have a great potential in the crop's market. Our study on fruit quality could help to develop new varieties in melon; in fact our RIL population is currently being evaluated by a seed company.

Furthermore, some of the major genes controlling fruit quality mapped in this work, the presence of sutures (*S-2*, Chapter 5) and the external color of immature fruit (*Wi*, Chapter 1), have been fine-mapped using a F2 population from the Ved x PS cross in our research group. In both cases, the final interval delimiting the major genes has been reduced to around 200 kb, containing less than 25 candidate genes (not shown). A similar strategy will be followed to identify the responsible gene of mottled rind (*Mt-2*, Chapter 1) and white/green flesh (*Wf*, Chapter 5).

New melon genetic resources

Different genetic resources have been developed in melon during the framework of this thesis. A high density genetic map, containing almost five thousand SNPs and INDELs generated by genotyping-by-sequencing, has been obtained using the Ved x PS RIL population. The map has already been used successfully to perform QTL mapping analysis, and it can be also employed to fine-tune the scaffolding of the melon genome sequence. In fact, some inconsistencies between the physical and the genetic map have been observed, as two chimeric scaffolds in chromosomes II and VII and an erroneously oriented scaffold in chromosome VI. Also, a few scaffolds or contigs belonging to chromosome 0 could be located in the pseudomolecules.

However, the most valuable genetic resource developed has been the two reciprocal IL collections with Ved and PS backgrounds. IL populations are powerful to study quantitative traits, since the effect of the interesting QTL is isolated from other genetic factors that interact and that are located in other regions of the genome. To characterize the effect of ripening QTLs in an accurate manner, IL collections promise to be very useful; in addition, the specific effects of the QTLs can be observed in two different and totally ripening-opposed backgrounds. In fact, some of the mapped QTLs in the RIL population have already been validated using the newly developed ILs with both PS and Ved introgressions, even though a more extensive evaluation of both complete IL collections will be performed during the 2018 season. Another of the main advantages of IL collections is their potential to fine map QTLs, through different methodologies as bulk-segregant analysis (Tzuri et al. 2015) or subNIL development (Argyris et al. 2017). A preliminary fine mapping of *ETHQV8.1* has been performed using some IL families, leading to a list of 14 candidate genes in the interval. One of them is the orthologue of *CTR1*, a gene involved in ethylene signal transduction by direct interaction with ethylene receptors. However, further experiments should be performed to validate CTR1 as the gene underlying *ETHQV8.1*, in which case we would corroborate that the ethylene signaling in melon fruit is analogous to the one already described in model species.

Another interesting opportunity for melon ILs may be the exploration of QTL x QTL interactions. It has been previously reported that, when the two QTLs *ETHQV6.3* and *ETHQB3.5* are stacked in the PS background, they act in an additive manner, leading to a higher and earlier ethylene peak when compared to the lines carrying only one of them

(Vegas et al. 2013). We have obtained ILs with the PS background carrying the Ved alleles for other distinct ripening-related QTLs, allowing the pyramiding of multiple ripening-associated QTLs in a non-climacteric background. A similar experiment was performed to investigate yield in tomato, exploring not only all the homozygous but also all the possible heterozygous combinations (Gur and Zamir 2015).

Finally, it is worth highlighting the great potential of IL collections as a breeding tool. The introduction of new alleles into a breeding program can be performed without any risk of altering many other traits, performing a driven selection, guided by molecular markers.

References

Abdi N, Holford P, McGlasson WB, Mizrahi Y (1997) Ripening behaviour and responses to propylene in four cultivars of Japanese type plums. Postharvest Biol Technol 12:21–34.

Argyris JM, Díaz A, Ruggieri V, et al (2017) QTL Analyses in Multiple Populations Employed for the Fine Mapping and Identification of Candidate Genes at a Locus Affecting Sugar Accumulation in Melon (*Cucumis melo* L.). Front Plant Sci 8:1–20.

Chernys JT, Zeevaart JAD (2000) Characterization of the 9-Cis-Epoxycarotenoid Dioxygenase Gene Family and the Regulation of Abscisic Acid Biosynthesis in Avocado. Plant Physiol 124:343–354.

Chervin C, El-Kereamy A, Roustan JP, et al (2004) Ethylene seems required for the berry development and ripening in grape, a non-climacteric fruit. Plant Sci 167:1301–1305.

Chung M-Y, Vrebalov J, Alba R, et al (2010) A tomato (*Solanum lycopersicum*) APETALA2/ERF gene, SlAP2a, is a negative regulator of fruit ripening. Plant J 64:936–947.

Concellón A, Añón MC, Chaves AR (2005) Effect of chilling on ethylene production in eggplant fruit. Food Chem 92:63–69.

Doerfler W (2011) Epigenetic consequences of foreign DNA insertions: de novo methylation and global alterations of methylation patterns in recipient genomes. Rev Med Virol 21:336–346.

Ezura H, Owino WO (2008) Melon, an alternative model plant for elucidating fruit ripening. Plant Sci 175:121–129.

Giovannoni J, Nguyen C, Ampofo B, et al (2017) The Epigenome and Transcriptional Dynamics of Fruit Ripening. Annu Rev Plant Biol 68:61–84.

Gross KC, Watada AE, Kang MS, et al (1986) Biochemical changes associated with the ripening of hot pepper fruit. Physiol Plant 66:31–36.

Gur A, Zamir D (2015) Mendelizing all Components of a Pyramid of Three Yield QTL in Tomato. Front Plant Sci 6:1–13.

Iannetta PPM, Laarhoven LJ, Medina-Escobar N, et al (2006) Ethylene and carbon dioxide production by developing strawberries show a correlative pattern that is indicative of ripening climacteric fruit. Physiol Plant 127:247–259.

Ito Y, Nishizawa-yokoi A, Endo M, et al (2017) Re-evaluation of the rin mutation and the role of RIN in the induction of tomato ripening. Nat Plants 3:866–874.

Jiang Y, Joyce DC, Macnish AJ (2000) Effect of abscisic acid on banana fruit ripening in relation to the role of ethylene. J Plant Growth Regul 19:106–111.

Katz E, Lagunes PM, Riov J, et al (2004) Molecular and physiological evidence suggests the existence of a system II-like pathway of ethylene production in non-climacteric Citrus fruit. Planta 219:243–252.

Leida C, Moser C, Esteras C, et al (2015) Variability of candidate genes, genetic structure and association with sugar accumulation and climacteric behavior in a broad germplasm collection of melon (*Cucumis melo* L.). BMC Genet 16:28.

Leng P, Yuan B, Guo Y, Chen P (2014) The role of abscisic acid in fruit ripening and responses to abiotic stress. J Exp Bot 65:4577–4588.

Liu Z, Wang Y, Shen Y, et al (2004) Extensive alterations in DNA methylation and transcription in rice caused by introgression from *Zizania latifolia*. Plant Mol Biol 54:571–582.

Mao L, Karakurt Y, Huber DJ (2004) Incidence of water-soaking and phospholipid catabolism in ripe watermelon (*Citrullus lanatus*) fruit: Induction by ethylene and prophylactic effects of 1-methylcyclopropene. Postharvest Biol Technol 33:1–9.

Moreno E, Obando JM, Dos-Santos N, et al (2008) Candidate genes and QTLs for fruit ripening and softening in melon. Theor Appl Genet 116:589–602.

Paul V, Pandey R, Srivastava GC (2012) The fading distinctions between classical patterns of ripening in climacteric and non-climacteric fruit and the ubiquity of ethylene-An overview. J Food Sci Technol 49:1–21.

Pereira L, Pujol M, Garcia-mas J, Phillips MA (2017) Non-invasive quantification of ethylene in attached fruit headspace at 1 p.p.b. by gas chromatography – mass spectrometry. Plant J 91:172–183.

Périn C, Gomez-Jimenez M, Hagen L, et al (2002) Molecular and Genetic Characterization of a Non-Climacteric Phenotype in Melon Reveals Two Loci Conferring Altered Ethylene Response in Fruit 1. Plant Physiol 129:300–309.

Perpiñá G, Esteras C, Gibon Y, et al (2016) A new genomic library of melon introgression lines in a cantaloupe genetic background for dissecting desirable agronomical traits. BMC Plant Biol 16:1–21.

Pitrat M (2016) Melon Genetic Resources: Phenotypic Diversity and Horticultural Taxonomy. Springer New York, New York, NY, pp 1–36

Saladié M, Cañizares J, Phillips MA, et al (2015) Comparative transcriptional profiling analysis of developing melon (*Cucumis melo* L.) fruit from climacteric and non-climacteric varieties. BMC Genomics 16:1–20.

Saltveit ME, Mcfeeters RF (1980) Polygalacturonase Activity and Ethylene Synthesis during Cucumber Fruit Development and Maturation. Plant Physiol 66:1019–1023.

Shima Y, Fujisawa M, Kitagawa M, et al (2014) Tomato FRUITFULL homologs regulate fruit ripening via ethylene biosynthesis. Biosci Biotechnol Biochem 78:231–237.

Tzuri G, Zhou X, Chayut N, et al (2015) A "golden" SNP in CmOr governs the fruit flesh color of melon (*Cucumis melo*). Plant J 82:267–279.

Vegas J, Garcia-Mas J, Monforte AJ (2013) Interaction between QTLs induces an advance in ethylene biosynthesis during melon fruit ripening. Theor Appl Genet 126:1531–1544.

Villavicencio L (1999) Ethylene and carbon dioxide production in detached fruit of selected pepper cultivars. J Amer Soc Hort Sci 124:402–406.

Villavicencio LE, Blankenship SM, Sanders DC, Swallow WH (2001) Ethylene and carbon dioxide concentrations in attached fruits of pepper cultivars during ripening. Sci Hortic 91:17–24.

Zaharah SS, Singh Z, Symons GM, Reid JB (2013) Mode of action of abscisic acid in triggering ethylene biosynthesis and softening during ripening in mango fruit. Postharvest Biol Technol 75:37–44.

Zhang M, Leng P, Zhang G, Li X (2009a) Cloning and functional analysis of 9-cis-

epoxycarotenoid dioxygenase (NCED) genes encoding a key enzyme during abscisic acid biosynthesis from peach and grape fruits. J Plant Physiol 166:1241–1252.

Zhang M, Yuan B, Leng P (2009b) The role of ABA in triggering ethylene biosynthesis and ripening of tomato fruit. J Exp Bot 60:1579–1588.

Zhang Y, Liu Z, Liu C, et al (2008) Analysis of DNA methylation variation in wheat genetic background after alien chromatin introduction based on methylation-sensitive amplification polymorphism. Chinese Sci Bull 53:58–69.

Conclusions

1. A RIL population, developed from a narrow cross between "Védrantais", from the *cantalupensis* group, and "Piel de Sapo", from the *inodorus* group, has been used to explore the segregation of fruit traits. For the first time two close elite varieties belonging to different botanical groups have been used as parents of a segregating population in melon.

2. The implemented strategy, using a RIL population and genotyping-by-sequencing, has been highly efficient for QTL mapping, obtaining QTL intervals of 1 Mb and containing one hundred genes, on average.

3. The Ved x PS RIL population showed a high segregation for fruit quality traits. Five major genes and 33 QTLs related to different aspects of fruit quality have been identified.

4. The Ved x PS RIL population presented a continuum spectrum of climacteric ripening, with a wide range for both the amount and the earliness of ethylene production. The first climacteric symptoms observed after ethylene production were the aroma production and the chlorophyll degradation, which appeared almost simultaneously. Around five days later, the abscission layer was formed.

5. A non-invasive method to measure ethylene in attached fruits was developed, leading to a resolution of 1 part per billion of ethylene. The new method has been successfully employed to evaluate ethylene production in two important horticultural crops, melon and tomato.

6. Fifteen QTLs related with ethylene production and ripening-associated traits were mapped in nine of the twelve melon chromosomes. Some of the mapped QTLs were widely modulating ripening and others were controlling exclusively a single trait.

7. A major QTL, named *ETHQV8.1*, was mapped for the majority of the evaluated ripening traits and was sufficient to trigger the climacteric response in a totally non-climacteric background. The QTL interval contains 14 candidate genes.

8. The climacteric ripening behaviour observed in melon may suggest that the traditional classification into two qualitative types of fruits may be reconsidered as a continuum.

9. The inheritance of climacteric behaviour observed in the NIL 8M35 is complex and highly environmental-dependent, hindering the positional cloning of the responsible gene.

10. The use of a diverse set of subNILs derived from 8M35 demonstrated that more than one genetic factor may be involved in climacteric ripening in the original NIL.

11. An integrative strategy, combining the results of the fine mapping with re-sequencing and transcriptomic data has allowed to propose some candidate genes that could be involved in the climacteric ripening observed in 8M35.

12. The two reciprocal IL collections, generated using "Védrantais" and "Piel de Sapo" as donor and recurrent parental lines alternatively, have shown a high potential to map QTLs and perform QTL x QTL and QTL x background interaction studies.

13. Due to the high complexity of the climacteric ripening process and its polygenic inheritance, the availability of ILs with totally opposed ripening backgrounds will facilitate the dissection of climacteric ripening in melon.